Università degli Studi di Ferrara

DOTTORATO DI RICERCA IN
SCIENZE CHIMICHE

CICLO XXVII

COORDINATORE Prof. Carlo Alberto Bignozzi

Molecular cocrystals
of pharmaceutical interest

Settore Scientifico Disciplinare CHIM/02

Dottorando   **Tutore**

Dott. Cvetkovski Aleksandar   Prof. Gilli Paola

Anni 2012/2014

Acronyms :

ANDA - Accelerated New Drug Application

API – An Active Pharmaceutical Ingredient

AUC - Area under the curve

BCS - Biopharmaceutical Classification System

CC - Cocrystal

CF- Coformer

CSD - Cambridge Structural Database

CT- Charge-transfer

C_{tr} - Transition concentration

DCA – Dichloroacetic acid

DSC- Different Scanning Calorimetry

EDA - Electron donor-acceptor

FDCs – Fixed-dose combinations

FT-IR – Furrier Transformed Infra-red Spectroscopy

GRAS - Generally Accepted As Safe

IPR - Intellectual Property Right

K_{sp} - Solubility product

MET – Metformin

MET·HCl – Metformin hydrochloride

NCEs - New Chemical Entities

PCCs – Pharmaceutical Cocrystals

PS –Pharmaceutical Salt

PT - Proton-transfer

SQA-Squaric acid

US FDA - United States Food and Drug Administration

XRPD – X-ray powder diffraction

List of tables and figures

ABSTRACT

L'enorme varietà delle forme cristalline (cocristalli, polimorfi, sali, idrati e solvati) è tutt'oggi una sfida scientifica con importanti implicazioni pratiche nell'industria farmaceutica, nello stadio finale di sviluppo di un farmaco o di una formulazione farmaceutica e negli stadi iniziali di sintesi ed isolamento di un API (principio attivo) in una definita forma cristallina favorevole. La scelta della forma cristallina ottimale di un API che influisca indisputabilmente sul programma di sviluppo del farmaco è direttamente relato alla solubilità dell'API in acqua. Siccome la solubilità in acqua di un API è il banco di prova per il trasporto e l'assorbimento del farmaco, attraverso un processo di screening, ottimizzazione e selezione è possibile controllare la velocità di dissoluzione dell'API e determinare l'entità della sua biodisponibilità e il profilo farmacocinetico, che sono strettamente relati alla solubilità ed alla forma cristallina. Pertanto comprendere le forze dell'impacchettamento cristallino ed il loro impatto sulle proprietà chimico-fisiche delle diverse forme cristalline dà accesso al controllo delle performance dell'API. L'ampia gamma di forme cristalline in cui il cristallo molecolare dell'API può esistere prevale sui suoi possibili polimorfi, sali, solvati e idrati in virtù del vasto numero di potenziali coformer, che non solo superano il limitato numero di controioni per la formazione di sali, ma sono anche molto più versatili e possono dare origine a più complesse interazioni molecolari basate su diversi legami ad idrogeno con l'API che portano a cambiamenti conformazionali e flessibilità per l'impacchettamento cristallino nel processo di cocristallizzazione. I cristalli molecolari di interesse farmaceutico sono propensi a superare la transizione di fase dell'API che da' luogo al polimorfismo. Ma d'altro canto, per la flessibilità conformazionale causata dal riconoscimento intermolecolare basato sul legame ad idrogeno, sfruttano le nuove forme polimorfe dell'API che possono essere stabilizzate in presenza di coformer opportunamente scelti. Un altro vantaggio dei cristalli molecolari cocristallizzati con appropriati coformer è il controllo della risoluzione stereoselettiva degli API racemici.

Il concetto di modificare le proprietà dell'API mediante formazione di cristalli molecolari che contengono un singolo API in combinazione con un coformer che può essere un altro API oppure un eccipiente funzionale capace di migliorarne le performance nel drug delivery o nelle formulazioni rispetto al cristallo dell'API originario è diventato un paradigma emergente per i programmi di sviluppo dei farmaci. Anche se le

combinazioni di formulazioni a dose fissa vengono frequentemente prescritte in terapia, i cristalli molecolari multi-API o "farmaco-farmaco" sono forme solide dell'API relativamente poco sfruttate. Questi cristalli molecolari nei quali sono cocristallizzati API di natura diversa ma complementari in termini di effetto farmacologico o di meccanismo di azione hanno importanza potenziale per migliorare le proprietà chimico-fisiche di entrambi gli API, la loro performance biofarmaceutica e la sinergia della risposta farmacologica.

Lo screening delle forme cristalline della metformina ha prodotto due gruppi di sali molecolari. Il primo gruppo comprende i sali molecolari della metformina con un'ampia gamma di acidi organici riconosciuti innocui come additivi alimentari, il secondo sali molecolari di metformina cocristallizzati con coformers che sono essi stessi API (diclofenac, acido dicloroacetico, acido glicolico e acido salicilico) ed eccipienti funzionali (saccarina ed acesulfame).

Prove preliminari per determinare la citotossicità dei cocristalli di metformina con acido dicloroacetico indicano una maggiore attività antitumorale in confronto all'effetto esercitato dai singoli farmaci e dalla loro miscela fisica.

ABSTRACT

Crystal form (cocrystals, polymorphs, salts, hydrates and solvates) assortment remains a scientific challenge that implicates practical issues in the pharmaceutical industry at the late stage of drug development of pharmaceutical formulations and in early stage of synthesis and isolation of an API in favorable defined crystalline form. Indeed, the selection of the optimal crystal form of an API that indisputably impacts the drug development program is directly related to the API's aqueous solubility. Since the aqueous solubility of an API is the benchmark for its drug delivery and absorption, by crystal form screening, optimization and selection it is possible to control the dissolution rate of API, and thus to determine the extent of its bioavailability and pharmacokinetics profile which are intricately interrelated to solubility and crystal forms. Therefore, understanding the crystal packing forces and their impact upon physicochemical properties of different crystal forms is threshold for controlling the performance of the API. The array of crystal forms in which molecular crystal of API may exist prevails over its possible polymorphs, salts, solvates and hydrates due to the vast number of potential coformers which, not only extend over the limited counterions for salt formation, but also they are much more versatile in nature and thus imply for more complex intermolecular interactions based on different H-bonding with API that lead to conformational changes and flexibility for crystal packing in process of cocrystallization. Molecular crystals of pharmaceutical interest are amenable to excel the phase transition in API which exert polymorphism. But on the other hand, due to the conformational flexibility caused by intermolecular recognition based on hydrogen bonding, they exploit the new polymorphic forms of the API that might be stabilized in the presence of favorable selected coformers. Another benefit of the molecular crystals cocrystalized with appropriate coformers is controlling the stereoselective resolution of the racemic APIs.

The concept of modifying the properties of the API by the forming the molecular crystals containing single API in combination with coformer that is another API or functional excipient that improves the performance of the drug delivery or in the formulations, compared to the native API crystal, has become emerging paradigm for drug development programs. Moreover the combination of fixed-doses formulation have been frequently prescribed for therapy, the multi-API or "drug-drug" molecular crystals are relatively unexploited solid forms of APIs. This molecular crystals cocrystallized of the

different by nature API, but complementary in terms of pharmacological effect or their mechanism of action have potential relevance for improving the physicochemical properties of both APIs, their biopharmaceutical performance and synergy in pharmacological respond.

Crystal form screening of metformin yields two groups of molecular salts. The one comprises the molecular salts of metformin with a wide range of organic acids recognized as safe for food additives, the other is referred to molecular salts of metformin cocrystallized with coformers which are APIs (diclofenac, dichloroacetic acid, glycolic acid, and salicylic acid) and functional excipients (saccharin and acesulfame).

Preliminary testing of cytotoxicity of the molecular crystals of metformin with dicloroacetic acid indicate an increased anticancer effect comparing to the effect exerted by the native drugs.

Part 1

Crystalline organic solids of pharmaceutical relevance

Organic crystals are described by unit cell that contains minimal number, but at least one molecule or ion which structural features and symmetry elements determine the nature of intermolecular interactions consequently of which molecules or ions are packed and oriented in three-dimensional space (Brittain & Byrn, 1999). Crystals of organic solids, depending on the arrangements and symmetry of their structural patterns, may be classified to one of the seven crystal classes defined by the relationship between the individual dimensions, a, b, and c of the unit cell and between the individual angles, α, β, and γ of the unit cell (Figure 1), to one of the 14 Bravais lattices (Table 1), and to one of the 230 space groups (Cullity, 1963).
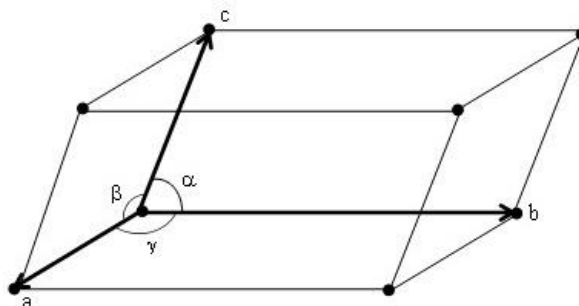
Figure 1.1. A unit cell and the lattice vectors

Individual symmetries and the symmetries of the diffraction patterns for all the 230 possible space groups are describes in the International Tables for Crystallography (Han, 1987). There is evidence for preferences solids to crystallize in certain space groups. Statistical analyses of all organic and organometallic compounds included in Cambridge Structural Database (CSD) indicates that about 90% of them belong to the 17 most common space groups, but about 76% crystallize in only five (5) space groups, $P2_1/c$, $P2_12_12_1$, $P\bar{1}$, $P2$ and C_2/c. Gavazzotti & Flack (2005) explained that this quite restricted number of space groups is result to the limited number of arrangements of symmetry operations: inversion through a point $\bar{1}$, the twofold screw rotation (2) and glide reflection (g) that organic molecules accomplished as a prerequisite for their strict packing into crystalline structures.

Table 1.1 The properties of the 14 Bravais lattices

Crystal system	Axial translation	Axial angles	Bravais lattice
Cubic	a = b = c	α = β = γ = 90°	simple body-centered face-centered
Tetragonal	a = b ≠ c	α = β = γ = 90°	simple body-centered
Orthorhombic	a ≠ b ≠ c	α = β = γ = 90°	simple body-centered face-centered side-centered
Trigonal	a = b = c	α = β = γ ≠ 90°	simple
Hexagonal	a = b ≠ c	α = β = 90°, γ = 120°	simple
Monoclinic	a ≠ b ≠ c	α = γ = 90° ≠ β	simple side-centered
Triclinic	a ≠ b ≠ c	α ≠ β ≠ γ ≠ 90°	simple

Organic crystals exist as single molecular entities or as multicomponent systems. The classification of the crystalline organic solids is presented on the **Figure 1.2**.
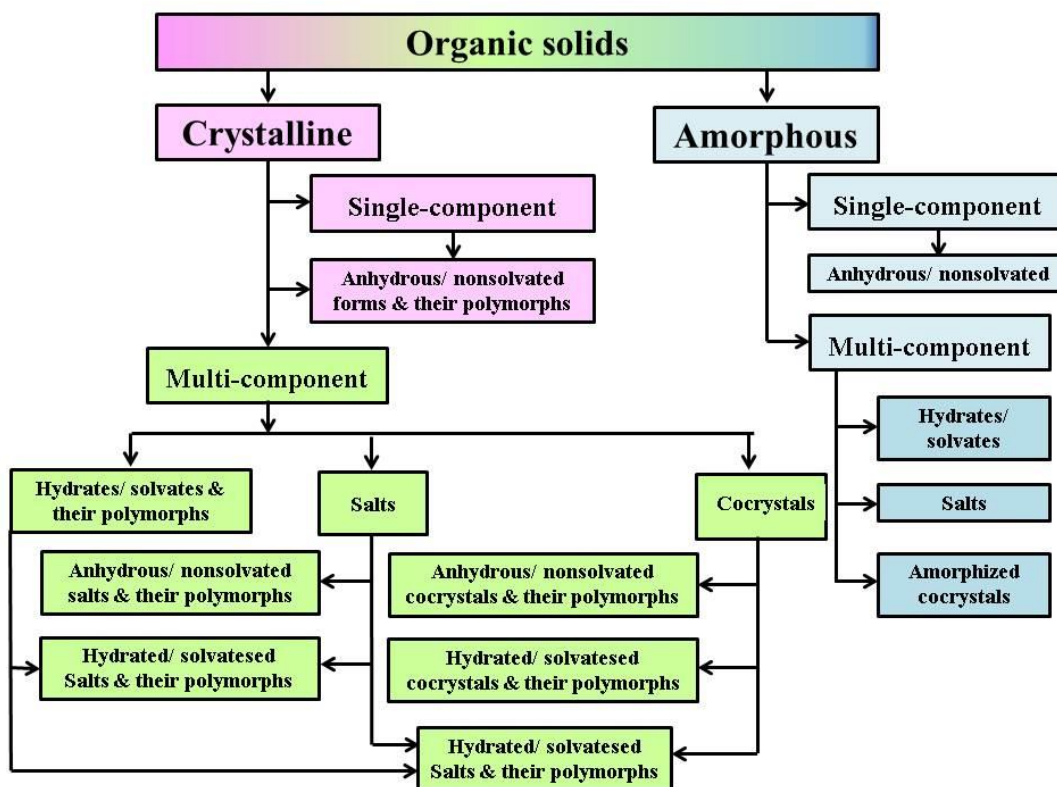
Figure 1.2. Classification of the organic solids (adapted from Stahly, 2007)

A common problem dealing with single component organic crystals is appearing of polymorphism as a propensity the molecules, during the crystallization, to be assembled (packed) in the crystal lattice in different spatial arrangements depending, either on the intermolecular interactions between several different functional groups (orientation polymorphism), or differences in structural flexibility of the molecules (conformational polymorphism) (Bernstein, 1993; Zerkowski *et al.*, 1997; Chin *et al.*, 1999). Different polymorphic forms of single-component crystal of one organic compound cause differences in physical properties listed in **Table 1.2**.

Multicomponent organic crystals cover diverse structures formed by stoichiometric or nonstoichiometric non-covalent bonding between at least two molecules with different polarity (ionizable, neutral or zwitterionic), chemical nature (acidic or basic compounds) and physical state at ambient conditions (solid, or liquid) (Peterson, 2006). Comparing to single-component crystals of one organic compound, its multi-component crystals have different chemical composition due to the nature and physical state of the molecules of the other components that participate in diverse non-covalent interactions with the molecules of the parent compound.

Crystalline solvates and hydrates represent molecular solvent-solute type of adducts. Since small-sized molecules of water or any other solvents are capable to participate in hydrogen bonding, they can link in the structure of organic molecules. Based on the location of crystallized water, crystalline hydrates may be classified in the following classes (Giron *et al.*, 2002; Morris & Rodigues-Hornedo, 1993):

- isolated hydrates (*e.g.* cefadrine dehydrate; Florey, 1973);

- ion-associated hydrates (*e.g.* dehydrate and trihydrate of disodium adenosine 5'-triphosphate; Morris *et al.*, 2001)

- channel hydrates (*e.g.* theophylline monohydrate; Morris *et al.*, 2001; Sugawara *et al.*, 1991), that may be additionally classified in the expanded channel or nonstoichiometric hydrates (*e.g.* cromolyn sodium; Chen *et al.*, 1999) and the planar hydrates (*e.g.* nedocromil zinc; Zhu *et al.*, 1997).

The molecular structure, and the thermodynamic conditions (the water or solvent activity in crystallization medium, temperature, and pressure) are responsible factors whether the hydrates and/ or solvates will be formed. Some of the hydrates structures can belong to more categories of the hydrates (Zhu *et al.*, 1997).

Clathrates are host-guest multi-component crystals wherein quite mobile guest molecules, without specific interactions, partially or fully occupy rigid tridimensional cavities- or

cage-shaped crystal lattice of the host molecule that controls the orientation of the individual molecules or aggregates of molecules (Andreetti, 1984).

Table 1.2. Property differences between single-component and multicomponent crystals and the different structures of their crystalline phases (polymorphs)

Packing properties	Molar volume and density
	Refractive index, optical properties
	Conductivity, electrical and thermal
	Hygroscopicity
Thermodynamic properties	Melting and sublimation temperatures
	Internal energy
	Enthalpy
	Heath capacity
	Entropy
	Free energy and chemical potential
	Thermodynamic activity
	Vapor pressure
	Solubility
Spectroscopic properties	Electrical transitions, UV-VIS spectra
	Vibrational transitions, Infrared and Raman spectra
	Rotational transitions
	Nuclear magnetic resonance chemical shifts
Kinetic properties	Dissolution rate
	Rates of solid state reactions
	Stability
Surface properties	Surface free energy
	Interfacial tensions
	Habit
Mechanical properties	Hardness
	Tensile strength
	Compactability, tabletability
	Handling, flow and blending

Molecular salts are multicomponent crystals composed of electrostatic interactions between charged (ionizable) acidic and basic molecular moieties as a result of which the proton transfer is occurred in range from acidic to basic component in ionic state (deprotonated acid/ acidic anion to protonated base/ basic cation) (Aakeröy et al., 2007).

Cocrystals (CCs) are subgroup of multicomponent crystals formed mainly through hydrogen bonding of at least two or more components: both neutral molecules; neutral molecule with cationic molecule; neutral molecule with anionic molecule; or neutral molecule with either positively or negatively charged ion. The term CC is synonym for

array of multicomponent crystals that have been explained with diverse terminology over the years: addition compounds (Grossmann, 1908), organic molecular compounds (Anderson, 1937), mixed binary molecular crystals (Remyga et al., 1969), molecular complexes (Damiani et al., 1965; Van Nieker&Saunder, 1948), solid-state complexes or heteromolecular complexes (Pekker et al., 2005).

The components coupled in structure of the multicomponent crystals are assembled through supramolecular synthons in fashion of complementarity of the hydrogen bond donor and acceptor functional groups forming homomeric or heteromeric structures (Etter, 1990; Etter, 1991, Aakeröy et al., 2004). The molecule of interest can crystallize in stoichiometric ratio with one or more coformer (CF) molecules in new crystalline structure of CC that acts as a different functional material due to the changes in physicochemical properties (*e.g.* solubility, melting point, morphology, thermal stability, hygroscopicity, etc., see in **Table 1.2**), while an active pharmaceutical ingredient (API) within the CC structure retains its chemical nature. Compounds that contain aromatic rings may form CCs by stacking (*Seaton, et al., 2013*) or charge transfer interactions (*Samanta et al., 2014*). Recent researches carried out by Grepioni *et al.* (2014), Braga *et al.* (2011), Smith *et al.* (2013) on multicomponent crystals revealed the ionic CCs involving inorganic salts and racemic drugs.

Depending on the thermodynamic and kinetic conditions, one organic compound may crystallize in a variety of solid phases which, as crystalline forms with different structural arrangement, may undergo to phase transition and appear as polymorphs, each of them exhibiting different physical properties (**Figure 1.2**).

Differences in long-range periodicity of assembled molecules in structure of organic crystals, arising by the differences in intermolecular forces, in turns cause differences in energy, and thus affect differences mainly in physical properties that consequently get implication to product development and formulation (selecting a crystalline form with prerequisite properties), processing (milling, granulation, drying, compaction, variations in cooling/ heating rates, seeding during the crystallization, that affect phase transition), performance (improved bioavailability due to altered solubility and dissolution profile, enhanced shelf-life as consequence of increased thermodynamic and kinetic stability), regulatory aspects (extending the process of the market authorization by substituting the solid form formulated in branded pharmaceutical product with the new crystalline form of the same composition) and intellectual right issue (patenting the new crystalline form) (Schultheiss & Newman, 2009; Morissette et al., 2004*) .

The emerging interest for research in solid state of pharmaceuticals is a consequence to the intention pharmaceutical industry to synthetize and isolate APIs and excipients in solid forms, higher demand for more than 80% of drugs as solid dosage forms to be available for oral administration in therapy, in spite of the fact that about 40% of them have low solubility that additionally cause 80-90% of drugs to be discarded from the R&D pipeline as a risk for proceeding in development drug delivery formulations and their clinical testing (Thayer, 2010).

Crystal engineering

Crystal engineering particularly addresses the molecular recognition phenomena in crystalline organic solids that are characterized by the regular extended in long-range and short-range highly ordered structures (Desiraju, 2013) in the crystal state, which is thermodynamically and kinetically the most stable condense phase of the matter (Goshe, 2002).

Braga *et al.* (2002) explained the crystal engineering as a concept that encompasses modeling, design, synthesis and application of crystalline solids with predefined and desired aggregation of molecules and ions. Its aim is to control the arrangement of the constitutive parts (neutral and polarizable molecules or ions), and thus to attain the final goal that is related to obtaining functional solids in crystalline state.

The major driving force to interplay molecules or ions are noncovalent bonds *e.g.* intermolecular interactions: hydrogen bonding (Gilli et al., 2007, 2010) and metal-ligand coordination (Sun *et al.*, 2002), as well as $\pi\cdots\pi$ stacking (Adams *et al.*, 2001), hydrophobic, ionic, and van der Waals forces (Mueller-Dethlefs *et al.*, 2000), and halogen bond (Metrangolo & Resnati, 2001; Auffinger *et al.*, 2004) .

Crystal engineering, well-known as "making crystals by design", refers to two-steps "bottom-up" approach where, firstly by devising synthetic routes of the covalent chemistry in solution, molecules or ions (building blocks) are modulated and characterized in order their physicochemical properties and intermolecular bonding capacity to be convoluted to the periodical distribution and symmetry of the supramolecular assembled building blocks which, secondly are spatially ranged into crystalline solids with desired properties (Braga *et al.* 2002). Molecular recognition between the functional groups encompassed in the structures of the "building blocks" with the well-defined molecular symmetries determines and controls the preference for their packing pattern into supramolecular lattice architecture with network topologies which crystallographic metrics (*e.g.* bond distances,

contact angles), through their systematic adjustment, tune the crystals functional properties allowing the design of functional materials (Nangia, 2010).

Crystal engineering explains the process of designing crystals at a molecular level that utilizes the tools of supramolecular chemistry to control solid-state properties. Thus, the scope of supramolecular chemistry that focuses on the intermolecular bonds and mutual recognitions in solution, firstly was explained by the 1987 Nobel Prize Laureate in Chemistry, Jean-Marie Lehn (1988) as a "chemistry beyond the molecules", and latter Desiraju (1989) applied it for defining the crystal engineering as: *"Understanding of intermolecular interactions in the context of crystal packing and in the utilization of such understanding in the design of new solid with desired physical and chemical properties"*

In the process of crystallization of organic solids, Desiraju (1995) indicated that the molecules or ions are assembled in crystal lattice through robust patterns of intermolecular interactions known as "synthons" that is kinetically defined structural units which by repeating regularly and extend spatially result in the growth of the crystalline phase. Hence, synthons, depending on the nature of the interactions between functional groups and their allocation in the molecules or ions, convey the essential feature of the molecular structure to crystal structure, thus playing role in approximation of the whole supramolecular crystal structure defined by Lehn (1990) as *"organized entity of higher complexity held together by intermolecular forces"*. This means that by manipulation with supramolecular chemistry tools in process of engineering crystals the focus put on generating collective properties of the assembled crystalline supramolecular structures and understanding the relationship between such collective properties and those of the individual constituents (molecules or ions).

Even though crystal engineering has become an emerging technology for designing molecular crystals, difficulties regarding the prediction of the crystal structure are caused by inability to control the multiplicity of possible orientations of the molecules in crystals, inaccuracies in estimating energies, and contribution of the variable interplay of the kinetic and the thermodynamical factors in process of nucleation and crystal growth.

The critical challenge in crystal engineering is that it is not easy to predict the crystal structure from just a few, for intermolecular interactions, favorable functional groups as a part of molecular structure wherein their behavior during the crystallization is influenced by their nature and positions of all other functional groups. Allan et al 1997 reported that hydrocarbon aromatic moiety as a part of 3-aminophenol acts as functional group for generating supramolecular synthons N—H···π which compete much more effectively with expected N—H···O synthon found both in 3-aminophenol and 4-aminophenol.

Though, since last decades the studying on the mechanisms for crystal nucleation and growth have been advanced (Braga *et al*., 1994; *Hulliger* 1994, *Perlstein et a.* 1994, Carter *et al.* 1994*)*, the ability to predict the organic crystal structure based on molecular structure, controlling the intermolecular forces that determine molecular packing patterns remain challenging, especially in designing the crystals that exhibit nonlinear optical properties (Gryl et al., 2015), ferromagnetic behavior (*Wriedt et al., 2013*), electrical conductivity (Huang et al., 2014) or solid-state reactivity (Atkinson et Al., 2011).

Beside the skepticism of the Maddox's (1988) statement "…general impossible to predict the structure of even the simplest crystalline solids from the knowledge of their chemical composition", and previous incentive by that Feynman (1960) stirred up the scientific community asking "*What would the properties of the materials be if we could really arrange the atoms the way we want them*", Schmidt (1971) in his research based on topochemical principles for minimum molecular movement in solid-state, correlated the structures obtained by solid-state reactivity of photodimerizable *trans*-cinnamic acid, and for first time coined the term crystal engineering. Referring to photochemical reactivity, Schmidt 1971 explained that the concept of crystal engineering enlightens that the properties and molecular recognition of the individual molecules determine their distribution within the crystal lattices, as a consequence to which crystalline solids exhibit distinct physical and chemical properties compared to native molecules. In last two decades crystal engineering emerged mainly in two directions; organo-metalic chemistry of polymers known as metal-organic frameworks, MOFs (Janiak, 2003; Cahill et al., 2007) and cocrystals, CCs (Desiraju, 2013).

The implications of crystal engineering extend far beyond organic and organometallic crystal design into supramolecular materials, nanotechnology, ligand-protein binding and crystal structure prediction (Nangia, 2010).

Despite many attempts for a comprehensive crystal structure prediction that remain elusive (Dunitz, 2003; Dunitz & Gavazzotti, 2005), since recently rapid advances are evident as a result of development of the computational methods (Price, 2004) and application of empirical strategies for convergent and divergent syntheses (Dubey et al., 2014) and crystal growth characterized by the state-of art instrumental techniques (Vogt et al., 2009, He et al., 2008).

Moreover Moulton & Zaworotko (2001) indicated to the inability of the precise control of the positions of the atoms in crystals, among non-covalent bonds, the hydrogen-bonding interactions between complementary functional groups of the molecules form robust one-dimensional (1D), two-dimensional (2D) or three-dimensional (3D) hydrogen-bonded

networks that control the degree of freedom for effective crystal packing in process of crystallization.

Whether the crystals will crystallize in single- or multicomponent crystals is enhanced, not only by the nature of the molecular constituents, but rather on the hierarchy fashion of the hydrogen bonds formation between potentially complementary functional groups (Bis et al., 2007, Kavuru et al., 2010; Shattock et al., 2008).

Molecular recognition in PCCs

Exploiting supramolecular synthons is a practical concept with aim to perceive and understand the design of PCCs. Properties of intermolecular interactions are appreciated in specific molecular recognition as an outcome of which specific synthons are formed. Process of molecular recognition is facilitated by balance of chemical and geometrical recognitions and it is hard to foresee which one might dominate in unknown crystal structure. The former is due to coupling of molecules or atoms in hierarchy fashion through strong, highly directional, specific and kinetically favored intermolecular interactions (Steiner, 2002). The latter considers Kitaigorodsky principle of close-packing based on molecular shape and size that leads to most stable structure (Kitaigorodsky, 1955). The concept of synthon is a qualitative and probabilistic descriptor that relies rather more on chemical nature of involved molecules then on topological or geometrical parameters. In the process of deriving a molecular structure based on crystallographic parameters, the strength of H-bonds in the structure of crystal impacts the topology and chemical nature of the synthons. This is retrosynthetic approach for designing crystal form the resolved structure of molecules which under the specific condition for crystallization forms network of crystal structure (Braga, 2004).

In general, two basic types of molecular recognition that drive the formation of molecular crystals (e.g. polymorphs, solvates and CCs) are classified by complementarity for intermolecular interactions of the functional groups encountered in the molecular structure. The self-complementary of the same by nature functional groups impacts the formation of the homosynthons, while the complementarity of the different functional groups is responsible for heterosyntons (Nangia, 2010). The **Scheme 1.3** represents the carboxylic acid and amide moieties capable for formation of homodimers *via* a two-point donor-acceptor molecular recognition path (Almarsson, & Zaworotko, 2004). Two primary patterns of the self-assembled carboxylic acid are dimer and catemer supramolecular homosynthons. This 'supramolecular isomerism" caused by diversity of hydrogen-bonding motifs involving carboxylic acid moieties is responsible for polymorphism that Kanters et

al. 1976 reported for two polymorphs of chloroacetic acid, one of which built-up by dimer motif (see **Scheme 1.3**), and another one composed by catemer supramolecular synthon that forms tetrameric supramolecular assembly. Apart of isomerism in dimer/catemer supramolecular homosynthons that causes polymorphism in carboxylic acids such as hydroxybenzoic acid (Gridunova, 1982), the oxalic acid (Derrisen & Smith, 1974), and the tetrolic acid (Benghiat & Leiserowiz, 1972), differences in packing arrangements of dimer motifs due to torsional flexibility of the molecular structures influence conformational polymorphism (Nangia, 2008, Bernstein & Hagler, 1978).

a   b

a. supramolecular homosynthons as
    exhibited by acid–acid and amide–amide dimers;
b. supramolecular heterosynthons as exhibited by acid–amide dimers.

Homosynthon   Heterosynthons

a   b

The self-organization modes seen in the two reported polymorphs of chloroacetic acid:
a. centrosymmetric dimer;
b. catemer motif, which leads to a tetrameric assembly
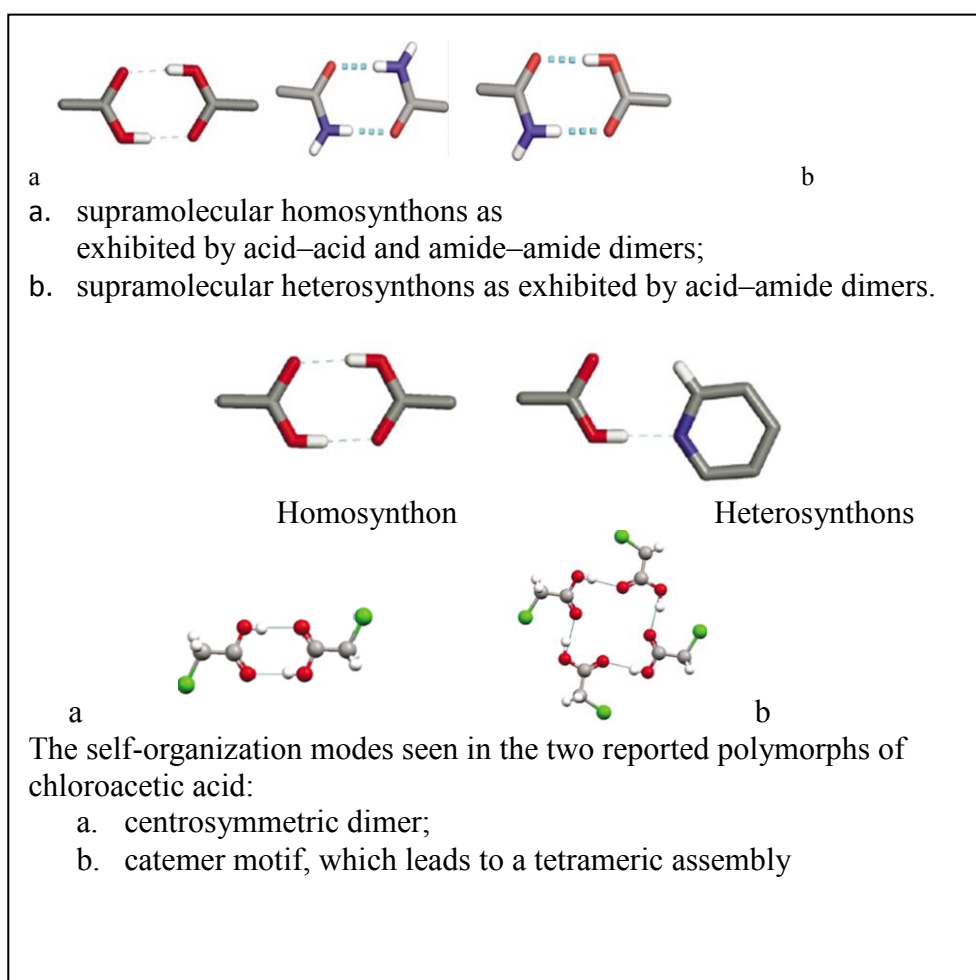
Scheme 1.3. Homosynthons and Heterosynthons

Statistical analyses performed by Allen (2002), and that relates to hydrogen-bond motifs of 4000 entries in the CSD of crystal structures in which at least one carboxylic acid moiety is present, revealed that supramolecular homosynthons (29.4% of dimer and 2.1% catemer motifs) are not dominant in solid state in comparison to heterosynthons recorded in the remaining crystal structures with carboxylic acid. However, among analyzed compounds

that include both carboxylic acid and aromatic nitrogen base that are deposited in CSD, 46.7% of them exhibit heterosynthon motifs mainly of pyridine-carboxylic acid type. Analogously to carboxylic acid moiety, both analyses in the CSD and reported results for chloracetamide and nootropic drug piracetam (2-oxo-1-pyrrolidinylacetamide), indicate that complementary hydrogen-bon donors and acceptors in the primary amides interplay one to another leading to formation of supramolecular homosynthon i.e. dimer that further impacts formation of supramolecular tapes or sheet structures. In case of chloroacetamide and piracetam, polymorphic forms that these compounds exhibit are result to isomerism of supramolecular carboxamide synthon that exist as catamer motifs (one polymorphic form of chlorocarboxamide 1-D tape structure, and one of three polymorphic forms of piracetam forming catamer chain structures based on cross-linked carboxamide homodimers) and homodimer (another polymorph of chlorcarboxamide with 1-D tape structure and two of three polymorphs of piracetam that form tape structures). In addition, analyses of structures with both included carboxylic acid and amide moieties which are deposited in CSD put in evidence the prevalence of acid-amide suprmolecular heterosynton. Hence, the preference and robustness of this heterosynton was confirmed in CC of anti-inflammatory drugs aspirin, and *rac*-flubiporfen with 4,4'-bipyridine, respectively (Bailey *Walsh* et al. 2003). The authors of this research reported that pyridine-carboxylic acid heterosynthon competes to carboxylic acid dimer homosynthon.

Within the family of the PCCs composed of pyrazinecarboxamide (PZA), drug for treatment of tuberculosis: PZA with 2,5-dihydroxybenzoic acid, ref. code XAQQOW (*McMahon* et al. 2005); 2-aminosalycilic acid, ref.code URUGIY (Grobenly et al. 2011); succinic and fumaric acid, respectively (Cherukuvada&Nangia, 2012); and vanilic, gallic, 1-hydroxy-2-naphtolic, and idnol-2-carboxylic acid, respectively (Adalder et al. 2012), structure determination showed that there is inconsistency in prevalence of acid-amide, aromatic NH─pyridine; hydroxyl-amide, amino-carbonyl heterosynthons, energetically more favored over the amide-amide homosynthons (mostly often with 50% probability for occurrence).

Hierarchy of hydrogen bond prevalence of the amide based N─H moiety for interaction with C=O or ─OH hydrogen-bond acceptors in heterosynthon and homosynthon interactions was tested by Aakeröy et al. (2007) on the 5 CCs and 2 salts formed by selecting CC models from the group of 4-acetaminopyridine derivatives and CFs from derivatives of dicarboxylic acids. The obtained results revealed that the primary heterosynthon for CC formation is achieved by locking the neutral H-bonding interaction O─H(acid)···N(pyr) between carboxylic acid and pyridine moiety, while charge-assisted

hydrogen-bond N─H$^+$···$\overline{}$O form the heterosynthon which favors the salts formation. The remaining N─H donor (on the amide moiety) exerts preference for interaction with carbonyl moiety (C=O) from the amide group, thus forming amide-amide homosynthon over the carbonyl C=O moiety and acidic O─H moiety, respectively, both from the carboxylic group.

Bis & Zaworotko (2005) reported the compliance of both experimental and statistical data of their research on cocrystallization of CC models from group of 2-aminopyridine derivatives with CF from the group of carboxylic acid derivatives. Their results indicate formation of rigid, two-point supramolecular heterosynthon, depicted as $R_2^2(8)$ graph set. Molecular recognition between 2-aminopyridinium and carboxylate moieties is favored by the charge-assisted H-bonding interactions (N-H$^+_{(pyr)}$···$\overline{}$O and N-H$_{(amino)}$···$\overline{}$O) observed in the ten reported structures, though the same recognition may result through the neutral H-bonding motifs.

Aakeröy et al. (2007) reported that in amide-pyridine heterosynthon, hydrogen bond acceptor strength of pyridine N is slighthly less then amide C=O moiety. Babu et al. (2007) conveyed research on utilizing oxidized pyridine amide to the corresponding pyridine N-oxide (N$^+$─$\overline{}$O) which exhibit higher basicity and anionic character, and thus behaves as stronger H-bond acceptor. The authors evaluated the utility of heterosynthon carboxamide-pyridine N-oxide that is sustained by *syn*(amide)─N···$\overline{}$O (oxide) hydrogen bond and auxiliary (N-oxide)C─H···O(amide) interaction in CCs obtained from amide-containing molecules and APIs (e.g. barbituric acid, barbital, saccharin, 4-hydroxybenzamide, and carbamazepine) with pyridine N-oxide CFs (e.g. quinoxcaline N,N-dioxide, pyridine N-oxide, picoline N-oxide, bipyridine N-oxide, etc.). The significantly different hydrogen bonding between the strongest H-bond donor CONH from amide and the strongest H-bond acceptor N$^+$─$\overline{}$O, found in the CCs, determines different physicochemical properties from those of the pure API and CF. The prevalence for formation of amide dimer is higher over the amide─N-oxide due to the competition of the OH group in CCs with 4-hydroxybenzamide, intamolecular H-bonding (e.g. in CC with picoline N-oxide) and steric factors relating to dibenzaazepine ring in CCs with carbamazepine (butterfly-shaped molecule) with pyridine N-oxide CFs (Babu et al., 2007).

Determined crystal structures of four polymorphs of anti-epileptic drug carbamazepine (Morissette et al., 2004), as well as its two solvates (acetonate and dihydrate) (Fleischman et al. 2003) indicate that presences of unsatisfied peripheral hydrogen-bond donor and acceptor pair in amide dimer of carbamazepine molecules, due to the steric (geometrical) constrains imposed by its dibenzazepine ring facilitate the formation of solvates with H-

bond acceptor solvents (e.g. DMSO, acetic, formic, butyric acid), and CCs (Vishweshwar et al., 2006) with CFs which are hydrogen-bond acceptors (e.g. benzoquinone, terephthaldehyde, 4,4'-bipyridine, and nicotinamide) and both hydrogen-bond donor and aceptor CFs (e.g. saccharin exerting hydrogen-donor effect through N—H···O hydrogen-bonds with carbonyl group from carbamazepine, while hydrogen-acceptor effect is result of through N—H···O=S (H-bond acceptor from saccharine structure).

Remenar et al. (2003) highlighted the outcome of undertaken high-throughput screening for expected and unexpected PCCs of antifungal drug itraconazole with set of dicarboxylic acids. Determined structures of obtained PCCs of *cis*-itraconazole with succinic acid and other 1,4-diacids with extended anti- conformations indicate to formation of supramolecular heterosynthons consisting of hydrogen-bonded trimers which are formed by bridging the triazole of each pair of drug molecules with one extended succinic acid molecule. Formation of this trimeric heterosynton is unexpected motif if the ΔpK_a rule for acid-base complementarity is followed (1,4-diacids with the stronger piperazine base in itraconazole structure compared to triazole moiety). Moreover, the inability of itraconazole to cocrystalize with maleic acid affected by Z-regiochemistry, 1,3- and 1,5-dicarboxylic acids proves that the structural conformation in comparison with acid-base complementarity, is favorable driving force for cocrystallization of itraconazole with 1,4-dicarboxylic acids resulting in formation of PCC which exhibits solubility and bioavailability profiles similar to that one obtained from the commercialized product Sporanox®, formulated by using amorphous itraconazole coated into the sucrose beads.

Moreover, Shattock et al. (2008) reported that the statistical analyses of heterosynthons of aromatic nitrogen bases with carboxylic acids and alcohols, respectively, in 15 entries in CSD (CCs out of which two are salts, composed of CFs which contain a permutation of carboxylic, alcohol and aromatic nitrogen base functional groups) revealed higher prevalence of the COOH···N$_{arom}$ hydrogen-bond over the O—H···N$_{arom}$ one.

Experimental work carried out by Etter and Reutzel (1991) showed that by applying the hydrogen bond selectivity criteria, it is possible to map the molecular recognition properties of a class of acyclic imides that depend on adopting the *cis-trans* and *trans-trans* conformations in their homomeric and heteromeric crystal forms with unique hydrogen bond properties. The cocrystallization process was explained as competition between homomeric and heteromeric aggregation. Imide cocrystallization patterns are predicted based on the competition of CF molecules that are proton donors (*e.g.* phenols or carboxylic acid) to the unused carbonyl group from the homomeric *cis-trans* forms (combination of independent primary amide forming dimers and a tertiary amide acting as

acceptor). In case proton donor of CF forms eight-membered ring hydrogen bonded chains (e.g. primary amides or carboxylic acids), then heterodimer type of CCs are formed. The two carbonyl groups act as bidentante ligand in *trans-trans* imides forming the CCs with metal ions form group I and II and with with strong proton acceptor such it is triphenylphosphyne oxide.

Difference of pK_a values of the acid and base, $\Delta pK_a = (pK_a)_{base} - (pK_a)_{acid}$ was proposed by Childs et al. (2007) as a rule of thumb to estimate the extent of proton transfer, and thus being indicator whether or not this lead to salt or CC formation. ΔpK_a is a descriptor that could be exerted for predicting salt formation in case it is higher than 3 (Stahly, et al. 2007), and CC formation in range of its negative values (Bhogala et al., 2005). Stahly 2007 pointed out that ΔpK_a rule is an empirical guidance for initial screening of salts or CCs because prediction for their formation is not reliable in range from 0 to 3.

Wenger & Bernstein (2006) applied statistical analyses in CSD (Allen 2002) and cocrystallization screening for anti-epileptic drug gabapentin with oxalic acid (host-guest combinations including amino and carbonyl groups) aiming, in a geometrically predictable way, to determine the probability for every combination of specific ammonium cation donors and carboxylate (COO$^-$) acceptor group to form three-center hydrogen bond which is commonly utilized is the main ring motif $R_4^2(8)$ (an eight-membered ring with four hydrogen-bond donors and two H-bond acceptors). The results showed that the high probability of charged groups (CO$^-$) to form charge-assisted three-center hydrogen bonds is due to their contribution to square charge arrangement which is utilized in $R_4^2(8)$ ring motif.

MacDonald et al. 2001 reported the modular approach for controlling molecular packing and physicochemical properties of the crystalline materials designed by using organic salts of imidazole and mono-, di- and tetracarboxylic acid derivatives as a building blocks. The authors explained that the advantage in using organic salts instead of the neutral molecules is based on simultaneous formation of two different motifs; one strong ionic (charge-assisted) $N^{(+)}-H\cdots O^{(-)}$ between imidazolium cations and carboxylate anions form carboxylic acid and O—H⋯O H-bonds between neutral moieties that are spatially modulated and tuned. 1D-chains are derived by imidazolium carboxylate salts in which the self-assembled ions form unique motif formed by the strong charge-assisted H-bond. In case dicarboxylic acids are used, exclusively generated "head-to-tail" chains of the strong O—H⋯$^-$O hydrogen bonds are formed by self-assembled monoanions which are acceptors for multiple hydrogen bonds. Imidazolium cations act as multidentate hydrogen bond

donors additionally forming three C—H···O hydrogen bonds which link anions in adjunct 2D polar imidazole carboxylate layers composed of intersecting chains.

Lemmerer et al. 2011 reported that carboxylic acid–pyridine heterosynthons was applied as scaffold in formation of PCC of anti-tuberculostatic drug isoniazid (isonicotinic acid hydrazide) with terephthalic acid 2:1. Authors reported that this heterosynthon in the structure of PCC exists in two geometric forms. One is related to co-planar conformation of the acid with pyridine ring, forming $R_2^2(7)$ ring-shaped hydrogen-bond motif (O—H···N supported by C—H···O) that generates finite triad which are linked along c-axis by extended assemblies formed by homosynthons $C(3)$ and ring-type homosynthon $R_2^2(10)$ along the a- and b-axes. Báthori et al. 2011 reported that in addition to discrete carboxylic acid-pyridine synthon (following the Etter's rule, the best donor and the best acceptor), homomeric amide-amide dimers $R_2^2(8)$ are present in the structures of the PCCs between isonocotinamide and, respectively, diclofenac and clofibric acid.

Guanidinium-carboxylate is type of robust heterosynthon that is reported by Nanuubolu et al. (2013) from their research on polymorphic forms of metformin embobnate salts. This synthon, closely resembled in hydrogen-bonding motif of urea-carboxylate, is beneficial over the previous one due to additional electrostatic attractions, and high protonation of the guanide moiety as result of resonance stabilization that lead to charge-assisted hydrogen bond interaction between guanidinium and carboxylate moieties.

Seaton et al (2013) reported that in acid/acid type of CCs formed by the derivatives of benzoic acid the magnitude of acidic proton (hydrogen atom) is proportional to Hammett constants used to describe the electron withdrawing ability of the substituents in structures of benzoic acid. Results indicate that the higher the difference of Hammett constant, the higher the probability two benzoic acid derivatives to form CCs.

Childs *et al.* 2009 analyzed similarity relationships of crystal packing motifs in 50 crystal structures of carbamazepine aiming to propose a semiquantitative predictive model as qualitative guidelines for the rational design of PCCs. The applied molecular descriptors implied to similarities based on the shape and polarity of the carbamazepine and cofomers and preference of carboxamide-carboxylic acid heterodimeric synthons favor CC formation.

Shattock *et al.* 2008 in their statistical analyses of the hierarchy of supramolecular heterosynthons in the context of APIs, carboxylic acids and alcohols, reported that heterosynthons between aromatic nitrogen (N) compounds and carboxylic acid and alcohols, respectively: COOH/OH···N$_{aroma}$ in the absence of other hydrogen bond donors and acceptors showed hierarchical prevalence over the corresponding supramolecular

homosynthons in carboxylic acid COOH···COOH and alcohol OH···OH dimers. However, when competing hydrogen bond moieties such COOH, OH and N_{aroma} are included in the same crystal structure, there is a lack of statistical evidence of predictability of the supramolecular heterosynthons.

MacDonald & Whitesides (1994) reported that by incorporating a variety of functional groups into majority of the derivatives with planar or nearly planar molecular structures from the identified three classes of diamides (cyclic ureas, cyclic diacylhydrazides and diketopiperazines), in process of crystallization there is a preference molecules to be packed and crystallized in rigid linear structures with tape motif due to the following structural features that influence functional properties of the crystals to be predicted: (i) equal number of donor and acceptor sites, (ii) rigidity of the diamide ring, (iii) size of diamide ring, (iv) steric bulk of substituents, (v) proximity of the configuration of donors and acceptors and (vi) competing hydrogen-bonding groups.

The computational methodology that Issa *et al.* 2009 proposed was based on the comparison of the lattice low-energies of 12 PCCs of 4-aminobenzoic acid, 8 PCCs of succinic acid and 6 PCCs of caffeine, with the sums of the lattice low-energies of their components. The minimization of the lattice energy, computed using the anisotropic intermolecular atom-atom potentials, with the electrostatic model and the intramolecular energy penalty for changes in specified torsion angles derived from ab initio calculations on the isolated molecules indicate that many of the CCs of these three CC formers are more stable than the sum of the lattice energies of their component structures. But, due to sufficiently small margin of this energy difference, comparing to the relative polymorphic energy differences and errors of computational model, the accurate prediction of the CC formation depends on approximations for accuracy of the chosen model for computing the CC energy landscape that determine the relative thermodynamic stability of the most stable CC structure. The thermodynamic stability is the driving force for CC formation; higher stability of CC then the crystals of its components implies to CC formation prevalence.

Role of Hydrogen bonds in designing multicomponent crystals

Systematical study on the nature of hydrogen bonds and intermolecular interactions driven by H-bonding is an essential and prerequisite factor for assessment of recognizable motifs of molecules (synthons) in solution and possible prediction of structural architecture of the CCs in solid state. The role of the proton transfer (PT) in the Brønsted-based H-Bond Theory, comprehensively elaborated by Gilli & Gilli 2007; 2010 as a Dual H-bond Model, aligned to charge-transfer ascribed in the alternative interpretation of the Lewis-based H-

bond Theory, put the focus to the prediction of H-bond energies and geometries and to unification of H-bonds in account to intermolecular interactions responsible for designing of the molecular crystals.

The Dual H-bond model refers to a bimolecular proton-transfer (PT) reaction pathway wherein the same proton is shared between two adjacent acceptors (—D: and :A), each carrying an electron pair and participating in competing bond with the central proton. Depending on the H-bond strength, the PT pathway in process of H-bond formation passes through one minimum or two minima in the reaction coordinate, thus depicting the three different profiles of PT reaction pathway described in **Table 1.3**.

The overall H-bond energy, E_{HB}, is the smaller of the two bond-dissociation energies, $D_0(D—H)$ and $D_0(H—A)$, by which —D: and :A are competitively bonded to the proton. The H-bond properties are function of the linear combinations of two variables, sum and difference of proton affinity (*pa*), that relate to mean donor/acceptor electronegativity and energy difference between tautomeric $D—H\cdots:A$ and $^-D\cdots:H—A^+$. On the base of thermodynamic data, Gilli et al. (2000; 1994; 1996; 2009) indicated that strong H-bonds can be classified in the following four chemical classes (the Chemical Leitmotifs) depending on specific chemical condition when $\Delta D_0 = \Delta pa = \Delta PA$ (gas phase) $= \Delta pK_a$ (condensed phase e.g. water) ≈ 0:

i.   (±)CAHB – double charge-assisted H-bonds: $(D—H\cdots:A)$ formed by acid and base with close donor-acceptor pK_a matching;

ii.   (—)CAHB – negative charge-assisted H-bonds: $[D\cdots H\cdots D]^-$ formed by two acids having lost one proton (identical pK_a)

iii. (+)CAHB – positive charge-assisted H-bonds: $[A:\cdots H\cdots:A]^+$ formed by two bases having gained one proton (identical pK_a)

iv.   RAHB – resonance-assisted H-bonds: $(D—H\cdots:A)$ formed by acidic donor and basic acceptor connected by a short π-conjugated and delocalized fragment which affects pK_a value;

All four Chemical Leitmotifs of strong H-bond fulfill the condition of PA/pK_a Equalization (Gilli et al., 2009; Gilli & Gilli, 2009).

Moreover,

v.   Ordinary H-bonds, encompassing all H-bonds that are neither charge- nor resonance-assisted, are week, dissymmetric, and mostly electrostatic in nature.

The H-bond strengths of any specific H-bond electronegativity class of the couple of donor D—H (e.g A—H acids) and acceptor :A (e.g. B bases) with fixed sum of proton affinities depend on the D—H /:A proton affinity difference $\Delta PA = PA(D^-) - PA(:A)$ (in gas phase) which is in relationship with $\Delta pK_a = pK_{AH}$ (D—H) $- pK_{BH+}(A—H^+)$ (in water). The estimation of the H-bond strength by PA/pK_a Equalization Method is possible by using the pK_a Slide Rule, which is a graphical tool for predicting H-bond strengths from the ΔpK_a differences: $\Delta pK_a = pK_{AH}(donor) - pK_{BH+}(acceptor)$.

Bertolasi et al. 2011 applied the pK_a-Equalization Method for estimating relationship of ΔpK_a, H-bond energy (E_{HB}) and H-bond distances ($d'_{D\cdots A}$, accounting for D—H—A angle changes) in 14 adducts formed by picric acid with aromatic N-bases and reported that short and high energy H-bonds are present in adducts where ΔpK_a is not far from zero and H-bond energies (E_{HB}) exponentially depend on the lengths of the H-bonds.

Table 1.3 H-bonds strengths as a function of PT reaction pathways

Possible Profiles of PT in reaction pathway	Strength of H-bonds	Properties of H-bonds
One assessable asymmetric single well (*a*SW)	High-barrier (HB) H-bonds	Weak, long, dissymmetric, ordered both in solution and in crystals, essentially electrostatic: D—H⋯:A
Two symmetric or slightly asymmetric double well (*s*DW, *sa*DW)	Low-barrier H-bonds (LBHB)	Strong, short, and tautomeric exchanged in solution and dynamic disordered in crystals, partly covalent (three-center-four-electron interactions)
Two symmetric or slightly asymmetric double well (*s*DW, *sa*DW)	Medium-barrier H bonds (MBHB)	Moderate strength, tautomeric exchange in solution and static disorder in crystals, partially covalent bonds
One symmetric single well (*s*SW)	No-barrier H bonds	Very strong and short, symmetric and linear, ordered both in solution and crystals, essentially covalent (three-center-four-electron interactions): D⋯H⋯A

Bertolasi et al 2011; 2012 proposed the "electron pair saturation rule" for rationalizing the crystal packing of three type of CCs: picric acid with planar N-bases, TCNQ with planar N-bases, and TCNQ with azo dyes (Gilli et al. 2013). According to the Lewis-based H-bond Theory, all electron donors - the Lewis base :A (n = neutral lone pair donors; n^- = negatively charged lone pair donors, σ = neutral donors of σ-bonding pairs; π = neutral donors of π-bonding pairs) have a propensity to be engaged in electron donor-acceptor (EDA) interactions with all available electron acceptors - the Lewis acid D—H (σ^* =

neutral acceptors with vacant σ* molecular orbital (MO); π* = neutral acceptors with vacant π* MO; π*(k) = neutral acceptors with vacant π* MO of ketonic type). The electron-pair saturation rule can be formulated as "all the electron donors of a closed-shell molecule, either nonbonding pairs of lone pairs or π-bonding pairs of multiple bonds, will display a definite tendency to become engaged in EDA interactions with all electron acceptors present as far as these are available; if acceptors are insufficient to saturate all donors, the latter will be saturated in order of decreasing EDA interaction strength". This saturation process of the maximum number of n donors by all available acceptors by means of charge-transfer (CT) or (EDA) interactions appear to be the main driving force in the formation of all molecular crystals.

The results of the three studied CT or EDA CCs indicate that in CCs with picric acid dominate H-bonds which, described according to the Lewis Theory, are a σ*←n EDA interactions (D─H←:A) that lead to packing geometry of planes or ribbons of planar molecules, while moderate π*←π potentiality causes parallel stacked packing (Bertolasi et al. 2011). In contrast, CCs of TCNQ exhibit moderate H-bonds and increased π*← π potentiality (Gilli et al. 2012), while in CCs with azo-dyes the H-bonds are absent, while the crystal packing has been dominated by π*← π interactions (Gilli et al. 2013). As an outcome of this research, CT or EDA interactions contribute to change our views on interacting molecules in molecular recognition processes, from spheroidal bodies attracting in a continuous molecular field, to similar objects interacting only by few scattered and complementary docking points.

In order to describe and label hydrogen bonds and topological analysis of the motifs in hydrogen-bonded molecular solids, Etter et al. (1990) for the first time proposed the graph-set notation $G_d^a(n)$ based on the following four descriptors: G (chains - C, dimers - D, rings - R, and intramolecular hydrogen bonds - S) where n is the number of atoms, a the number of hydrogen bond acceptors, and d the number of hydrogen-bond donors. This graph-set notation in combination with "hydrogen bond rules" is based on estimation the prevalence for H-bond donors and H-bond acceptors interaction. To enable the design of hydrogen bonded CCs of pyridine and benzenpolycarboxylic acid, Dale et al. (2004) revealed guidelines for criteria for hydrogen-bonding that refer to (*i*) all best proton donors and acceptors are engaged in hydrogen-bonding, (*ii*) prevalence six-membered rings to form intramolecular, rather than intermolecular hydrogen bonds; and (*iii*), once intramolecular hydrogen bond is established, the best proton donors and acceptors remaining available for intermolecular hydrogen bonding.

Significance of molecular CCs of pharmaceutical interest

For last twenty years in academic and industrial communities, the research in PCCs has been emerging due to the fact that, through the noncovalent modification of the crystalline phases without changing the molecular structure of the APIs themselves, selected without particular restriction of the magnitude of the their polarity (from neutral up to ionizable) and cocrystallized in the unit cell of the PCC together with appropriate CFs, selected from compounds that extended the traditional counterions for salt selections, the physical properties of solid APIs are controlled (Datta & Grant, 2004; Morisette *et al.*, 2004).

Wide range of the definitions and accuracy for the nomenclature of the CCs have been resulted by different approaches of the scientists who invented the names based on the composition of resolved CC structure and properties of the components within the CC. Moreover Bond (2007) proposed the definition of a CC as a multicomponent molecular crystal that has scientific prove, and the subclass of PCCs for first time was coined by Vishweshwar & Zaworotko (2006), emphasizing that one CC component is an API in molecular or ionic form and another one, CF, is a solid substance under the ambient condition. The term CC is used to denote togetherness of two or more molecular components, each of which must be solid at ambient temperature and unnecessarily to retain any degree of its individual crystalline identity within the CC. Following the concept of togetherness, Dunitz 2003 defined CCs a subset of multicomponent crystals that "*encompasses molecular compounds, molecular complexes, solvates, inclusion compounds, channel compounds, clathrates and possibly a few types of multi-component crystals*". However, aligning to this standpoint and emphasizing the formation of CCs as unique crystalline phases, Stahly (2007) proposed the following definition: "*co-crystals consist of two or more components that form unique crystalline structure having unique properties*". The attraction for PCCs evolved from the variety of crystal forms of API which exhibit alteration of physicochemical properties of clinical relevance comparing to the properties of the native API.

Moreover the term PCCs is scientifically ambiguous for being distinguished among other multicomponent crystals, it is seemingly that its nomenclature is overwhelmed by the legal concerns. Hence, the PCCs meet the following criteria of regulatory affairs: patentability (*e.g.* new and unique crystalline phase), namely novelty (*e.g.* new composition of API-CF), non-obviousness (selection of CF based on synthon theory in the strategy for PCCs design is unlikely as criteria for counter ions identification for salt formation) and utility (benefits of altered properties that impact the performance and functionality).

Hence, so far, the PCCs are only recognized by the US FDA within the final guidance that was issued in April 2013. According to this guidance, the PCCs are determined as drug product intermediate of the dissociable "API-excipient" molecular complexes wherein the same API molecules interact with the crystal lattice of the molecules of CFs defined as excipients. This means that, comparing to novel salts of an API which are regulated by the FDA as NCEs, and thus undergo to entire testing of their properties, PCCs are analogues to API-excipent physical mixtures or complexes (e.g. such are inclusion compounds of drugs with cyclodextrins) and are considered not to be new drugs, consequently allowing them to be eligible for approval under an ANDA procedure.

This definition allows to generic pharmaceutical companies to meet IPR requirements for issuing patents for PCCs as competitive products that are still considered to be the same API as the original one. Hence, PCCs cannot circumvent the patent for the original API. Therefore, use of PCCs can delay or divert generic competition during the product lifecycle management extending the market authorization and exclusivity of the pharmaceutical products formulated with PCCs.

In addition, this FDA's definition compulsorily requires PCC must provide assurance that complete dissociation of the API occurs prior to reaching the site of absorption or receptor for obtaining pharmacological response.

In order to contribute the draft version of US FDA guidance for regulatory classification of PCCs released in 2011, upon the growing number of patent applications in the field of APIs CCs, the expert group in solid state chemistry in the published report (Aitipamula *et al*. 2012) has voiced concerns regarding ambiguous classification of many of the multicomponent crystals by the three mutually exclusive classes of the pharmaceutical solids: pharmaceutical salts (PSs), and polymorphs. Therefore, Aitipamula *et al*. 2012 underlined the following reasons why some of PCCs, PSs, and their solvates/ hydrates and polymorphs overlap with one another (**Figure 1.4**), and thus, due to their diversity in nature (*e.g.* ionic CCs *i.e.* CCs of salts, zwitterionic CCs) why it is not possible to distinguish PCCs form PSs and why they proposed PCCs should naturally be grouped together with salt forms:

Proton transfer (position, location) in salt-CC continuum.
PCCs and PSs have been envisaged as two extremes of a continuum of multicomponent solids ranging from fully charge delocalized, and nonionized molecular species (neutral PCCs) to fully charge separated, and ionized species (PSs). For some cases of acidic and basic molecules that cocrystallize, despite the crystalline environment of each of the

components and the magnitude of the differences in their strengths for dissociation (ΔpKa), in a particular range of ΔpKa it is not always possible to distinguish the extent of proton transfer, and thus whether the formed solid is a PS or a PCC. This occurs because either the proton is shared or the structure contains equilibrated mixture of disordered ionized and non-ionized states in the salt-CC continuum (Childs *et al.* 2007). This is the intermediate state of variable degree of ionized and neutral traits for components into ionic CCs (e.g. fluoxetine cation and chloride anion from fluoxetine hydrochloride salt cocrystallized with neutral molecules of carboxylic acids (Childs *et al.* 2004), alkali and alkaline earth metal halides cocrystallized with barbituric acid (Braga et al., 2010, 2011, 2012), and ionized fluconazole cocrystallized with one molecule neutral and one ionized maleic acid in 1:2 molar ratio (Kastelic et al., 2010).
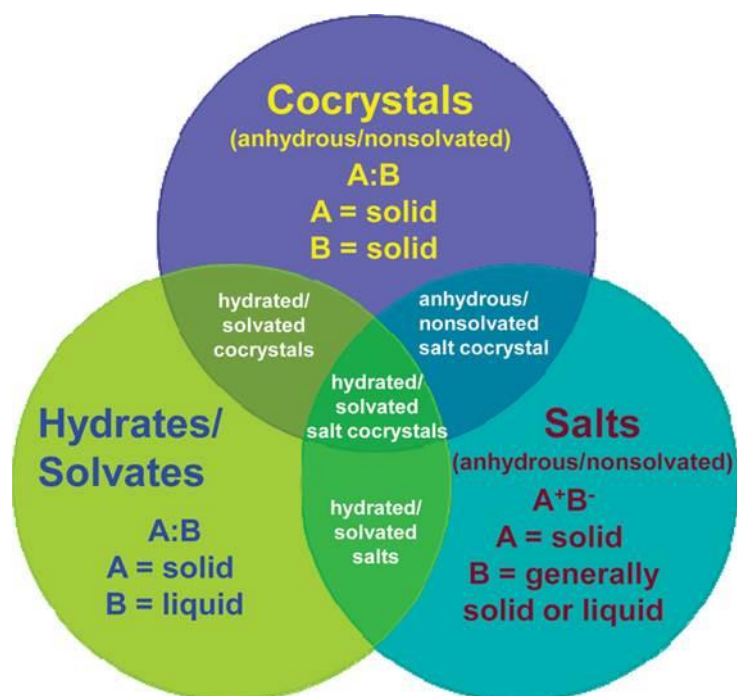
Figure 1.4. Salt – Cocrystal continuum

(with permission of Aitipamula, S. , *Cryst. Growth Des*. 2012, *12*)

While the long-range Coulombic interactions between charged pairs that form ionic crystals differently affect their properties (e.g. aqueous solubility and stability) comparing to their neutral counterparts which, connected by H-bonds, could at least partially control the structural traits, it is expected that in continuum of particular range of ΔpK_a, mixture of the ionized structures formed by anisotropic, non-directional ionic interactions, and structures formed by neutral molecules that interplay through directional hydrogen bonding

interactions exert combined and very often unpredictable properties leading to a behavior that is neither strictly typical of purely PS crystals or purely neutral PCCs, nor easily described as intermediate states. The structure determination by neutron diffraction of the urea/ phosphoric acid 1:1 salt (Wilson, 2001), revealed that increase temperature is a crucial factor for PT (shifting of the average hydrogen position) from structures with ionic character (in range of low temperatures) to neutral CC (in range of high temperatures) (Li et al., 2006; Steiner et al., 2001).   Differences in bond lengths, ΔD_{C-O}, for two values of the symmetric carboxylate anion and dissymmetric and neutral (protonated) carboxylic group measured in single crystals of 2-aminopyrimidine with CFs from series of carboxylic acids (Aakeröy $et\ al.$, 1994) are in correlation with ΔpK_a and determine the degree of PT. A small value for D_{C-O} (carboxylate anion) and high value of ΔpK_a lead to salt formation while large D_{C-O} values (neutral carboxylic group or protonated carboxylate group) for negative ΔpK_a influence CC formation. Based on the experimental crystallographic and spectroscopic data for determination of the hydrogen atom position along a single hydrogen bond, Childs e$t\ al.$ 2007 highlighted that change in polarity that accompanies the inclusion or exclusion of water (hydrate formation) and the subsequent change in crystal structure environment are responsible for the different ionization states of the multiple solids of the complexes of amphiprotic drug theophylline (both proton donor and acceptor) with acids and amine bases. Apart of the determined PCCs for complexes of theophylline with acids, 5-sulfosalicylic acid and hydrochloric acid, the structure refinement of its hydrated complex with ethylendiamine (2:1:1 theophylline : ethylendiamine : water), commercially well known as an aminophylline, indicates to ionized interactions between two theophylline molecules and halves of the two ethylenamine molecules, along with one water molecule packed in asymmetric unit cells since the proton has been transferred to the nitrogen base of the etilendiamine molecule. Beside of aminophylline hydrate salt, aminophylline anhydrous crystal is composed of equilibrated solid-state wherein 75% of the components are ionized and 25% non-ionized, the latter which, in addition, is equally shared between two different states. This mixture of ionized and non-ionized state causes that it is not possible classification of anhydrous aminophylline to be assigned either to PS, or PCC class.

Defined stoichiometry

Both PSs and PCCs are formed without of stoichiometric restriction for content of the CC model compound and CF (e.g. pyridine and formic acid in 1:1 molar ratio form neutral CC via O─H···N hydrogen bond and salt in 1:4 ratio where pyridinium cation and formate

anion are bound with three formic acid molecules (Wiechert et al., 1999); pyridine and 3,5-dinitrobenzoic acid form CC in 1:2 molar ratio an salt monohydrate in 1:1:1 (Arora et al., 2005) and 2,3-lutidine and fumaric acid form CC in 2:1 and salt in 1:2 (Haynes et al., 2006)). Based on the complementarity interaction in a O─H···N hydrogen bond, Aakeröy et al. 2007 demonstrated the preference for CC formation in "expected stoichiometry" of 1:1 and 1:2 established between monocarboxylic acid and N-heterocyclic compounds with difference in basicity (pyrazole and benzimidalozle, pyridine, pyrimidine compounds) and 2:1 stoichiometry in CCs of neutral dicarboxylic acid which is less demanded for forming two symmetry-related O─H···N H-bonds with more competitive H-bond donor site such as benzimidazol derivative, more basic than pyrazole. Charge-assisted O^-···$H─N^+$ interaction lead to salt formation and solvated forms with unexpected stoichiometries.

Solubility

The changing of equilibrated solubility and dissolution rate of API has impact on the extent of its absorption that directly affects its bioavailability (Dokoumetzidis, & Macheras, 2006). Alteration of the API solubility from PCC causes reversible transformation into parent API which by nature can be free base or acid (Rodrigues-Hornado et al., 2005, Stanton et al, 2011). When the solubility of the PCC exceed the solubility of the API (maximum measurable concentration of soluble API in saturated solution), and both CF and API are completely dissociable in solution, thus the solubilizing effect is absent, and dissolution rate enhances the API concentration beyond the value of its equilibrated solubility. As a consequence of this supersaturated state of API in solution, precipitation of the API that is in equilibrium with solid PCC as thermodynamically more stable crystal form at the normal atmospheric conditions is very likely to be occurred in vitro. In case PCC or API form hydrates, Qu et al., 2006 demonstrated that carbamazepine exerts dihydrate-anhydrate phase boundary at water activity of approximately 0.64 and 25°C, and it precipitates in hydrate form (Rodrigues-Hornado et al., 2005).

Like common counter-ion effect that occurs in PSs, multiple ionization of API and CF in solution of the PCCs may exhibit common-component effect, self-association and complexation. This behavior in solution is determined by solubility product K_{sp} (defined as a product of API and CF solution concentrations calculated from the slope of a line yielded from the plot of API concentrations in equilibrium with PCC as a function of reciprocal CF concentrations, Nehm et. al. 2006) and a pH_{max} that determines the thermodynamic stability region of the CC (Nehm et al., 2006). K_{sp} is a constant that describes the strength of CC solid-state interactions of API and CF in relation to their interactions with the

solvent. The value of K_{sp} for CC reflects association of the high CF concentration with low degree of the API in solution.

pH-solubility relationship of free acid/base and the salt form determines the type of the formed salt, dissociation into acid/base forms, common ion effect and dissolution patterns in physiologically relevant pH conditions. At pH_{max} both the free base and the salt can co-exist as solids. Phase conversion of base to its crystalline salts is occurred in supersaturated solution of base at pH that decreases below pH_{max} by addition in excess of the acid, and in reverse mode for conversion of a salt to the free base (Serajuddin, 2007). The solubility of PCCs composed by neutral molecules of APIs and CFs might be pH dependent in range of pH wherein the APIs and CFs are partially ionized. Apparent solubility product pK_{sp} for salts in presence of common ion determines an extent of the salt solubility (higher solubility and higher pK_{sp} have less impact to common ion effect, and vice versa). Similar to salts, and unless PCC does not dissociate into API and CF in solution, in presence of high complexation in solution the drug is highly solubilized with the higher concentration of CF (Good & Rodríguez-Hornedo, 2009; Jayasankar et al., 2009; Nicoli et al., 2008), the high value for pK_{sp} of PCC requires high concentration of CF (in excess of its molar ratio in PCC) in order to increase the PCC solubility equivalent to solubility of the API (Nehm et al. 2006).

Good & Rodríguez-Hornedo, 2009 proposed a method for predicting solubility and thermodynamic stability of the PCCs using the experimental measurements of the solubility of the PCC of carbamazepine (low water soluble drug model) in pure solvent wherein solid phases of the PCC (either stable or metastable) and its components (carbamazepine and CF) coexist in equilibrium with solution. Determined solubility of carbamazepine PCC in equilibrium condition corresponds to transition concentration (C_{tr}) known as eutectic point that determine the thermodynamic stability of carbamazepine PCC relative to its components (Rodríguez-Hornedo et al., 2006; Klussmann et al. 2008; Childs et al., 2008; Chiarella et al. 2007). Calculated values for pK_{sp} of carbamazepine PCC using the measured concentrations at C_{tr} indicate that solubility of carbamazepine PCC is directly proportional to the solubility of the CC components, C_{tr} for CF increases with the solubility of CF and carbamazepine PCC, respectively, and 10-fold increased CF solubility then solubility of carbamazepine influences increased solubility of carbamazepine PCC compared to the solubility of the native carbamazepine. In this study Good & Rodríguez-Hornedo, 2009 reported that seven carbamazepine PCC exhibit aqueous solubility 2-152 times greater than the solubility of the stable carbamazepine dihydrate form.

Stanton et al, 2011 reported that many of the highly soluble in water PSs and PCCs showed rapid precipitation in physiological media forming less soluble free APIs and CFs. Authors demonstrated that rapid dissolution of carboxylic acid PCCs of AMG 517 (Amgen compound) was followed by slow crystallization. This patterns of changing the solubility has been described as 'spring and parachute' effect (Cheney et al. 2010). The 'spring' explained the fast dissolution rate, while 'parachute' effect refers to the slow kinetics of conversion to the less soluble form. The initial, fast dissolution rate prevails *in vivo* conditions exerting higher values for AUC (Stanton et al, 2011). By using the precipitation inhibitors, Guzmán et al., 2007 reported that it is possible to prevent PSs or PCCs from their supersaturated solutions in gastric media to precipitate out in intestinal fluid.

The assessment of PCCs stability with respect to solid-solid conversion of its component forms under the normal atmospheric conditions of temperature and humidity in the work of Schartman 2009 indicates to relationships between conversion of the PCC to its components in solvent systems (Childs et al., 2004; Task et al., 2005; McNamara et al., 2006), hydrate-anhydrate phase boundaries determined by the modified slurry method (Zhu et al., 1996; Zhu and Grant, 1996) and the relative stability of polymorphs (Giordano et al., 2001, Gu et al., 2001, Getsoian et al., 2008).

Perspective for research and utilization of PCC in designing drug delivery systems

The PCCs have opened new paradigm in solid-state modification of physicochemical properties of APIs. Bioavailability of API in context of structure-property-performance relationships is directly determined by its solubility and dissolution/permeability rate, that API exerts when it is cocrystallized in the unique structure of the PCC. The erratic solubility of APIs selected from the WHO Model List for Essential Medicines caused, only for period of 2010-2011, out of all 263 drug candidates for ANDA submissions to US-FDA in process of approval for market authorization, only 20.9 % to belong to APIs from the group of BCS's (Biopharmaceutical Classification System) Class II referring to APIs which exert low solubility/high permeability, and no one to the BCS Class IV of low solubility/slow permeability APIs (Nair et al. 2012). **Table 1.4** covers the examples of PCCs in respect to the solubility/permeability relationship of the APIs according to BSC and potential utilization of nutraceutical and drug for obtaining functional PCCs of drug-drug type.

Even though crystal engineering has become emerging technology for designing molecular crystals, difficulties regarding the prediction of the crystal structure are caused by inability

to control the multiplicity of possible orientations of the molecules in crystals, the inaccuracies in estimating energies, and contribution of the variable interplay of kinetics and thermodynamics in process of nucleation and crystal growth.

Table 1. 4 PCCs in respect to the solubility/permeability relationship of the APIs according to BCS; potential drug-drug type of PCC and nutraceuticals CC

Classification	API	CF	Modulated properties	Reference
BCS Class I High solubility High permeability	Fluoxetine hydrochloride	Succinic acid	two fold increase in solubility	Childs et al. 2004
	Caffeine	Oxalic, Malonic, Maleic and Glutaric acid	improved hydration stability	Trask et al. 2005
	Caffeine	4-hydroxybenzioc acid	Improved thermal stability	Aitipamula et al., 2012
	Theophylline	Oxalic acid	Improved hydration stability	Zhanga, 2012
BCS Class II Low solubility High permeability	Ibuprofen & Flurbiprofen	Nicotinamide	Increased dissolution	Chow et al. 2012
	*AMG-517	Aliphatic & aromatic carboxylic acids	Enhanced dissolution patterns	Stanton & Bak, 2008
	Carbamazepine (Tegretol®)	Saccharin	Enhanced dissolution and suspension stability	Hickey et al., 2007
	Itraconazole (Sporanox®)	Succinic acid	Improved dissolution	Remenar et al. 2003
	Griseofulvin	Acesulfame	Monohydrated PCC Increased thermodynamic stability Increased solubility	Aitipamula et al., 2012
	Ethenzamide	4-hydroxybenzioc acid	Increased solubility/dissolution	Aitipamula et al., 2012
BCS Class III High solubility Low permeability	Adefovir Dipivoxil	Saccharin	Kinetic stability, pH independent dissolution	Gao et al., 2011
	Pyrazinamide	Dicarboxylic acids	Enhanced solubility	Luo & Sun, 2013
	Metformin	Embonic acid	Decreased solubility	Babu et al., 2013
BCS Class IV Low solubility Low permeability	Furosemide	Caffeine	Enhanced solubility	Goud et al., 2012
	Norfloxacin	Isonicotinamide	Solvated form Enhanced solubility	Basavoju et al., 2006
Drug-Drug PCC	Meloficam	Aspirin	Increased solubility of meloxicam	Cheney et al. 2011
	Pyrazinamide	Diflunisal	increased solubility of diflunisal, reduced side effects	Évora et al. 2011
	Lamivudine	Zidovudine	Increased solubility/dissolution	Bhatt et al., 2009
Nutraceuticals CC	Quercetin	Caffeine	Enhanced solubility	Smith eta l., 2011
	Curcumin	Resorcinol Pyragallol	Enhanced solubility	Sanphui et al., 2011
	Petrostilbene	Piperazine	Improved hydration and thermal stability, increased solubility	Bethune et al., 2011

*Antagonist of transient receptor potential vaniloid 1 (TRPV1)

The physical proprieties of APIs in form of CCs are altered without chemical modification of the API. CC design become approach of the first choice for APIs that do not form useful salts (e.g. nonionizable and highly lipophilic APIs) or require improvement of the physical properties, mainly solubility and dissolution rate that directly impact the

bioavailability and pharmacokinetic profiles, and thermodynamic stability that influences the shelf-life due to the changes in crystal packing caused in specific range of values for temperature and humidity. This unpredictability or lack of obviousness of crystal structures and physical properties impel the challenges for legal issues in terms of obtaining and managing patent protection for any of crystalline form for an API. Anyhow, the decision for designing API in form of CC could be justified by the improvement of the physical properties that are desirable over the properties of the API itself (*e.g.* obtaining CC of API which exist in amorphous form, improve melting points, enable improved chemical purity, reduce chemical degradation by light exposition, remove the risk of hydrate formation in a formulation, and improve the solubility to enable enhanced bioavailability). In addition, the advantage of PCCs comparing to PSs is sought in vast opportunities for selection of a "pharmaceutically acceptable" conformer from the group of nontoxic substances included in US-FDA's GRAS list (Generally Accepted As Safe) of substances approved as food additives which number and structure versatility exceed over pharmaceutically acceptable salt former (only acids and bases).

The efficient design of PCCs with desired properties, favorable for solving drug delivery problems, relies on understanding the structure-property-performance relationships. Therefore, strategic shift from property enhancement to property modulation address the comprehensive approaches for substituting serendipitously discovery of PCC with systematic design based on mastering the techniques for PCC screening that enable single crystal growth of PCCs, applying convenient *in silico* technologies for molecular modeling and structure prediction, as well protocols for scale-up efficient bulk cocrystallization, environmental impact, purity and stability (Sun, 2013).

PCCs design strategies

Determination of the particular CF candidate or set of CFs to crystallize with targeted API as a drug model is well-known as PCC screening. Various screening methods are related to the two main and complementary approaches. Firstly, to select methods for growing PCCs with quality, suitable for absolute structure determination using the single-crystal diffraction, and second one for studying the propensity for PCCs formation based on physicochemical and thermodynamical properties.

Solvent evaporation is suitable method for growing single crystals of PCC by evaporation of the pure solvent of solvent mixture wherein API and CF with similar solubilities form stoichiometric solution (Basavoju et al., 2008; Bis et al., 2007; Weyna et al., 2009). On the contrary, non-equivalent solubility of API and CF in solution lead to formation of single

component crystals because supersaturation is obtained with respect to less soluble component (either API or CF, depend of their solubilities) or both one of less soluble reactant and PCC (Blagden et al., 2008). This last approach has been utilized by Childs et al., 2008 for so-called reaction crystallization method for screening carbamazepine PCCs from a set of 18 different CFs. This method is performed by adding the API into the saturated or nearly saturated solution of CF reaching the level of supersaturation of the solution with respect to formed PCC.

Cooling crystallization method based on the precipitation of the PCC once it is formed in the point of supersaturation solution in heating-cooling cycle was successfully applied for obtaining PCC of caffeine with p-hydroxybenzoic acid in methanol (He et al., 2010).

Over the past few years, great progress in PCCs screening is achieved by utilizing grinding of the stoichiometric mixture of API and CF that represent mechanochemical solid-state reactions for producing PCCs (Friščić & Jones, 2009; Trask&Jones, 2005). One of the two common techniques for grinding relates to neat grinding of API and CF which exhibit significant vapor pressure in the solid state that is driving force for formation of intermediate distinct phases (a gas, a liquid or an amorphous) with respect to starting crystalline phases of API and CF. This technique, being modified by grinding of API and CF in presence of droplets of solvent is known as liquid-assisted grinding, or kneading. Task et al., 2004 reported that the nature of solvent and the solubility of one of the component in the solvent is crucial factor for controlling the polymorphism in PCC of caffeine with glutaric acid. This is the cost-effective and environmentally friendly method for reliable and rapid PCC screening (Basavoju et al. 2008; Braga & Grepioni, 2005; Task et al., 2004, Weyna et al. 2009). In addition to these methods, hot-stage thermal microscopy method, so-called Kofler technique in the study carried out by Berry et al., 2008 for initial screening of PCC with nicotinamide in combination with one of several APIs, was exerted as beneficial, particularly in heating-cooling cycle for visualizing and mapping the phase transformation that contribute the binary phase diagram and thermodynamic properties in process of PCC formation. Since recently, advantages for indomethacin-saccharin PCC screening have been highlighted by applying supercritical fluid technology in the research done by Padrela et al., 2009. Ultrasound-assisted crystallization that contribute the solution crystallization method, has been utilized by Aher et al., 2010 as novel method for obtaining PCC of caffeine and maleic acid 2:1.

Part 2

History of metformin

The origin of the globally well reputed drug metformin is from the medicinal plant *Galega Officinalis* (Leguminosae) which, since medieval ages has been used in traditional medicine for treatment of many illnesses and symptoms, nowadays ascribed as consequence of the type 2 diabetes. Before the World War I, in France, Watanabe performed the first chemical analyses on the composition of this medicinal plant detecting the presence of guanidine, a compound which shows hypoglycemic activity in animals. In order to avoid the high toxicity of the guanidine base, other two French scientists, Muller (1927) and Simonnet (1927) prepared less toxic extracts of this plant wherein they identified the structure of the alkaloid gelagine (isoamylene guanidine) and tested its hypoglycemic activity. In order to improve its hypoglycemic effects and avoid adverse effects, synthetic ancestors, decamethylen diguanide (Synthalin A) and dodecamethylene diguanide (Synthalin B) were developed and clinically used.

For the first time, in 1927, the German scientists Hesse at al. and Frank et al. synthesized the biguanide derivatives including the dimethylbiguanide and tested their non-toxicity and glucose-lowering effect on animal models, but not on humans. The first who explored the antidiabetic properties of dimethylbiguanide in clinical development was the French pharmacologist Jane Sterne, who in 1956 proposed the generic name "Glucophage" (glucose eater) for metformin. In the published results in 1956, Stern addressed the metformin effect on lowering blood glucose in patients with type 2 diabetes, but not in health population. Although numerous studies on pharmacovigilance has monitored the safety profile of metformin, its natural ancestor, *Gelega Officinalis*, up-to-date is being cited both as medicinal plant in *British Herbal Pharmacopoeia* (1976) and in Handbook of Medicinal Herbs (Duke JA, 2002) as well it is appeared on the U.S Poisonous Plant Database (U.S. FDA Center for Food Safety & Applied Nutrition) as a poisonous weed. This contradicted status could be justified by the famous quote of the founder of Toxicology, Paracelsus, that "the right dose differentiates a poison from a useful medicine".

The successive research on aryl biguanide derivative phenformin and alkylbuformine buformine which exerted effect of increased lactic acidosis shed reputation of metformin until the published result from UK Prospective Diabetes Study (Lancet 1998) claimed that

early use of metformin reduced risks of myocardial infarction and increased survival in overweight and obese type 2 diabetic patients beyond that expected for the prevailing level of glycaemic control. As a result metformin became the first-choice treatment for obese patients with type 2 diabetes.

Since 1995, metformin enjoyed the status of blockbuster drug under the franchise to Bristol Mayer in US and brand name "Glucophage".

Metformin market outlook

The Drug Trend Report from 2013 indicated that the diabetes therapy class had the highest per-member-per-year spend, at $270.62, and the highest trend, at 14.5%. Based on the sale of metformin generic forms from Teva and Mylan, together with branded lucophage, that in total was $1.57 billion in 2011, metformin was ranked on thirteen position among top 20 generic molecules (FiercePharma web portal in 2012)

Global drug market for diabetes care values a $45 billion, and it gradually grows in demographics favor. Worldwide population affected by diabetes form 382 million people today is expected to be increased to 592 million by 2035, as a prevalence rises from 8.3% to 10.1%.of the population. Though the type 1 diabetes has tendency to rise, the growing prevalence of Type 2 diabetes increases due to an increasingly urbanized, sedentary, and obese global population.

According to the diabetes market outlook report (Conover *et al* 2014), it is expected diagnosis and treatment rates to climb, particularly in emerging markets, where access to care is improving. Branded drugs that share the diabetes market with annual growth rate of 12% is going to grow to $58 billion in 2018 from $33 billion in 2013. This is slightly higher tendency than the 10.5% 10-year historical market growth rate (which incorporates sales of generic products like metformin), but lower than growth in more recent years.

The Glucophage, Bristol-Myers Squibb's brand of the drug whose generic name is metformin, was the only one brand of metformin on the U.S. market until 2002 when the patent of metformin expired and other pharmaceutical manufacturers gained approval from the U.S. FDA to market their own generic forms of metformin. Up to now there are at least 15 manufacturers which hold market authorization for selling generic forms of metformin on U.S. market.

Several generic versions of the drug metformin (previously sold only as Glucophage or Glucophage XR) are now available. The combinations of metformin and glyburide

(Glucovance) and metformin and glipizide (Metaglip) are available as generic drugs. Dinsmoor in 2008 reported that the combinations of metformin and rosiglitazone (Avandamet), metformin and pioglitazone (Actoplus Met), metformin and sitagliptin (Janumet), and metformin and repaglinide (PrandiMet), however, are still sold only as brand-name products.

Among the top 200 products in 2012 listed by total prescriptions, Bartholow ranked the generic forms of metformin in following order: Metformin from Zydus on the position 40; Metformin from Teva on the position 41; metformin from Mylan on the position 73; Metformin from Aurobindo on the and position 97.

Physicochemical properties of metformin

Metformin basicity and structure relationships

As a representative of the biguanide class of compounds, metformin exhibits strong basic properties (stronger base then ammonia). It is a diacid base. In biguanide structure, formed by the two condensed guanidine moieties, the positive charge is distributed among four almost equivalent amino groups forming a π-conjugated system that determines MET to exist in three resonance-stabilized forms, *i.e.* as neutral molecule (MET), monoprotonated (METH$^+$) or diprotonated (METH$_2^{2+}$) cation with high difference in values of primary and secondary dissociation constants.
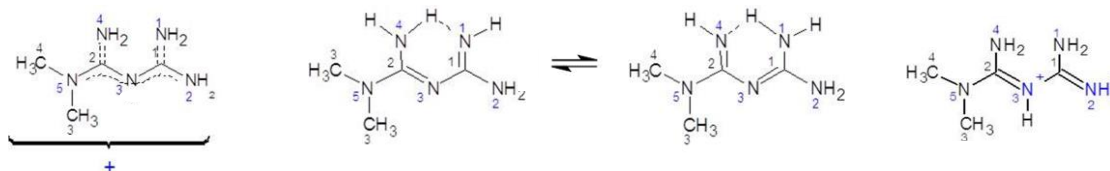
* Monoprotonated MET   Neutral MET   Diprotonated MET

* (Hariharan, et al., 1989, *ActaCryst*. C45, Childs, et al., 2004, *Cryst.Growth.Des*. 4, 3)

Figure 1.5 MET resonance-stabilized forms

The pK_a values of MET reported in the NIST database (Martell *et al.*, 2004) are the following:

Metformin = L;

[HL]/[L][H] pK_{a1}(N−H$^+$) ~ 12.40;

[H$_2$L]/[HL][H] pK_{a2}(N−H$^+$) = 2.96

(NIST database)

Margetic (2009) reported that both in the gas phase and in the solution, basicity is in correlation with increasing number of amino groups in the molecule of biguanides. Hence, metformin with three amino groups is a stronger base than guanidines that have two amino groups which are stronger bases than amidines with only one amino group, while amidines are stronger bases than imines which have no amino group. The pK_a values in acetonitrile obtained for biguanides (27–32) were larger than for the corresponding guanidines (23–26) reported by Kaljurand et al. (2005).

The high basicity of pK_{a1} and the difference between the pK_a values qualify MET as organosuperbase and determine the stability of its monoprotonated form $METH^+$ within a wide range of pH.

Rainbolt et al. (2010) reported that protonation of the Lewis basic nitrogen and formation of iminium ion in alkanoguanidines increase their electrophylicity for nucleophylic addition reaction with acidic gas carbon dioxide from atmosphere. Thus, through non-covalent interactions with carbon dioxides alkanoguanidines convert either in ionic liquids, or form crystalline carbonate salts. This capacity that strong organic bases exerts in capturing carbon dioxide has been confirmed with our research on providing crystallization protocols for isolation in crystals of the neutral form of metformin. As a result of our research, we succeeded to crystallize only carbonate and hydrogen carbonate salts of metformin for which the crystal structures have been determined (data in process of publication). The affinity of carbon dioxide (CO_2) uptake, indicated by Heldebrant et al. (2011), make biguanides and alkanoguanides as promising reagents for fuel gas streams and materials for energy sources.

Antioxidant capacity of metformin

In the comprehensive study for confirming antioxidant properties of metformin, Trouillas et al. (2013) outlined that concomitant metformin consumption and formation of its oxidation products in pH 2.8, 7.15 and 11.6, respectively is depending on radiation dose that caused radical-induced oxidation of metformin.   In presence of $HO^\bullet$ and $O^{\bullet-}_2$ at pH 7, $O^{\bullet-}_2$ at pH 7.15 and 11.6 and acidic form of $HO^\bullet_2$ at pH 2.8, the lower value of radiolytic yield for metformin consumption at pH 2.3 then the obtained values in neutral and basic environment, indicates to dismutation process in which part of metformin is regenerated during the radical reactions. Reaction between one molecule of metformin and $HO^\bullet$ radical leads to no regeneration of metformin. By applying the Density Functional Theory (DFT), the calculated bond dissociation enthalpies (BDE) for carbon atoms from methyl groups of metformin, even in values higher compared to O─H BDEs for polyphenol type of

antioxidants, showed that methyl groups are equivalent targets for HO$^{\bullet}$ attack confirming that *N*-dimethyl moiety of metformin is reactive site. After attacking HO$^{\bullet}$ to metformin, and consequently formation of primarily carbon-centered radical ([MTF─H]•) located on C8 (or C9) which undergo to conformational reorganization (depending of the pH value it is easily for diportonated metformin) through N7-C8(C9) bond formation and transformation to cyclic radical which in bi radical reaction in presence of other radical species is transformed to neutral metformin molecule in solution. This dismutation mechanism described by Trouillas et al. (2013) allows regeneration of metformin and confirm its antioxidative property in relation to pH value.

Metformin in metal-organic chemistry (Chelating properties of metformin)

Zhu et al. (2002) synthetized and crystallized the metal-organic red cooper complex of deprotonated metformin (an anionic ligand). Metformin as a bidentate ligand which lacks aromatic character, through four N atoms of two ligands, chelates copper in unusual pseudoaromatic square-planar ring coordinative structures characterized by the high value for affinity constant (equilibrium constant). The deprotonation of the ligand causes extensive delocalization in π conjugation of the conjugated C─N─C system, reducing the bond angle at the central N atom to nearly 120°. Electron delocalization in the chelate complex of metformin and copper in the study of Logie *et al.* (2012) was tested in the cellular action of biguanides to regulate AMPK, glucose production, gluconeogenic gene expression, mitochondrial respiration, and mitochondrial copper binding. In contrast, regulation of S6 phosphorylation is prevented only by direct modification of the metal-liganding groups of the biguanide structure, supporting recent data that AMPK and S6 phosphorylation are regulated independently by biguanides. Logie *et al.* (2012) explained that apolar dimeric metformin complex with Cu^{2+} which exhibits hydrophobic property, and thus slowly passes the plasma membranes inside the cells, is a crucial factor in the complex I (NADH-ubichinone-reductase) responsible for the respiratory chain located in the inner mitochondrial membrane (Logie et al. 2012, Rena et al. 2012).

Other metal-organic complexes of metformin were reported, that include cobalt (Rafat *et al,* 2014) and technetium and rhenium (Marchi et al. 1999).

Since Li *et al.* (2009) confirmed on animal model the antidiabetic effects of Vanadium (III, IV, V)-chlorodipicolinate (dipic-Cl) complexes, Chatkon *et al.* (2014) synthetized crystalline double salt of polyoxovanadate *i.e.* decavanadate ($V_{10}O_{28}{}^{6-}$) anions with two metformium monocations, and a hydrolyzed product of metformin, protonated guanylurea (HGU+) enganed with two crystallized water molecules: $(HGU^+)_4(HMet^+)_2(V_{10}O_{28}$

$^{6-}$)·2H$_2$O. The ions and the two water molecules of solvation are engaged in extensive multiple H-bonded network, and crystallize in the triclinic space group $P-1$ ($Z = 1$).

The FTIR spectroscopic study on interface properties for testing the hydrogen-bonding properties of the non-water soluble decavanadate salt of metformin in the water and sodium bis (2-ethylhexyl) sulfosuccinate (AOT) reverse micelles, carried out by Chatkon *et al.* (2013), showed that decavanate counter anion (V$_{10}$O$_{28}^{6-}$) affects the solubility of the salt in aqueous solution and in reverse micelles due to effect of metforminium monoprotonated cations on hydrogen-bonding pattern in water phase of the reverse micelles.

Fabbrizzi et al (1978) on their study of biguanide complexes with nickel(II) and copper(II) in solution reported that the process of formation of metal-nitrogen π bonds in complexes between square coordination of the metal ions and delocalized planar configurations of monoprotonated biguanide cations is accompanied with high exothermicity characterized by negative changes for configurational and translational entropy due to release of water molecules of solvation.

Metformin as a chemoselective catalyst in Henry reactions

For first time Alizadeh *et al.* (2012) utilized the metformin in neutral form to catalyze the Henry reaction (nitro-aldol reaction of aldol-type C—C bond formation) of a variety of aliphatic, aromatic and heteroaromatic aldehydes with nitromethane without resulting the side reactions such as aldol-condensation, Cannizzaro reaction, nitroalkene formation, Michael reaction, retro-aldol reaction and Nef reaction. The benefits of metformin to catalyze the Henry reactions are in unnecessity to use organic solvents, its recycling use in repeated reactions in which reversible proton transfer occurs between metformin and acidic substrate, and its easy removal. These advantage contribute this catalyzed Henry reaction with metformin to be classified as green or environmentally friendly.

Metformin salts

Metformin is a drug marketed as hydrochloride, embonate (pamoate) and *p*-chlorophenoxy acetate salt.

Measurements by UV spectroscopy for the hydrochloride salt of metformin at pH 1, pH 4, pH 7 and pH 13 shown that its UV spectra is pH dependent. The maximum of the absorption at around 230 nm is due to π-π* transition and it is not affected by the single protonation that only may induce a decrese in intensity (Prugnard & Noel). Clement (1999) comparative study on monoprotonated metformin, phenfomin and buformin in forms of hydrochloride salts by applying ^{15}N NMR spectroscopy indicated that for all three

biguanides, the protonation occurs at the position of the most basic nitrogen atom N-2 and that the neutral metformin in solution predominantly exists in form of 1. This result has been confirmed by Hariharan *et al.* (1989) whose crystallographic study on last resolved structure of metformin hydrochloride revealed that the imino group attached to C5 is a site for protonation, due to which intermolecular H-bonds are formed. Moreover, results of Hariharam study showed that two guanide groups laid in planes between which the angle has value of 67.9° which corresponds to dihedral-angle values reported for related structures. Crystallographic analyses underlined that intermolecular N—H⋯N type of hydrogen bond does not exist in structure of metformin hydrochloride though previously Shapiro *et al*. (1959) has reported that this type of hydrogen bond is responsible for hypoglycemic activity of biguanides. The molecules of metformin hydrochloride in the unit cell are stabilized by N—H⋯N and N—H⋯Cl types of hydrogen bonds, chlorine atoms are interspersed between layers of metformine molecules along the *b* axis and each chlorine participate in five hydrogen bonds. The crystals of metformin hydrochloride belong to a monoclinic group and on macroscopic scale they are white needles in shape.

Metformin hydrochloride as a solute in its aqueous solution was used in the work of Maheshwari et al. (2009) as hydrotropic agent to enhance the solubilization of the aqueous solubility of the poorly-water soluble drug atenolol from its dosage forms. The statistically validated data   indicate that metformin hydrochloride in concentration range of 50-300μg/ml obeyed to Beer's law and did not interfere with excipients from atenolol formulation at 275 nm. The reported results of analysis by the method proposed by Maheshwari et al. are in compliance with the method proposed for metformin assay in the British Pharmacopea and are beneficial in terms of avoiding organic solvents.

Results from the assessment of thermal stability of metformin hydrochloride salts obtained by Sharma et al. (2010) highlighted that 10% of the drug will decompose within 208 h on 30 ºC. The decompensation constant calculated from the slope of the Arrhenius plot for temperature-concentration indicates that metformin decomposition follows a zero order kinetic. This work of Sharma et al. anticipates that storage and processing conditions for formulations with metformin hydrochloride salt influence its thermal stability.

Sensitivity (0.02 mg/L detection limit in human plasma), and highly reproducibility of the reversed phase high-performance liquid chromatography   with a new precolumn derivatization method using 9,10-anthraquinone-2-sulfonyl chloride as the derivatization agent developed by Juan *et al.* (2006) overcomes the disadvantages associated with complexity for performing and costs for reverse-phase, ion-pair liquid chromatography

(LC) (Vasudevan. *et al.*, 2001), LC–mass spectrometry (MS)–MS (Zhang *et al.*, 2001), or cation exchanging with normal phase (Koseki *et al.*, 2005).

Poor flowability and compressibility of needle-shaped and large size (>400 μm) crystals of metformin hydrochloride was improved in work of Barot et al. (2012) by its recrystallization in solution of 2% polyvinylpyrrolidone (PVP K30), well known excipient for pharmaceutical formulations and crystallization inhibitor to its effect to adsorb to the surface of the particles modifying only the crystal habits (size and shape). The values for the selected as dependent variables (flowability - Carr's index and tensile strength calculated from the Kawakita equation and Heckel plot, respectively) obtained for optimized batch by method of 3^2 factorial design showed that bulk powder (mean size 184 μm for spherical particles) of recrystallized metformin hydrochloride salts with 2% PVP in comparison to commercial, untreated metformin salt, exerts higher degree of densification, lower porosity under zero pressure, less resistance force required for compression. These results are promising in terms of favorable properties of bulk powder of recrystallized metformin hydrochloride salt in presence of 2%PVP for high-dose sustained release tablet formulations.

Inconsistent flow behavior of the batches of blends of metformin hydrochloride salts with other excipients which were undergone to milling, after the processing and during the storage at different temperatures and relative humidity ambient was investigated by Vippagunta *et al.* (2010). The results for surface energy values obtained by the density functional theory (DFT) method, together with X-ray diffraction patterns, thermally stimulated current measurements, and dynamic vapor sorption isotherms indicated to detectible defects on the surfaces of its crystals which were absent in the samples of the storage (aged) sample. Vippagunta *et al.* underlined that these change on the surface of metformin hydrochloride crystal is a factor for difference in flow behavior.

Amorha *et al.* (2013) studied the concomitant *in vitro* dissolution profiles of 500 mg (Glucophage® 500mg) and 10 mg (Zestril® 10) and reported that lisinopril decreases the percentage of released metformin at pH 1.2, 4.5, and 6.8. Increased percentage of released lininopril in presence of metformin is statistically significant only at pH 1.2 and 6.8. These results anticipate the alertness of optimizing the dosage regimen in therapy with metformin and lisinopril.

First reported metastable polymorph of metformin hydrochloride was reported by Childs *et al.* (2004) who succeeded obtaining single crystals of form B grown from the mixture of metformin hydrochloride and ethylene glycol by manipulating the temperature of the hot-stage during the crystal growth process. The thermodynamic study of highly metastable

Form B indicate its rapid crystal growth in constrained *in situ* conditions and complete conversion to more stable Form A over a 24 to 36 h period at temperatures between 0°C and 140°C. By comparing the determined structures of Form A and Form B, both collected at 100 K, Shild *et al.* pointed out the 5.5 % difference in density what is in agreement with previous work of Gavezzotti & Filippini (1995) who reported that 93% of polymorphic pairs included in the Cambridge Crystallographic Database differ in density less than 5%. Both polymorphs crystallize in monoclinic (*P*21/*c*) space group with one complete metformin cation and one chloride anion in the asymmetric unit. The charge-assisted hydrogen bonds N-H···Cl confined to a layer are in the *bc* plane of Form B, and the *ac* plane for Form A. In the metastable Form B a centrosymmetric 0D dimer is presented by the hydrogen bonds between cations, while in Form A neutral N-H···N bonds form one-dimensional (1D) rod motif. The differences in values for torsion or dihedral angle (N5–C2–N1–C1), −53.7° and 129.1° for Form A and Form B, respectively, influence the differences in conformations of the metformin cations in structures of both polymorphs. In the Form A, the –C(NH$_2$)$_2$ group is close to –N(CH$_3$)$_2$ group resulting in more compact packing in the asymmetric unit, while Form B has a more extended molecular backbone.

Embonate or pamoate is another salt of metformin that was patented for many years in France (FR2037002A1), but in recent study of Nanubolu *et al.* (2013) its polymorphism was reported. Authors revealed that the two polymorphic forms are in enantiotropic relation; Form I is theromdinamically more stable at higher temperatures, while Form II at room temperature, and this latter displays lower solubility and lower intrinsic dissolution rate comparing to the former Form I. Moreover, a polymorphic mixture of Forms I and II at room temperature in water converts to more stable Form II after one day. Crystal packing analyses of the determined structures for Form I and II consist of metformin and enbonate in 2:1 stoichiometric ratio. Form I crystalizes in monoclinic *P*2$_1$/*c* and Form II in triclinic *P*−1 space group. The analyses of hydrogen bonding motifs underlined that in both forms between metformin monoprotonated and first carboxylate of the embonate exists a two-point dimer synthon with symmetry independent metformin; R$_2^4$(16) motif of N4B–H4N···O5 and N5A–H6N···O5, and four-point tetramer synthon; R$_4^2$(8) motif of N2B–H8N···O3 and N4B–H9N···O3 including another carboxylate of embonate form and independent metformin. The difference in arrangement of these two similar synthons have been confirmed in work of Nanubolu *et al.* as important feature for difference in packing due to which metformin embonate exists in two polymorphic forms. Form I is formed by connecting one dimeric unit to another screw-related dimer through single N–H···O interaction in which participate the NH donor of metforminium cation and the O acceptor

of the carboxylate (N4A–H3N···O6). This mode of packing propagates infinite zig-zag arrangements along the *b*-axis. In Form II, one dimeric unit is linked to its inversion-related dimeric unit by two point motifs $R_2^2(8)$ including two N4A–H3N···O6 interactions leading to ladder patterns of arrangements along *a*-axis. The conformation proposed by Childs *et al.* for Form B (value of torsion angle 129.1°) was confirmed to exist in two metformin molecules included in both polymorphs of metformin embonate salts, Form I with values for torsion angles –156.8° and –151.5°, and Form II with values for torsion angles –161.5° and –148.1°. Additional DFT computations for relative conformer energy, in the work of Nanubolu *et al.*, confirmed the crystallographic analyses that the stable conformer of monoprotonated metformin (metforminium cation) in solid state is that one with value for the torsion angle around 150° (N1–C3–N3–C4) and the lower energy.

In addition, the survey in the Cambridge Structural Database (CSD) revealed that there are 12 deposited structures of metformin salts wherein metformin exists as monocation (monoprotonated): two polymorphs of hydorchloride, bromide, nitrate and acetate salts and five structures where it is dication (diportonated): oxalate, sulfate, perchlorate, squarate and calixarene-sulfonate salts.

In acetate and nitrate salts, monoportonated metformin exists in the same, most stable conformation as it was explained in hydrochloride and embonate salts (Childs *et al*; Nanubolu *et al.*), while in bromide salt its conformation correspond to the less stable at Form B (Childs *et al.*). Pérez-Fernández *et al.* (2013) reported salicylate salts of metformin prepared from metformin hydrochloride and sodium salicylate

Quality specification for metformin hydrochloride described in the monograph of the European Pharmacopoeia (Ph EUr) includes tests for description, identification (IR, PhEur), solubility (Ph Eur), melting point (Ph Eur), Loss on drying (Ph Eur), heavy metals (Ph Eur), content (Ph Eur, 98.5-101.0%), impurities (HPLC), residual solvents (GC), and particle size.

Mechanism of action of metformin in diabetes mellitus type 2

Conducted research by Inzucchi et al. 1998 showed that biguanide group of drugs affect the inhibition of liver glucose production. However, the mechanism of action of metformin remains unclear in spite of its wide application as a first line oral therapy in diabetes type 2 (Goodarzi et al. 2005). Previously demonstrated metformin mode of action through activation of the kinase AMPK (Shaw *et al.* 2005, Zgou et al, 2001) has been disputed by the recent study done by Foretz *et al.* 2010 involving livers and primary hepatocytes with

missed either AMPK or its upstream activating enzyme LKB14.The experiments from this study are associated with the Miller et al. work on the inhibition of the glucagon signaling pathway caused by metformin, since the abnormal secretion of the hormone glucagon, having partial role in controlling glycogenesis and gluconeogenesis during the fasting state, is a major factor for hyperglycemia in individuals with diabetes mellitus type 2 (D'Alessio *et al.* 2010, Jiang *et al.* 2003, Unger *et al.* 2012).Unlike sulfonylureas, metformin did not stimulate insulin release, but increased its peripheral uptake and also reduced the release of glucose from the liver. Cellular effects of biguanides are associated their metal-binding properties. Logie et al (2012) demonstrated that biguanide/copper interactions, stabilized by extensive π-electron delocalization, enables biguanides to regulate AMPK, glucose production, gluconeogenic gene expression, mitochondrial respiration, and mitochondrial copper binding. In contrast, regulation of S6 phosphorylation is prevented only by direct modification of the metal-liganding groups of the biguanide structure, supporting recent data that AMPK and S6 phosphorylation are regulated independently by biguanides.

Anticancer activity of Metformine

Recently, Pollac (2013) proposed that metformin or related biguanides may have antineoplastic activity. The study performed on breast cancer cells (Zakhikani et al. 2006) showed that metformin-induced inhibition of oxidative phosphorylation leads to AMPK activation and to AMPK-dependent antiproliferative effects, which are mediated by processes such as AMPK-mediated inhibition of fatty acid synthesis (Algire et.al. 2010) and AMPK-mediated inhibition of mRNA translation (Larson et al, 2012). Pernicova *et al.* 2014 reported that combination of tumor genetics, patient metabolic profile and the cellular microenvironment determine the antitumor effect of treatment with metformin. In the work of Giovannuci *et al.* 2010 is reported that metformin reduced the risk of cancer incidence to the patients with diabetes mellitus by approximately 40% compared with the other antidiabetic treatments.

Metformin exerts direct effects in cancer through interplay of 5' AMP-activated protein kinase, AMPK-independent and AMPK-dependent mechanisms (Liu et al. 2014). The LKB1-dependent and AMPK-dependent suppression of the mammalian target of rapamycin 9mTOR pathway is possibly most potent antineoplastic effect of metformin because mTOR inhibition interrupts protein synthesis, and consequently tumor cell proliferation. Inhibition of proto-oncogene c-MYC and hypoxia-inductible factor 1α (HIF-1α) via AMPK and proteins level in breast cancer models indicate to its antiproliferative

effects (Blandino et al. 2012). Independently of AMPK, metformin inhibits mitochondrial complex I responsible for production of reactive oxygen species, oxidative stress and DNA damage, therefore it reduce the risk of mutagenesis (Aigire C et al 2012).

Anti-inflammatory activity of metformin in treatment of psoriasis

Glossmann *et al.* 2013 outlined the arguments that the metformin could be useful as an add-on therapy to methotrexate for the treatment of psoriasis and, perhaps, for rheumatoid arthritis as well.

Their claim is based on the biochemical data suggesting that both drugs may share a common cellular target, the AMP-activated protein kinase (AMPK). Clinical observations as well as experimental results argue for anti-inflammatory, antineoplastic and antiproliferative activities of metformin and a case-control study suggests that the drug reduces the risk for psoriasis. Patients with psoriasis have higher risk of metabolic syndrome, type 2 diabetes and cardiovascular mortality. Glossmann *et al.* expect that addition of metformin to methotrexate can lead to positive effects with respect to the The *Psoriasis Area Severity Index* (PASI score), reduction of the weekly methotrexate dose and of elevated cardiovascular risk factors in patients with metabolic syndrome and psoriasis.

Biopharmaceutical profile of metformin

Metformin (MET) is a low-molecular-weight hydrophilic compound with value for distribution coefficient log$D$ of –3.37 at pH 4 and water solubility higher than 100 mg/mL within the entire physiological pH range (Bretnall & Clarke, 1998). The major window of absorption for metformin is the proximal small intestine, and the primary route of elimination is through the kidneys (Trucker *et.al,* 1981). Based on Caco-2 cell model for testing process of permeation through cell membrane proposed by Nicklin *et al.*(1996), the absorption of MET is proposed to occur by diffusion in extent of 91-95% by paracellular, and 5-9% by transcellular, respectively.

After oral administration, metformin is slowly absorbed from the proximal small intestine (e.g., duodenum) and mainly excreted from urine (>90%) without undergoing significant biotransformation (Scheen, 1996; Bell and Hadden, 1997). The intestinal absorption of metformin is the rate-limiting step of its disposition, due to its slower rate of absorption than of plasma elimination. (Scheen, 1996; Bell and Hadden, 1997). The absorption of metformin is dose-dependent and incomplete (Scheen, 1996; Bell and Hadden, 1997). A

lower dose affects higher extent of metformin absorption rather than higher dose does (Tucker et al., 1981), and an inverse relationship was observed between the amount of metformin ingested (from 0.25 to 2.0 g) and its bioavailability (from 86 to 42%) (Scheen, 1996; Bell and Hadden, 1997). Dose-dependent absorption kinetics supported the suggestions that metformin absorption is mediated by an active, saturable absorption process (Scheen, 1996; Bell and Hadden, 1997; Klepser and Kelly, 1997). However, the further investigations remain as a challenge to reveal which of the transporters are responsible for the active uptake process of metformin in the intestine.

The transport activity of the organic cation transporters (OCTs), polyspecific transporters expressed in the liver and kidney where they are responsible for elimination of the organic cations from systemic circulation (Koepsell, 1998), in general is significantly decreased at lower pH (Wang *et al*., 2002), and the acidic environment in the gut lumen (pH 4.0-7.0) may limit their ability in metformin absorption. A novel organic cation transporter, plasma membrane monoamine transporter (PMAT), transports many classic organic cations (e.g., monoamine neurotransmitters, 1-methyl-4-phenylpyridinium) in a pH-dependent manner and its mRNA is expressed in multiple human tissues (Engel and Wang, 2005). The study of Zhou et al (2007) showed that metformin is avidly transported by PMAT, the concentration-velocity profile of PMAT-mediated metformin uptake is sigmoidal, and is greatly stimulated by acidic pH, with the uptake rate being ~4-fold higher at pH 6.6 than at pH 7.4.

After single oral doses administration of MET (0.5 and 1.5 g), Trucker et al. (1981) showed that the maximal plasma concentration and urinary rate of excretion have been reached about 2 h. In urinary tract, the drug is reabsorbed about 30% in unchanged form, and through the fecal the unchanged forms is recovered about 30%. Urinary recoveries were significantly lower after the higher dose. Absolute oral bioavailability was estimated 50-60% of the dose. Beside the results reported by Shu *et al.* 2008 that addressed genetic variations on organic cation transportes (OCT) in enterocytes, small intestine, and hepatocytes in facilitation of the process of absorption of metformin, Zhou *et al.* (2007) reported that the significant differences in oral absorption of metformin in patients with genetic variation of OCT and the specific OCTs have not been identified. Metformin-associated lactic acidosis is the major side effect of metformin (Lalau, 2010).

The bioavailability of APIs is determined by their solubility and permeability. Lipinski *et al* (2000, 2001) reported that for the well water soluble APIs formulated in dosage forms for oral administration, the crucial factor is their permeability.

Biopharmaceutical Classification System (BCS) outlines two benchmarks for the high water solubility of APIs: one considers to 85% dissolution of the dose within 30 min at all pH values from 1 to 7.5, and another is related to the solubility of the released dose in not more the 250 mL. The high-solubility and low-solubility compound differ one to another in range of million-fold (0.1 μg/mL–100 mg/mL). One API is classified as highly intestinal permeable if more than 90% of its administered dose is absorbed in comparison with intravenous administration. Kerns *et al*. (2008) pointed out that the difference between a high-permeability and a low-permeability compound can be 50-fold (0.001–0.05 min^{-1}) The permeability of the APIs formulated in oral dosage forms depends on several factors, such as intestinal permeability, solubility in gastrointestinal system, drug release from the dosage form, liability to efflux and metabolism (Thakker, 2008).

Kerns et all. (2008) reported that the strategies for improving the permeability encompass modification of the API molecules through reduction of ionizability, increase of lipophilicity, reduction of polarity or reduction of hydrogen bond donors or acceptors. Another strategy address to changing in formulation in relation to substitution or involvement of the functional excipients, such are permeability enhancers, surfactants or pharmaceutical complexing agents.

According to Biopharmaceutics Classification System, MET belong to class III (BCS III) of compounds, which exert high solubility, poor permeability (Cheng *et al*., 2004, Blume *et al*. 1996). Several studies (Cheng *et al*. 2004, Kortejarvi *et al*. 2007, Jantratid *et al*. 2006,) enlightened that the controlling factor for the process of absorption of the pharmaceutical dosage forms is not the solubility of API in formulation, in case API belong to BSC III. Moreover, the absorption of these compounds form BSC III is affected by the gastrointestinal (GI) transit time (Sinko *et al*. 1991, Zhou *et al*. 2007 , Tsume *et al*. 2010). Sinco *et al*. (1991) observed that though the *in vitro* release profiles are slower than *in vivo* release profiles, compared to the fraction of dose absorbed, both are faster, thereby confirming that the permeability and transit time in the intestine are rate limiting to absorption and not to solubility. Hence, in order to compare bioequivalence of the two dosage forms formulated with APIs from BSC III, the release time must be within the boundaries of the absorption window in the intestine (Homsek et al., 2010).

On the basis of comparative in vitro release profiles of API from two different dosage forms formulated with the same doses, it is possible the predicted changes in dosage forms that not affect in vivo performance to be approved by applying the biowaiver approach (Homsek et al., 2010). Biowaiver concept allows minimizing review burdens in process of

marketing authorizations of the dosage forms, avoiding unnecessary clinical trials and expenses (Blume *et al.* 1996).

European Medicines Agency guidelines allow application of biowaiver in the case of BCS III compounds under very specific conditions of excipient composition of the compared materials and where dissolution is very rapid, not less than 85% dissolved in 15 min across the physiological pH range. The study carried out by Zhou *et al.* 2007 applying the validated computer simulations from a mechanistically based *in silico* permeability and intenstinal transit time within the framework of compartmental absorption transit model in the human subject, demonstrated that predicted nonlinear pharmacokinetics (PK) parameters respect to doses (maximum plasma concentration, Cmax and area under the curve, AUC), compared with corresponding human pharmacokinetics (PK) data, are not significantly affected when 100% of metformin is released within 2h of oral 500mg metformin single doses, formulated in immediate and extended release dosage forms, respectively. Hence, combining the PK modeling tool with *in vitro* dissolution, it is possible to set a range of release rates that are expected to have no impact of PK, and therefore result in bioequivalence. Crison *et al.* (2012) emphasized that the advantage of this biopharmaceutics-based approach for proposing biowaiver is to avoid the need for very rapid dissolution times and challenges of current similarity factor assessments for *in vitro* dissolution profiles, which may show nonsimilarity for bioequivalent drug products.

Bioavailability of the salts in GI tract depends on the properties of the salts and its corresponding base and acid. Salts of the basic drugs in GI tract exist as dissolved in gastric fluid, and thus remain in solution or may precipitate out in form of free base when once it passaged to intestinal compartment. Hydrochloride salts exert a common ion effect owing to the presence of chloride ions in the stomach. The bioavailability of the sulfate salts is more than three times greater than that of the hydrochloride salt. Recent studies indicate that fast interfacial counterion exchange and the presence of chloride ions quickly inhibit dissolution of free base and other acid salts not limiting to the HCl salts (Marianne Ashforl 2013). Another potential disadvantage outlined in literature (Le Heewoon, 2014) relates to the general physical properties of hydrochloride salts, such it is volatility of formed HCl, is related to its high hygroscopic nature and lower melting points and/ or decomposition temperatures comparing to salts formed with other acidic counterions. Both cases are threatened for risks of metal contamination of batches and processing equipment.

By historical backward perspective Serajuddin (2007) and Paulekuhn et al. (2007) reported that beside of all commercially marketed and approved by FDA APIs, in form of salts, 40%-60% of them exist as hydrochloride salts. The water solubility od metformin in pH range of 1.2-6.8 is 300 mg/mL and its dissolution rate is pH independent. The evidence of slower dissolution profiles exhibited by immediate-released 850 mg metformin hydrochloride tablet formulation at pH 1.2 (0.1 N HCl) and at pH 4.5 (acetate buffer) compared to that in pH 6.8 (phosphate buffer), designated as dissolution media in the United States Pharmacopeia (USP) for metformin tablets, and majority of metformin fixed-dose tablet formulation, has been attributed to the additional protonation of the monoprotonated metforminium cation at the acidic pH resulting in higher solvation and a larger hydrodynamic radii that cause slower diffusion and dissolution. The solubility of the released portion of highly dosed sustained-release metformin tablets, in the work of Desai et al. (2014), was facilitated by adding the wetting agent lauryl sulfate to the dissolution media with aim of decreasing the diffusion layer on the surface of drug released. The results of this study (Dasai et al. 2014), obtained by diffusion-ordered spectroscopy nuclear magnetic resonance technique, indicated that the decreasing release of metformin at pH 1.2 and 4.5 was associated with formation of hydrophobic and insoluble salts due to interaction of the metforminium cation with the lauryl sulfate anion in 1 : 2 stoichiometry in dissolution medium at pH 1.2 and 4.5, while this effect was absent at pH 6.8.

Metformin formulations (drug delivery systems)

Since the metformin was introduced as single dose table formulation on the U.S market by Bristol Myers Squibb, up-to-date, on the health care market have been authorized single-dose formulations (SDFs) for immediate released (IR) and extended released (XR) of the drug, as well fixed-doses combinations (FDCs) of metformin and another anti-hyperglycemic drug.

Metformin extended release (XR) versus immediate release (IR) single-dose formulation (SDFs)

The results form clinical trials headed by Fujioka *et al.* 2003, Schwartz *et al.* 2006 indicated that metformin extended released (XR) tablets with dose of 1000 mg showed to have comparable effects to that of immediate-release (IR) tablets loaded with metformin 500 mg per tablet and ordinated in twice-daily doses.

In addition, to comparable efficacy, Schwartz *et al.* 2006, Ali *et al.* 2012, Chacra *et al.* 2014, based of performed clinical trials, claimed that the metformin XR formulation given

once daily was associated with less gastrointestinal (GI) side effects than metformin IR. Metformin XR formulations were proposed (Schwartz *et al.* 2006, Ali *et al.* 2012, Donnelly *et al.* 2009) as option for therapy to patients who experience an unacceptable level of GI side effects with metformin IR.

However, a retrospective cohort study conducted by Blonde, *et al.*(2004) investigating relative GI tolerability only showed a lower incidence of GI side effects for patients who had been switched from metformin IR to patented metformin extended-released (XR) formulation, based on GelShield diffusion drug delivery system, after GI upset, or for treatment-naïve patients who had been started on metformin XR. This study did not show any difference overall in GI adverse events between groups given IR or XR formulations (Blonde, *et al.* 2004).

In a population-based study, Donnelly *et al.* (2009) demonstrated improved adherence in patients taking XR compared with IR formulations, but it is unclear from this small observational study whether the improvement in adherence was attributable to once-daily dosing or to reduced side effects.

Metformin fixed-doses formulations (FDCs)

Fixed-dose combinations (FDCs) drugs are formulations comprised of two or more drugs that are combined in a fixed ratio of doses and available in a single dosage form.

International and national guidelines for therapy do not recommend FDCs for the treatment of diabetes.

In comparison to India pharmaceutical market review (PharmTrac report) where metformin FDCs dominated over metformin single-dose formulations, SDFs, by a ratio of 3:1 between the years 2007-2012, comprising 56% of oral diabetes drugs sold in volume in 2012, in E.U. markets, according to the report issued by European Medicines Agency (EMA), exist 11 metformin FDCs authorized products. Of these four products are listed in the UK's British National Formulary (March, 2013) and Monthly Index of Medical Specialities (MIMS). The EMA publishes an European public assessment reports (EPAR), full scientific assessment reports, for every medicine granted a central marketing authorisation by the European Commission following an assessment by the EMA's Committee for Medicinal Products for Human Use (CHMP).
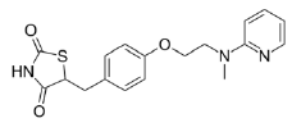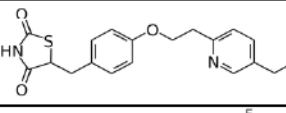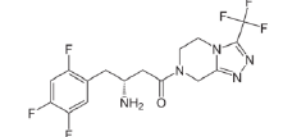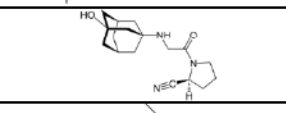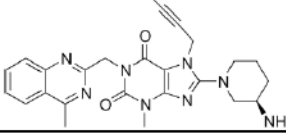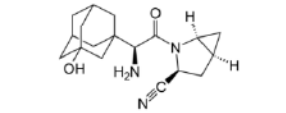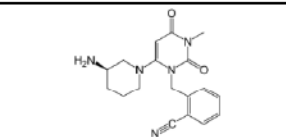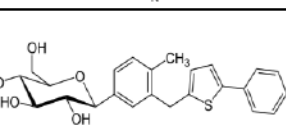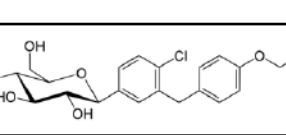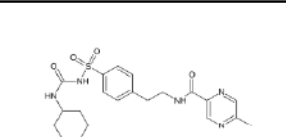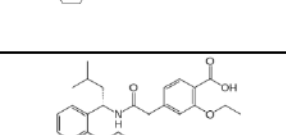
In Table 2.1 are presented metformin FDCs formulations authorized in E.U and US markets. Table 2.2 includes the chemical formulas of the eleven (11) ant diabetic drugs approved in FDCs with metformin.

Table 2.1 Metformin FDCs

APIs	Medicine name Brand	Marketing Authorization Holder	Authorized status
rosiglitazone / metformin·HCl	Avandamet	SmithKline Beecham Plc	EMA, October 2003
	Avandamet	SmithKline Beecham Plc	FDA, October 2002
pioglitazone / metformin·HCl	Competact	Takeda Pharma A/S	EMA, July 2006
	Glubrava	Takeda Global Research and Development Centre (Europe) Ltd.	EMA, December 2007
	Actoplus Met XR	Takeda	FDA approved, August 2005
sitagliptin / metformin·HCl	Efficib	Merck Sharp & Dohme Ltd.	EMA, July /2008
	Janumet	Merck Sharp & Dohme Ltd.	EMA, July 2008
	Ristfor	Merck Sharp & Dohme Ltd.	EMA, March 2010
	Velmetia	Merck Sharp & Dohme Ltd.	EMA, July 2008
	Janumet	Merck Sharp & Dohme Ltd.	FDA, March 2007
	Janumet XR	Merck Sharp & Dohme Ltd.	FDA, February 2012
vildagliptin / metformin·HCl	Eucreas	Novartis Europharm Ltd	EMA, November 2007
	Icandra (previously Vildagliptin / metformin·HCl Novartis)	Novartis Europharm Ltd.	EMA, December 2008
	Zomarist	Novartis Europharm Ltd.	EMA, Decembre 2008
linagliptin / metformin	Jentadueto	Boehringer Ingelheim International GmbH	EMA, December 2012
	Jentadueto	Boehringer Ingelheim Pharmaceuticals, Inc.	FDA, February 2012
saxagliptin hydrochloride/ metformin·HCl	Komboglyze	AstraZeneca AB	EMA, November 2011
	Kombiglyze XR	E.R. Squibb & Sons, L.L.C.	FDA, November 2010
alogliptin benzoate / metformin·HCl	Vipdomet	Takeda Pharma A/S	EMA, Spetember 2013
canagliflozin / metformin·HCl	Vokanamet	Janssen-Cilag International N.V.	EMA, April 2014
metformin·HCl / dapagliflozin propanediol monohydrate	Xigduo	Bristol-Myers Squibb/AstraZeneca EEIG	EMA, January 2014
Glipizide/ metformin·HCl	Metaglip	Bristol-Myers Squibb	FDA, October 2002
Repaglinide / metformin·HCl	PrandiMet	Novo Nordisk	June 2008

Sources: European public assessment reports, http://www.ema.europa.eu/ema/index. FDA-Approved Diabetes Medicines, http://www.fda.gov/ForPatients/Illness/Diabetes/ucm408682.htm

Table 2.2 Review of antidiabetic drugs in FDCs with metformin

Generic name	Chemical name	Chemical formula	Therapy class
Rosiglitazone	(*RS*)-5-[4-(2-[methyl(pyridin-2-yl)amino]ethoxy)benzyl]thiazolidine-2,4-dione		thiazolidinedione (TZD) class of drugs PPAR receptors (Khandoudi *et al*.,2002)
Pioglitazone	(*RS*)-5-(4-[2-(5-ethylpyridin-2-yl)ethoxy]benzyl)thiazolidine-2,4-dione		TZD class of drugs (Bogacka *et al*., 2004)
Sitagliptin	(*R*)-4-oxo-4-[3-(trifluoromethyl)-5,6-dihydro[1,2,4]triazolo[4,3-*a*]pyrazin-7(8*H*)-yl]-1-(2,4,5-trifluorophenyl)butan-2-amine		dipeptidyl peptidase-4 (DPP-4) inhibitor (Aschner *et al*, 2006)
Vildagliptin	(*S*)-1-[*N*-(3-hydroxy-1-adamantyl)glycyl]pyrrolidine-2-carbonitrile		DPP-4 inhibitor (Kalra S, 2011)
Linagliptin	, 8-[(3*R*)-3-aminopiperidin-1-yl]-7-(but-2-yn-1-yl)-3- methyl-1-[(4-methylquinazolin-2-yl)methyl]-3,7-dihydro-1*H*-purine-2,6-dione		DPP-4 inhibitor (Forst *et al* 2010)
Saxagliptin,	(1*S*,3*S*,5*S*)-2-[(2*S*)-2-amino-2-(3-hydroxy-1-adamantyl) acetyl]-2-azabicyclo[3.1.0]hexane-3-carbonitrile		DPP-4 inhibitor (Tahrani *et al*., 2009)
Alogliptin	2-({6-[(3*R*)-3-aminopiperidin-1-yl]-3-methyl-2,4-dioxo-3,4-dihydropyrimidin-1(2*H*)-yl}methyl)benzonitrile		DPP-4 inhibitor (Ndefo, *et al*., 2014)
Canagliflozin	(2*S*,3*R*,4*R*,5*S*,6*R*)-2-{3-[5-[4-Fluoro-phenyl)-thiophen-2-ylmethyl]-4-methyl-phenyl}-6-hydroxymethyl-tetrahydro-pyran-3,4,5-triol		Inhibitor of subtype 2 of the sodium-glucose transport proteins (SGLT2) (Nisly *et al*. ,2013)
Dapagliflozin	(2*S*,3*R*,4*R*,5*S*,6*R*)-2-[4-chloro-3-(4-ethoxybenzyl)phenyl]-6-(hydroxymethyl)tetrahydro-2*H*-pyran-3,4,5-triol,		SGLT2 inhibitor (Plosker *et al*., 1 2012)
Glipizide	*N*-(4-[*N*-(cyclohexylcarbamoyl)sulfamoyl]phenethyl)-5-methylpyrazine-2-carboxamide		a second generation sulfonylurea drugs, short-acting drug (Lebovitz *et al* .,1983)
Repaglinide	, (*S*)-(+)-2-ethoxy-4-[2-(3-methyl-1-[2-(piperidin-1-yl)phenyl]butylamino)-2-oxoethyl]benzoic acid		Second-generation sulfonylureas drug (Lebovitz *et al*., 1983)

Part 3

 EXPERIMENTAL SECTION

Cocrystallization screenings for selected DMs clopidogrel (thienopyridine derivative), enediol derivatives (L-ascorbic, D-ascorbic and squaric acids) and metformin (biguanide derivative) were carried out with CFs enumerated in tables 3.1; 3.2 and 3.3 respectively (supplementary part).

Cocrystallization of copidogrel. For the purpose of cocrystallization screening clopidogrel in neutral form of free base was prepare by treating the commercially available form of colopidogrel bisulfate with sodium hydrogen carbonate and using the methylene dichloride clopidogrel free base was extracted and isolated in form of oily liquid which was assay by UV-Vis spectroscopy and purity of *S* –isomer was confirmed by measuring thespecific optical rotation. The ORTEP (Burnett et al., 1996) views of the two polymorphic forms of the molecular salts of clopidogrel with picric acid was presented in Figure 3.1. The protocol for cocrystallization of clopidogrel with CFs from group of acidic compounds included dissolving the clopidogrel free base with CF in 1:1 molar ration in mixture of organic solvents and leaving the solutions for slow rate evaporation in order to obtain single crystal growth with quality for structure determination.

Cocrystallization of zwitterionic molecular crystals. The ORTEP (Burnett et al., 1996) diagrams for the resolved structures of zwiterionic CCs obtained from group of enediole derivatives with zwitterionic CFs in preparation protocol presented in table 3.2 are reported in figure 3.2.

Cocrystallization of metformin. MET·HCl used for cocrystallization screening was available from commercial supplier, USV Limited (India), with quality specification according to British Pharmacopoeia. The batch of a MET was prepared according to procedure in the patent EP 2432320 A1. MET·HCl and sodium hydroxide in equal quantity of 7 mmol, respectively ware added to 150 mL 2-propanol. The slurry was agitated on magnetic stirrer at 40°C during the 3 hours. The suspension was filtered through Celite$^®$ under the vacuum. Clear solution of the filtrate was dried under the reduced pressure by roto-evaporation method. Residue of the white dried powder in yield of 62% from the reaction of the neutralization MET·HCl was collected and tested on the 13C and 1H NMR and FT-IR spectroscopies, both spectra confirming the presence of MET in form of neutral free base.

The structures of the carbonated forms of MET determined from single crystals grown after recrystallization of neutral MET in organic solvents according to preparation protocols shown in table 3.5 are presented in figure. 3.4.

CFs saccharine and acesulfame (listed in tables 3.1; 3.2 and 3.3) in neutral, acidic forms were prepared by neutralizing the sodium salt of saccharine and potassium salt of acesulfame, respectively with mineral acid, follow by extraction and slow solvent evaporation. All other CFs (tables 3.1; 3.2, and 3. 3) utilized in cocrystallization screening were supplied with quality of Sigma Aldrich, without previous purification.

Method of preparation of the four groups of molecular crystals of MET, classified according to nature and functionality of the selected CF, and which structures have been determined is showed in the table 3.6.1 (MET PCCs with strong acidic compounds; compounds numerated 1-5) , in the table 3.6.2 (MET PCCs with monocarboxylic acids), in the table 3.6.3 (MET PCCs with the dicarboxylic acids) and in the table 3.6.4 (functional MET PCCs).

Crystal Structure Determination. Crystal data of all compounds were collected using a Nonius KappaCCD diffractometer with graphite-monochromated Mo-$K\alpha$ radiation; data sets were integrated with the Denzo-SMN package (Otwinowski [,] [1997]) and corrected for Lorentz and polarization. All structures were solved by direct methods (SIR97) (Altomare et al., [1999]) and refined by full-matrix least-squares with anisotropic non-hydrogen and isotropic hydrogen atoms. The treatment of the disordered atoms occurring in some of the structures will be described in the final publications. All calculations were performed by the SHELXL-97 (Sheldrick, 1997), PARST (Nardelli, 1995) and PLATON (Spek [,] [2005]) programs implemented in the WINGX system (Farrugia).

ORTEP (Burnett et al., 1996) views of compounds with the thermal ellipsoids at 30% probability are reported in Figures 3.5 - 3.30a,b. Crystal data, selected bond distances and angles, and H-bond and contact distances are collected in Tables 3.8.1-3.8.26. The values for the torsion angles and the angles between the planes in structure of MET cocrystallized with CF in all MET PCCs are presented in Tables 3.91-3.9.4.

Preparation by cocrystallization of reproducible batches of MET-Dichloroacetic acid 1:1 and MET-Dichloroacetic acid 1:2

The cocrystallization protocols for both MET PCCs, MET-Dichloroacetic acid 1:1 and MET-Dichloroacetic acid 1:2 were performed by following and adapting the proposed procedure for synthesys of metformin salicylate (Pérez-Fernández, 2013).

Cocrystallization of MET-Dichloroacetic acid 1:1. A methanol solution (30 mL) of MET·HCl (588.7 mg, 3.55 mmol) and sodium dichloroacetate (536,4 mg, 3.55 mmol) was stirred for 12h at room temperature. The solvent was removed under the reduced pressure in rotoevaporator, and 2-propanol (100 mL) was added to the residue solid of the reaction. The solid part (sodium chloride) of the slurry was filtered off through Celite® under the vacuum, and the clear solution was evaporated under reduced pressure by roto-evaporator. The quality of the resulting crystalline white powder was studied by X-ray powder diffraction (XRPD), that confirmed the presence of the pure solid phase of molecular crystal MET-Dichloroacetic acid 1:1.

Cocrystallization of MET-Dichloroacetic acid 1:2. To the methanol solution (30 mL) of MET·HCl (562.7 mg, 3.4 mmol) was added equal mole of sodium dichloroacetate (512.8 mg, 3.4 mmol) and dichloroacetic acid (438,1 mg, 3.4 mmol), respectively. After 12h stirring of solution at room temperature, the solvent was evaporated under reduced pressure, and 2-propanol (100 mL) was added to the solid sediment. The slurry was filtered removing the solid sodium chloride and the clear solution was evaporated under reduced pressure. The quality of the residue of white solid crystalline powder that was tested by X-ray powder diffraction (XRPD) confirmed the presence of the pure solid phase of molecular crystal MET-Dichloroacetic acid 1:2.

The XRPD patterns of MET-Dichloroacetic acid 1:1 and MET-Dichloroacetic acid 1:2 are reported in Figure 3.31.

X-Ray Powder Diffraction. Crystalline powder samples were analyzed by an X-ray powder diffractometer Bruker D8 Advance with graphite-monochromated Cu Kα radiation (λ= 1.5406 Å, generator set at 40 kV and 40 mA). Scans were performed from 3° to 40° (2θ) at a step size of 0.02° with a measuring time of 2 s per step.

 X-Ray Powder Pattern Calculation. X-ray powder diffraction patterns were calculated by the use of the Mercury CSD 2.3 program (Macrae et al, 2008) for all the crystalline powder samples prepared for biological testing, in order to assess their identity with the corresponding structures determined by single-crystal X-ray diffraction.

The Furrier Transformed Infrared (FT-IR) Spectroscopy. FT-IR spectra were generated on the Bruker Vertex 70 FT-IR instrument in range of 4000−400 cm^{-1} in

mixture of KBr powder. The FT-IR spectra for MET-Dichloroacetic acid 1:1 and MET-Dichloroacetic acid 1:2 are showed in Figure 3.32.

Differential Scanning Calorimetry (DSC) measurements were performed with a Mettler–Toledo model 820 calibrated with a standard-grade indium sample. A portion of the samples, weighting 8–9 mg, was heated in an aluminum pan from −100 to 200°C at a heating rate of 20°C/min under continuous nitrogen purge. For each sample, the glass transition temperature (Tg), melting temperature (Tm), and melting enthalpy (ΔH) were determined. Tg was taken during the second heating scan as the onset temperature point. The DSC thermograms for MET-Dichloroacetic acid 1:1 and MET-Dichloroacetic acid 1:2 are reported in the Figure 3.33.

Preliminary Tests of the Biological Activity of two PCCs. The two Metformin-Dichloroacetic acid (DCA) salts (Metformin-DCA 1:1 and Metformin-DCA 1:2) were tested on the B leukemic cell line EHEB, purchased from DSMZ (Deutsche Sammlung von Mikroorganismen und Zellkulturen GmbH, Braunschweig, Germany). EHEB cells was routinely cultured in RPMI-1640 supplemented with 10% FBS, L-glutamine and Penicillin/streptomycin. The cells were treated with a range of concentration (from 30 mM to 300uM) of the two salts or with a mix of the two compounds used in the same stoichiometric ratio. For the *in vitro* treatments, cells were seeded at a density of 1x10^6 cells/mL and cell viability was examined by Trypan blue dye exclusion after 24 and 48 hours of treatment.

The results of this first experiment on the EHEB cell line reported in the Table 3.11.

Part 4

RESULTS AND DISCUSSION

Cocrystallization screening with DM clopidogrel. Clopidogrel hydrogensulphate, which exists in two enantiomeric forms, i.e., $R(-)$ and $S(+)$ enantiomer, is a potent platelet anti-aggregation drug. The corresponding R-isomer at carbon 8 is less active and less well tolerated in pharmaceutical use (Kotar-Jordan et al. 2005). (+)Clopidogrel hydrogensulphate salt is known to crystallize in different polymorphic and pseudopolymorphic forms among which polymorphic forms 1 and 2 are commercially used in solid dosage forms on the market (Koradia et al. 2004). The cocrystallization screening for molecular salts of clopidogrel with strong organic acids indicated that it was not possible to obtain a crystalline phase with quality of single crystal for absolute structure determination were the CF was a drug, a nutraceutical or an excipient. Only screening protocol for cocrystallization using picric acid resulted in single crystal growth which determined structure indicated the existence of two polymorphic forms of clopidogrel picrate in 1:1 molar ratio (ORTEP structures reported in Figure 3.1). The undertaken experiments suggest that steric factors in the structure of clopidogrel have prevalence over the differences in   pK_a values between clopidogrel and acidic CFs preventing to the two components to find a favourable packing mode leading to cocrystallization.

Cocrystallization screening with enediol derivatives. The approach for exploring the cocrystallization of enediole derivatives was based on previously reported structures of CCs of the L-ascorbic acid (vitamin C) with zwitterionic compouns (nicotinic acid, sacrosine and betaine) (Kavuru et.al. , 2010). In the cocrystallyzation screening undertaken in experimental work, D-ascorbic acid (Isoascorbic acid) as enantiomer of L-ascorbic acid, and squairc acid (SQA) another acid with similar enediol structure were included in the protocol, aiming to explore opportunities for cocrystallization of the three enedioles with an extended series of zwitterionic CFs (listed in Table 3.2). Moreover the SQA is much more acidic than the ascorbic acids according to their pK_a values (reported in Table 3.2).

The results of the cocrystallyzation screening show that single crystals of suitable quality for X-ray diffraction structural determination could be obtained only in samples cocrystallized with SQA and seven of the 19 zwitterionic CFs reported in Table 3.2

(nicotinic acid, 2-aminopyridine-3-carboxylic acid, betaine, creatine monohydrate, sarcosine, γ-Aminobutyric acid, and ciprofloxacin). The ORTEP diagrams of all seven (7) CCs obtained are presented in Figure 3.2 (with the thermal ellipsoids at 30% probability). In the structures of six (6) CCs (i.e., SQA−nicotinic acid 1:1; SQA−2-aminopyridine-3-carboxylic acid 1:1; SQA−betaine 1:1; SQA−sarcosine 1:1; and SQA−γ-Aminobutyric acid 1:1) H-bonded carboxylate-hydroxyl supramolecular heterosynthons are present. In all these six CCs of SQA, the carboxylate moieties present in the structures of zwitterionic CFs persistently form charge-assisted H-bonds with acidic hydroxyl group of the SQA molecule. Only the CC structure of SQA with DM ciprofloxacin, which is a second-generation quinolone antibiotic, indicates that the interaction of the SQA and ciprofloxacin is related to the capacity of SQA to protonate the external N-atom in the piperazine ring of ciprofloxacine, that is responsible for its basic properties. This series of 7 CCs SQA−zwitterion will not be further discussed in this thesis because, since SQA is neither a drug nor an excipient, these CCs are of chemical interest but not of pharmaceutical relevance and will be submitted to a chemistry journal.

Unfortunately, it was not possible obtaining a crystalline solid with crystal quality sufficient for structure determination in all samples of zwitterionic compounds cocrystallized with L-ascorbic acid and D-ascorbic acid, respectively. Even when crystals were formed they were not stable. Their color turned from colorless to yellow or brownish and a deliquescent glue was formed. The crystallization procedure was repeated in a vacuum and in nitrogen atmosphere without producing suitable crystals. Not obtaining solid phases as an outcome of cocrystallization protocol with zwitterionic compounds, suggests that L-ascorbic and D-ascorbic acids have undergone to a possible redox process as result of which their structures were decomposed in presence of zwitterionic compounds.

Cocrystallization screening with metformin (MET). As a derivative of the biguanide compounds, MET contains two guanidine groups of which only one is involved in the active hydrogen bonding while the other is substituted by two methyl groups at the N-position (Figure 3.3). The biguanide structure makes MET to exist as highly resonance-stabilized system due to the conjugation between the double bonds and loan pairs of the N-atom that impacts the delocalization of the positive charge. The consequence of the conformational flexibility for resonance-stabilization of MET structure is occurrence of multiple sites for effective charge-assisted hydrogen bonding (Dumitrescu et al., 2012). Survey in the latest version of the CSD revealed that MET exists in form of

monoprotonated and diprotonated salts. Additionally, patents review indicated that there are no reported structures of the neutral form of MET. The biguanidinium mono-cation exists in five structures of MET: two polymorphs of hydrochloride salts (Hariharan , 1989; Childs et al. 2004), bromide (Lu et.al, 2004); nitrate (Zhu et al., 2003) and acetate salts (Wei et al, 2014). MET in form of biguanidinium dication has been found in structures of six salts; oxalate (Lu et al.., 2004), sulfate (Fridrichova et al., 2012), perchlorate (Guo et al, 2012), squarate salts (Serb et al., 2011).

Our attempt to grown, in a vacuum or under the purge of nitrogen, the single crystals of neutral MET from the mother liquid after the neutralization and isolation of the MET free base failed, resulting in obtaining only crystalline phases whose structure determination revealed that MET is transformed in carbonate salts of its monoprotonated cation. This preference for formation of carbonate salts is determined by the strong basicity of MET confirmed by the value for the first protonation constant (pK_{a1} above 12, see Table 3.3). The ORTEP diagrams of the carbonated forms of MET obtained in recrystallization of the freshly prepared free base of MET (protocol details see in Table 3.5) are reported in Figure 3.4.

Once the first protonation occurs in MET, the large pK_{a1} value ensures that the biguanide structure of MET remains protonated over a wide pH range. Existence of protonated MET favors the interactions with complementary functional groups with well aligned hydrogen bond donor and acceptor moieties.

The cocrystallization protocol (details shown in Tables 3.61-3.6.4) included as DM both MET and MET·HCl in combination with a large number of CFs (for a total of 96 experiments). In order to obtain PCCs of both monoprotonated and diprotonated MET, all cocrystallization experiments were carried out both in the 1:1 and 1:2 DM:CF ratio.

A total number of 26 PCCs of quality suitable for crystal structure determination were obtained, 20 containing MET in form of monoprotonated and 6 of diprotonated cation.

The crystallographic data for the unit cell parameters of all the resolved structures for 26 MET PCC revealed that, apart the MET-Saccharine 1:1 Polymorph I which crystallizes in orthrombic space group, all other MET PCCs crystallize either in triclinic or monoclinic space groups (details reported in Table 3.7).

In the six (6) PCCs of diprotonated MET the CF is always a very strong acid (dichloroacetic, trichloroacetic, oxalic, picric acid and squaric acid) having pK_a values in the range -0.5−1.2.

The molecular crystals of MET (MET PCCs) in which MET was determined to exist as diprotonated are: MET-Picric Acid 1:2 (Figure 3.8); MET-Trichloroacetic acid 1:2 (Figure

3.15a); MET-Oxalic acid hydrate 1:1:1 (Figure 3.17a); MET-Oxalic acid hydrate 1:2.5:1 (Figure 3.18), MET-Squaric acid hydrate 1:1:1 (Figure 3.9a) and MET-Dichloroacetic acid 1:2 (Figure 3.2.4).

Strong similarities can be observed in the crystallographic features, intermolecular interactions and geometry of packing motifs of the structures obtained in cocrystallization of MET

(i) with simple monocarboxylic acids: MET-Formic acid 1:1 (Table 3.8.6/ Fig 3.10); MET-Acetic acid 1:1 (Table 3.8.7/ Fig.3.11a & 3.11b); MET-Monochloracetic acid 1:1 (Table 3.8.8/ Fig.3.12a/ 3.12b); MET-Trifluoroacetic acid 1:1 (Table 3.8.9/ Fig.3.131 & 3.13b); MET-Trichloroacetic acid 1:1 (Table 3.8.10/ Fig.3.14a & 3.14b) and MET-Trichloroacetic acid 1:2 (Table 3.8.11/ Fig.3.15a & 3.15b),

(ii) with dicarboxylic acids (malonic and maleic acids) which due to intramolecular H-bond formation act as monocarboxylic acids: MET-Malonic acid 1:1 (Table 3.8.12/ Fig. 3.16a & 3.16b) and MET-Maleic acid 1:1 (Table 3.8.15/ Fig. 3.19a & 3.19b), as well as

(iii) in the structures of the compounds described as functional MET PCC as a result of dual pharmacological activity of DM and CF and which are formed with CFs from the group of monocarboxylic acids: MET-DCA 1:1 (Table 3.8.19/ Fig.3.23a & 3.23b); MET-DCA acid 1:2 (Table 3.8.20/ Fig.3.24a & 3.24b), MET-Glycolic acid 1:1 (Table 3.8.21/ Fig.3.25a & 3.25b), MET-Diclofenac 1:1 (Table 3.8.22/ Fig.3.26a & 3.26b) and MET-Salicylic acid 1:1 (Table 3.8.23/ Fig. 3.27a & 3.27b).

In all the structures of MET PCC obtained with both monocarboxylic and dicarboxylic acids is evident the presence of a well-conserved heteromeric dimer composed of a guanidinium-carboxylate synthon linked by two parallel charge-assisted H-bonds N^+—H$\cdots^-$O. This guanidinium-carboxylate synthon formed in interaction of two resonance-stabilized functional moieties (carboxylate and guanidinium) is favored by two strong charge-assisted H-bonds that direct the molecular aggregation in the formation of different packing patterns, depending whether or not N—H$\cdots$O dimers are connected in chains forming tapes of inversely related heterodimers linked one to another through centrosymmetric N—H$\cdots$O tetramers forming extended zig-zag ribbons. The heteromeric N—H$\cdots$O dimer is described as a planar ring motif composed of two proton donors and two proton acceptors forming a ring of eight atoms, corresponding to the graph set $\boldsymbol{R_2^2}$ (8), while the graph set for the N—H$\cdots$O tetramer, an eight-member ring with two proton acceptors and four proton donors, is $\boldsymbol{R_4^2}$ (8). The formation of N—H$\cdots$O tetramers is supported by two sets, each of two parallel N—H$\cdots$O H-bonds.

The structure of MET, consisting of two fused guanidine moieties, is not planar. The conformations of the MET cations in structures of all 26 MET PCCs are related to the values for the N5─C2─N1─C1 torsion angle with respect to the values found in two polymorphic forms of MET hydrochloride salt. Only the torsion angle measured in MET-Saccharine 1:1 with value of -71.2^o (Table 3.9.4, num. 24) is close to the value of -53.7^o reported in commercially available polymorph of MET hydrochloride salt which structure was resolved by Hariharan et at., (1989). In all the remaining 25 MET PCCs the values of the N5─C2─N1─C1 torsion angle are in the range from 129.1 to -162.7^o, which is in accordance to the value of 129.1^o observed in the second metastable polymorph of MET hydrochloride reported by Childs et al. (2004). The differences in torsion angles influence by steric effect the conformation placement of the ─C(NH$_2$) group in respect to the ─N(CH$_3$)$_2$ group in the structure of MET cations. The measured values for the angle between the planes P1 and P2 (the average planes of the two guanidine moieties) in structure of MET cations in all 25 MET PCCs are around 55°, and $72°$ in MET-Saccharine 1:1 (data shown in Tables 3.9.1-3.9.4). The N5─C2─N1─C1 torsion angle and the angle between the P1 and P2 planes impact the linearity of H-bonds in charge-assisted interactions with the proton acceptor groups. This inclination of the bond-angles in the parallel H-bonds formed in heteromeric N─H···O dimers impacts the zig-zag packing patterns of formation of ribbons.

Another well conserved packing motif found in almost all MET PCCs is the homomeric N─H···N dimer described as an eight-membered planar ring formed by two proton donors and acceptors ($\textbf{\textit{R}}_\textbf{2}^\textbf{2}$ (8)). This dimer corresponds to an homosynthon generated by two parallel N─H···N H-bonds between the N3 and N2H positions. Formation of the homomeric N─H···N dimers influences the lateral connection of the N─H···O heterodimers in direction of formation of the zig-zag tapes or planes. The zig-zag planes or tapes are linked one to the others in parallel packing formations through perpendicular N─H···O H-bonds formed by participation of the protons from the ─N4H2 group, which interact with H-bond acceptor atoms of the CFs.

In the MET PCCs where MET exists as dication (MET-Picric Acid 1:2 (Figure 3.8); MET-Trichloroacetic acid 1:2 (Figure 3.15a); MET-Oxalic acid hydrate 1:1:1 (Figure 3.17a); MET-Oxalic hydrate acid 1:2.5:1 (Figure 3.18), MET-Squaric acid hydrate 1:1:1 (Figure 3.9a), and MET- MET-DCA 1:2 (Figure 3.24)), another N─H···O heterodimer is observed formed by interaction between the second carboxylate moiety and the second protonation site in N3 position of the MET dication.

In the structures of MET PCCs formed with dicarboxylic acids (malonic, maleic, formic and succinic acids) there is evidence of formation of parallelly packed infinite planes of molecules.

Only in the structure of MET-Adipic acid 1:1 is evident a channel type of packing as a result of the conformational flexibility of the aliphatic chain in the molecule of adipic acid. These channels are not empty but are filled by infinite chains of H-bonded adipic acid molecules in extended conformation (Figure 3.22b).

Besides the well-known fact that MET is the drug of first choice in the oral antidiabetic therapy (Rojas & Gomes, 2013), recent studies reported its anticancer activity (Dowling et al., 2011). In addition, the anticancer effect of DCA has been reported from the clinical trials (Papandreou et al., 2011). Therefore the possible combination of these two drugs cocrystalized in form of molecular crystal that was obtained in the determined structures of MET-DCA acid 1:1 and MET-DCA acid 1:2 offered an opportunity for further studing this system of "drug-drug" CCs. For the purpose of preliminary testing the physicochemical properties and pharmacological activity of the combination of two drugs, MET and DCA cocrystallized in form of molecular crystals, methods for large-scale preparation were performed in order to optimize the reproducibility of the batches of MET-DCA 1:1 and MET-DCA 1:2, respectively.

The peak position in the experimental XRPD patterns of MET-DCA 1:1 and MET-DCA 1:2 showed in Fig.3.31 completely correspond with the calculated XRPD patterns obtained from single crystal structure determination. The FT-IR spectra of the MET-DCA 1:1 and MET-DCA 1:2 presented in Fig. 3.32 are different compared to the spectra of the native compounds. DSC thermograms for MET-DCA 1:1 and MET-DCA 1:2 in Figure 3.33 clearly indicate to the difference in values of the melting points of these two compounds recorded in heating cycle.

Furthermore, both MET-DCA 1:1 and MET-DCA 1:2 represent "drug-drug" molecular salts and their potential relevance for therapeutical purposes in treatment of cancer was assessed based on *in vitro* measurement of the vitality of the B leukemic cell line EHEB after treatment with these two molecular crystals.

The results of this first experiment on the EHEB cell line reported in the Table 3.11 show that the two Metformin–DCA salts, and in particular the 1:2, seem to exert a little greater cytotoxic activity compared to the treatment with the physical mixture of the two compounds used in the same stoichiometric ratio of the salts.

In addition, from the group of functional MET PCCs, the resolved structures of MET-Diclofenac 1:1, MET-Glycolic acid 1:1 and MET-Salicylic acid represent other molecular

crystals of the 'drug-drug" type. Moreover, the two polymorphs of the MET-Saccharine 1:1 and MET-acesulfame are functional molecular crystals composed of the combination of a drug with functional excipients from the group of artificial sweeteners.

The recently outlined effects of the topical treatment of the skin keratosis with diclofenac (Nelson, 2011), glycolic acid (Khater et al., 2014) and salicylic acid (Kootiratrakarn T, 2015) imply the opportunity to explore the molecular salts of MET in combination with each of these drugs widely used in treatment of the skin disorders.

Part 5

Conclusion and Further Perspectives

Cocrystallization of DM Colopidogrel with mono- & di- carboxylic acids failed maybe due to conformational flexibility of the thienopyridine ring.

Cocrystallization with zwitterionic compounds resulted in 7 CCs with SQA based on carboxylate… squarate heterosynthon formation (*obtained CCs are not of pharmaceutical interest*).

Cocrystallization with DM MET led to formation of 26 molecular divided in 4 groups (MET-strong acids; MET- monocarboxylic acids, MET- dicarboxylic acids & functional MET CC ("drug-drug" type of CCs).

MET CCs with mono- & di- carboxylic acids are based on guanide···carboxylate heterosynthons that result in conserved packing motifs recognized in all structures: N─H···O heterodimers and N─H···N homodimers, as well as N─H···O tetramers.

Complex packing motifs in MET CCs imply the need of systematic study on molecular recognition phenomena at the early stage of the drug development process (isolation of "lead" compounds and pharmaceutical preformulation screening).

Crystallography, method of first choice for absolute structure determination, is the best for crystallization screening, and thus reveling the intermolecular interactions between API-API and API-excipients that contribute rational approach in development of pharmaceutical formulations based on single API or fixed-dose combinations of two or more API in the solid dosage forms.

Table 3.1 Corystallization screening for clopidogrel free base and acidic compounds (part 1)

No	Coformers (CFs)	§pKa/pKb dissociation constant	Molar ratio DM:CF	Solvent(s)	Outcome of cocrystallization
1	Saccharine	*pKa 1.9	1:1	methanol/ n-pentanol 50/50 V//V %	No single crystal growth
2	Acesulfame	*pKa 2.7	1:1	methanol/ n-pentanol 50/50 V//V %	No single crystal growth
3	Picric acid	pKa 0.35	1:1	methanol/ n-pentanol 50/50 V//V %	Single crystal growth
4	Trifluoromethanesulfonic acid	pKa -12	1:1	methanol/ n-pentanol 50/50 V//V %	No single crystal growth
5	Squaric acid	pKa$_1$ 0.55 pKa$_2$ 3.48	1:1	methanol/ n-pentanol 50/50 V//V %	No single crystal growth
6	Formic acid	pKa 3.74	1:1	methanol/ n-pentanol 50/50 V//V %	No single crystal growth
7	Acetic Acid	pKa 4.75	1:1	methanol/ n-pentanol 50/50 V//V %	No single crystal growth
8	Trichloroacetic acid	pKa 0.5	1:1	methanol/ n-pentanol 50/50 V//V %	No single crystal growth
9	Trifluoroacetic acid	pKa 0.2	1:1	methanol/ n-pentanol 50/50 V//V %	No single crystal growth
10	Acetylsalicylic acid	pKa 3.64	1:1	methanol/ n-pentanol 50/50 V//V %	No single crystal growth
11	Salicylic acid	pKa1 2.95 pKa2 13.7	1:1	methanol/ n-pentanol 50/50 V//V %	No single crystal growth
12	DL-Alpha lipoic acid	pKa 4.82	1:1	methanol/ n-pentanol 50/50 V//V %	No single crystal growth
13	Benzoic acid	pKa 4.20	1:1	methanol/ n-pentanol 50/50 V//V %	No single crystal growth
15	Oxalic acid x 2H2O (Ethanedioic acid)	pKa$_1$ 1.25 pKa$_2$ 4.88	1:1	methanol/ n-pentanol 50/50 V//V %	No single crystal growth

Table 3.1 Corystallization screening for clopidogrel free base and acidic compounds (part 2)

No	Coformers (CFs)	§pKa/pKb dissociation constant	Molar ratio DM:CF	Solvent(s)	Outcome of cocrystallization
16	Fumaric acid	pKa_1 3.02 pKa_2 4.48	1:1	methanol/ n-pentanol 50/50 $V//V$ %	No single crystal growth
17	Maleic acid	pKa_1 1.93 pKa_2 6.28	1:1	methanol/ n-pentanol 50/50 $V//V$ %	No single crystal growth
18	Malonic acid	pKa_1 2.85 pKa_2 5.69	1:1	methanol/ n-pentanol 50/50 $V//V$ %	No single crystal growth
19	Succinic acid	pKa_1 4.20 pKa_2 5.65	1:1	methanol/ n-pentanol 50/50 $V//V$ %	No single crystal growth
20	DL-Malic acid	pKa_1 3.45 pKa_2 5.11	1:1	methanol/ n-pentanol 50/50 $V//V$ %	No single crystal growth
21	D-Malic acid	pKa_1 3.45 pKa_2 5.11	1:1	methanol/ n-pentanol 50/50 $V//V$ %	No single crystal growth
22	DL-Tartaric acid	pKa_1 3.17 pKa_2 4.91	1:1	methanol/ n-pentanol 50/50 $V//V$ %	No single crystal growth
23	L-Tartaric acid	*pKa_1 3.16 *pKa_2 4.02	1:1	methanol/ n-pentanol 50/50 $V//V$ %	No single crystal growth
24	Adipic acid	pKa_1 4.42 pKa_2 5.42	1:1	methanol/ n-pentanol 50/50 $V//V$ %	No single crystal growth
25	Suberic acid	pKa_1 4.52 pKa_2 5.41	1:1	methanol/ n-pentanol 50/50 $V//V$ %	No single crystal growth
26	Citric acid	pKa_1 3.12 pKa_2 4.79 pKa_3 6.39	1:1	methanol/ n-pentanol 50/50 $V//V$ %	No single crystal growth

§ NIST database

* *Reaxys*, version 1.7.8; Elsevier; 2012; RRN 969209 (accessed Aug 13, 2012).

Clopidogrel free base: pKa 5.3 *(est)* (tertiary amine)

(Ref. SPARC; pKa/property server. Ver 3. Jan, 2006. Available from, as of Apr 20, 2006: http://ibmlc2.chem.uga.edu/sparc/
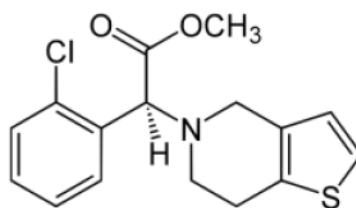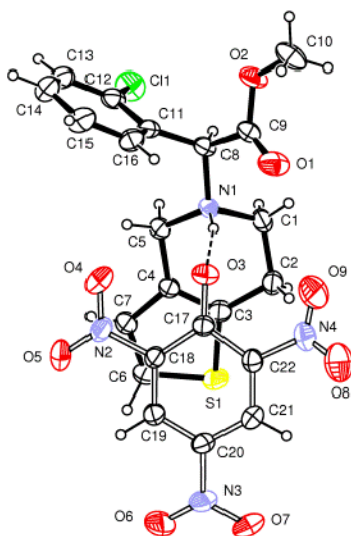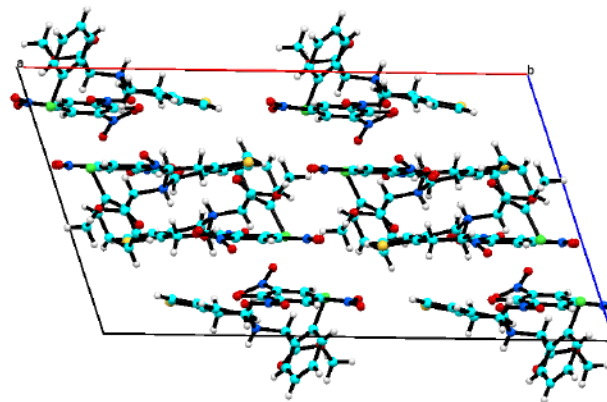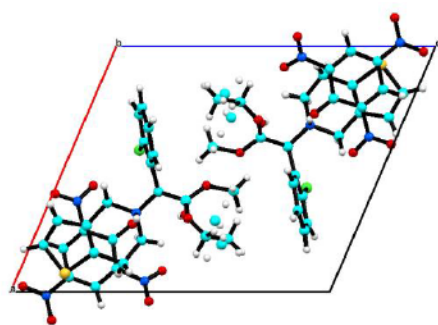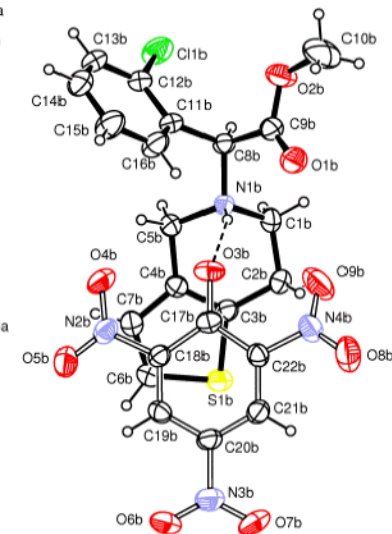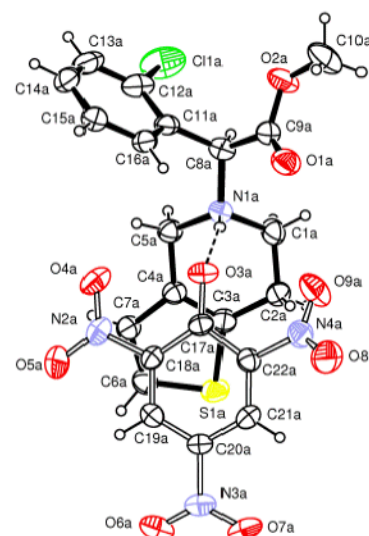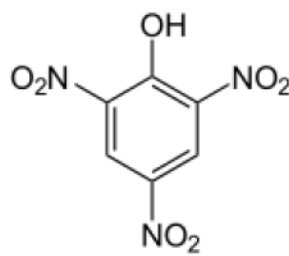
Polymorph I Clopidogrel Picrate (1:1)

Polymorph II Clopidogrel Picrate (2:2)

Figure 3.1. Clopidogrel – Picric acid 1:1 cocrystals (polymorphs I and II)

Table 3.2 Corystallization screening for enedioles derivatives (part 1)

No	CFs Studied Models	L (+) Ascorbic Acid (LAA) Mw176.12: pKa₁; 4.17p Ka₂; 11.57	D-Isoascorbic acid (DAA) Mw 176.12: pKa₁; 4.17 Ka₂; 11.57	Squaric acid (SQA) Mw 114.06: pKa₁; 1.5 pKa₂; 3.5
1	Nicotinic Acid (NIC) Mw 123.1 pKa₁: 4.82 pKa₂: 2.03	No crystalline solid/ Amorphous black flasks Methanol	No crystalline solid/ Amorphous black flasks Methanol	Single crystal grown/ White spherical crystals Resolved Structure Methanol/ Water 60/40 *V/V*
2	Isonicotinic Acid (INIC) Mw 123.1 pKa₁: 4.88 pKa₂: 1.72	No crystals/ yellow-black glassy, amorphous solid Slow rate solvent evaporation	No crystals/ yellow-black glassy, amorphous solid Slow rate solvent evaporation	Solid/ Crystalline powder mixed in amorphous mass Small size crystals Methanol/ Water 60/40 *V/V*
3	3,5-Pyridinedicarboxylic acid (3,5PDCA) Mw167.1 pKa₁: 4.03 pKa₂: 2.1 pKa₃: 1.1	Solid/ / yellow-brown crystalline powder Small size crystals Methanol/ Acetonitrile 60/40 *V/V*	Solid/ yellow-brown crystalline powder Small size crystals Two type of crystal Methanol/ Acetonitrile 60/40 *V/V*	Single crystal growth White crystals Not determined new structure Methanol/ Acetonitrile 60/40 *V/V*
4	2,4-Dihydroxypyrimidine-5-carboxylic Acid Isoorotic acid, Uracil-5-carboxylic acid Mw156.1 156,10 pKa₁: 4.05 pKa₂: 8.7	Solid/ Crystalline powder Small size crystals Methanol/ Acetonitrile 60/40 *V/V*	Solid/ Crystalline powder Methanol/ Acetonitrile 60/40 *V/V*	Solid/ white crystalline powder Small size crystals Acetonitrile
5	2,5 – Pyridinedicarboxylic Acid Mw 167.12 pKa₁: 5.02 pKa₂: 2.38	No crystals/ amorphous solid

Dissolved in Carbon tetrachloride | Solid/ crystalline powder

Dissolved in Carbon tetrachloride | Single crystal growth Solid/ bad diffraction Not determined new structure Dissolved in Carbon tetrachloride |
6	2,6 dihydroxypyridine 4-carboxylate, Citrazinic Acid Mw155.11 155.11 g/ pKa₁: 10.88 pKa₂: 3.11 pKa₃: 1.4	Solid/ Crystalline powder Small size crystals Methanol/ Acetonitrile 60/40 *V/V*	No crystals/ amorphous solid Methanol/ Acetonitrile 60/40 *V/V*	Single crystal growth Solid Not determined new structure Methanol/ Acetonitrile 60/40 *V/V*
7	2-Aminopyridine-3-carboxylic acid Mw 138.12 pKa₂:2.2 pKa₁: 6.5 (est.)	Solid/ Crystalline powder Small size crystals Methanol/ Water 60/40 *V/V*	Solid/ Crystalline powder Small size crystals Methanol/ Water 60/40 *V/V*	Single crystal growth Resolved Structure Methanol/ Water 60/40 *V/V*
8	Betaine monohydrate (x 1H₂O) Mw 135.16 pKa₁: 1.82	Solid/ no crystalline Methanol/ Acetonitrile 60/40 *V/V*	No crystals/ amorphous solid Methanol/ Acetonitrile 60/40 *V/V*	Single crystal growth Resolved Structure Methanol/ Water 60/40 *V/V*
9	L Aspartic acid Mw133.11 pKa₁: 10.88 pKa₂: 3.9 pKa₃: 1.99	Solid/ Crystalline powder Small size crystals Methanol/ Water 60/40 *V/V*	Solid/ Crystalline powder Small size crystals Methanol/ Water 60/40 *V/V*	Solid/ powder Methanol/ Water 60/40 *V/V*

Table 3.2 Corystallization screening for enedioles derivatives (part 2)

CFs — Studied Models	L (+) Ascorbic Acid (LAA) Mw176.12: pKa₁; 4.17p Ka₂; 11.57	D-Isoascorbic acid (DAA) Mw 176.12: pKa₁; 4.17 Ka₂; 11.57	Squaric acid (SQA) Mw 114.06: pKa₁; 1.5 pKa₂; 3.5
10 Aspartame N-(L-α-Aspartyl)-L-phenylalanine methyl ester, Asp-Phe methyl ester, Asp-Phe-OMe Mw 294.30 pKa₂; 3.19 pKa₁; 7.87	No crystals/ amorphous solid Ethanol/water/ Tetrahydrofuran 30/30/30 V/V/V % Amorphous solid	No crystals/ amorphous solid Ethanol/water/ Tetrahydrofuran 30/30/30 V/V/V % Amorphous solid	No crystals/ amorphous solid 30/30/30 V/V/V % Amorphous solid
11 Creatine monohydrate Mw 149.15: pKa₂;: 2.63 pKa₁: 14.3	Single crystal growth Determined Creatine crystals Water/ Ethanol 50/50 V/V %	Single crystal growth Determined Creatine crystals Water/ Ethanol 50/50 V/V %	Single crystal grown Resolved Structure Water/ Ethanol 50/50 V/V %
12 L-Carnitine inner salt Mw 161.20: pKa₁;: 4.83 pKa₂ 9.2	No crystals/ amorphous solid Water/ ethanol 50/50 V/V %	No crystals/ amorphous solid Water/ ethanol 50/50 V/V %	No crystals/ amorphous solid Water/ ethanol 50/50 V/V %
13 L-Theanine Nγ-Ethyl-L-glutamine, L-Glutamic acid γ-(ethylamide) Mw 160.19: pKa₂; 2.35 pKa₁;9.31	Glassy solid Water/ Methanol 50/50 V/V %	Single crystal grown Small sized crystals Water/ Methanol 50/50 V/V %	No crystals/ amorphous solid Water/ Methanol 50/50 V/V %
14 Sarcosine N-methylglycine Mw 89.09: pKa₁; 2.23 pKa₂; 10.01	Single crystal growth Determined Sarcosine crystals Water/ Methanol 50/50 V/V %	No crystals/ amorphous solid Water/ Methanol 50/50 V/V %	Single crystal grown Resolved Structure Methanol/ Water 50/50 V/V
15 Taurine Mw 125.15: pKa₁: 1.5 pKa₂: 9.06	Single crystal growth Determined Taurien crystals Water/ Methanol 50/50 V/V %	Single crystal growth Determined Taurien crystals Water/ Methanol 50/50 V/V %	Single crystal growth Determined Taurien crystals Kneaded with methanol Dissolved in methanol
16 γ-Aminobutyric acid Mw 103.12: pKa₂; 4.23, pKa₁.10.43	Crystalline solid Water/ Tetrahydrofurane 50/50 V/V %	No crystals/ amorphous solid	Single crystal grown Resolved Structure Methanol/ Water 50/50 V/V
17 Gabapentin Mw 103.12: pKa₁; 3.68 pKa₂.; 10.70	No crystals/ amorphous solid	No crystals/ amorphous solid	Single crystal grown Squaric Acid determined crystals Ethanol/Water 80/20 V/V %
18 Ofloxacin Mw 361.37 pKa₂: 6.22 pKa₁: 7.81	No crystals / Solid white powder	No crystals / Solid white powder	No crystals/ amorphous solid powder
19 Ciprofloxacin Mw 385.8 pKa₂: 6.42 pKa₁: 8.79	No crystals / Solid white powder Methanol	No crystals / Solid white powder Methanol	Single crystal grown Resolved structure Methanol/ Water 80/20 V/V %

pKa values (Sources: NIST database and *Reaxys*, version 1.7.8; Elsevier; 2012; RRN 969209 (accessed Aug 13, 2012).

Samples of crystallization of multicomponent crystals
 (Studied models - Conformer 1: 1 molar ratio)

Squaric Acid –Nicotinic hemihydrate Acid 1 : 1 :1
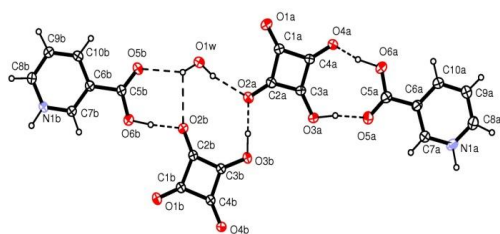
Squaric Acid - 2-Aminopyridine-3-carboxylic acid 1:1

Squaric Acid - Ciprofloxacin 1:1

Squaric Acid- Betaine 1 : 1
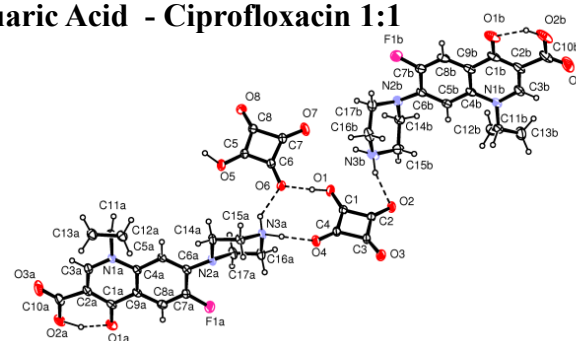
Squaric Acid - Sarcosine 1:1
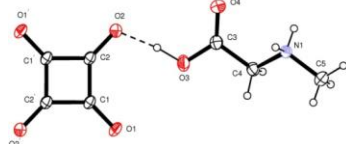
Squaric Acid - Creatine 1: 1
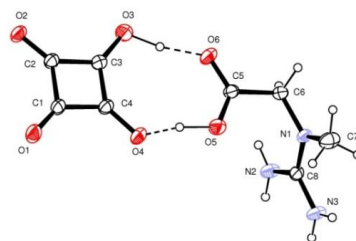
Squaric Acid - γ- Aminobutyric acid 1: 1
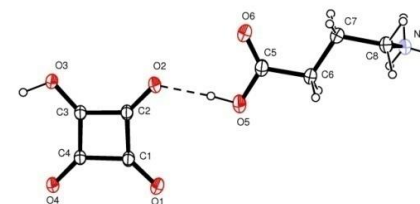
Fig. 3.2. Cocrystalof Squaric acid (SQA) with zwitterionic compounds

Table 3.3. Cocrystallization screening carried out with neutral MET (part 1)

No	Coformers (CFs)	§pKa/pK_b dissociation constant	Molar ratio DM:CF	Solvent(s)	Outcome of cocrystallization
1	Saccharine	*pKa 1.9	1:1	n-pentanol	crystalline solid; single crystals grown
2	Acesulfame	*pKa 2.7	1:1	n-pentanol	Crystalline solid, single crystal grown
3	Picric acid	pKa 0.35	1:1	n-pentanol	crystalline solid; single crystals grown
			1:2	n-pentanol	crystalline solid; single crystals grown
4	Trifluoromethanesulfonic acid	*pKa -12	1:1	methanol/ n-pentanol 50/50 $V//V$ %	no crystalline solid phase
5	Aniline-2-sulfonic acid	*pKa$_1$ 2.41	1:1	methanol/ acetonitrile 40/60 $V//V$ %	no crystalline solid phase
6	Phosphoric acid 85 wt% in water	pKa$_1$ 0.0 pKa$_1$ 2.148 pKa$_2$ 7.198 pKa$_3$ 12.37	1:1	methanol	no crystalline solid phase
			1:2	methanol	no crystalline solid phase
			2:1	methanol	crystalline solid; single crystals grown
7	Nitric acid 90%	pKa$_1$ -1.3	1:1	methanol	crystalline solid; single crystals grown
			1:2	methanol	no crystalline solid phase
			2:1	methanol	no crystalline solid phase
8	Sulfuric acid	pKa$_1$ -3 pKa$_2$ 1.99	1:1	methanol	no crystalline solid phase
			1:2	methanol	no crystalline solid phase
			2:1	methanol	no crystalline solid phase
9	L (+) Ascorbic acid	pKa$_1$ 4.17 pKa$_2$ 11.72	1:1	methanol	no crystalline solid phase
			1:1	ethanol	no crystalline solid phase
			1:2	methanol	no crystalline solid phase
			1:2	ethanol	no crystalline solid phase

Table 3.3. Cocrystallization screening carried out with neutral MET (part 2)

No	Coformers (CFs)	[§]pKa/pK_b dissociation constant	Molar ratio DM:CF	Solvent(s)	Outcome of cocrystallization
10	D-Isoascorbic acid	pKa$_1$ 4.26 pKa$_2$ 11.64	1:1	methanol	no crystalline solid phase
			1:1	ethanol	no crystalline solid phase
			1:2	methanol	no crystalline solid phase
			1:2	ethanol	no crystalline solid phase
11	Squaric acid	pKa$_1$ 0.55 pKa$_2$ 3.48	1:1	ethanol	crystalline solid; single crystals grown
			2:1	ethanol	no crystalline solid phase
12	Formic acid	pKa 3.74	1:1	methanol/ n-pentanol 50/50 V/V %	crystalline solid; single crystals grown
13	Acetic Acid	pKa 4.75	1:1	methanol	crystalline solid; single crystals grown
			1:2	methanol	crystalline solid; single crystals grown
14	Dehydroacetic acid	[*]pKa 6	1:1	methanol	no crystalline solid phase
15	Monochloroacetic acid	pKa 2.82	1:1	methanol/ n-pentanol 50/50 V/V %	crystalline solid; single crystals grown
			1:2	methanol/ n-pentanol 50/50 V/V %	crystalline solid; single crystals grown
16	Dichloroacetic acid	pKa 1.1	1:1	methanol/ n-pentanol 50/50 V/V %	crystalline solid; single crystals grown
			1:2	methanol/ n-pentanol 50/50 V/V %	crystalline solid; single crystals grown
17	Trichloroacetic acid	pKa 0.5	1:1	methanol/ water 20/80 V/V %	crystalline solid; single crystals grown
			1:2	methanol/ water 20/80 V/V %	crystalline solid; single crystals grown
18	Trifluoroacetic acid	pKa 0.2	1:1	methanol/ n-pentanol 50/50 V/V %	crystalline solid; single crystals grown
			1:2	methanol/ n-pentanol 50/50 V/V %	crystalline solid; low quality of single crystals

Table 3.3. Cocrystallization screening carried out with neutral MET (part 3)

No	Coformers (CFs)	§pKa/pK$_b$ dissociation constant	Molar ratio DM:CC	Solvent(s)	Outcome of cocrystallization
19	Glycolic Acid	pKa 3.83	1:1	methanol/n-pentanol 50/50 V/V %	crystalline solid; single crystals grown
			1:2	methanol/ n-pentanol 50/50 V/V %	no crystalline solid phase
20	Acetylsalicylic acid	pKa 3.64	1:1	n-pentanol	crystalline solid; single crystals grown
			1:2	n-pentanol	no crystalline solid phase
21	Salicylic acid	pKa$_1$ 2.95 pKa$_2$ 13.7	1:1	ethanol/ n-pentanol 20/80 V/V %	no crystalline solid phase
			1:2	ethanol/ n-pentanol 20/80 V/V %	no crystalline solid phase
			2:1	ethanol/ n-pentanol 20/80 V/V %	no crystalline solid phase
22	DL-Alpha lipoic acid	*pKa 4.82	1:1	ethanol/ n-pentanol 20/80 V/V %	no crystalline solid phase
				ethanol	no crystalline solid phase
			1:2	ethanol/ n-pentanol 20/80 V/V %	no crystalline solid phase
				ethanol	no crystalline solid phase
			2:1	ethanol/ n-pentanol 20/80 V/V %	no crystalline solid phase
				ethanol	no crystalline solid phase
23	Benzoic acid	pKa 4.20	1:1	n-pentanol	no crystalline solid phase
24	4-Methylbenzoic acid (*p*-Toluic acid)	pKa 4.37	1:1	methanol/ n-pentanol 50/50 V/V %	no crystalline solid phase
25	2,4-Dimethylbenzoic acid	pKa 4.20	1:1	n-pentanol	no crystalline solid phase
26	2,4-Dimethoxybenzoic acid	pKa 3.50	1:1	n-pentanol	crystalline solid; no single crystals grown of MET PCC
27	2,4-Dihydroxybenzoic acid	pKa$_1$ 3.32 pKa$_2$ 8.64	1:1	n-pentanol	no crystalline solid phase
28	*trans*-4-Hydroxycinnamic acid (*p*-Coumaric acid)	*pKa 4.08	1:1	n-pentanol	no crystalline solid phase

Table 3.3. Cocrystallization screening carried out with neutral MET (part 4)

No	Coformers (CFs)	§pKa/pK_b dissociation constant	Molar ratio DM:CC	Solvent(s)	Outcome of cocrystallization
29	3,4,5-Trihydroxybenzoic acid (Gallic acid)	pKa$_1$ 4.44 pKa$_2$ 9.11 pKa$_3$ 11.38	1:1	dimethyl sulfoxide (DMSO)	no crystalline solid phase
30	2-Hydroxy-2-phenylacetic acid (DL-Mandelic Acid)	pKa 3.40	1:1	n-pentanol	no crystalline solid phase
31	Pyridine-3-carboxylic acid	pKa$_1$ 2.03 pKa$_2$ 4.82	1:1	n-pentanol	no crystalline solid phase
32	Pyridine-4-carboxylic acid (Isonicotinic acid)	pKa$_1$ 2.72 pKa$_2$ 4.88	1:1	dimethyl sulfoxide (DMSO)	no crystalline solid phase
33	2-Aminopyridine-3-carboxylic acid (2-Aminonicotinic acid)	*pKa 9.1	1:1	n-pentanol	no crystalline solid phase
34	2,6-Dihydroxypyridine-4-carboxylic acid (Citrazinic acid)	*pKa$_1$ 2.78	1:1	dimethyl sulfoxide (DMSO)	no crystalline solid phase
35	2,4-Dihydroxypyrimidine-5-carboxylic acid (Uracil-5-carboxylic acid)	pKa$_1$ 4.05 pKa$_2$ 8.79 (-N1-H)	1:1	n-pentanol	no crystalline solid phase
36	Furan-3-carboxylic acid (3-Furoic acid)	*pKa$_1$ 3.82	1:1	dimethyl sulfoxide (DMSO)	no crystalline solid phase
37	Diclofenac (free acid form) 2-[(2,6-Dichlorophenyl) amino]benzeneacetic acid	*pKa 3.99	1:1	methanol /n-pentanol 50/50 *V/V* %	crystalline solid; single crystals grown
38	Indomethacin 1-(4-Chlorobenzoyl)-5-methoxy-2-methyl-3-indoleacetic acid	*pKa 4.5	1:1	methanol	no crystalline solid phase
			1:1	methanol /n-pentanol 10/90 *V/V* %	no crystalline solid phase
39	Ibuprofen (±)-2-(4-Isobutylphenyl) propanoic acid	*pKa 4.31	1:1	methanol	no crystalline solid phase
			1:1	methanol/ acetonitrile 50/50 *V/V* %	no crystalline solid phase
40	Clofibric acid 2-(*p*-Chlorophenoxy)-2-methylpropionic acid	*pKa 4.62	1:1	methanol	crystalline solid; low quality of single crystals grown
			1:1	methanol/ acetonitrile 50/50 *V/V* %	no crystalline solid phase
41	Bezafibrate 2-[4-[2-(4-Chlorobenzamido) ethyl]phenoxy]-2-methylpropanoic acid	*pKa 5.09	1:1	methanol	no crystalline solid phase
			1:1	methanol/ acetonitrile 50/50 *V/V* %	no crystalline solid phase

Table 3.3. Cocrystallization screening carried out with neutral MET (part 5)

No	Coformers (CFs)	§pKa/pKb dissociation constant	Molar ratio DM:CF	Solvent(s)	Outcome of cocrystallization
42	Gemfibrozil Dimethylphenoxy)-2,2-dimethylpentanoic acid	*pKa 4.7	1:1	methanol	no crystalline solid phase
			1:1	methanol/ acetonitrile 50/50 V/V %	no crystalline solid phase
43	Salsalate (Salicylsalicylic acid)	**pKa$_1$ 3.5 **pKa$_2$ 9.8	1:1	ethanol	no crystalline solid phase
44	Oxalic acid x 2H$_2$O (Ethanedioic acid)	pKa$_1$ 1.25 pKa$_2$ 4.88	1:1	methanol/ n-pentanol 50/50 V/V %	crystalline solid; single crystals grown
			1:2	methanol/ n-pentanol 50/50 V/V %	crystalline solid; single crystals grown
45	Fumaric acid	pKa$_1$ 3.02 pKa$_2$ 4.48	1:1	methanol/ n-pentanol 50/50 V/V %	crystalline solid; single crystals grown
46	Maleic acid	pKa$_1$ 1.93 pKa$_2$ 6.28	1:1	n-pentanol	crystalline solid; single crystals grown
47	Malonic acid	pKa$_1$ 2.85 pKa$_2$ 5.69	1:1	methanol/ n-pentanol 50/50 V/V %	crystalline solid; single crystals grown
48	Succinic acid	pKa$_1$ 4.20 pKa$_2$ 5.65	1:1	methanol/ n-pentanol 50/50 V/V %	crystalline solid; single crystals grown
49	DL-Malic acid	pKa$_1$ 3.45 pKa$_2$ 5.11	1:1	methanol/ n-pentanol 50/50 V/V %	crystalline solid; no single crystals grown of MET PCC
50	D-Malic acid	pKa$_1$ 3.45 pKa$_2$ 5.11	1:1	methanol/ n-pentanol 50/50 V/V %	crystalline solid; no single crystals grown of MET PCC
51	DL-Tartaric acid	pKa$_1$ 3.17 pKa$_2$ 4.91	1:1	methanol/ n-pentanol 50/50 V/V %	crystalline solid; no single crystals grown of MET PCC
52	L-Tartaric acid	*pKa$_1$ 3.16 *pKa$_2$ 4.02	1:1	methanol/ n-pentanol 50/50 V/V %	crystalline solid; no single crystals grown of MET PCC
53	Adipic acid	pKa$_1$ 4.42 pKa$_2$ 5.42	1:1	methanol/ n-pentanol 30/70 V/V %	crystalline solid; single crystals grown
			2:1	methanol/ n-pentanol 30/70 V/V %	crystalline solid; single crystals grown
54	Suberic acid	pKa$_1$ 4.52 pKa$_2$ 5.41	1:1	methanol/ n-pentanol 50/50 V/V %	no crystalline solid phase
			2:1	methanol/ n-pentanol 50/50 V/V %	no crystalline solid phase
55	Itaconic acid	pKa$_1$ 3.85 pKa$_2$ 5.57	1:1	methanol/ n-pentanol 50/50 V/V %	no crystalline solid phase

Table 3.3. Cocrystallization screening carried out with neutral MET (part 6)

No	Coformers (CFs)	§pKa/pK_b dissociation constant	Molar ratio DM:CF	Solvent(s)	Outcome of cocrystallization
56	3,5-Pyridinedicarboxylic acid	pKa$_1$ 2.10 pKa$_2$ 4.30	1:1	methanol	no crystalline solid phase
57	2,5-Pyridinedicarboxylic acid	pKa$_1$ 2,25 pKa$_2$ 5.02	1:1	methanol	no crystalline solid phase
58	2,6 dimethyl-3,5-pyridinedicarboxylic acid	n.a	1:1	methanol	no crystalline solid phase
59	Phthalic acid (1,2-Benzenedicarboxylic acid)	pKa$_1$ 2,95 pKa$_2$ 5.41	1:1	methanol	crystalline solid; no single crystals grown of MET PCC
60	Isocitric acid lactone (DL-2-Oxotetrahydrofuran-4,5-dicarboxylic acid)	pKa$_1$ 3.06 pKa$_2$ 4.29 pKa$_3$ 5.05	1:1	methanol/ n-pentanol 50/50 *V/V*%	no crystalline solid phase
61	Folic acid (Pteroyl-L-glutamic acid)	*pKa$_1$ 4.92 *pKa$_2$ 8.04	1:1	DMSO/ water 50/50 *V/V*%	no crystalline solid phase
			1:1	ethanol/ water 20/80 *V/V*%	no crystalline solid phase
			2:1	ethanol / water 20/80 *V/V*%	no crystalline solid phase
62	Trimesic acid (Benzene-1,3,5-tricarboxylic acid)	pKa$_1$ 3.12 pKa$_2$ 4.10 pKa$_3$ 5.18	1:1	ethanol	no crystalline solid phase
63	Citric acid	pKa$_1$ 3.12 pKa$_2$ 4.79 pKa$_3$ 6.39	1:1	ethanol	crystalline solid; no single crystals grown of MET PCC
64	Phloroglucinol	pKa$_1$ 8.42 pKa$_2$ 8.79	1:1	n-pentanol	crystalline solid; no single crystals grown of MET PCC
65	Quercetin (2-(3,4-dihydroxyphenyl)-3,5,7-trihydroxy-4H-chromen-4-one)	*pKa$_1$ 5.70 *pKa$_2$ 7.0 *pKa$_3$ 9.6 *pKa$_4$ 11.8	1:1	methanol/ n-pentanol 10/90 *V/V*%	no crystalline solid phase
66	Curcumine	*pKa$_1$ 8.1 *pKa$_2$ 10.45	1:1	ethanol	no crystalline solid phase
67	Pyridixine	pKa$_1$ 4.09 pKa$_2$ 8.9	1:1	n-pentanol	crystalline solid; no single crystals grown of MET PCC
68	Nicotinamide	pKa$_1$ 3.35	1:1	n-pentanol	no crystalline solid phase
69	Pyridine *N*-oxide	*pKb$_1$ 0.79	1:1	methanol	crystalline solid; no single crystals grown of MET PCC
70	4-Nitropyridine *N*-oxide	*pKb$_1$ -1.7	1:1	methanol/ acetonitrile 50/50 *V/V*%	crystalline solid; no single crystals grown of MET PCC

Table 3.3. Cocrystallization screening carried out with neutral MET (part 7)

No	Coformers (CFs)	§pKa/pK$_b$ dissociation constant	Molar ratio DM:CF	Solvent(s)	Outcome of cocrystallization
71	Caffeine (1,3,7-Trimethylxanthine)	*pKb$_1$ 0.61	1:1	ethanol/ n-pentanol 50/50 V/V%	no crystalline solid phase
72	Theophylline (1,3-Dimethylxanthine)	*pKa$_1$ 8.55	1:1	ethanol/ n-pentanol 50/50 V/V%	no crystalline solid phase
73	Theobromine (3,7-Dimethylxanthine)	*pKa$_1$ 0.3 *pKa$_2$ 11	1:1	methanol/water 20/80 V/V%	no crystalline solid phase
74	Pentoxifylline (3,7-Dimethyl-1-(5-oxohexyl)xanthine)	**pKa$_1$ 0.28	1:1	n-pentanol	no crystalline solid phase
75	Pyrazine	***pKa$_1$ 0.97	1:1	methanol/ n-pentanol 10/90 V/V%	no crystalline solid phase
76	2,3,5,6-Tetramethylpyrazine	*pKa$_1$ 3.7 *pKa$_2$ 11	1:1	methanol/ n-pentanol 50/50 V/V%	no crystalline solid phase
77	Aminopyrazine (Pyrazinamine)	pKa$_1$ 11.2	1:1	methanol/ n-pentanol 10/90 V/V%	crystalline solid; no single crystals grown of MET PCC
78	Aspartame	pKa$_1$ 2.98 pKa$_2$ 7.87	1:1	ethanol/ water 90/10 V/V%	Solid powder/ no crystal grown
79	Creatine monohydrate	*pKa$_1$ 2.63 *pKa$_2$ 11.0	1:1	ethanol	no crystalline solid phase
80	L-Carnitine inner salt	*pKa$_1$ 4.83 *pKa$_2$ 9.2	1:1	ethanol	no crystalline solid phase
81	L-Theanine L-Glutamic acid γ-ethylamide	*pKa$_1$ 2.35 *pKa$_2$ 9.31	1:1	ethanol	no crystalline solid phase
82	Sarcosine (N-methylglycine)	pKa$_1$ 2.11 pKa$_2$ 10.2	1:1	ethanol	no crystalline solid phase
83	Taurine	pKa$_1$ -0.33 pKa$_2$ 9.06	1:1	ethanol	no crystalline solid phase
84	γ-Aminobutyric acid	*pKa$_1$ 4.07 *pKa$_2$ 10.37	1:1	ethanol	no crystalline solid phase
85	Gabapentin	*pKa$_1$ 3.712 *pKa$_2$ 9.37	1:1	ethanol	no crystalline solid phase
86	2,4-Diamino-6-phenyl-1,3,5-triazine (Benzoguanamine)	*pKa$_1$ 10.14	1:1	methanol/ n-pentanol 10/90 V/V%	no crystalline solid phase
87	7,7,8,8-Tetracyanoquinodimethane (TCNQ)	*pKa$_1$ 7.10 *pKa$_2$ 10.30	1:1	methanol	no crystalline solid phase

§ NIST database

* *Reaxys*, version 1.7.8; Elsevier; 2012; RRN 969209 (accessed Aug 13, 2012).

** In "*Analytical Profiles of Drug Substances and Excipients*", Volume 25, Harry G. Brittain

*** Journal of Heterocyclic Chemistry, 1985, vol.22, p.1143–1144

Drug Model (DM): neutral metformin (MET): pKa$_1$ 12.40; pKa$_2$ 2.96 (NIST database)

Table 3.4. Cocrystallization screening carried out with the monoprotonated salt MET·HCl

No	Coformers (CFs)	§pKa/pK_b dissociation constant	Molar ratio DM:CF	Solvent(s)	Outcome of cocrystallization
1	Saccharinate sodium	*pKa 1.9	1/1	n-pentanol	crystalline solid; single crystals grown
2	Acesulfame potassium	*pKa 2.7	1/1	n-pentanol	crystalline solid; single crystals grown
3	Diclofenacs sodium	*pKa 3.99	1/1	n-pentanol	crystalline solid; single crystals grown
4	Calcium pantothenate	pKa$_1$ 4.41 pKa$_2$ 9.698	1/1	n-pentanol	no crystalline solid phase
5	Sodium ascorbate	pKa$_1$ 4.17 pKa$_2$ 11.72	1/1	n-pentanol	no crystalline solid phase
6	L-Ascorbic acid 2-phosphate trisodium salt	pKa$_1$ 4.17 pKa$_2$ 11.72	3/1	n-pentanol	no crystalline solid phase
7	Sodium chloroacetate	pKa 2.82	1/1	n-pentanol	crystalline solid; single crystals grown
8	Sodium dichloroacetate	pKa 1.1	1/1	n-pentanol	crystalline solid; single crystals grown
9	Pyruvic acid sodium salt, (α-Ketopropionic acid sodium salt)	pKa$_1$ 2.48	1/1	isopropanol	crystalline solid; no single crystals grown of MET PCC

§ NIST database
* *Reaxys*, version 1.7.8; Elsevier; 2012; RRN 969209 (accessed Aug 13, 2012).
** In "*Analytical Profiles of Drug Substances and Excipients*", Volume 25, Harry G. Brittain
*** Journal of Heterocyclic Chemistry, 1985, vol.22, p.1143–1144
Drug Model (DM): neutral metformin (MET): pKa$_1$ 12.40; pKa$_2$ 2.96 (NIST database)

monoprotonated metformin

neutral metformin

diprotonated metformin,
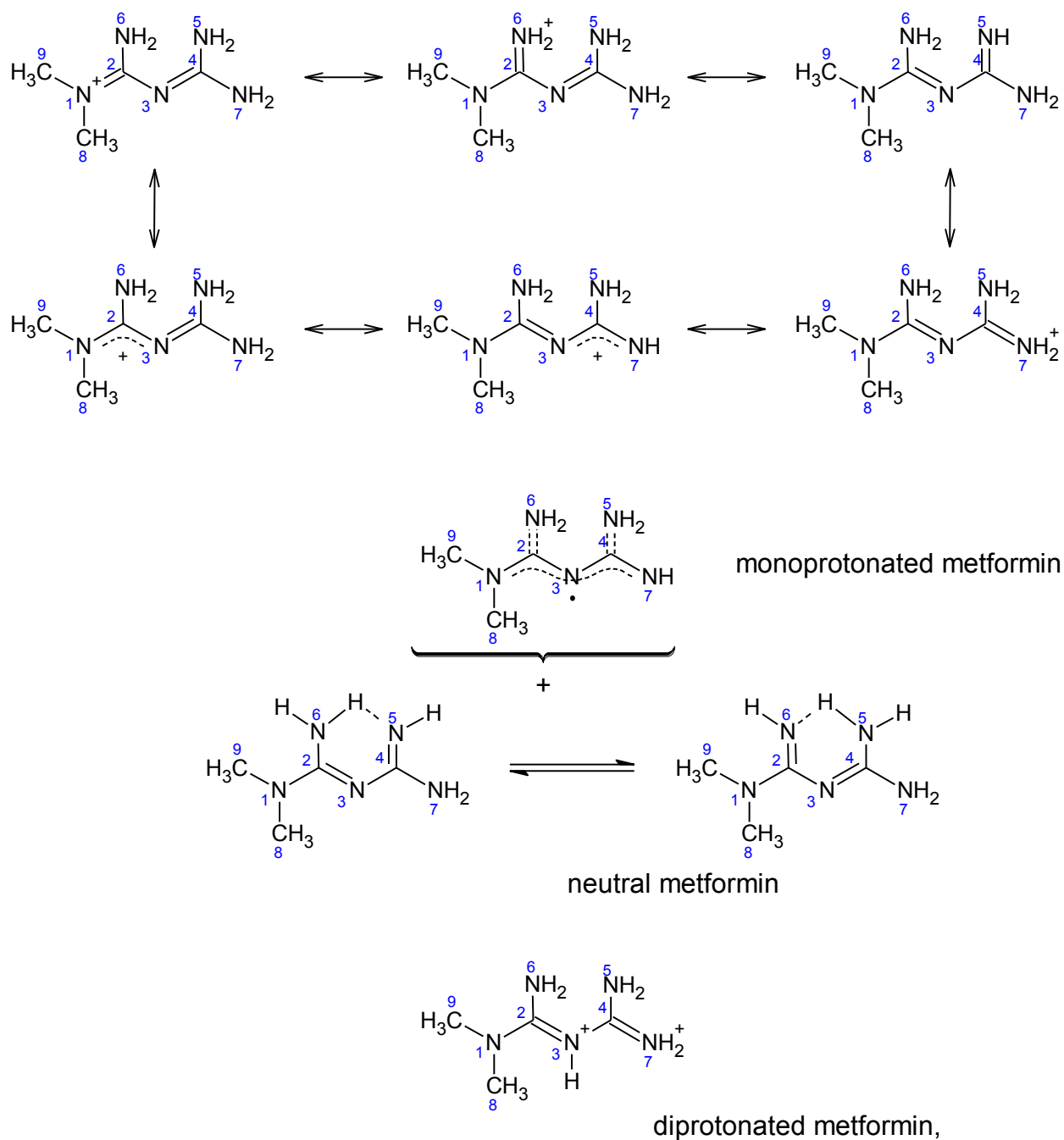
Ref: Alizadeh, et. Al, 2012; Clement & Girreser, 1999; Nanubolu et. Al, 2013; Trouillas et.al., 2013; Bharatam et al. 2005

Fig. 3.3 Resonance stabilized monoprotonated, deprotonated and neutral form of MET

Table 3.5. Experimental screening for single crystal growth of neutral metformin (MET)

Lab code	Metformin carbonated molecular salts	Method of preparation
METF2	$METF^+ + HCO_3^-$	Metformin free base recrystallized in benzene. Complete dissolved in benzene, slightly heated. Clear solution left for slow solvent evaporation
METF3	$METF^+ + GUA^+ + CO_3^{--}$	Metformin free base dissolved in ethanol, heated up to boiling. Complete dissolved. Clear solution left for slow solvent evaporation
METF7	$2METF^+ + CO_3^- + i\text{-}Pr\text{-}OH + 3H_2O$	Metformin free base dissolved in toluene, slightly heated. Complete dissolved. Clear hot solution left for slow solvent evaporation
METF	$4METF^+ + 2.CO_3^- + 6H_2O$	Part of Metformin mother liquid: Filtered solution of neutralized metformin HCl with NaOH in isopropyl alcohol). Filtered isopropyl alcohol solution of neutralized metformin HCl left for slow solvent evaporation on ambient temperature and pressure. Bulk isopropyl solution of neutralized metformin HCl was transformed in free metformin base by roto-evaporation.
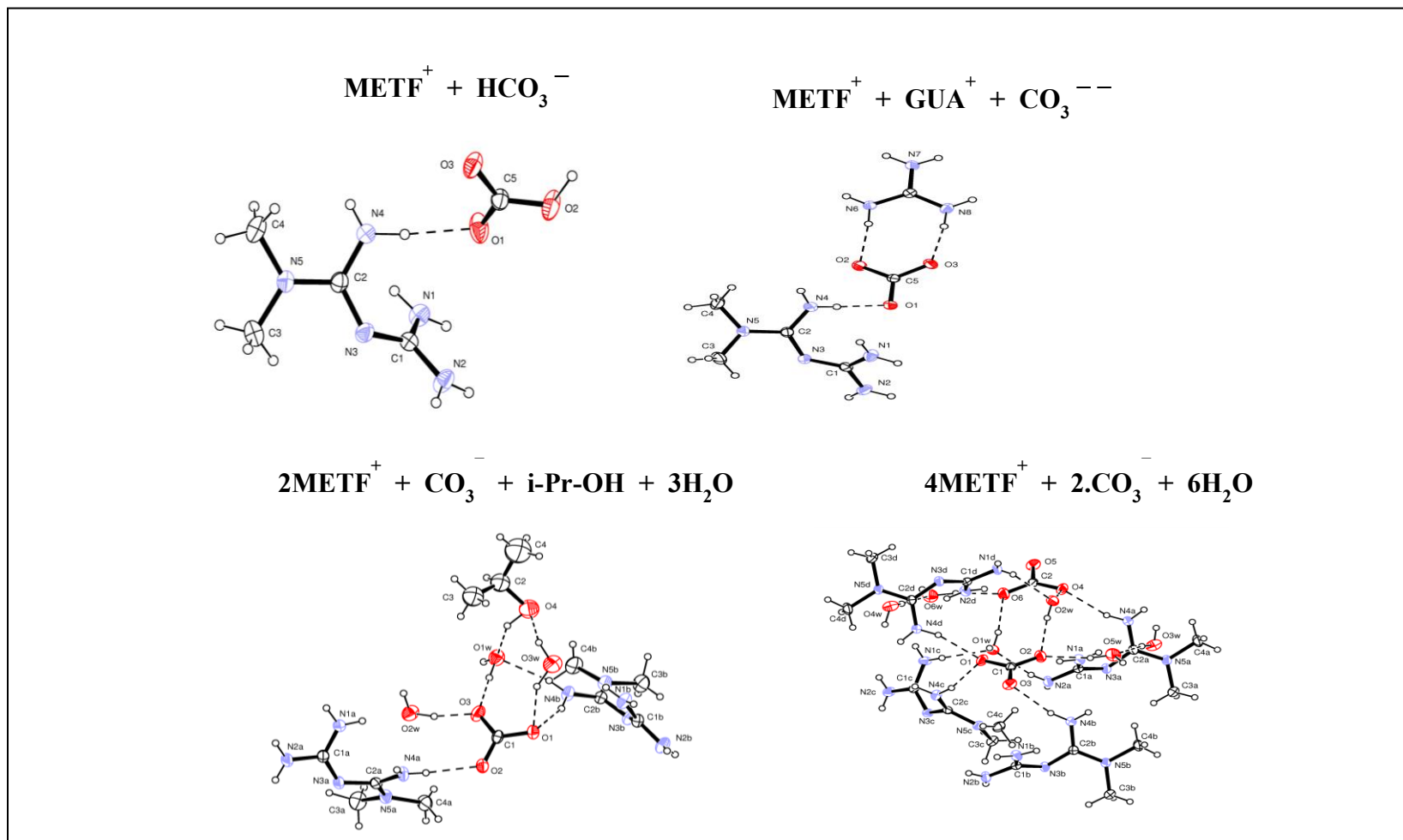
Fig. 3.4. Structures determined of carbonated form of single crystals of MET grown from mother liquid solutions of neutral MET

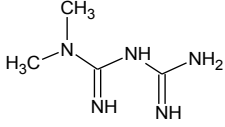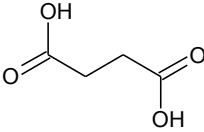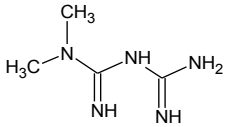**Table 3.6.1 Method of preparation of MET PCCs with strong acidic compounds (compounds no. 1-5)**
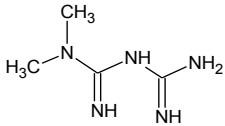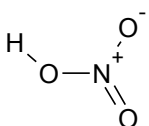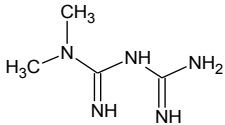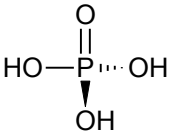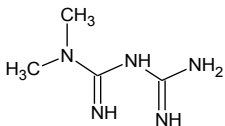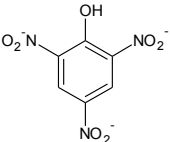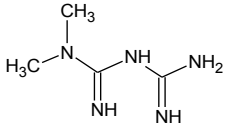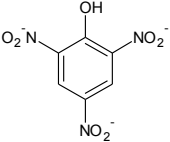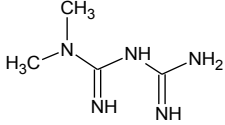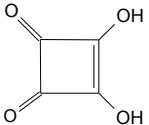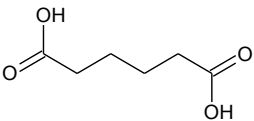
No	MET PCCs (structure determined)	Drug Model	Coformer	Preparation of the solution used for single crystal growth by slow solvent evaporation method
1	MET7b: MET-Nitric acid 1:1 $(C_4H_{12}N_5)^+•(NO_3)^-$	MET	Nitric acid	25.27 mg (0.2 mmol) MET and 19 mg (0.2 mmol) nitric acid ≥65% dissolved in methanol. Clear solution.
2	MET3b: MET-Phosphoric acid trihydrate 2:1:3 $2(C_4H_{12}N_5)^+ •(HPO_4)^=•3(H_2O)$	MET	Phosphoric acid	33.6 mg (0.26 mmol) MET and 12.8 mg (0.13 mmol) conc. phosphoric acid dissolved in methanol. Clear solution
3	MET39: MET-Picric acid 1:1 $(C_4H_{12}N_5)^+ •(C_6H_2N_3O_7)^-$	MET	Picric acid	2.1 mg (0.02 mmol) MET and 3.8 mg (0.04 mmol) picric acid dissolved in n-pentanol. Clear solution.
4	MET41: MET-Picric acid 1:2 $(C_4H_{13}N_5)^{++} •2(C_6H_2N_3O_7)^-$	MET	Picric acid	2.1 mg (0.02 mmol) MET and 6.6 mg (0.04 mmol) picric acid dissolved in n-pentanol. Clear solution.
5	METFSQ: MET-Squaric acid-hydrate 1:1:1 $(C4H13N5)++ •(C4O4)= •(H2O)$	MET	Squaric acid	10.6 mg (0.06 mmol) and 9.3 mg squaric acid dihydrate (0.06 mmol) kneaded with a few drops conc. ethanol. Solid dissolved in hot ethanol. Clear solution.

Table 3.6.2 Method of preparation of MET PCCs with monocarboxylic acids (compounds no. 6-11), part 1
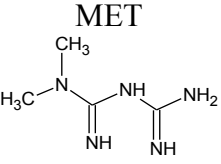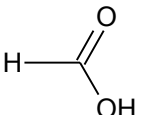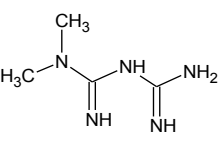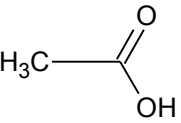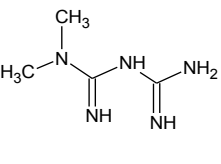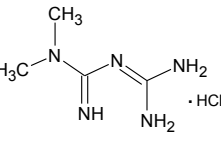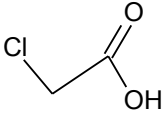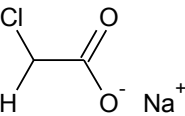
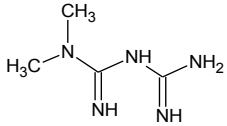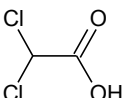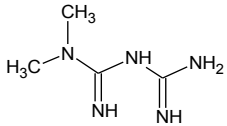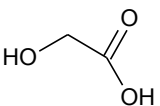| No	MET PCCs (structure determined)	Drug Model	Coformer	Preparation of the solution used for single crystal growth by slow solvent evaporation method
6	METFORMA: MET-Formic acid 1:1 $(C_4H_{12}N_5)^+ \cdot (CHO_2)^-$	MET	Formic acid	17.5 mg (0.13 mmol) MET and 6.27 mg (0.13 mmol) formic acid dissolved in mixture of methanol and n-pentanol 50/50 *V/V* %. Clear solution.
7	MET10b: MET-Acetic acid 1:1 $(C_4H_{12}N_5)^+ \cdot (CH_3O_2)^-$	MET	Acetic acid	*Sample 1:* 17.31 mg (0.13 mmol) MET and 16.8 mg (0.27 mmol) conc. acetic acid dissolved in methanol. Clear solution. *Sample 2:* 99.8 mg (0.78 mmol) MET and 46.39 mg (0.78 mmol) conc. acetic acid dissolved in methanol. Clear solution.
8	METClA6: MET-Monochloracetic acid 1:1 $(C_5H_{12}N_5)^+ \cdot (C_2H_2ClO_2)^-$	MET MET•HCl	Chloroacetic acid Na•Chloroacetate	*Sample 1:* 6.5 mg (0.05 mmol) MET and 4.75 mg (0.05 mmol) chloroacetic acid dissolved in mixture of methanol and n-pentanol 50/50 *V/V* %. Clear solution. *Sample 2:* 5 mg (0.039 mmol) MET and 7.3 mg (0.078 mmol) chloroacetic acid dissolved in mixture of methanol and n-pentanol 50/50 V/V %. Clear solution. *Sample 3:* 68.8 mg (0.4 mmol) MET•HCl and 47.9 mg (0.4 mmol) sodium chloroacetic acid dissolved in n-pentanol, filtered sediment of NaCl, clear solution of the filtrate left for slow rate solvent evaporation.

Table 3.6.2 Method of preparation of MET PCCs with monocarboxylic acids (compounds no. 6-11), part 2
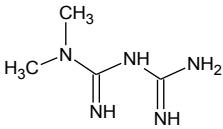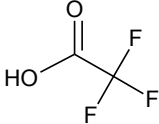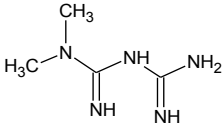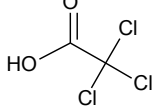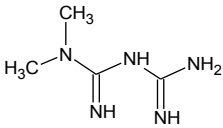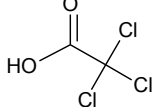
No	MET PCCs (structure determined)	Drug Model	Coformer	Preparation of the solution used for single crystal growth by slow solvent evaporation method
9	METTRIFA: MET-Trifluoroacetic acid 1:1 $(C_4H_{12}N_5)^+ \cdot (C_2F_3O_2)^-$	MET	Trifluoroacetic acid	85.3 mg (0.7 mmol) MET and 75.3 mg (0.7 mmol) trifluoroacetic acid dissolved in mixture of methanol and n-pentanol 50/50 *V/V* %. Clear solution.
10	METTRIClA24 MET-Trichloroacetic acid 1:1 $(C_4H_{12}N_5)^+ \cdot (C_2Cl_3O_2)^-$	MET	Trichloroacetic acid	5.3 mg (0.04 mmol) MET and 6.5 mg (0.04 mmol) trichloroacetic acid dissolved in mixture of methanol and n-pentanol 20/80 *V/V* %. Clear solution.
11	METTRIClA2 MET-Trichloroacetic acid 1 :2 $(C_4H_{13}N_5)^{++} \cdot 2(C_2Cl_3O_2)^-$	MET	Trichloroacetic acid	8.22 mg (0.06 mmol) MET and 20.8 mg (0.12 mmol) trichloroacetic acid dissolved in mixture of methanol and n-pentanol 20/80 *V/V* %. Clear solution.

Table 3.6.3 Method of preparation of MET PCCs with dicarboxylic acids (compounds no. 12-18), part 1
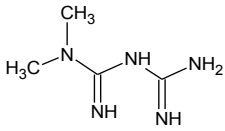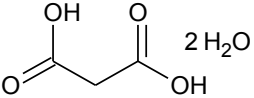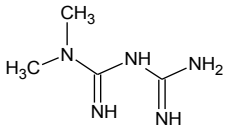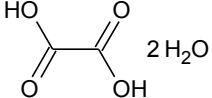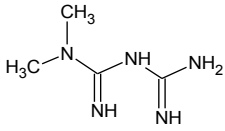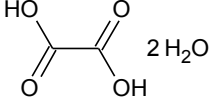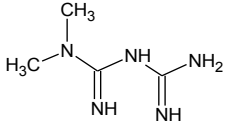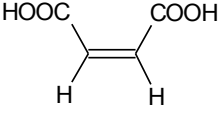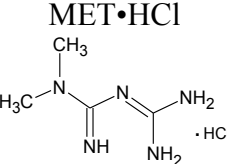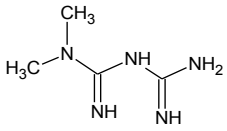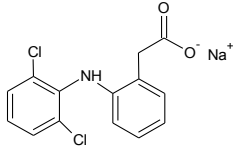
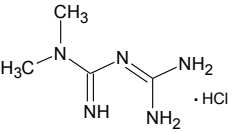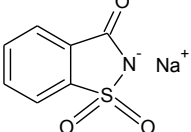| No	MET PCCs (structure determined)	Drug Model	Coformer	Preparation of the solution used for single crystal growth by slow solvent evaporation method
12	MET34: MET-Malonic acid 1:1 $(C_4H_{12}N_5)^+ \bullet (C_3H_3O_4)^-$	MET	Malonic acid $2\,H_2O$	5.4 mg (0.03 mmol) MET and 5.8 mg malonic acid dihydrate (0.04 mmol malonic acid) dissolved in mixture of methanol and n-pentanol 50/50 *V/V* %. Clear solution.
13	MET33: MET-Oxalic acid-hydrate 1:1:1 $(C_4H_{13}N_5)^{++} \bullet (C_2O_4)^= \bullet (H_2O)$	MET	Oxalic acid dihydrate $2\,H_2O$	3.7 mg (0.03 mmol) MET and 3.6 mg oxalic acid dihydrate (0.03 mmol oxalic acid) dissolved in mixture of methanol and n-pentanol 50/50 *V/V* %. Clear solution.
14	MET68: MET-Oxalic acid-hydrate 1:2.5:1 $(C_4H_{13}N_5)^{++} \bullet 2(C_2HO_4)^- \bullet 1/2(C_2H_2O_4) \bullet (H_2O)$	MET	Oxalic acid dihydrate $2\,H_2O$	4.2 mg (0.033 mmol) MET and 8.4 mg oxalic acid dihydrate (0.066 mmol oxalic acid) dissolved in mixture of methanol and n-pentanol 50/50 *V/V* %. Clear solution.
15	MET17: MET-Maleic acid 1:1 $(C_4H_{12}N_5)^+ \bullet (C_4H_3O_4)^-$	MET	Maleic acid	4.6 mg (0.035 mmol) MET and 4 mg (0.035 mmol) maleic acid dissolved in n-pentanol. Clear solution.

Table 3.6.3 Method of preparation of MET PCCs with dicarboxylic acids (compounds no. 12-18), part 2
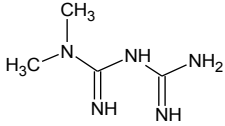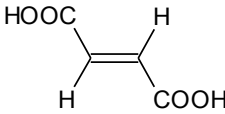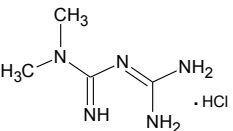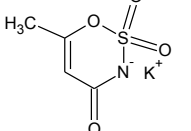
No	MET PCCs (structure determined)	Drug Model	Coformer	Preparation of the solution used for single crystal growth by slow solvent evaporation method
16	MET18: MET-Fumaric acid 1:0.5 $(C_4H_{12}N_5)^+ \cdot 1/2(C_4H_2O_4)^=$	MET	Fumaric acid	4 mg (0.031 mmol) MET and 3.6 mg (0.031) fumaric acid dissolved in mixture of methanol and n-pentanol 50/50 *V/V* %. Clear solution.
17	MET15: MET-Succinic acid 1:0.5 $(C_4H_{12}N_5)^+ \cdot 1/2(C_4H_4O_4)^=$	MET	Succinic acid	4 mg (0.03 mmol) MET and 3.65 mg (0.03 mmol) succinic acid dissolved in mixture of methanol and n-pentanol 50/50 *V/V* %. Clear solution.
18	METADA22: MET-Adipic acid 1:1 $(C4H12N5)+ \cdot 1/2(C6H8O4)= \cdot 1/2(C6H10O4)$	MET	Adipic acid	17.3 mg (0.12 mmol) MET and 19.6 mg (0.13 mmol) adipic acid dissolved in mixture of methanol and n-pentanol 30/70 V/V %. Clear solution.

Table 3.6.4 Method of preparation of functional MET PCCs (compounds no. 19-26), part 1
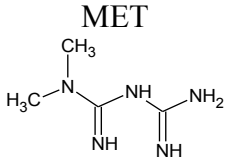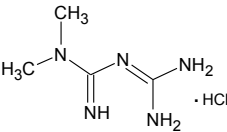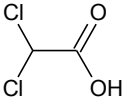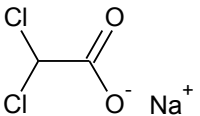
No	MET PCCs (structure determined)	Drug Model	Coformer	Preparation of the solution used for single crystal growth by slow solvent evaporation method
19	METDIClA1: MET-Dichloroacetic acid 1:1 $(C_5H_{12}N_5)^+ \cdot (C_2HCl_2O_2)^-$	MET MET•HCl 	Dichloroacetic acid Na•dichloroacetate 	*Sample 1:* 8.5 mg (0.07 mmol) MET and 8.5 mg (0.07 mmol) dichloroacetic acid dissolved in mixture of methanol and n-pentanol 50/50 *V/V* %. Clear solution. *Sample 2:* 68.8 mg (0.4 mmol) MET•HCl and 47.9 mg (0.4 mmol) sodium chloroacetic acid dissolved in n-pentanol, filtered sediment of NaCl, clear solution of the filtrate left for slow rate solvent evaporation.
20	METDIClA3: MET-Dichloroacetic acid 1:2 $(C_4H_{13}N_5)^{++} \cdot 2(C_2HCl_2O_2)^-$	MET 	Dichloroacetic acid 	8.8 mg (0.07 mmol) MET and 17.5 mg (0.14 mmol) dichloroacetic acid dissolved in mixture of methanol and n-pentanol 50/50 *V/V* %. Clear solution.
21	METGLY23: MET-Glycolic Acid 1:1 $(C_4H_{12}N_5)^+ \cdot (C_2H_3O_3)^-$	MET 	Glycolic acid 	49.9 mg (0.39 mmol) MET and 42.8 mg (0.56 mmol) 70% liquid glycolic acid dissolved in mixture of methanol and n-pentanol 50/50 *V/V* %. Clear solution.

Table 3.6.4 Method of preparation of functional MET PCCs (1-26), part 2
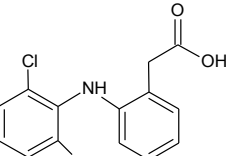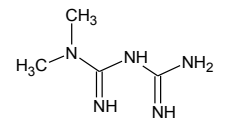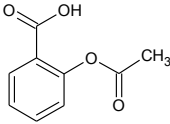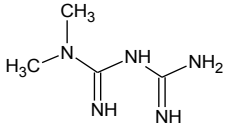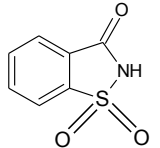
No	MET PCCs (structure determined)	Drug Model	Coformer	Preparation of the solution used for single crystal growth by slow solvent evaporation method
22	METDCF9: MET-Diclofenac 1:1 $(C_4H_{12}N_5)^+ \cdot (C_{14}H_{10}NCl_2O_2)^-$	MET•HCl MET	Diclofenac•Na Diclofenac neutral	*Sample 1:* 2.2 mg (0.013 mmol) MET•HCl and 4.3 mg (0.013 mmol) diclofenac•Na kneaded with a few drops conc. ethanol. Solid dissolved in mixture of methanol and n-pentanol 50/50 *V/V* %. Clear solution. *Sample 2:* 22.37 mg (0.17 mmol) MET and 51.3 mg (0.17 mmol) diclofenac (acidic form) dissolved in mixture of methanol and n-pentanol 50/50 *V/V* %. Clear solution.
23	MET30: MET-Salicylic acid 1:1 $(C_4H_{12}N_5)^+ \cdot (C_7H_5O_3)^-$	MET	Acetylsalicylic acid	4 mg (0.03 mmol) MET and 5.57 mg (0.03 mmol) acetylsalicylic acid dissolved in n-pentanol. Clear solution.
24	MET43: MET-Saccharine 1:1 Polymorph I $(C_4H_{12}N_5)^+ \cdot (C_7H_4NO_3S)^-$	MET	Saccharine	6 mg (0.05 mmol) MET and 8.5 mg (0.05 mmol) saccharine neutral form dissolved in n-pentanol. Clear solution.

Table 3.6.4 Method of preparation of functional MET PCCs (1-26), part 3

No	MET PCCs (structure determined)	Drug Model	Coformer	Preparation of the solution used for single crystal growth by slow solvent evaporation method
25	METHCl6: MET-Saccharine 1:1 Polymorph II $(C_4H_{12}N_5)^+ \cdot (C_7H_4NO_3S)^-$	MET•HCl	Saccharine•Na	24.5 mg (0.15 mmol) MET•HCl and 24.5 mg (0.15 mmol) saccharine •Na kneaded with a few drops conc. ethanol. Solid dissolved in hot n-pentanol, removed sediment of NaCl. Clear solution of filtrate.
26	METACSU7: MET-Acesulfame 1:1 $(C_4H_{12}N_5)^+ \cdot (C_4H_4NO_4S)^-$	MET•HCl	Acesulfame•K	26.4 mg (0.16 mmol) MET•HCl and 32.07 mg (0.16 mmol) acesulfame •K kneaded with a few drops conc. ethanol. Solid dissolved in hot n-pentanol, removed sediment of NaCl. Clear solution of filtrate.

Neutral metformin (MET): Mw (129.16 g·mol-1)

Metformin hydrochloride salt (MET•HCl): Mw (165.62 g·mol-1)

Table 3.7 Crystallographic data MET PCCs (1-26); part 1

Crystallographic data	MET-Nitric acid 1:1 MET7b	MET-Phosphoric acid trihydrate 2:1:3 MET3b	MET-Picric acid 1:1 MET39	MET-Picric acid 1:2 MET41
Formula	$(C_4H_{12}N_5)^+ \bullet (NO_3)^-$	$2(C_4H_{12}N_5)^+ \bullet (HPO_4)^= \bullet 3(H_2O)$	$(C_4H_{12}N_5)^+ \bullet (C_6H_2N_3O_7)^-$	$(C_4H_{13}N_5)^{++} \bullet 2(C_6H_2N_3O_7)^-$
Molecular mass (Mr)	192.20	410.40	358.29	587.41
Crystal system	Triclinic	Triclinic	Monoclinic	Triclinic
Space group	$P\text{-}1$	$P\text{-}1$	$P2_1/c$	$P\text{-}1$
a, Å	7.3002(2)	9.4750(2)	11.4876(3)	10.5937(3)
b, Å	7.5460(3)	9.6849(2)	5.6401(1)	11.2322(3)
c, Å	8.9078(3)	10.8896(3)	24.2262(8)	12.2961(5)
α, deg	78.138(2)	77.8210(8)	90	102.623(1)
β, deg	74.496(2)	84.7487(9)	94.370(1)	105.189(1)
γ, deg	84.991(2)	88.7943(9)	90	115.272(2)
V, Å^3	462.48(3)	972.69(4)	1565.08(7)	1181.83(7)
Z	2	2	4	2
D_c, Mg m^{-3}	1.380	1.401	1.521	1.651
μ, mm^{-1}	0.116	0.194	0.130	0.146
$F(000)$	204	440	744	604
$\theta_{min}-\theta_{max}$, deg	2.42-29.97	3.46-30.06	3.99-25.99	3.52-24.99
Index ranges min./max. h,k,l	-10,10;-10,9;-11,12	-13,12;-10,13;-14,15	-14,14;-6,5;-29,29	-12,12;-12,13;-14,14
Measured Reflections	3964	8258	5096	6904
Unique Reflections	2645	5622	3036	4145
R_{int}	0.0295	0.0189	0.0260	0.0275
Obs. Reflections[I > 2σ(I)]	2044	4391	2182	2774
No. Variables/Restraints	166/0	359/0	282/0	439/0
$R(F^2)$ [I > 2σ(I)]	0.0569	0.0403	0.0502	0.0552
$wR (F^2)$ (all data)	0.1741	0.1149	0.1427	0.1591
Goodness of fit, S	1.075	1.028	1.041	1.018
$\Delta\rho$ (max., min.) e Å^{-3}	0.540,-0.384	0.309,-0.449	0.444,-0.483	0.438,-0.300

Table 3.7 Crystallographic data MET PCCs (1-26) ; part 2

Crystallographic data	MET-Squaric acid-hydrate 1:1:1 METSQ	MET-Formic acid 1:1 METFORMA	MET-Acetic acid 1:1 MET10b	MET-Monochloracetic acid 1:1 METClA6
Formula	$(C_4H_{13}N_5)^{++} \cdot (C_4O_4)^= \cdot (H_2O)$	$(C_4H_{12}N_5)^+ \cdot (CHO_2)^-$	$(C_4H_{12}N_5)^+ \cdot (CH_3O_2)^-$	$(C_5H_{12}N_5)^+ \cdot (C_2H_2ClO_2)^-$
Molecular mass (Mr)	261.25	175.20	189.23	223.67
Crystal system	Monoclinic	Monoclinic	Monoclinic	Monoclinic
Space group	$P2_1/c$	$P2_1/n$	$P2_1/n$	$P2_1/n$
a, Å	7.1369(2)	9.6766(3)	10.0007(5)	10.0229(3)
b, Å	10.8618(3)	8.9183(2)	8.8974(5)	8.7967(2)
c, Å	15.9179(4)	10.4766(4)	10.7080(5)	11.6851(4)
α, deg	90	90	90	90
β, deg	92.876(2)	90.787(1)	91.241(3)	96.823(1)
γ, deg	90.00	90	90	90
V, Å^3	1232.40(6)	904.03(5)	925.58(8)	1022.96(5)
Z	4	4	4	4
D_c, Mg m^{-3}	1.408	1.287	1.319	1.452
μ, mm^{-1}	0.117	0.101	0.101	0.359
$F(000)$	552	376	408	472
$\theta_{min}-\theta_{max}$, deg	3.60-30.02	3.65-28.00	4.68-30.06	3.43-30.06
Index ranges min./max. h,k,l	-10,10;-12,15;-22,22	-12,12;-9,11;-13,13	-14,14;-12,11;-15,15	-14,14;-10,12;-16,16
Measured Reflections	6022	4021	4433	5094
Unique Reflections	3566	2175	2752	2962
R_{int}	0.0278	0.0241	0.0254	0.0181
Obs. Reflections [I > 2σ(I)]	2339	1598	2109	2411
No. Variables/Restraints	224/0	161/0	178/0	183/0
$R(F^2)$ [I > 2σ(I)]	0.0452	0.0421	0.0474	0.0406
$wR(F^2)$ (all data)	0.1155	0.1212	0.1415	0.1139
Goodness of fit, S	1.027	1.023	1.052	1.043
$\Delta\rho$ (max., min.) e Å^{-3}	0.298,-0.180	0.183,-0.175	0.274,-0.257	0.518,-0.564

Table 3.7 Crystallographic data MET PCCs (1-26) ; part 3

Crystallographic data	MET-Trifluoroacetic acid 1:1 METTRIFA	MET-Trichloroacetic acid 1:1 METTRIClA24	MET-Trichloroacetic acid 1 :2 METTRICla2	MET-Malonic acid 1:1 MET34
Formula	$(C_4H_{12}N_5)^+ \bullet (C_2F_3O_2)^-$	$(C_4H_{12}N_5)^+ \bullet (C_2Cl_3O_2)^-$	$(C_4H_{13}N_5)^{++} \bullet 2(C_2Cl_3O_2)^-$	$(C_4H_{12}N_5)^+ \bullet (C_3H_3O_4)^-$
Molecular mass (Mr)	243.21	292.56	455.93	233.24
Crystal system	Monoclinic	Monoclinic	Monoclinic	Monoclinic
Space group	$P2_1/n$	$P2_1/n$	$P2_1/a$	$P2_1/c$
a, Å	10.8169(3)	10.6569(2)	10.3129(1)	12.5523(3)
b, Å	8.9417(3)	8.8735(2)	22.4379(3)	5.0134(1)
c, Å	11.1235(3)	13.7575(3)	16.7563(3)	17.6365(5)
α, deg	90	90	90	90
β, deg	92.106(2)	105.600(1)	100.8384(7)	91.955(1)
γ, deg	90	90	90	90
V, Å^3	1075.15(6)	1253.04(0.05)	3808.24(9)	1109.21(5)
Z	4	4	8	4
D_c, Mg m^{-3}	1.502	1.551	1.590	1.397
μ, mm^{-1}	0.147	0.726	0.923	0.115
$F(000)$	504	600	1840	496
$\theta_{min}-\theta_{max}$, deg	3.44-27.00	3.92-30.03	2.71-25.00	4.05-30.02
Index ranges min./max. h,k,l	-13,13;-11,10;-14,14	-14,15;-11,12;-19,18	-12,12;-26,26;-19,19	-17,17;-7,6;-24,24
Measured Reflections	4279	6632	12817	4989
Unique Reflections	2331	3637	6699	3192
R_{int}	0.0208	0.0180	0.0224	0.0169
Obs. Reflections [I > 2σ(I)]	1744	2843	4866	2470
No. Variables/Restraints	193/0	193/0	496/66	205/0
$R(F^2)$ [I > 2σ(I)]	0.0614	0.0452	0.0877	0.0425
$wR (F^2)$ (all data)	0.1842	0.1227	0.2521	0.1255
Goodness of fit, S	1.062	1.052	1.167	1.021
$\Delta\rho$ (max., min.) e Å^{-3}	0.646,-0.451	0.852,-0.627	1.126,-0.957	0.201;-0.209

Table 3.7 Crystallographic data MET PCCs (1-26) ; part 4

Crystallographic data	MET-Oxalic acid-hydrate 1:1:1 MET33	MET-Oxalic acid-hydrate 1:2.5:1 MET68	MET-Maleic acid 1:1 MET17	MET-Fumaric acid 1:0.5 MET18
Formula	$(C_4H_{13}N_5)^{++}$ •$(C_2O_4)^=$ •(H_2O)	$(C_4H_{13}N_5)^{++}$ • $2(C_2HO_4)^-$ • $1/2(C_2H_2O_4)$ •(H_2O)	$(C_4H_{12}N_5)^+$•$(C_4H_3O_4)^-$	$(C_4H_{12}N_5)^+$•$1/2(C_4H_2O_4)^=$
Molecular mass (Mr)	237.23	372.28	245.25	187.21
Crystal system	Monoclinic	Triclinic	Monoclinic	Monoclinic
Space group	$P2_1/c$	P -1	$P2_1/n$	$P2_1/n$
a, Å	6.7793(2)	5.7106(4)	10.6035(2)	9.6757(3)
b, Å	10.7696(3)	9.9488(8)	8.9059(2)	8.7927(2)
c, Å	14.7388(4)	14.8902(13)	13.6459(4)	10.8808(4)
α, deg	90	87.761(3)	90	90
β, deg	92.554(1)	80.392(3)	107.772(1)	90.824(1)
γ, deg	90	76.244(4)	90	90
V, Å^3	1075.02(5)	810.2(1)	1227.13(5)	925.59(5)
Z	4	2	4	4
D_c, Mg m^{-3}	1.466	1.526	1.327	1.343
μ, mm^{-1}	0.126	0.141	0.107	0.104
F(000)	504	390	520	400
θ_{min}–θ_{max}, deg	3.76-30.05	2.52-24.99	3.91-30.01	2.98-27.78
Index ranges min./max. h,k,l	-9,9;-15,13;-20,20	-6,6;-11,11;-17,17	-14,14;-12,12;-19,19	-12,12;-11,9;-14,14
Measured Reflections	5470	5010	6599	3977
Unique Reflections	3135	2801	3563	2178
R_{int}	0.0222	0.0500	0.0207	0.0183
Obs. Reflections [I > 2σ(I)]	2330	2211	2424	1736
No. Variables/Restraints	205/0	267/3	214/0	171/1
$R(F^2)$ [I > 2σ(I)]	0.0417	0.0870	0.0491	0.0593
wR (F^2) (all data)	0.1126	0.2581	0.1428	0.1487
Goodness of fit, S	1.020	1.154	1.040	1.044
$\Delta\rho$ (max., min.) e Å^{-3}	0.299,-0.244	0.407,-0.310	0.212,-0.199	0.815,-0.631

Table 3.7 Crystallographic data MET PCCs (1-26) ; part 5

Crystallographic data	MET-Succinic acid 1:0.5 MET15	MET-Adipic acid 1:1 MET-ADA22	MET-Dichloroacetic acid 1:1 METDIClA1
Formula	$(C_4H_{12}N_5)^+ \cdot 1/2(C_4H_4O_4)^=$	$(C_4H_{12}N_5)^+ \cdot$ $1/2(C_6H_8O_4)^= \cdot 1/2(C_6H_{10}O_4)$	$(C_5H_{12}N_5)^+ \cdot (C_2HCl_2O_2)^-$
Molecular mass (Mr)	188.22	275.32	258.11
Crystal system	Monoclinic	Triclinic	Monoclinic
Space group	$P2_1/n$	$P\text{-}1$	$P2_1/n$
a, Å	9.5569(3)	7.5497(2)	10.6346(2)
b, Å	8.8294(2)	9.1036(2)	9.0263(2)
c, Å	10.8542(3)	10.2423(3)	12.6154(4)
α, deg	90	89.914(1)	90
β, deg	92.484(1)	82.124(1)	105.5040(9)
γ, deg	90	79.296(1)	90
V, Å^3	915.04(4)	684.97(3)	1166.90(5)
Z	4	2	4
D_c, Mg m^{-3}	1.366	1.335	1.469
μ, mm^{-1}	0.105	0.104	0.547
$F(000)$	404	296	536
$\theta_{min}-\theta_{max}$, deg	3.76-30.00	3.99-29.97	4.52-28.00
Index ranges min./max. h,k,l	-13,13;-12,10;-15,15	-8,10;-12,11;-13,14	-13,14;-11,11;-16,16
Measured Reflections	4398	5305	5032
Unique Reflections	2654	3914	2766
R_{int}	0.0245	0.0227	0.0141
Obs. Reflections [I > 2σ(I)]	1889	3056	2401
No. Variables/Restraints	174/0	256/0	188/1
$R(F^2)$ [I > 2σ(I)]	0.0433	0.0463	0.0662
$wR (F^2)$ (all data)	0.1209	0.1290	0.1785
Goodness of fit, S	1.022	1.045	1.044
$\Delta\rho$ (max., min.) e Å^{-3}	0.235,-0.221	0.308,-0.220	0.647,-0.748

Table 3.7 Crystallographic data MET PCCs (1-26) ; part 6

Crystallographic data	MET-Dichloroacetic acid 1:2 METDIClA3	MET-Glycolic Acid 1:1 METGLY23	MET-Diclofenac 1:1 METDCF9	MET-Salicylic acid 1:1 MET30
Formula	$(C_4H_{13}N_5)^{++}$ • $2(C_2HCl_2O_2)^-$	$(C_4H_{12}N_5)^+$•$(C_2H_3O_3)^-$	$(C_4H_{12}N_5)^+$• $(C_{14}H_{10}NCl_2O_2)^-$	$(C_4H_{12}N_5)^+$•$(C_7H_5O_3)^-$
Molecular mass (Mr)	387.05	205.23	425.32	267.30
Crystal system	Triclinic	Triclinic	Monoclinic	Monoclinic
Space group	*P-1*	*P-1*	*P2$_1$/c*	*P2$_1$/n*
a, Å	8.8368(2)	5.8145(2)	8.8865(4)	15.3440(6)
b, Å	9.6189(2)	8.6576(3)	10.1845(5)	6.0542(3)
c, Å	10.3659(3)	10.3719(3)	22.4124(12)	15.8769(10)
α, deg	83.7093(8)	93.199(2)	90	90
β, deg	72.7342(9)	91.403(2)	94.260(2)	116.658(2)
γ, deg	84.4839(10)	106.448(1)	90	90
V, Å^3	834.45(4)	499.53(3)	2022.8(2)	1318.1(1)
Z	2	2	4	4
D_c, Mg m^{-3}	1.540	1.364	1.397	1.347
μ, mm^{-1}	0.729	0.110	0.348	0.101
$F(000)$	396	220	888	568
θ_{min}–θ_{max}, deg	4.19-28.00	3.94-29.93	3.04-26.50	4.43-24.99
Index ranges min./max. h,k,l	-10,11;-12,12;-12,13	-5,8;-12,9;-12,14	-11,11;-12,11;-28,28	-18,18;-7,7;-18,18
Measured Reflections	6096	3833	6784	4264
Unique Reflections	3997	2849	4028	2311
R_{int}	0.0240	0.0244	0.0440	0.0321
Obs. Reflections [I > 2σ(I)]	3288	2353	2969	1586
No. Variables/Restraints	256/6	187/0	341/0	241/0
$R(F^2)$ [I > 2σ(I)]	0.0713	0.0440	0.0484	0.0480
$wR (F^2)$ (all data)	0.1992	0.1295	0.1397	0.1318
Goodness of fit, S	1.031	1.049	1.041	1.050
$\Delta\rho$ (max., min.) e Å^{-3}	1.130, -0.955	0.286,-0.205	0.247,-0.353	0.185,-0.172

Table 3.7 Crystallographic data MET PCCs (1-26) ; part 7

Crystallographic data	MET-Saccharine 1:1 Polimorph I MET43	MET-Saccharine 1:1 Polymorph II METHCl6	MET-Acesulfame 1:1 METACSU7
Formula	$(C_4H_{12}N_5)^+\bullet$ $(C_7H_4NO_3S)^-$	$(C_4H_{12}N_5)^+\bullet$ $(C_7H_4NO_3S)^-$	$(C_4H_{12}N_5)^+\bullet(C_4H_4NO_4S)^-$
Molecular mass (Mr)	312.36	312.36	292.33
Crystal system	orthorhombic	monoclinic	Monoclinic
Space group	$P2_12_12_1$	$C2/c$	$P2_1/n$
a, Å	7.1858(1)	29.9130(6)	8.4931(2)
b, Å	9.9319(2)	12.6385(2)	13.6704(3)
c, Å	20.2161(4)	15.6051(4)	12.2991(2)
α, deg	90	90	90
β, deg	90	103.6450(8)	99.935(1)
γ, deg	90	90	90
V, Å^3	1442.80(5)	5733.1(2)	1406.56(5)
Z	4	16	4
D_c, Mg m^{-3}	1.438	1.448	1.380
μ, cm^{-1}	0.245	0.247	0.251
$F(000)$	656	2624	616
$\theta_{min}-\theta_{max}$, deg	3.65-30.03	3.80-28.00	27.1-28.00
Index ranges min./max. h,k,l	-10,10;-13,13;-28,28	-39,39;-16,14;-20,20	-11,11;-18,16;-16,16
Measured Reflections	4193	12121	5908
Unique Reflections	2409	6868	3372
R_{int}	0.0233	0.0238	0.0151
Obs. Reflections [I > 2σ(I)]	1957	5036	2784
No. Variables/Restraints	254/0	507/0	245/0
$R(F^2)$ [I > 2σ(I)]	0.0353	0.0410	0.0554
$wR(F^2)$ (all data)	0.0880	0.1131	0.1605
Goodness of fit, S	1.029	1.025	1.060
$\Delta\rho$ (max., min.) e Å^{-3}	0.194,-0.327	0.250,-0.359	0.673,-0.544

Table 3.8.1 Intromolecular contacts and Packing motifs of the MET-Nitric acid 1:1

1	MET-Nitric acid 1:1	D−H/Å	H⋯A/Å	D⋯A/Å	<D−H ⋯A/ °	Symmetry code
Lab code MET7b	N−H⋯O dimer - $R_2^2(8)$					
	N1−H12⋯O2	0.89(2)	2.06(2)	2.934(3)	167(2)	x, y, z
	N2−H21⋯O1	0.90(2)	2.08(2)	2.983(2)	176(2)	x, y, z
	N−H⋯N dimer - $R_2^2(8)$					
	N2−H22⋯N3	0.85(2)	2.164(2)	3.017(2)	177(2)	-x,-y+1,-z
	N−H⋯O tetramer - $R_4^2(8)$					
	N4−H41⋯O1 (nitrate)	0.83(3)	2.21(3)	3.028(2)	168(2)	-x,-y,-z
	N4−H42⋯O1 (nitrate)	0.85(2)	2.20(2)	3.023(2)	163(2)	x,+y,+z+1
	N1−H11⋯O2 $R_4^2(8)$	0.56(3)	2.16(3)	2.952(3)	154(2)	-x+1,-y,-z
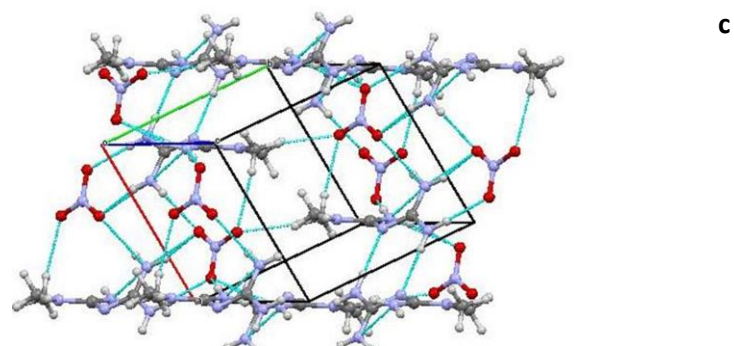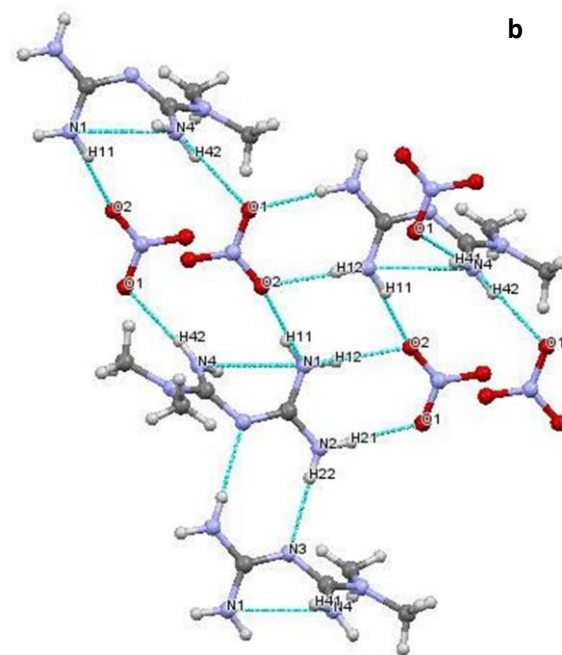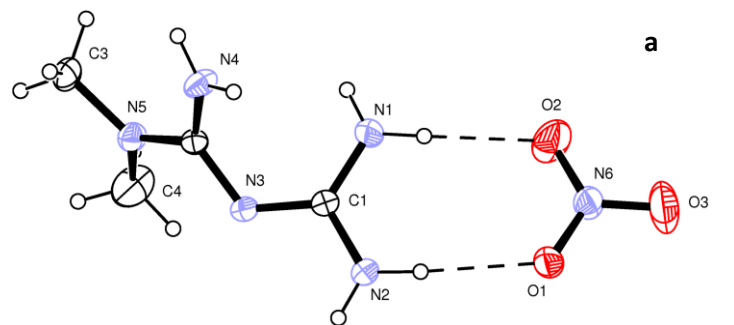
Fig. 3.5 Packing motifs of the MET-Nitric acid 1:1

Table 3.8.2 Intremolecular contacts and Packing motifs of the MET-Phosphoric acid trihydrate 2:1:3

| 2	MET-Phosphoric acid trihydrate 2:1:3	D−H/Å	H···A/Å	D···A/Å	<D−H ···A/ °	Symmetry code
	N−H···O dimer - $R_2^2(8)$					
	N1A−H11A···O4 (phosphate)	0.86(2)	1.97(2)	2.821(2)	172(2)	x, y, z
	N2A−H22A···O3 (phosphate)	0.86(2)	2.01(2)	2.870(2)	174(2)	x, y, z
	N−H···N dimer - $R_2^2(8)$					
	N2B−H21B···N3B	0.90(2)	2.15(2)	3.041(2)	173(2)	-x+2,-y+2,-z+2
	Bifurcated N−H···O H-bonds					
	N1B−H12B···O3	0.86(2)	2.20(2)	2.977(2)	149(2)	x, y, z
	N2B−H22B···O3	0.77(2)	2.34(2)	3.063(2)	157(2)	x, y, z
	N1A−H11A···O3	0.86(2)	2.20(2)	2.977(2)	149(2)	x, y, z
	N2A−H22A···O3	0.77(2)	2.34(2)	3.063(2)	157(2)	x, y, z
	Tetramer					
	N1A−H11A···O4 (phosphate)	0.86(2)	1.97(2)	2.821(2)	172(2)	x, y, z
Lab code	N4A−H42A···O4	0.90(2)	2.10(2)	2.912(2)	151.(2)	-x+1,-y+1,-z+1
MET3b	Tetramer (O−H···O)					
	O2W−H22W···O3W	0.79(3)	2.42(4)	2.798(3)	111(3)	-x+1,-y+1,-z+1
	O3W−H32W···O2W	0.86(4)	2.06(4)	2.897(2)	166(3)	x+1,+y,+z
	O1W−H12W···O2	0.93(3)	1.84(3)	2.768(1)	175(2)	x, y ,z
	O1W−H11W···O2	0.84(2)	1.96(2)	2.796(2)	173(2)	-x+2,-y+1,-z+2
	Other H-bonds					
	N4B−H42B···O1	0.84(2)	2.21(2)	2.984(2)	153(2)	x+1,+y,+z
	N4B−H41B···O2	0.87(2)	1.95(2)	2.797(1)	163(2)	-x+2,-y+1,-z+2
	N1B−H12B···O1W	0.86(2)	2.90(2)	3.263(2)	108(2)	x, y, z
	N1B−H11B···O2W	0.82(2)	2.94(2)	3.396(2)	117(2)	x+1,+y,+z
	N2B−H22B···O1	0.78(2)	2.83(2)	3.489(2)	146(2)	x, y, z
	N1A−H12A···O2W	0.81(2)	2.08(2)	2.881(2)	172(2)	x, y, z
	O2W−H22W···N1A	0.789(3)	2.87(4)	2.881(2)	83(2)	x, y, z
	O1−H1···N4B	0.87(2)	2.98(2)	2.984(2)	82.17(1)	x-1,+y,+z
	O2W−H21W···O1W	0.88(3)	1.82(3)	2.680(2)	167(3)	x-1,+y,+z
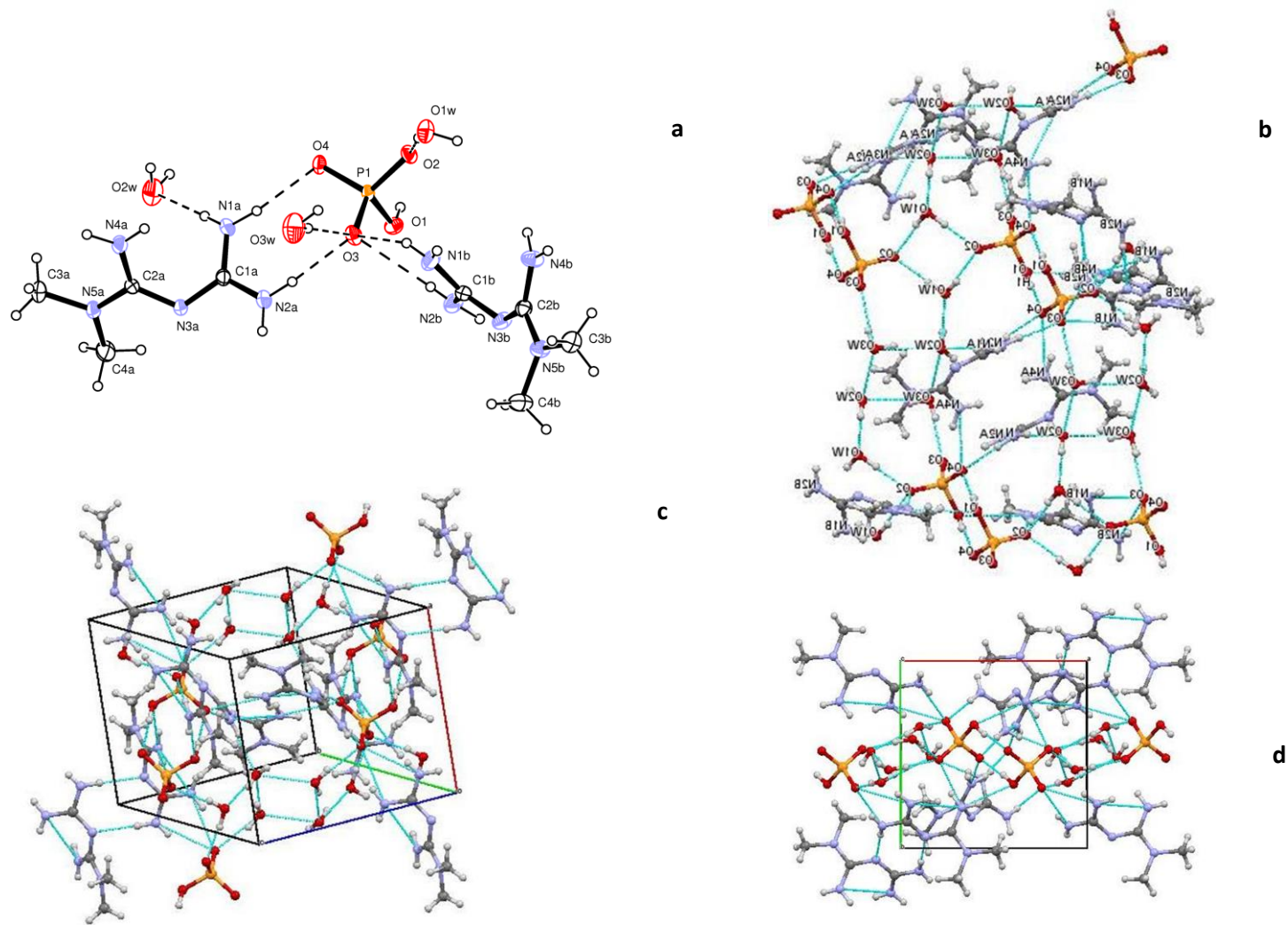
Fig.3.6 Packing motifs of the MET-Phosphoric acid trihydrate 2:1:3

Table 3.8.3 Intremolecular contacts and Packing motifs of the MET-Picric acid 1:1

3	MET-Picric acid 1:1	D−H/Å	H···A/Å	D···A/Å	<D−H ···A/ °	Symmetry code
	Bifurcated H-bonds					
	N1−H1···O1	0.86(3)	2.12(3)	2.897(3)	153(2)	x, y, z
	N2−H1···O1	0.83(3)	2.18(3)	2.906(3)	146(2)	x, y, z
	N−H···N dimer - $R_2^2(8)$					
	N2−H2···N3	0.85(3)	2.17(3)	3.025(3)	176(2)	-x,-y+2,-z+1
Lab code	Other H-bonds					
MET39	N2−H1···O2	0.83(2)	2.39(3)	3.095(4)	143(2)	x, y, z
	N1−H2···O7	0.80(3)	2.32(3)	3.104(3)	165(2)	-x+1,-y+1,-z+1
	N4−H1···O6	0.86(3)	2.28(3)	3.088(3)	157(3)	-x+1,-y+2,-z+1
	N4−H2···O1	0.95(3)	2.16(3)	3.089(3)	165(3)	x,+y+1,+z
	N4−H2···O6	0.95(3)	2.72(3)	3.279(3)	118(2)	x,+y+1,+z
	N1−H1···O6	0.86(3)	2.81(3)	3.466(3)	135(2)	x, y, z
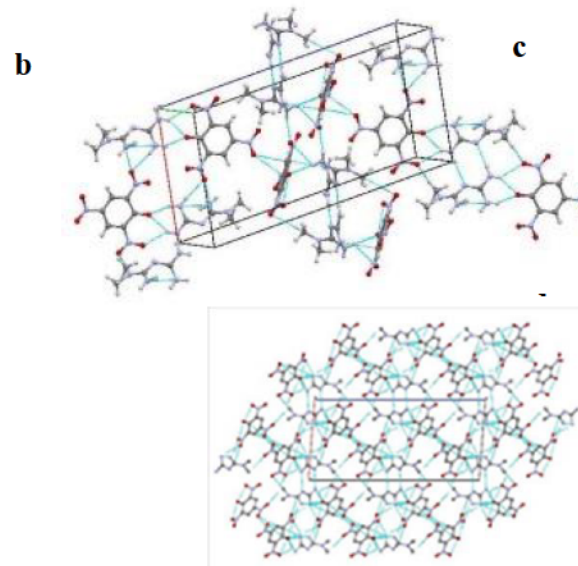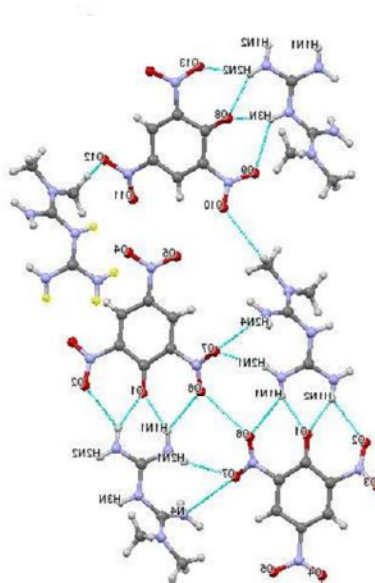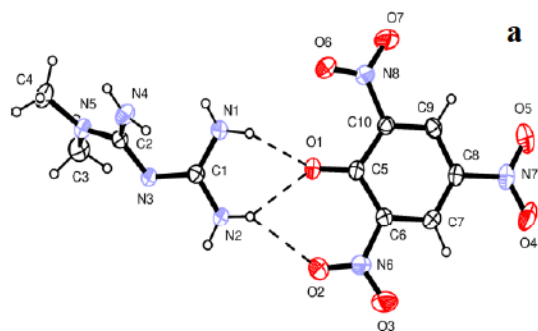
Fig. 3.7 Packing motifs of the MET-Picric acid 1:1

Table no. 3.8.4 Intremolecular contacts and Packing motifs of the MET-Picric acid 1:2

4	MET-Picric acid 1:2	D−H/Å	H⋯A/Å	D⋯A/Å	<D−H ⋯A/ °	Symmetry code
	Bifurcated H bonds					
	N1−H1⋯O1	0.87(4)	2.01(5)	2.791(5)	149(4)	x, y, z
	N2−H1⋯O1	0.89(4)	1.93(3)	2.731(3)	149(4)	x, y, z
	N2−H2⋯O8	0.79(3)	2.19(3)	2.871(3)	144(4)	x, y, z
	N3−H3⋯O8	0.84(3)	1.90(4)	2.694(3)	158(4)	x, y, z
	Other H-bonds					
	N2−H1⋯O2	0.89(4)	2.44(5)	3.156(5)	138(4)	x, y, z
Lab code	N1−H1⋯O6	0.87(4)	2.43(3)	3.141(3)	140(4)	x, y, z
MET41	N1−H2⋯O7	0.86(5)	3.14(5)	2.322(5)	158(4)	-x,-y,-z+1
	N3−H3⋯O9	0.84(3)	2.51(3)	3.074(3)	126(3)	x, y, z
	N4−H1⋯O7	0.85(5)	2.78(3)	2.893(4)	89(3)	-x,-y,-z+1
	N1−H2N1⋯O11	0.86(5)	2.92(4)	3.468(5)	123(3)	x-1,+y-1,+z
	N4−H1N4⋯O14	0.85(5)	2.08(5)	2.894(5)	160(4)	x,+y-1,+z
	N4−H2N4⋯O13	0.87(5)	2.17(4)	3.016(4)	165(4)	-x+1,-y+1,-z+1
	N4−H2N4⋯O2	0.87(4)	2.65(4)	3.040(5)	109(3)	-x+1,-y+1,-z+1
	N2−H2⋯O13	0.79(3)	2.33(4)	2.999(4)	143(4)	x, y, z
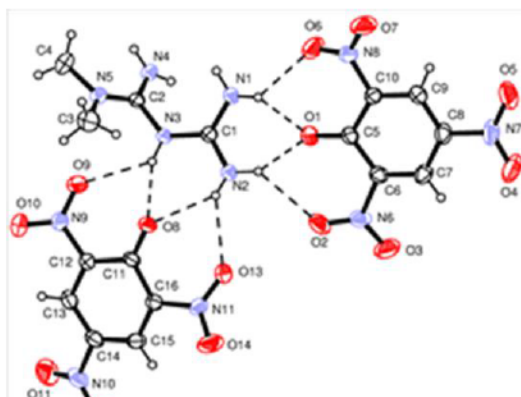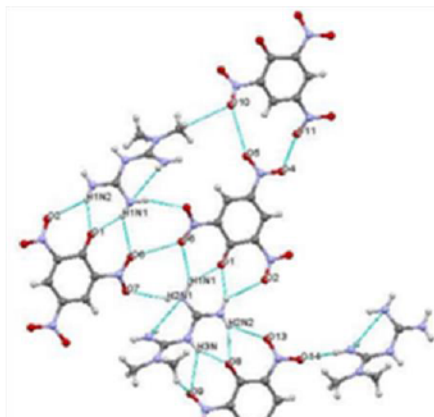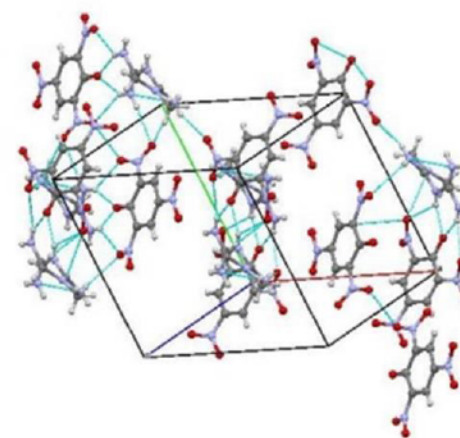
Fig. 3.8 Packing motifs of the MET-Picric acid 1:2

Table 3.8.5 Intremolecular contacts and Packing motifs of the MET-Squaric acid-hydrate 1:1:1

5	MET-Squaric acid-hydrate 1:1:1	D−H/Å	H···A/Å	D···A/Å	<D−H ···A/ °	Symmetry code
	N1−H1···O1	0.83(2)	2.36(2)	2.988(2)	134(2)	x, y, z
	N1−H1···O2	0.83(2)	2.522)	3.1992)	140(2)	x, y, z
	N2−H1···O2	0.89(2)	1.97(2)	2.822(2)	163(2)	x, y, z
	N2−H2··O3	0.91(2)	1.92(2)	2.807(2)	164(2)	x, y, z
Lab code	N3−H3··O4	0.92(2)	1.73(2)	2.625(2)	165(2)	x, y, z
METFSQ	N4−H1···O1	0.92(2)	1.88(2)	2.792(2)	169(2)	-x+1,+y-1/2,-z+1/2
	N4−H2···O3	0.90(2)	2.06(2)	2.923(2)	159(2)	-x,-y,-z
	N1−H2···O5W	0.92(2)	1.85(2)	2.760(2)	167(2)	x, y, z
	O5W−H52W···O2	0.82(3)	1.92(3)	2.731(2)	171(3)	x,-y+1/2,+z+1/2
	O5W−H51W···O4	0.86(3)	2.02(3)	2.865(2)	165(3)	-x,+y+1/2,-z+1/2
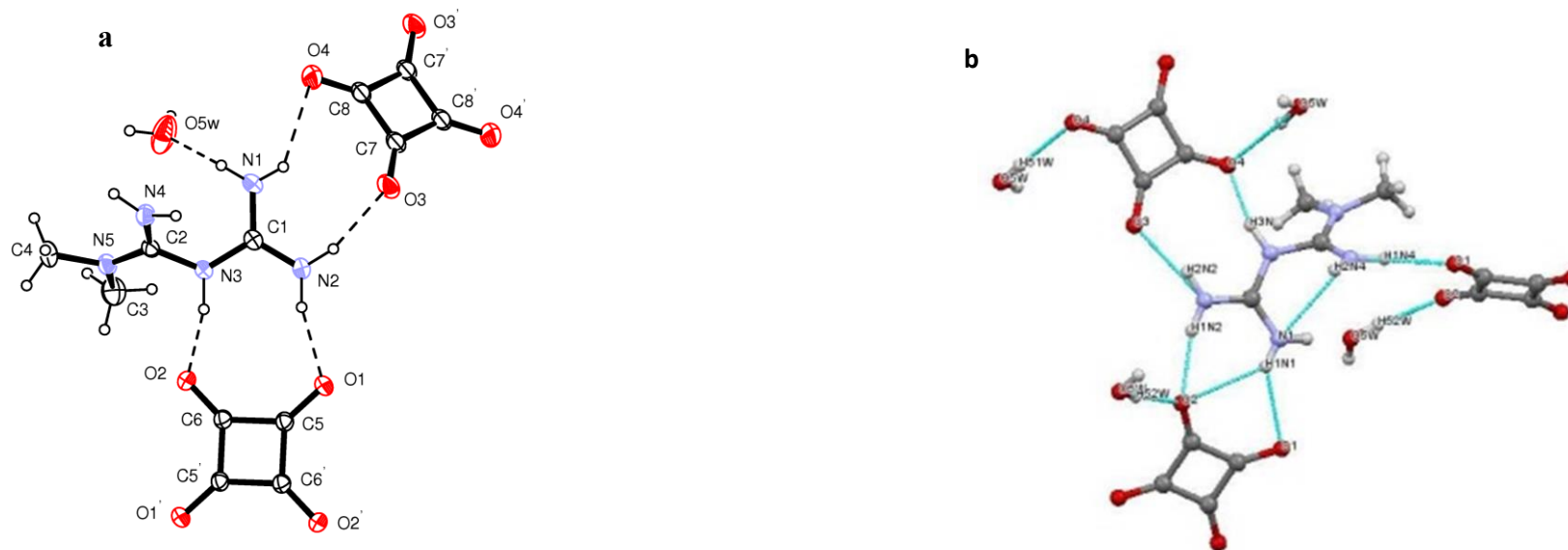
Fig. 3.9a Packing motifs of the MET-Squaric acid-hydrate 1:1:1

c

d
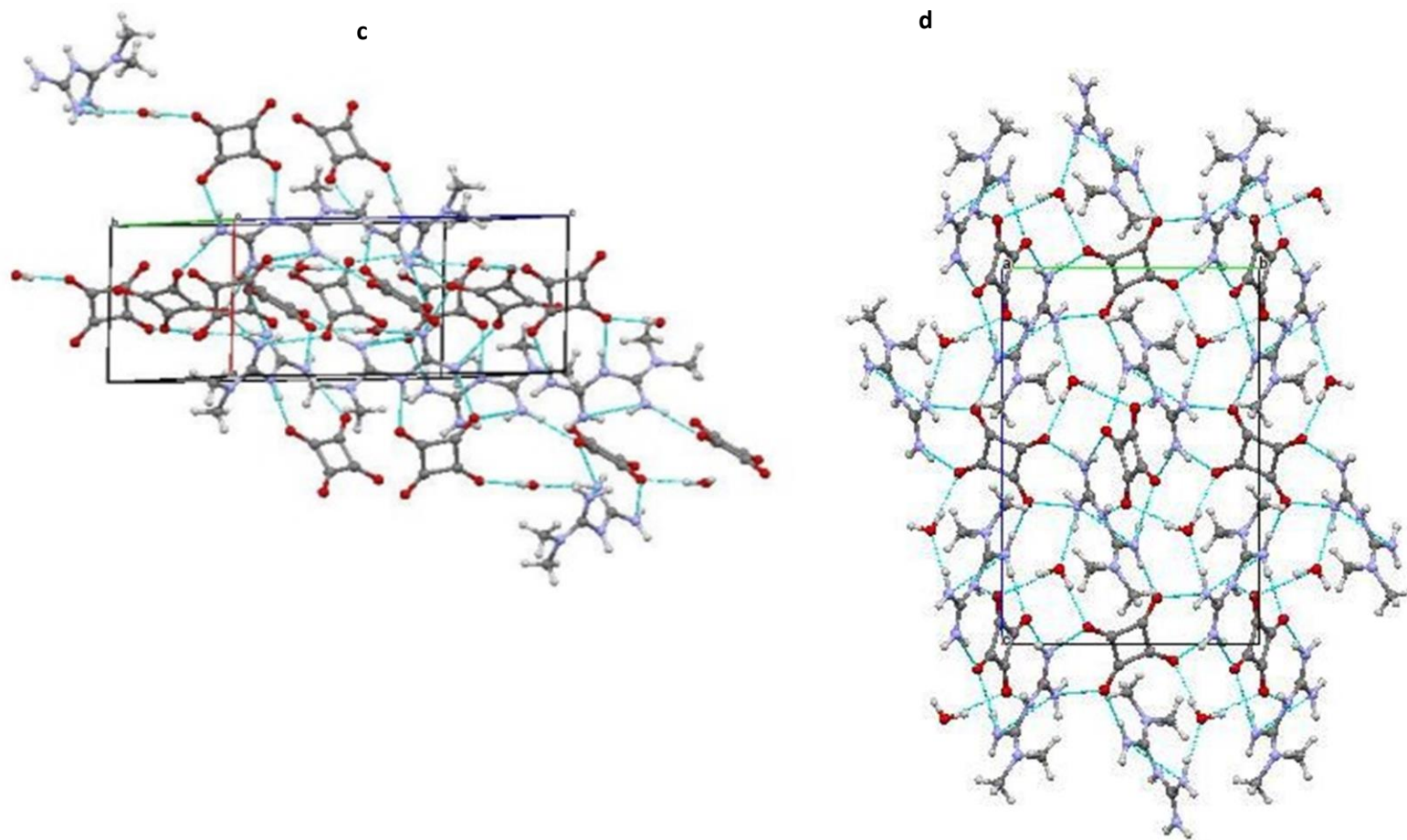
Fig.3.9.b Packing motifs of the of the MET-Squaric acid-hydrate 1:1:1

Table 3.8.6 Intremolecular contacts and Packing motifs of the MET-Formic acid 1:1

6	MET-Formic acid 1:1	D−H/Å	H···A/Å	D···A/Å	<D−H ···A/ °	Symmetry code
	N−H···O dimer - $R_2^2(8)$					
	N1−H1···O1	0.87(2)	2.04(2)	2.911(2)	173(2)	x, y, z
	N2−H1−O2	0.86(2)	2.09(2)	2.946(2)	178(2)	x, y, z
	N−H···O tetramer - $R_4^2(8)$					
	N1−H2···O1	0.90(2)	2.04(2)	2.861(2)	152(2)	-x+1,-y+1,-z+1
Lab code	N1−H1···O1	0.87(2)	2.04(2)	2.911(2)	173(2)	x, y, z
METFORMA	N−H···N dimer - $R_2^2(8)$					
	N2−H2···N3	0.85(2)	3.03(2)	2.180(2)	174(2)	-x+1,-y+1,-z+2
	Connected ribbons					
	N4−H1···O2	0.85(2)	2.08(2)	2.922(2)	174(2)	x,+y-1,+z
	Connected planes					
	C4−H42···O1	0.93(3)	2.65(3)	3.565(3)	167(2)	x-1/2,-y+1/2,+z+1/2
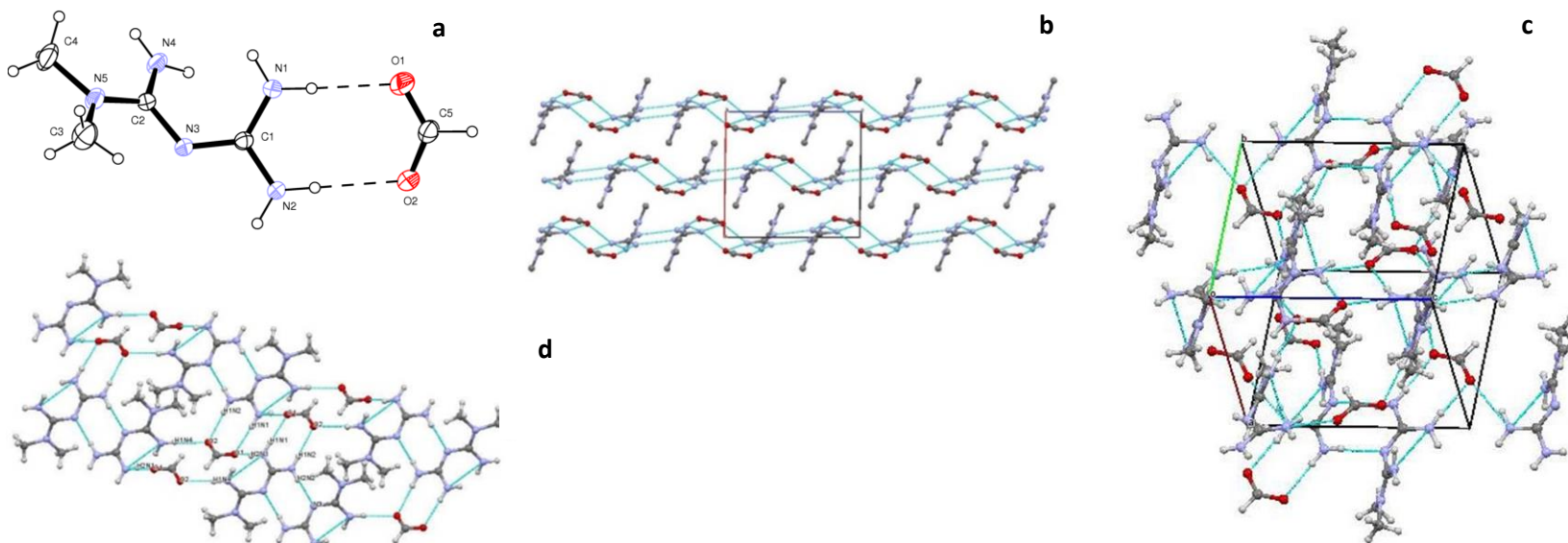
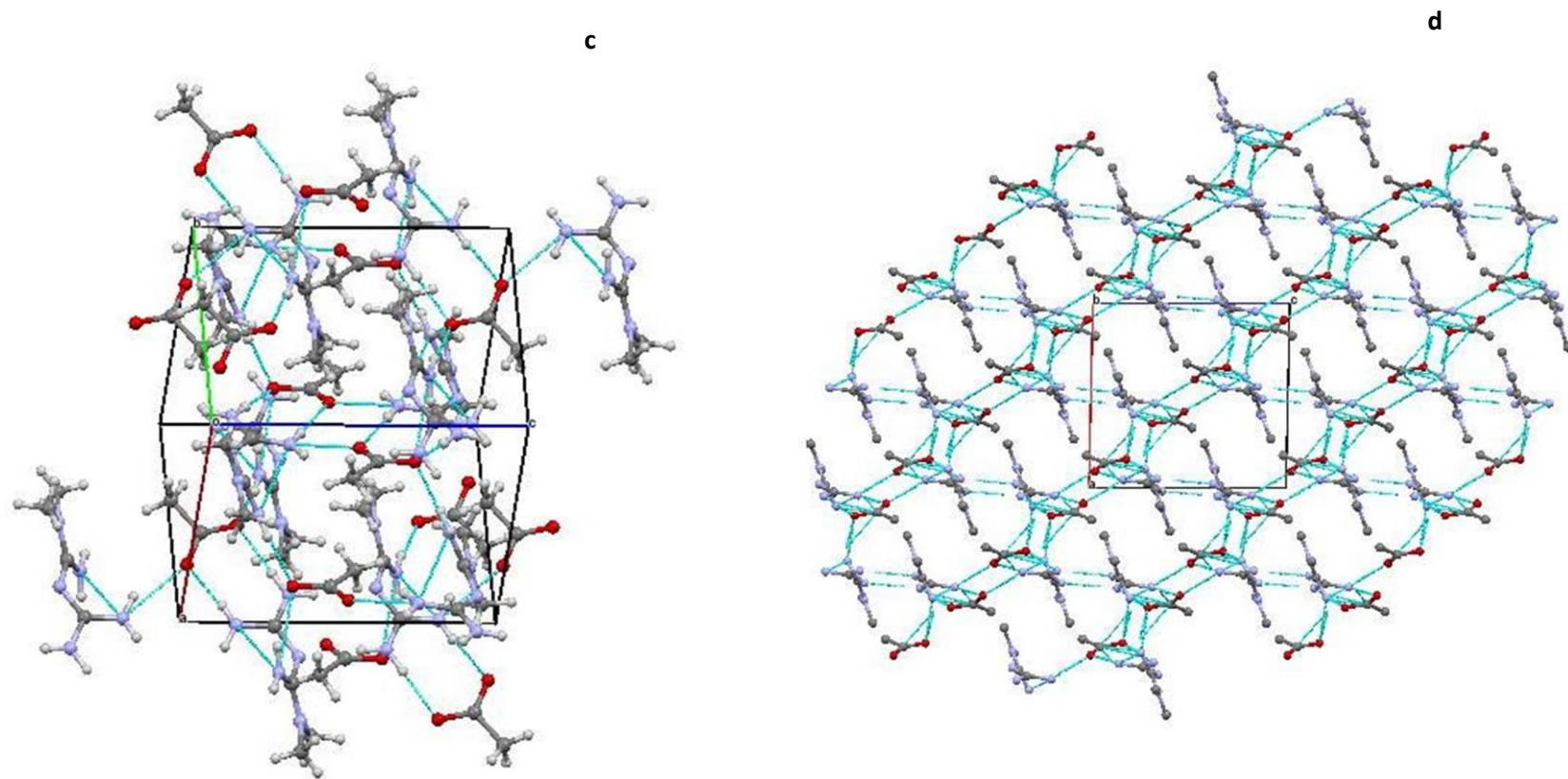**Fig.3.10 Packing motifs of the MET-Formic acid 1:1**

Table 3.8.7 Intremolecular contacts and Packing motifs of the MET-Acetic acid 1:1

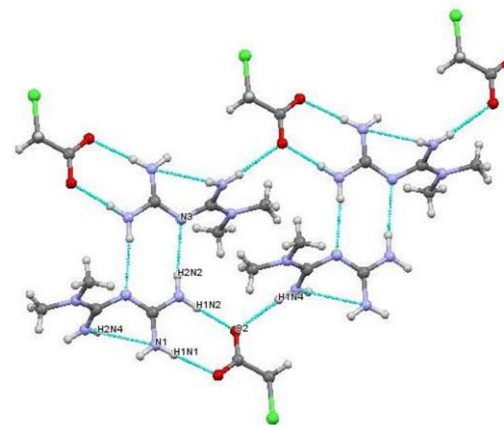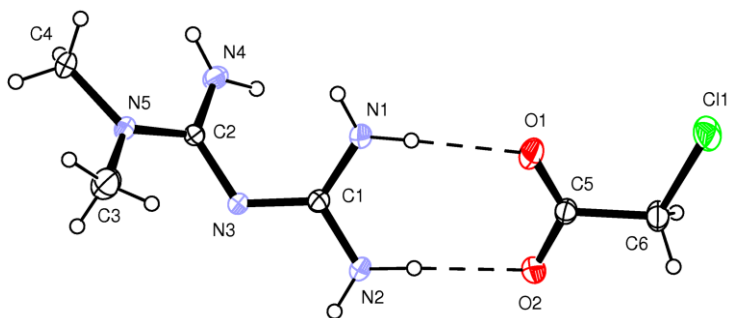| 7	MET-Acetic acid 1:1	D−H/Å	H···A/Å	D···A/Å	<D−H ···A/ °	Symmetry code
Lab code MET10b	N−H···O dimer - $R_2^2(8)$					
	N1−H1···O1	0.84(2)	1.97(2)	2.808(2)	174(2)	x, y, z
	N2−H2···O2	0.93(2)	2.02(2)	2.950(1)	177(2)	x, y, z
	N−H···O tetramer - $R_4^2(8)$					
	N1−H2···O1	0.90(2)	2.04(2)	2.861(2)	152(2)	-x+1,-y+1,-z+1
	N−H···N dimer - $R_2^2(8)$					
	N2−H2···N3	0.85(2)	2.18(2)	3.030(2)	174(2)	-x+1,-y+1,-z+2
	Connected heteromeric dimer					
	N4−H1···O2	0.85(2)	2.08(2)	2.922(2)	174(2)	x,+y-1,+z
	Connected planes					
	N4−H2···O2	0.89(2)	2.20(2)	3.04(2)	163(2)	-x+1/2+1,+y-1/2,-z+1/2
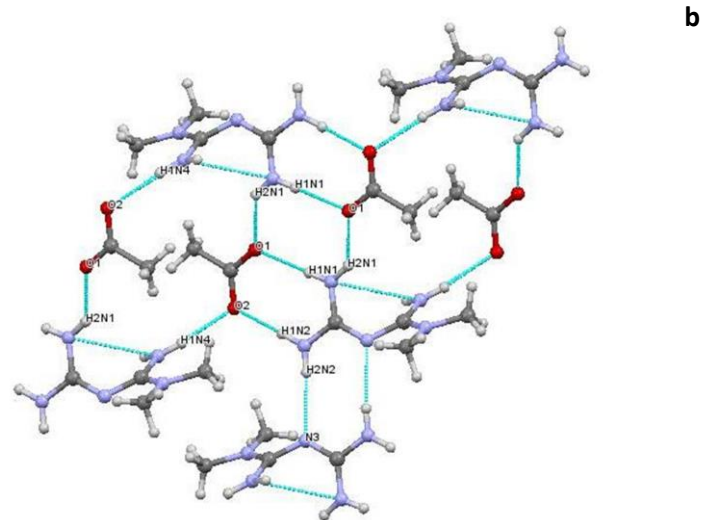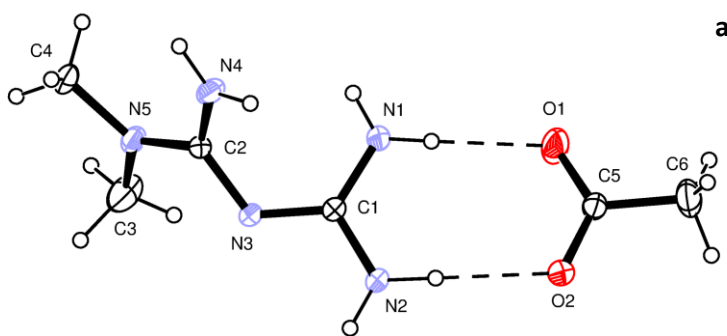
Fig.3.11a Packing motifs of the MET-Acetic acid 1:1

c

d

Fig.3.11b Packing motifs of the MET-Acetic acid 1:1

Table 3.8.8 Intermolecular contacts and Packing motifs of the MET-Monochloracetic acid 1:1

8	MET-Monochloracetic acid 1:1	D−H/Å	H···A/Å	D···A/Å	<D−H···A/ °	Symmetry code
	N−H···O dimer - $R_2^2(8)$					
	N1−H1···O1	0.86(2)	2.02(2)	2.875(2)	175(2)	x, y, z
	N2−H1···O2	0.90(2)	2.00(2)	2.864(2)	171(2)	x, y, z
	N−H···N dimer - $R_2^2(8)$					
	N2−H2···N3	0.87(2)	2.31(2)	3.175(2)	172(2)	-x,-y,-z+1
Lab code METClA6	N−H···O dimer - $R_2^2(8)$					
	N4−H2···O2	0.81(2)	2.17(2)	2.982(2)	173(2)	- x,+y+1,+z
	Other H-bonds					
	N1−H2···Cl 1	0.83(2)	2.894(2)	3.68(1)	157(2)	-x,-y,-z+2
	N1−H1···O1	0.86(2)	2.02(2)	2.875(2)	175(2)	x, y, z
	Connecting haring-bone tapes					
	N4−H2···O2	0.87(2)	2.20(2)	3.033(2)	163(2)	-x+1/2,+y+1/2,-z+1/2+1

Fig.3.12a Packing motifs of the MET-Monochloracetic acid 1:1
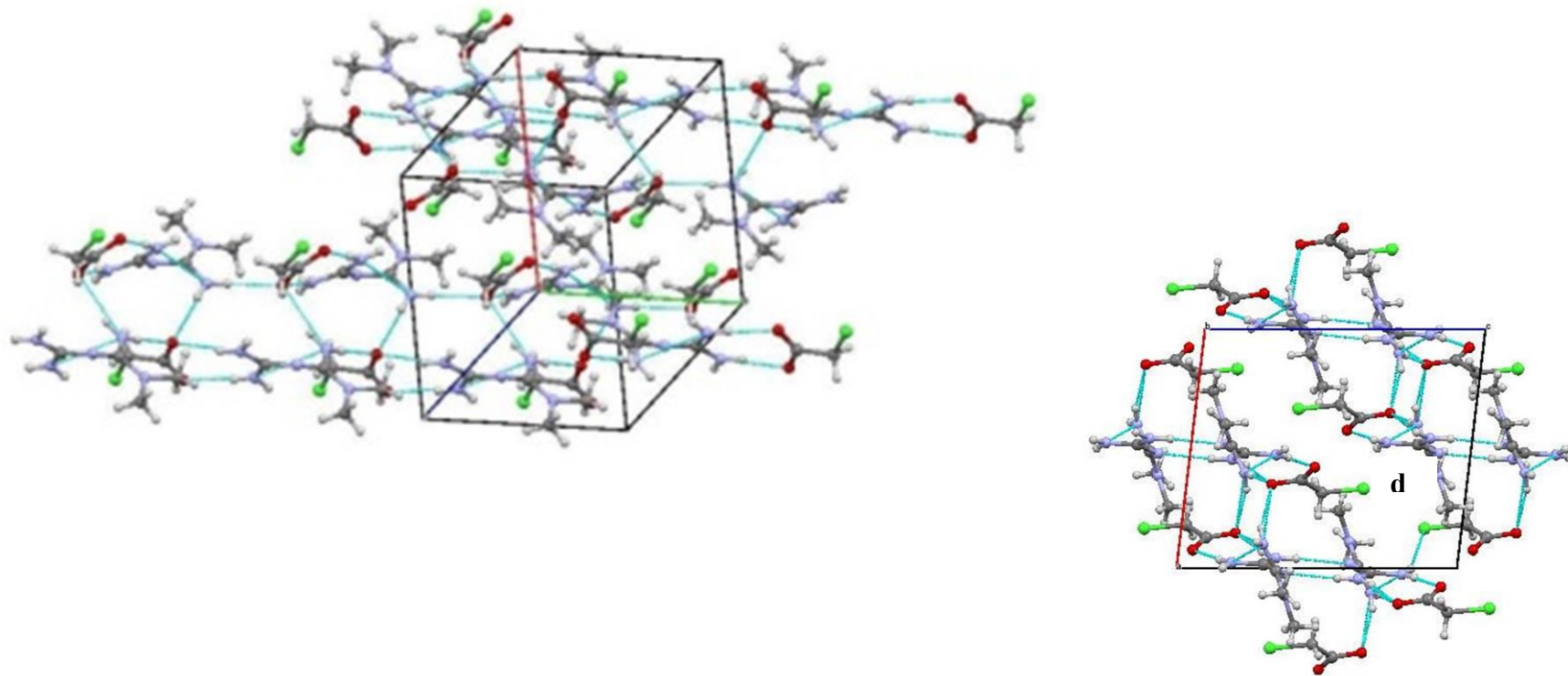
Fig.3.12b Packing motifs of the MET-Monochloracetic acid 1:1

Table 3.8.9 Intremolecular contacts and Packing motifs of the MET-Trifluoroacetic acid 1:1

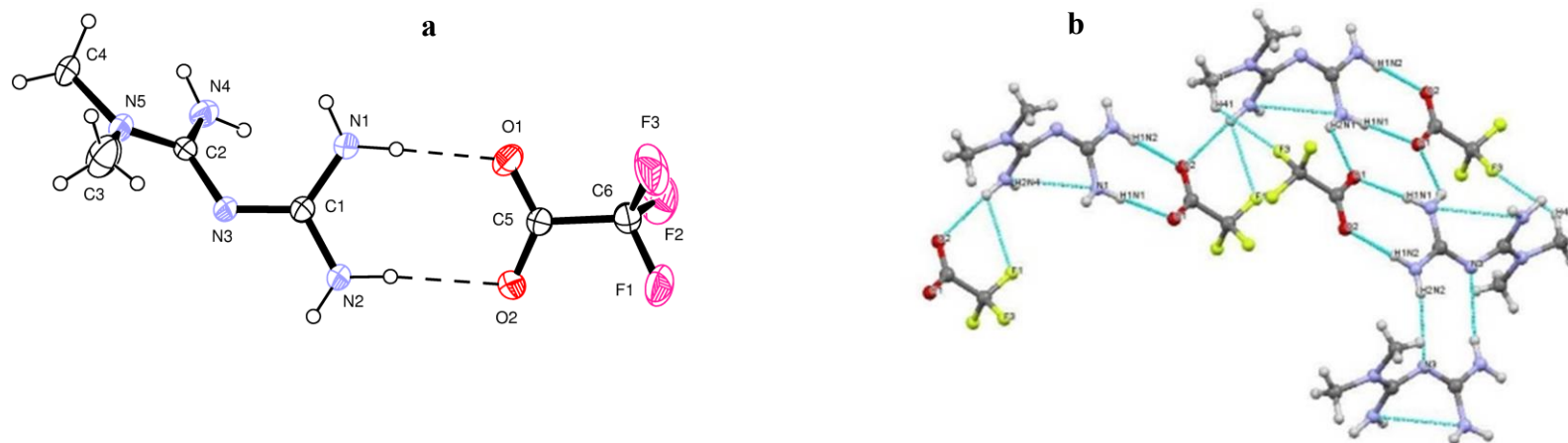| 9	MET-Trifluoroacetic acid 1:1	D−H/Å	H···A/Å	D···A/Å	<D−H ···A/ °	Symmetry code
Lab code METTRFA	N−H···O dimer - $R_2^2(8)$					
	N1−H1···O1	0.88(3)	1.98(3)	2.862(3)	178(3)	x, y, z
	N2−H1···O2	0.90(3)	2.11(3)	3.002(3)	175(3)	x, y, z
	N−H···N dimer - $R_2^2(8)$					
	N2−H2···N3	0.81(3)	2.43(3)	3.230(3)	170(3)	-x+1,-y+1,-z+1
	N−H···O tetramer - $R_4^2(8)$					
	N1−H1···O1	0.88(3)	1.98(3)	2.862(3)	178(3)	x, y, z
	N1−H2···O1	0.85(3)	2.33(3)	2.994(3)	135(3)	-x+1,-y+1,-z
	Other H-bonds					
	N2−H1···O1	0.90(3)	2.90(3)	3.593(3)	135(2)	x, y, z
	N2−H2···O1	0.85(3)	2.33(3)	2.994(3)	135(3)	x, y, z
	N4−H2···O2	0.88(3)	2.36(3)	3.194(3)	161(3)	-x+1/2,+y+1/2,-z+1/2
	N4−H1···O2	0.86(4)	2.23(4)	3.078(3)	172(3)	x,+y+1,+z

a

b

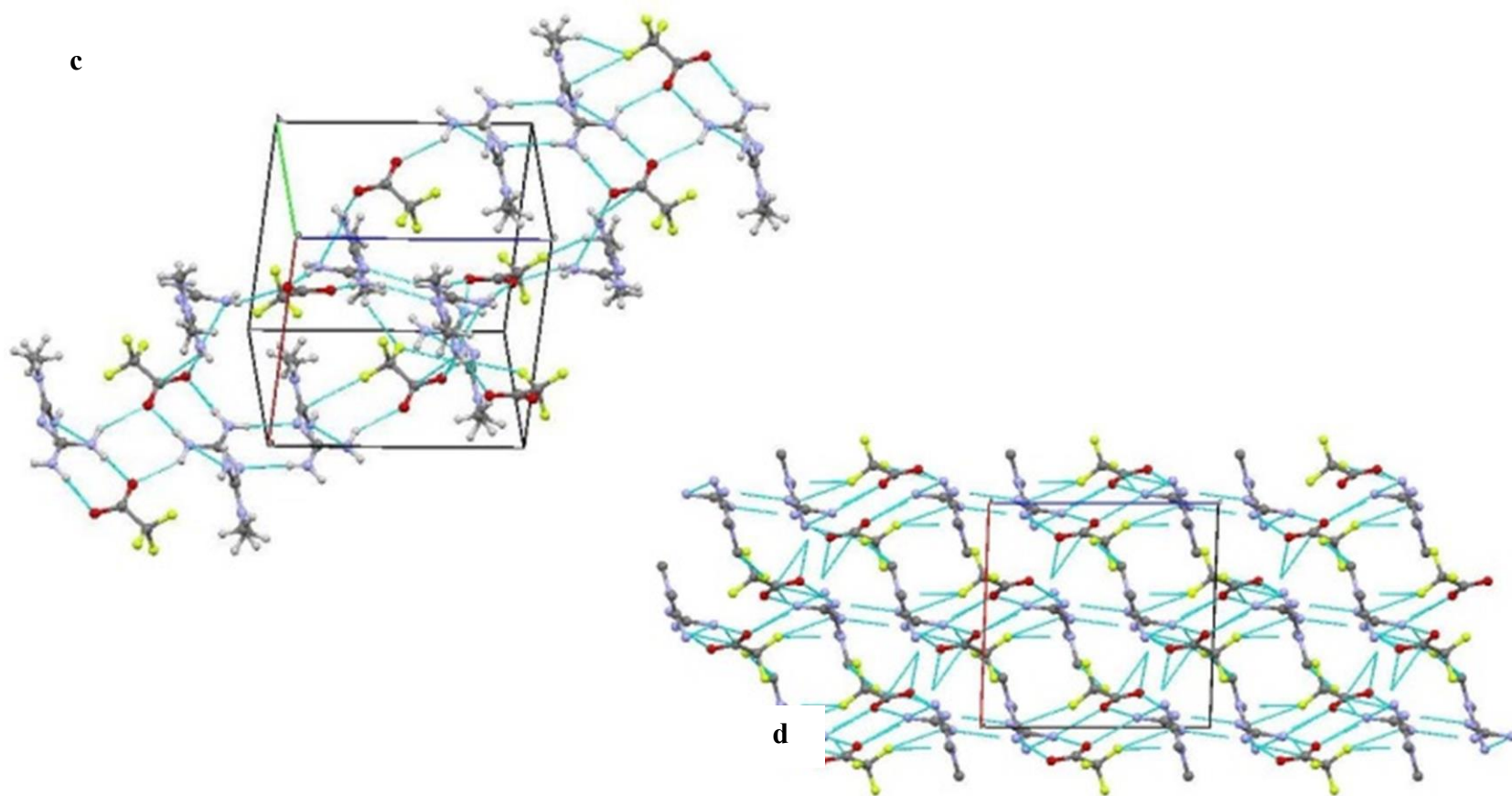**Fig.3.13a Packing motifs of the MET-Trifluoroacetic acid 1:1**

Fig.3.13b Packing motifs of the Packing motifs of the MET-Trifluoroacetic acid 1:1

Table 3.8.10 Intremolecular contacts and Packing motifs of the MET-Trichloroacetic acid 1:1

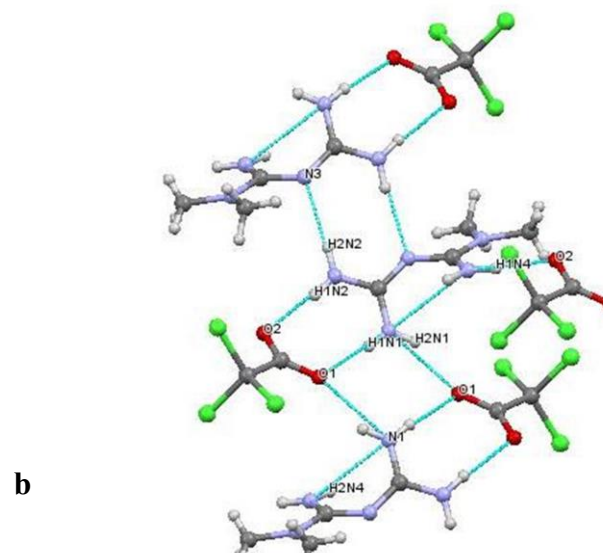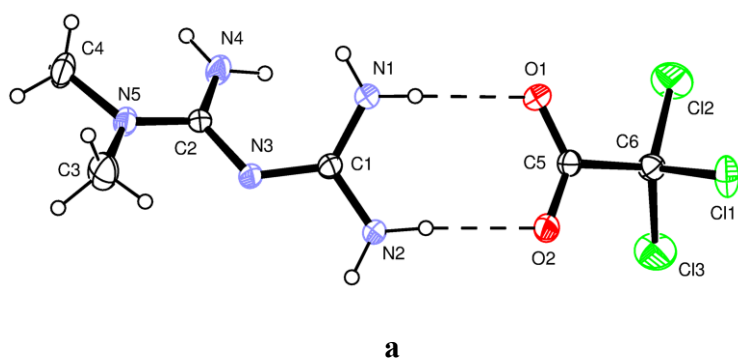| 10	MET-Trichloroacetic acid 1:1	D−H/Å	H···A/Å	D···A/Å	<D−H ···A/ °	Symmetry code
Lab code METTRIClA24	N−H···O dimer - $R_2^2(8)$					
	N1−H1···O1	0.81(3)	2.14 (3)	2.927(2)	165.49(2)	x, y, z
	N2−H1···O2	0.86(3)	2.03(3)	2.888(2)	174(3)	x, y, z
	N−H···O tetramer - $R_4^2(8)$					
	N1−H1···O1	0.83(3)	2.10(3)	2.819(2)	145(3)	-x+1,-y+2,-z+1
	N1−H2···O1	0.83(3)	2.10(3)	2.819(2)	145(3)	-x+1,-y+2,-z+1
	N−H···N dimer - $R_2^2(8)$					
	N2−H2···N3	0.88(3)	2.17(3)	3.041(2)	173.56(3)	-x,-y+2,-z+1

a

b

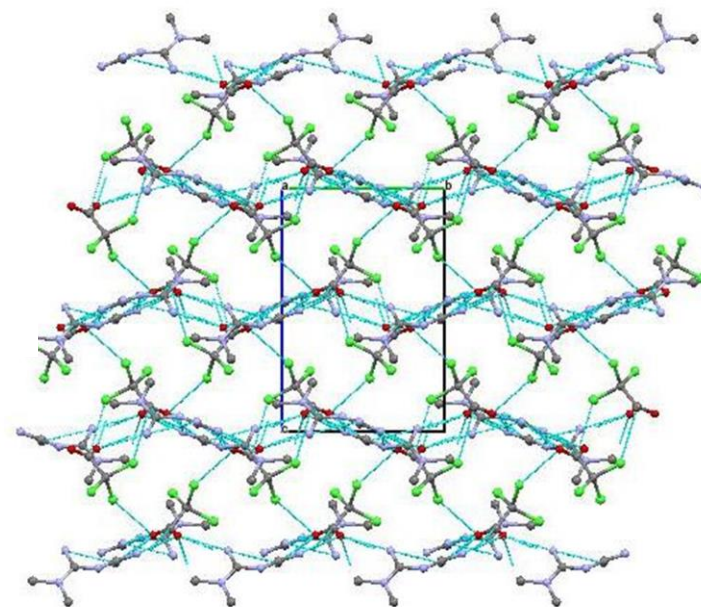**Fig.3.14a Packing motifs of the MET-Trichloroacetic acid 1:1**

c
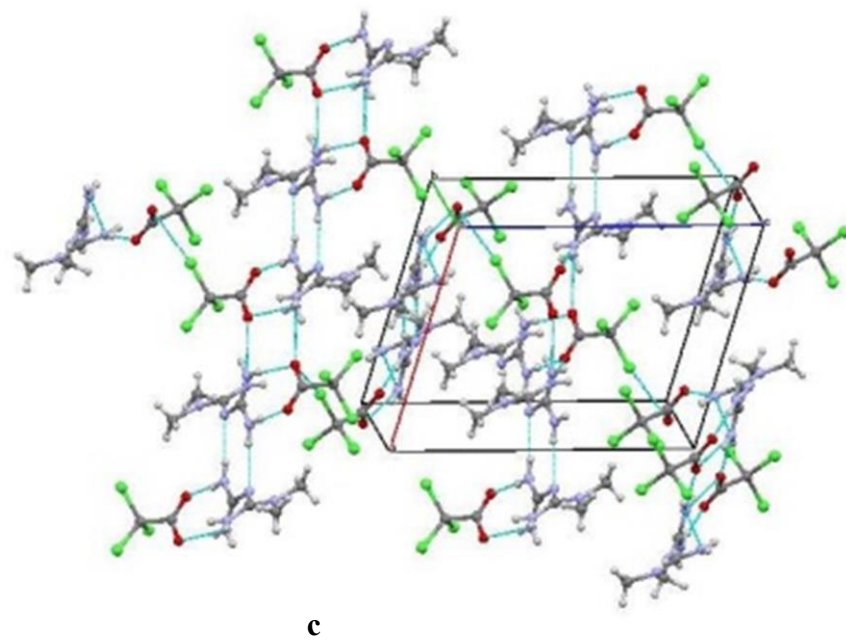
d

Fig.3.14b Packing motifs of the MET-Trichloroacetic acid 1:1

Table 3.8.11 Intremolecular contacts and Packing motifs of the MET- Trichloroacetic acid 1 : 2

11	MET-Trichloroacetic acid 1 :2	D−H/Å	H···A/Å	D···A/Å	<D−H ···A/ °	Symmetry code
	N−H···O dimer - $R_2^2(8)$					
	N1A−H11A···O1	0.80(6)	1.98(7)	2.780(7)	177(7)	x, y, z
	N2A−H21A···O2	0.67(6)	2.22(6)	2.903(8)	177(7)	x, y, z
	N2B−H22B···O7	0.84(9)	1.99(8)	2.795(7)	161 (9)	x, y, z
	N3B−H3B···O8	0.83(8)	1.84(8)	2.652(7)	166(8)	x, y, z
Lab code	N2A−H22A···O4	0.92(7)	3.05(7)	2.161(7)	165(7)	x, y, z
METTRIClA2	N3A−H3A···O3	0.79(7)	1.93(7)	2.717(7)	174(7)	x, y, z
	Other H-bond contacts					
	N2B−H21B···O4	0.81(9)	2.28(8)	3.013(8)	150(8)	x, y, z
	N1B−H11B···O4	0.81(7)	2.10(8)	2.874(9)	162(7)	x, y, z
	N1B−H12B···O5	0.76(7)	2.19(6)	2.832(7)	142(6)	x, y, z
	N4A−H42A···O5	0.84(7)	2.03(7)	2.864(7)	173(7)	x, y, z

Fig.3.15a Packing motifs of the MET-Trichloroacetic acid 1:2

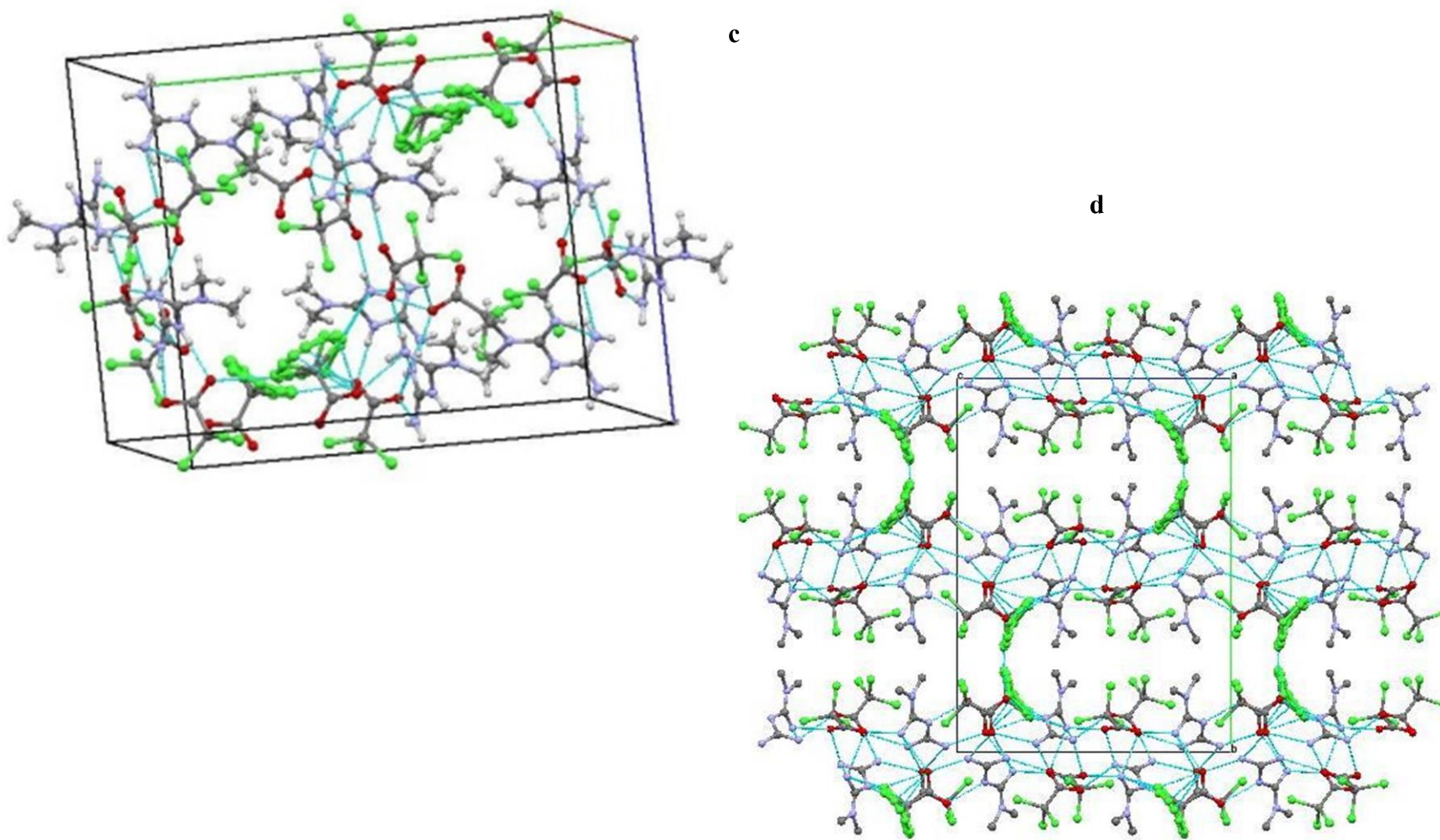**Fig.3.15b Packing motifs of the MET-Trichloroacetic acid 1:2**

Table 3.8.12 Intremolecular contacts and Packing motifs of the MET- Malonic acid 1:1

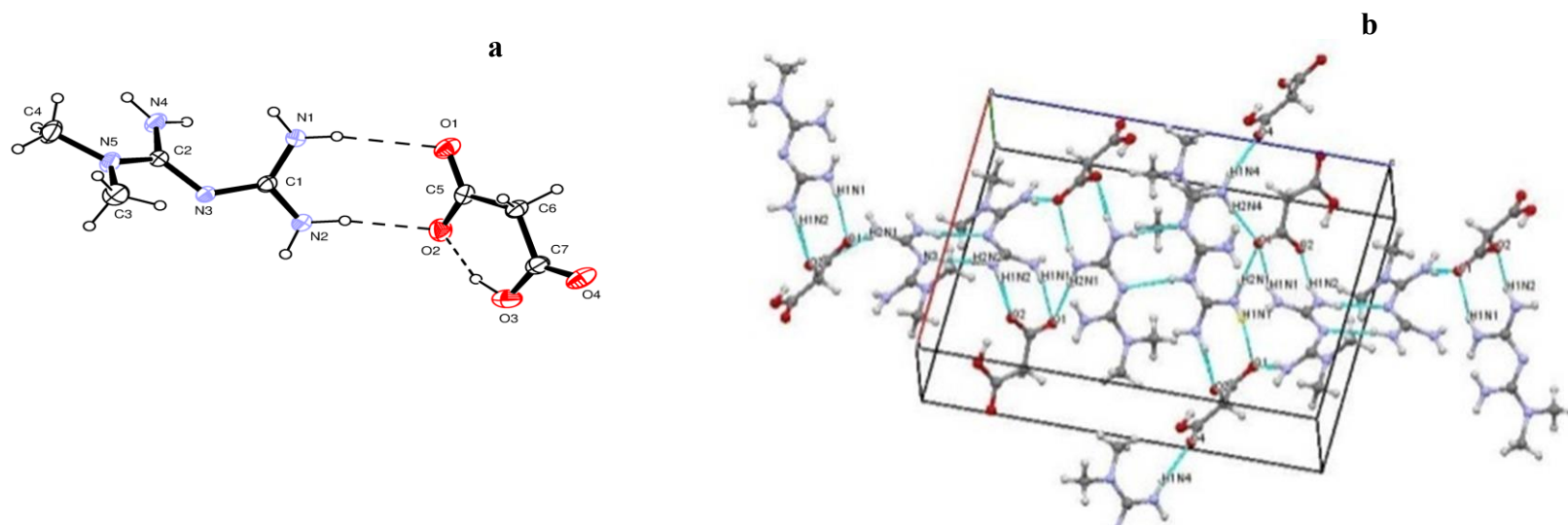| 12	MET-Malonic acid 1:1	D−H/Å	H···A/Å	D···A/Å	<D−H ···A/ °	Symmetry code
	N−H···O dimer - $R_2^2(8)$					
	N2−H1···O2	0.89(1)	1.98(1)	2.862(1)	168(1)	x, y, z
	N1−H1···O1	0.85(2)	2.29(2)	3.132(1)	168(2)	x, y, z
	N−H···N dimer - $R_2^2(8)$					
	N2−H2···N3	0.88(2)	2.18(2)	3.053(1)	170(2)	-x+1,-y+1,-z+2
Lab code	Other H-bonds					
MET34	N1−H2···O1	0.912)	2.74(2)	3.026(1)	100(2)	x, y, z
	N1−H1···O1	0.85(2)	2.29(2)	3.132(1)	168(2)	x, y, z
	N4−H2···O1	0.90(2)	2.12(2)	3.008(2)	168(2)	-x+1,+y+1/2,-z+1/2+1
	N4−H1···O4	0.88(2)	2.09(2)	2.951(1)	169(2)	x+1,+y,+z
	Intramolecular H-bond					
	O3−H30···O2	0.98(3)	1.55(3)	2.484(1)	156(2)	x, y, z

b

a

Fig.3.16a Packing motifs of the MET- Malonic acid 1:1
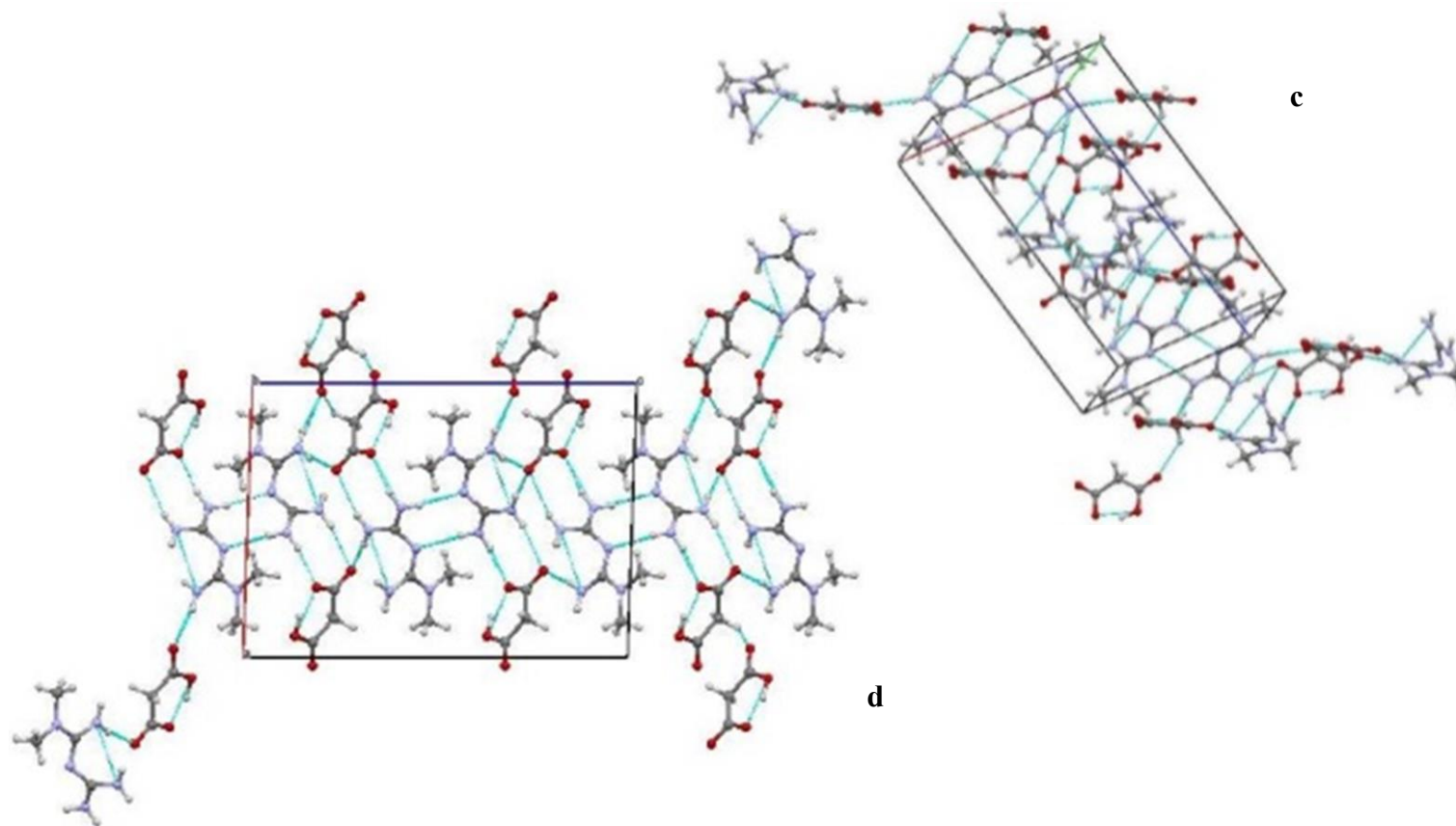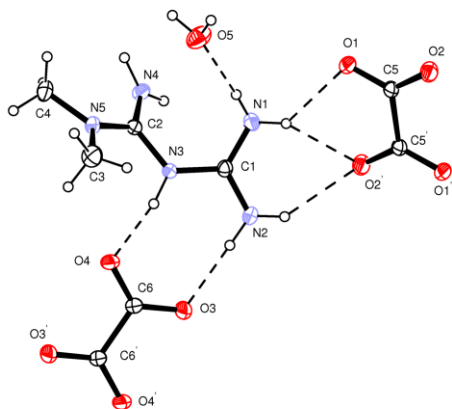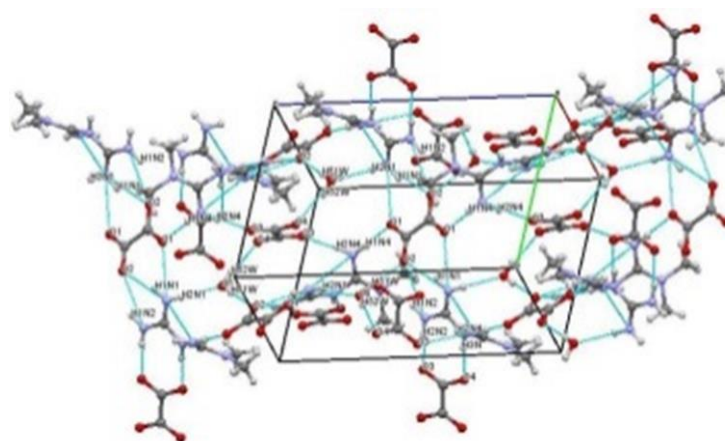
Fig.3.16b Packing motifs of the MET- Malonic acid 1:1

Table 3.8.13 Intremolecular contacts and Packing motifs of the MET-Oxalic acid-hydrate 1:1:1

13	MET-Oxalic acid-hydrate 1:1:1	D−H/Å	H···A/Å	D···A/Å	<D−H ···A/ °	Symmetry code
Lab code MET33	N−H···O dimer - $R_2^2(8)$					
	N2−H2···O3	0.89(2)	1.95(2)	2.830(2)	173(2)	x, y, z
	N3−H3N···O4 (0)	0.89(2)	1.78(2)	2.654(1)	169(2)	x, y, z
	Other H-bonds					
	N1−H1···O1	0.84(2)	2.32(2)	2.908(2)	128(2)	x, y, z
	N1−H2···O1	0.84(2)	2902)	2.908(2)	81(1)	x, y, z
	N4−H1···O1	0.93(2)	1.84(2)	2.773(1)	176(2)	-x+1,+y+1/2,-z+1/2
	N2−H1···O2	0.84(2)	2.27(2)	2.987(2)	142 (2)	-x+1,-y,-z
	N1−H1···O2	0.842)	2.102)	2.875(2)	154(2)	-x+1,-y,-z
	N4−H2···O3	0.88(.2)	2.07(2)	2.881(1)	153(2)	-x,-y+1,-z
	O5−H52W···O4	0.81(2)	2.13(2)	2.933(2)	167(2)	-x,+y-1/2,-z+1/2
	O5−H51W···O2	0.89(2)	1.91(2)	2.787(2)	172(2)	-x+1,+y+1/2,-z+1/2
	N1−H2···O5	0.84(2)	2.11(2)	2.927(2)	165(2)	x, y, z

a

b

Fig.3.17a Packing motifs of the MET-Oxalic acid-hydrate 1:1:1

Fig.3.17b Packing motifs of the MET-Oxalic acid-hydrate 1:1:1

Table 3.8.14 Intremolecular contacts and Packing motifs of the MET-Oxalic acid-hydrate 1:2.5:1

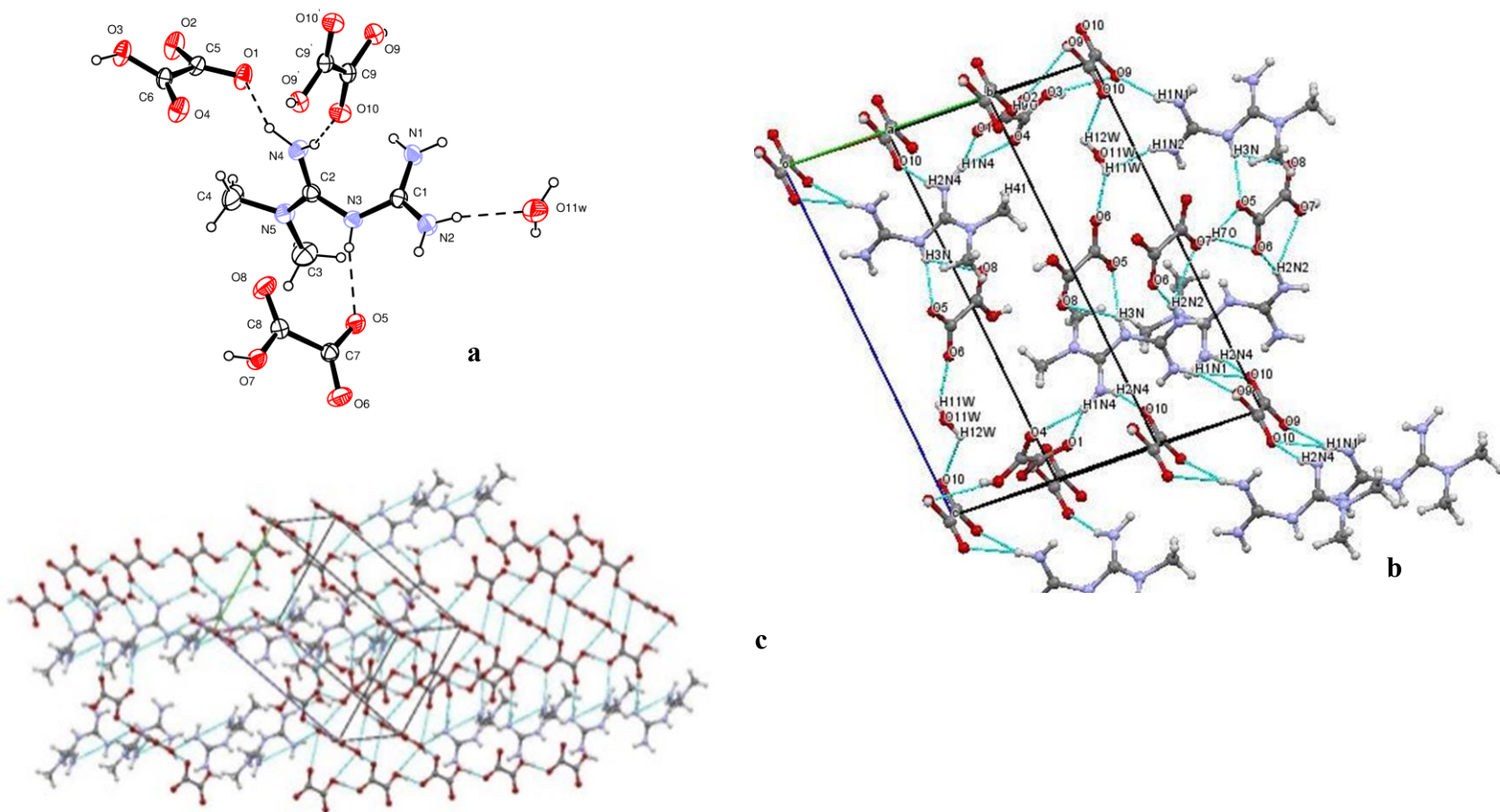| 14	MET-Oxalic acid-hydrate 1:2.5:1	D−H/Å	H···A/Å	D···A/Å	<D−H ···A/ °	Symmetry code
	Dimer carboxylate					
	O9−H9O···O2	0.89(5)	1.65(5)	2.526(5)	167(6)	-x+1,-y+1,-z
	Other H-bonds					
	N1−H1···O2	0.86(5)	2.95(5)	3.190(7)	98(3)	-x+1,-y+1,-z
	N1−H2···O2	0.86(5)	2.95(5)	3.190(7)	98(3)	-x+1,-y+1,-z
	N1−H1···O9	0.86(5)	2.35(3)	3.060(6)	141(3)	-x+1,-y,-z
	N1−H1O···10	0.86(5)	2.33(4)	3.104(7)	150(3)	x-1,+y,+z
	N1−H2···O4	0.86(5)	2.18(4)	3.001(6)	159(3)	x-1,+y,+z
	N2−H2···O7	0.86(7)	2.53(7)	3.140(7)	129(6)	-x+1,-y,-z+1
	N2−H2···O6	0.86(7)	2.07(7)	2.881(7)	157(6)	-x+1,-y,-z+1
	N2−H1O···11W	0.81(7)	2.07(7)	2.867(9)	168(6)	x, y, z
	N2−H2···O5	0.86(7)	2.96(7)	3.399(7)	114(5)	x, y ,z
	N3−H3···O5	0.74(4)	2.01(7)	2.731(7)	167(8)	x, y ,z
Lab code	N3−H3···O8	0.74(7)	2.64(7)	3.101(8)	122(6)	x, y ,z
MET68	N4−H1···O1	0.98(1)	2.00(9)	2.859(6)	145(8)	x, y ,z
	N4−H1···O4	0.98(1)	2.51(1)	3.336(7)	141(7)	x, y ,z
	N4−H2O···10	0.98(7)	1.97(6)	2.919(6)	164(6)	x, y ,z
	O11W−H11W···N2	0.89(7)	2.86(9)	2.867(9)	81(5)	x, y ,z
	O11−WH12W···O9	0.90(7)	2.83(8)	3.154(6)	103(4)	-x+1,-y,-z
	O11W−H12W···O10	0.90(7)	2.67(8)	3.222(6)	121(5)	x-1,+y,+z
	O11W−H11W···O6	0.89(7)	2.05(7)	2.811(6)	143(6)	-x,-y,-z+1
	O11−WH12W···O2	0.90(7)	2.88(8)	3.758(8)	167(5)	x-1,+y-1,+z
	O11−WH12W···O3	0.90(7)	2.85(7)	3.414(7)	123(4)	x-1,+y-1,+z
	O3−H3O···O1	1.00(6)	1.56(5)	2.560(5)	175(5)	x+1,+y,+z
	O3−H3O···O2	1.00(6)	2.80(6)	3.550(6)	132(4)	x+1,+y,+z
	O3−H3O···O1	1.00(6)	2.98(5)	3.180(5)	92(3)	-x+2,-y+1,-z
	O3−H3O···O9	1.00(6)	2.90(5)	2.928(6)	82(3)	-x+2,-y+1,-z
	O7−H7O···O5	0.87(9)	1.79(8)	2.604(6)	153(8)	x+1,+y,+z
	O7−H7O···O6	0.87(9)	2.64(9)	3.421(6)	150(7)	x+1,+y,+z
	O7−H7O···O7	0.87(9)	2.99(7)	3.143(5)	92(5)	-x+2,-y,-z+1
	O9−H9O···O3	0.89(5)	2.80(7)	2.928(6)	89(5)	-x+2,-y+1,-z

Fig.3.18 Packing motifs of the MET-Oxalic acid-hydrate 1:2.5:1

Table 3.8.15 Intermolecular contacts and Packing motifs of the MET-Maleic acid 1:1

15	MET-maleic acid 1:1	D−H/Å	H···A/Å	D···A/Å	<D−H ···A/ º	Symmetry code
Lab code MET17	N−H···O dimer - $R_2^2(8)$					
	N1−H1···O1	0.85(2)	2.90(2)	2.044(2)	177(2)	x, y, z
	N2−H1···O2	0.88(2)	2.19(2)	3.053(2)	169(2)	x, y, z
	N−H···N dimer - $R_2^2(8)$					
	N2−H2···N3	0.87(2)	2.19(2)	3.057(2)	173(2)	-x+1,-y+1,-z+2
	Other H-bonds					
	N4−H1···O2	0.88(2)	2.12(2)	2.998(2)	175(2)	x,+y-1,+z
	N4−H2···O2	0.90(2)	2.17(2)	3.019(2)	159(2)	-x+1/2,+y-1/2,-z+1/2+1
	N1−H2···O3	0.88(2)	2.43(2)	3.063(2)	129(2)	-x+1,-y+1,-z+1
	N1−H2···O4	0.88(2)	2.21(2)	3.075(2)	168(2)	-x+1,-y+1,-z+1
	Intramolecular H-bond in maleic acid					
	03−H1···O1	0.98(3)	1.46(2)	2.427(2)	173(3)	x, y, z
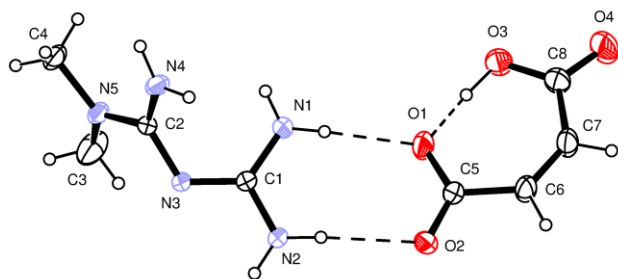
a
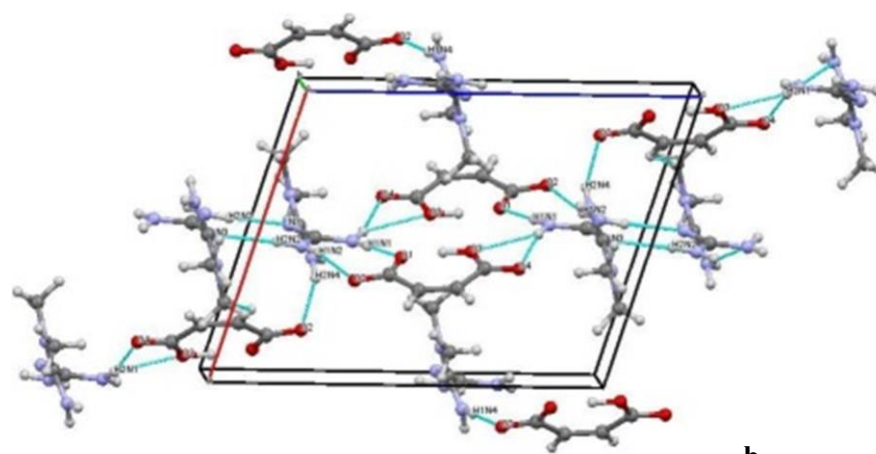
b

Fig.3.19a Packing motifs of the MET-Maleic acid 1:1
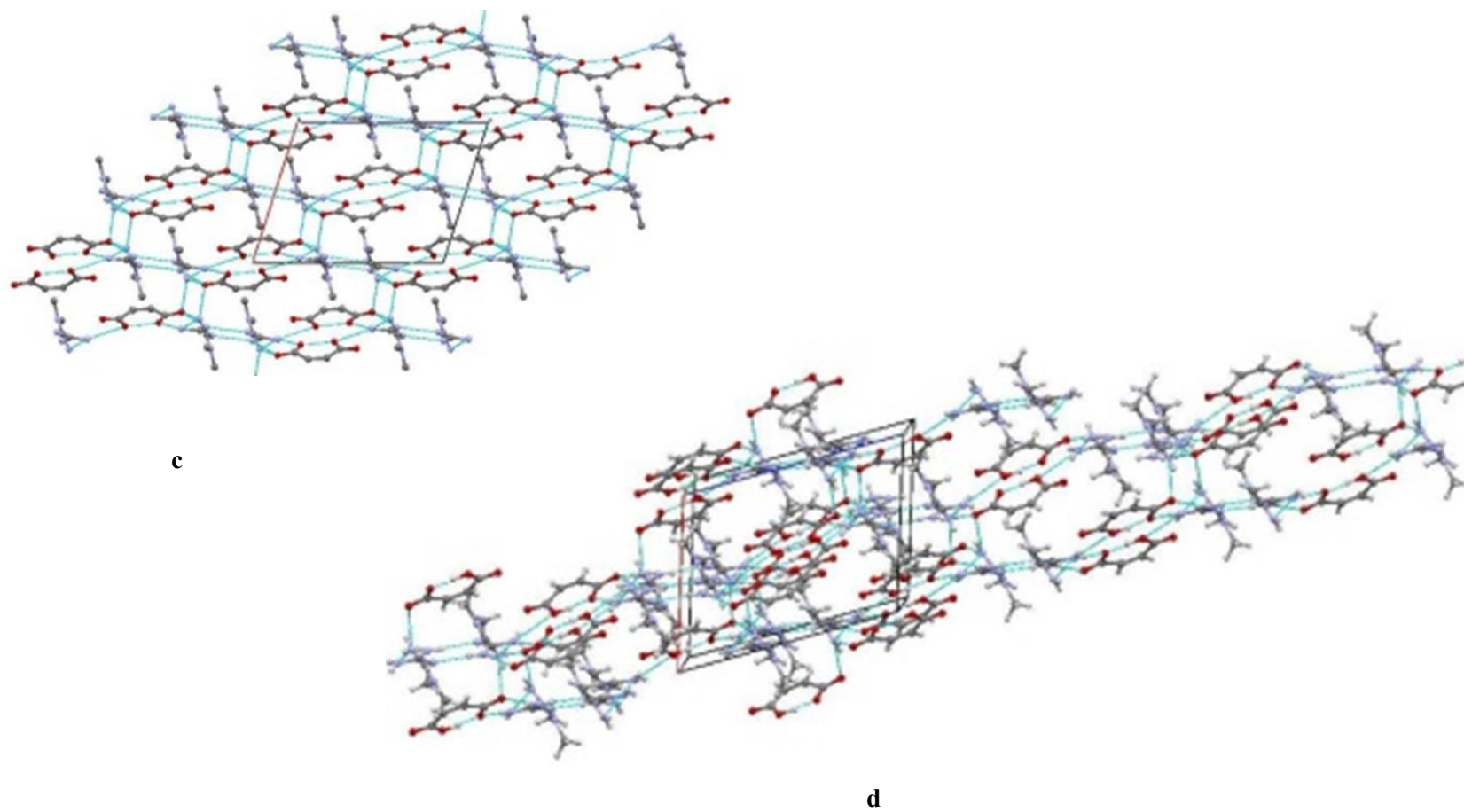
c

d

Fig.3.19b Packing motifs of the MET-Maleic acid 1:1

Table 3.8.16 Intremolecular contacts and Packing motifs of the MET-Fumaric acid 1 : 0.5

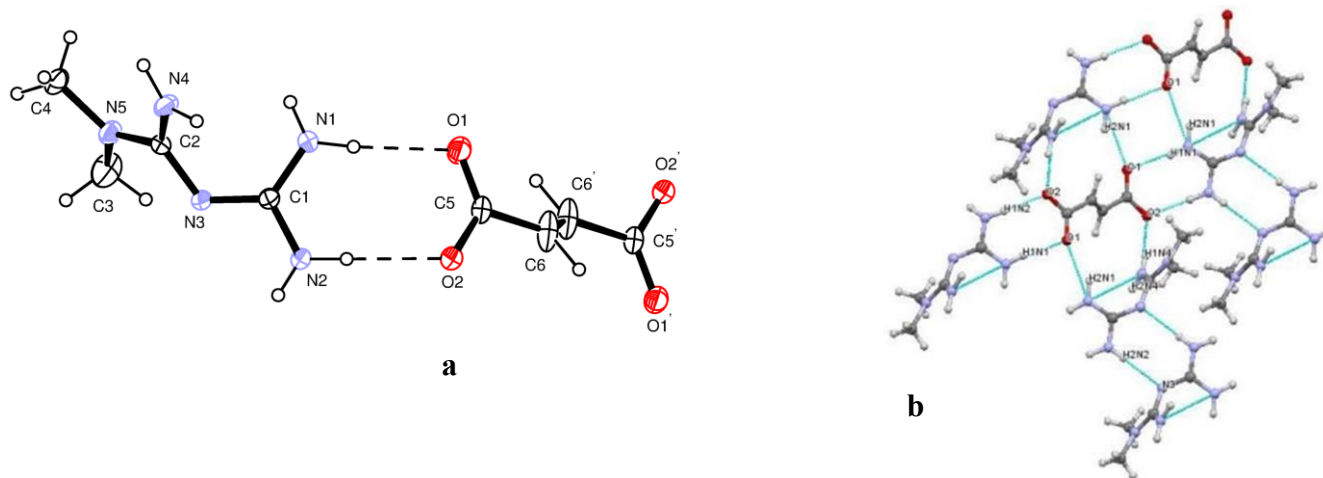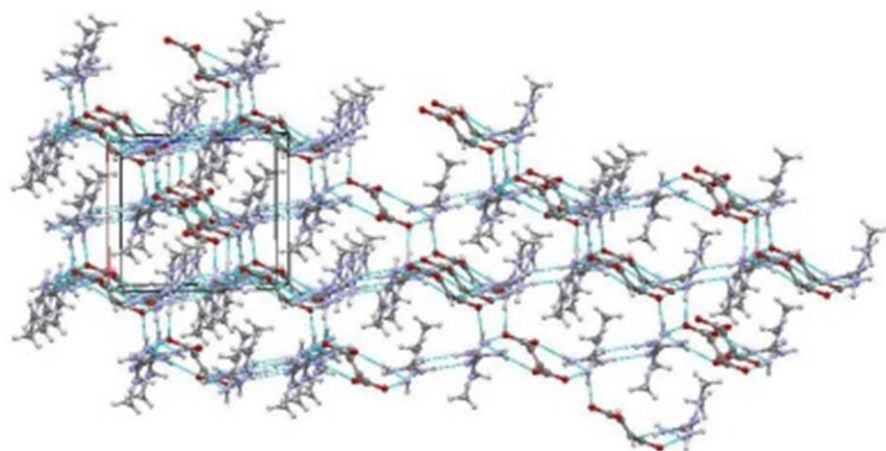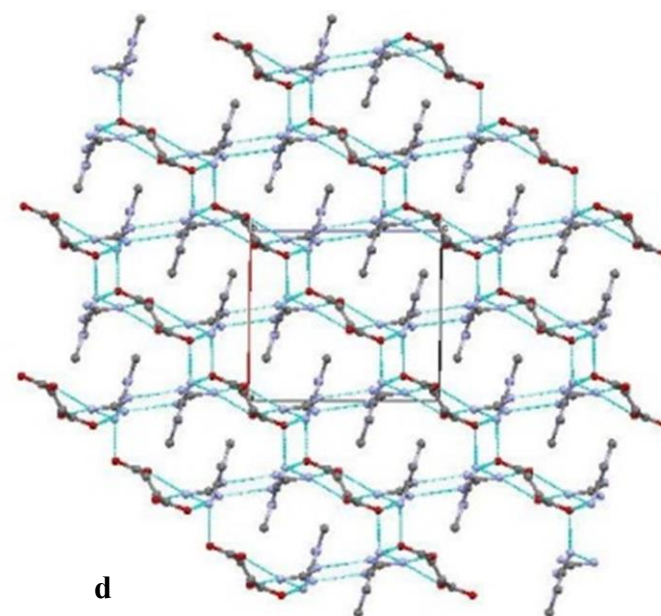| 16	MET-Fumaric acid 1 : 0.5	D−H/Å	H···A/Å	D···A/Å	<D−H ···A/ °	Symmetry code
Lab code MET18	N−H···O dimer - $R_2^2(8)$					
	N1−H1···O1	0.89(3)	2.94(3)	2.061(3)	169(3)	x, y, z
	N2−H1···O2	0.89(3)	2.04(3)	2.927(2)	176(3)	x, y, z
	N−H···O tetramer - $R_4^2(8)$					
	N1−H2···O1	0.90(3)	2.12(3)	2.902(2)	145(3)	-x,-y+1,-z
	N1−H1···O1	0.89(3)	2.94(3)	2.061(3)	169(3)	x, y, z
	Homomer N−H···N dimer - $R_2^2(8)$					
	N2−H2···N3	0.83(3)	2.23(3)	3.060(3)	176(3)	-x,-y+1,-z+1
	Other H-bonds (connecting of the planes)					
	N4−H2···O2	0.91(3)	2.97(3)	3.576(3)	126(2)	-x+1/2,+y+1/2,-z+1/2
	N4−H1···O2	0.91(3)	2.07(3)	2.977(2)	174(3)	-x+1/2,+y+1/2,-z+1/2

a

b

Fig.3.20a Packing motifs of the MET-Fumaric acid 1 : 0.5

c

d

Fig.3.20b Packing motifs of the MET-Fumaric acid 1 : 0.5

Table 3.8.17 Intremolecular contacts and Packing motifs of the MET-Succinic acid 1 : 0.5

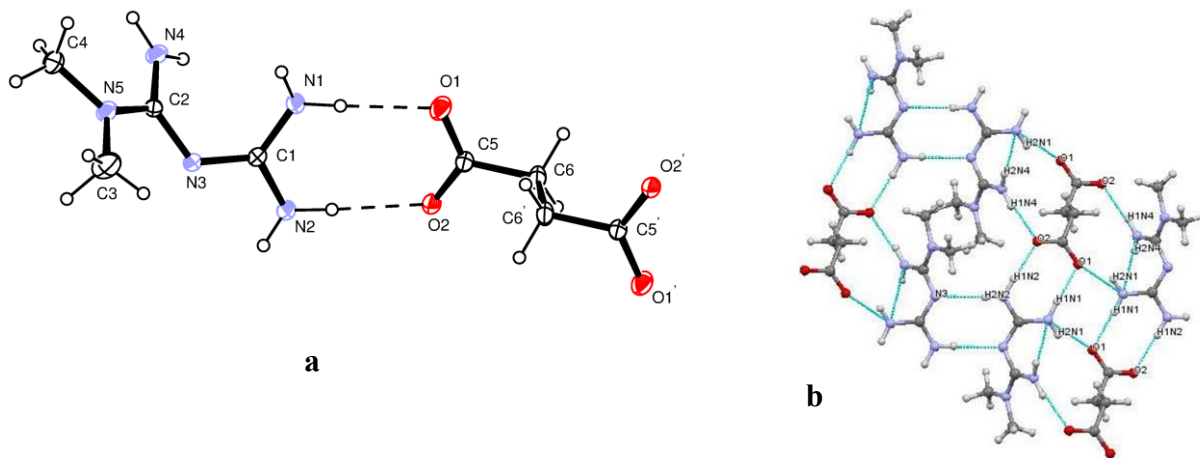| 17	MET-Succinic acid 1:0.5	D−H/Å	H···A/Å	D···A/Å	<D−H ···A/ °	Symmetry code
	N−H···O dimer - $R_2^2(8)$					
	N1−H1···O1	0.91(2)	2.01(2)	2.908(1)	169(2)	x, y, z
	N2−H1···O2	0.93(2)	2.02(2)	2.944(1)	178(2)	x, y, z
	N1−H2···O1	0.86(2)	2.07(2)	2.841(1)	148(2)	-x+1,-y+2,-z+1
	Homomer N−H···N dimer - $R_2^2(8)$					
Lab code	N2−H2···N3	0.85(2)	2.24(2)	3.089(2)	177(2)	-x+1,-y+2,-z
MET15	N−H···O tetramer - $R_4^2(8)$					
	N1−H2···O1	0.86(2)	2.07(2)	2.841(1)	148(1)	-x+1,-y+2,-z+1
	N1−H1···O1	0.91(2)	2.01(2)	2.908(1)	169(2)	x, y, z
	Other H-bonds (connecting of the planes)					
	N4−H2···O2	0.88(2)	2.17(2)	3.040(1)	171(2)	-x+1/2,+y-1/2,-z+1/2
	N4−H1···O2	0.88(2)	2.02(2)	2.898(1)	171(2)	x,+y-1,+z

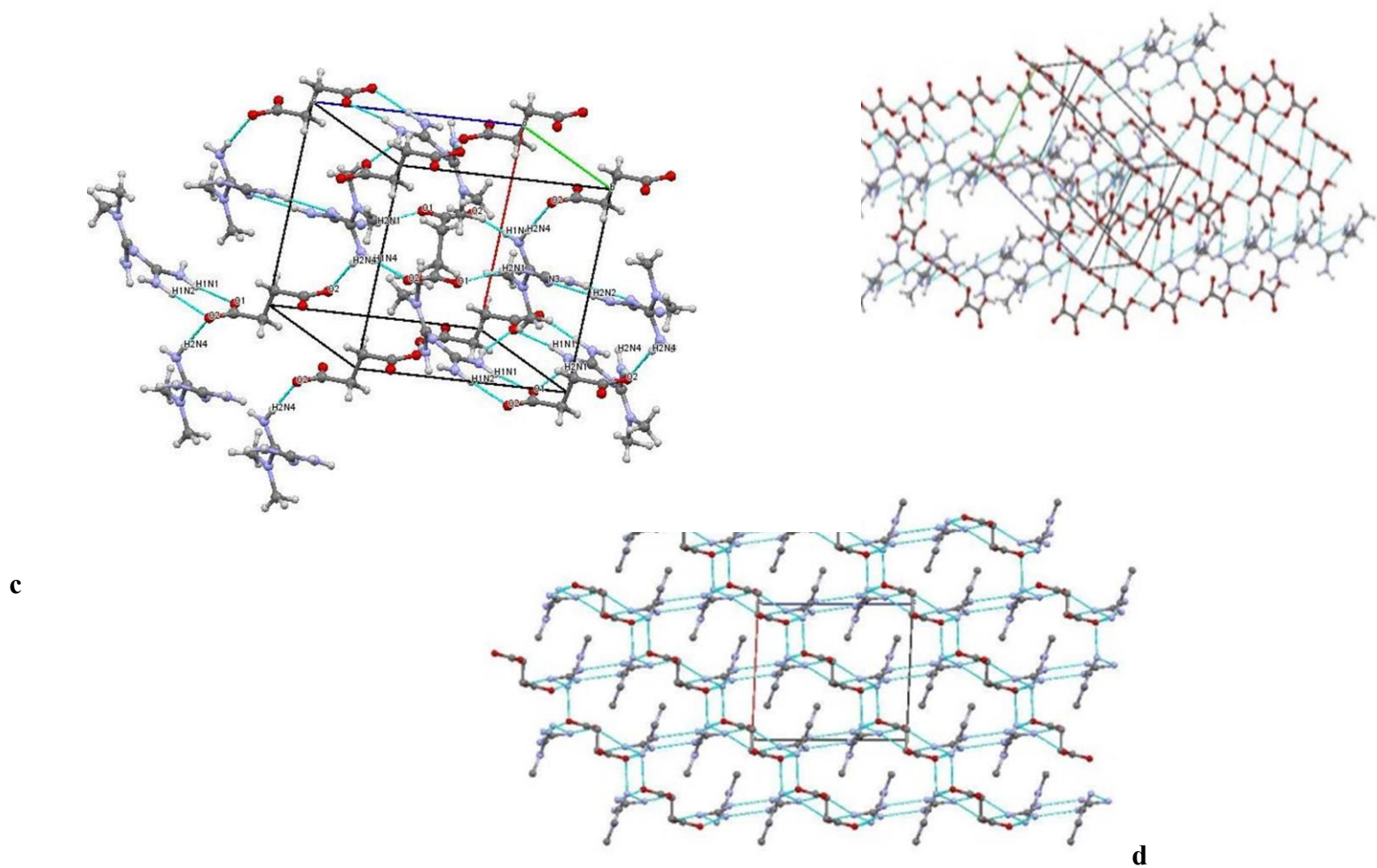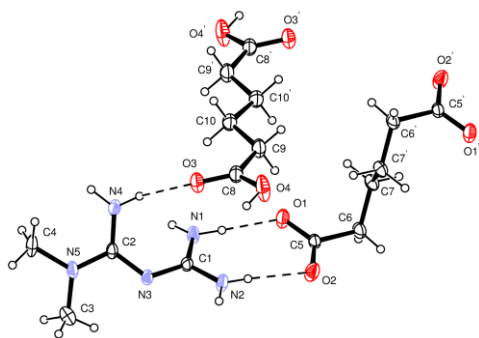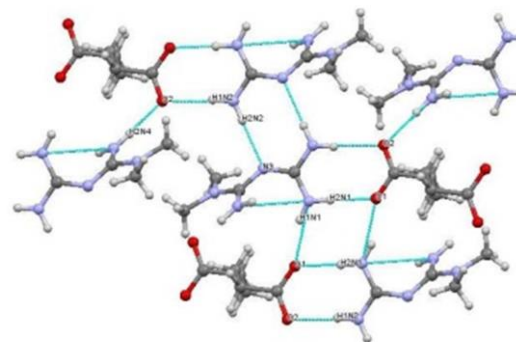**Fig.3.21a Packing motifs of the MET-Succinic acid 1 : 0.5**

c

d

Fig.3.21b Packing motifs of the MET-Succinic acid 1 : 0.5

Table 3.8.18 Intremolecular contacts and Packing motifs of the MET-Adipic acid 1:1

18	MET-Adipic acid 1:1	D−H/Å	H···A/Å	D···A/Å	<D−H ···A/ °	Symmetry code
	N−H···O dimer - $R_2^2(8)$					
	N1−H2···O1	0.91(2)	1.95(2)	2.852(1)	178.62(2)	x, y, z
	N2−H1···O2	0.86 (2)	2.07(2)	2.932(1)	174.64(2)	x, y, z
	Homomer N−H···N dimer - $R_2^2(8)$					
	N2−H2··N3	0.87(2)	2.16(2)	3.020(2)	177.45(2)	-x,-y+1,-z+2
	N−H···O tetramer - $R_4^2(8)$					
	N1−H2···O1	0.91(2)	1.95(2)	2.852(1)	178.62(2)	x, y, z
Lab code	N1−H1O1	0.87(2)	2.04(2)	2.870(1)	160(2)	-x,-y+1,-z+1
METADA22	Chains of homomeric O−H···O carboxyle dimer $R_2^2(8)$					
	Other H-bonds					
	C3−H31···O3	0.94(3)	2.53(3)	3.367(2)	148(2)	x+1,+y,+z
	C4−H43···O4	0.96(3)	2.57(2)	3.100(2)	115(2)	x+1,+y-1,+z
	N4−H1··O3	0.86(2)	2.24(2)	3.035(1)	154.29(2)	x, y, z
	N4−H2··O2	0.90(2)	2.02(2)	2.906(2)	170.97(2)	x,+y-1,+z

a

b

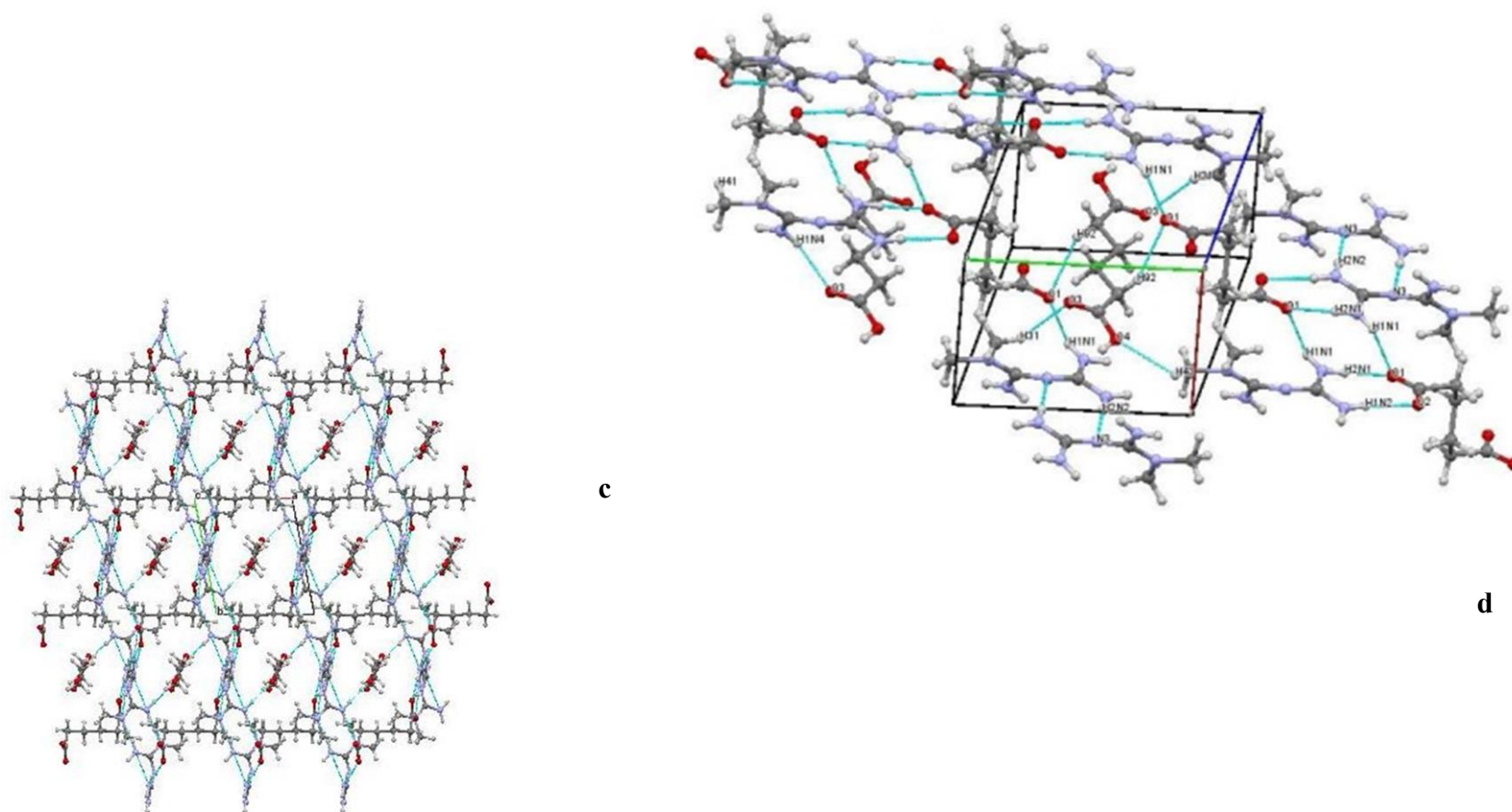**Fig.3.22a Packing motifs of the MET-Adipic acid 1:1**

c

d

Fig.3.22b Packing motifs of the MET-Adipic acid 1:1

Table 3.8.19 Intremolecular contacts and Packing motifs of the MET-Dichloroacetic acid 1:1

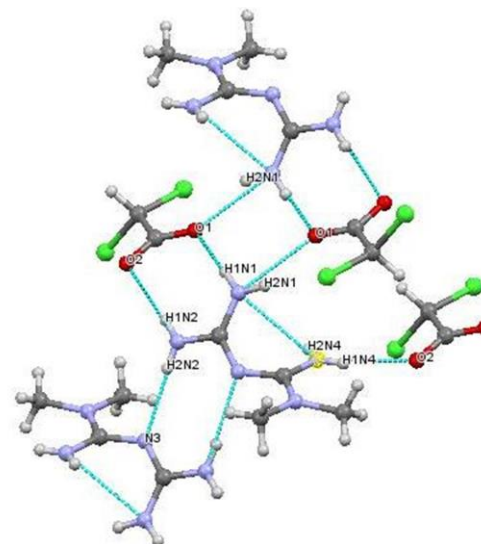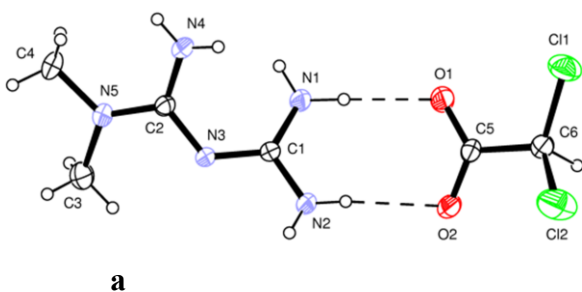| 19	MET-Dichloroacetic acid 1:1	D−H/Å	H···A/Å	D···A/Å	<D−H ···A/ °	Symmetry code
Lab code METDICLA1	N−H···O dimer - $R_2^2(8)$					
	N1−H1···O1	0.89(3)	2.03(3)	2.909(4)	174(3)	x, y, z
	N2−H1···O2	0.81(3)	2.91(3)	3.547(4)	172(3)	x, y, z
	N−H···O tetramer - $R_4^2(8)$					
	N1−H2···O1	0.87(3)	2.04(4)	2.780(3)	142(3)	-x+1,-y+1,-z+1
	N−H···N dimer - $R_2^2(8)$					
	N2−H2···N3	0.81(3)	2.24(3)	3.034(3)	169(4)	-x+2,-y+1,-z+1
	Connecting of ribbons in the zigzag planes					
	N4−H1···O2	0.79(4)	2.10(4)	2.861(3)	164(4)	x,+y-1,+z

Fig.3.23a Packing motifs of the MET-Dichloroacetic acid 1:1
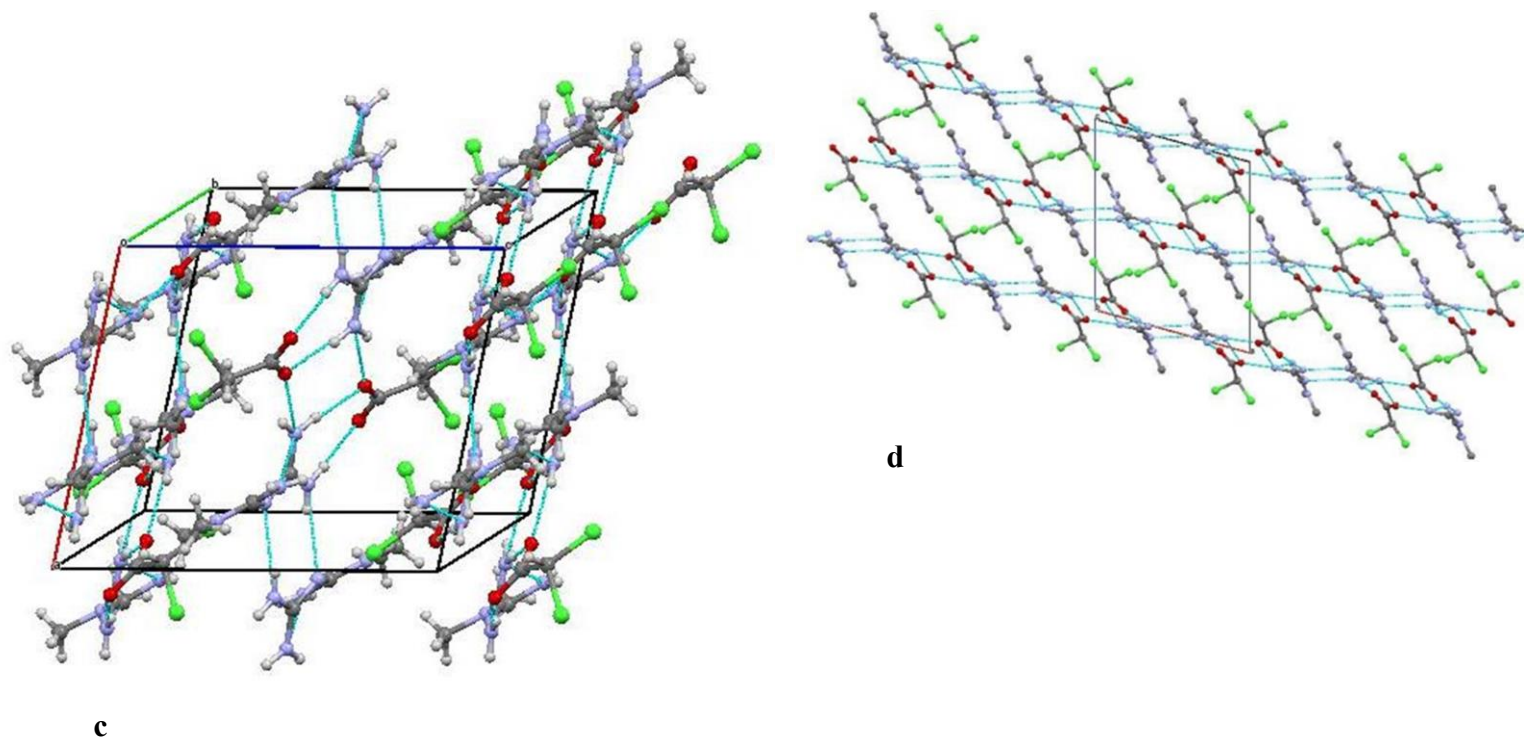
c

d

Fig.3.23b Packing motifs of the MET-Dichloroacetic acid 1:1

Table 3.8.20 Intremolecular contacts and Packing motifs of the MET-Dichloroacetic acid 1 : 2

20	MET-Dichloroacetic acid 1:2	D−H/Å	H···A/Å	D···A/Å	<D−H ···A/ °	Symmetry code
	N−H···O dimer - $R_2^2(8)$					
	N1−H1···O1	0.75(3)	2.09(4)	2.836(4)	176(4)	x, y, z
	N2−H1···O2	0.85(4)	2.06(4)	2.912(3)	179(4)	x, y, z
	N2−H2···O3	0.97(5)	1.82(5)	2.786(4)	175(4)	x, y, z
	N3−H1···O4	0.84(4)	1.86(4)	2.692(4)	177(4)	x, y, z
	N−H···O tetramer - $R_4^2(8)$					
	N1−H1···O1	0.75(3)	2.09(4)	2.836(4)	176(4)	x, y, z
	N1−H2···O1	0.80(5)	2.63(4)	2.964(4)	132(4)	x, y ,z
	N−H···O tetramer - $R_8^4(18)$					
Lab code METDIClA3	N4−H1···O2	0.82(4)	2.06(4)	2.878(4)	173(4)	x+1,+y,+z
	N1−H2···O1	0.80(5)	2.06(5)	2.811(4)	156(4)	-x-1,-y+1,-z+2
	Connecting of the dimers in chain					
	N4−H1···O2	0.82(4)	2.06(4)	2.878(4)	173(4)	x+1,+y,+z
	N4−H3···O3	0.81(4)	2.06(4)	2.848(3)	163(4)	-x-1,-y,-z+2
	Other H-bonds					
	N4−H2N4···O3	0.81(4)	2.06(4)	2.85(3)	163(4)	-x-1,-y,-z+2
	N3−H1N3···O3	0.84(4)	2.95(4)	3.569(4)	132(3)	x, y, z
	N2−H2N2···O4	0.97(5)	2.71(4)	3.421(4)	131(4)	x, y, z
	N2−H1N2···O1	0.85(4)	2.90(4)	3.53(4)	132(4)	x, y, z
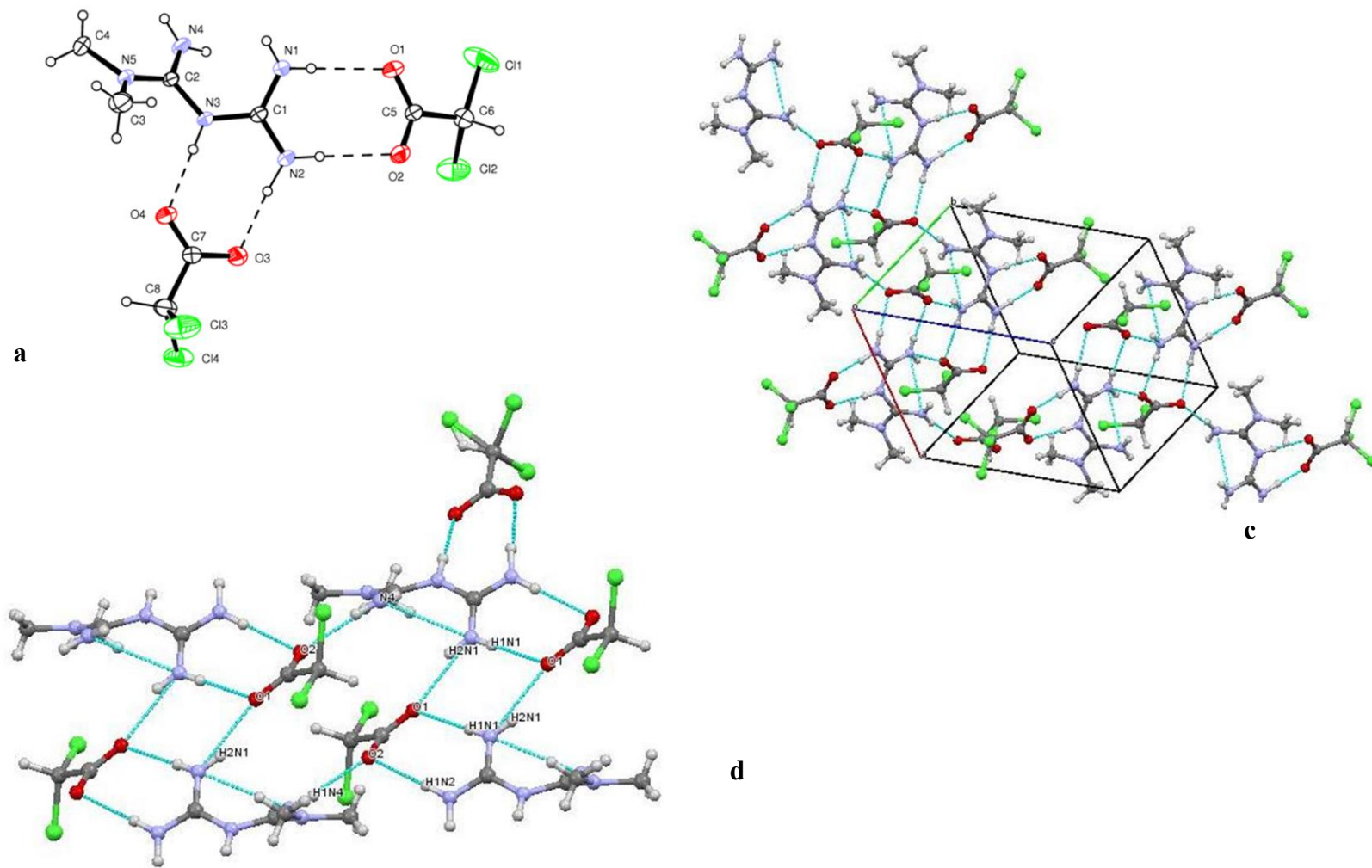
Fig.3.24 Packing motifs of the MET-Dichloroacetic acid 1 : 2

Table 3.8.21 Intremolecular contacts and Packing motifs of the MET-Glycolic Acid 1:1

21	MET-Glycolic Acid 1:1	D−H/Å	H···A/Å	D···A/Å	<D−H ···A/ °	Symmetry code
Lab code METGLY23	N−H···O dimer - $R_2^2(8)$					
	N1−H1···O1	0.90(2)	1.99(2)	2.844(1)	159(2)	x, y, z
	N2−H1···O2	0.93(2)	2.03(2)	2.959(1)	174(2)	x, y, z
	N−H···N dimer - $R_2^2(8)$					
	N2−H2···N3	0.88(2)	2.19(2)	3.066(1)	173(2)	-x+1,-y,-z+1
	O−H···O dimer - $R_2^2(10)$					
	O3−H3···O1	0.90(3)	2.23(3)	3.069(2)	155(2)	-x,-y,-z
	Tetramer $R_4^2(8)$					
	N1−H2···O1	0.85(2)	2.07(2)	2.826(1)	148(2)	-x+1,-y,-z
	N1−H1···O1	0.90(2)	1.99(2)	2.844(1)	159(2)	x, y, z
	Tetramer $R_4^4(18)$					
	N4−H2···O3	0.89(2)	2.19(2)	3.064(2)	166(2)	-x,-y,-z
	N4−H1···O2	0.93(2)	2.03(2)	2.959(1)	174(2)	x+1,+y+1,+z

a

b
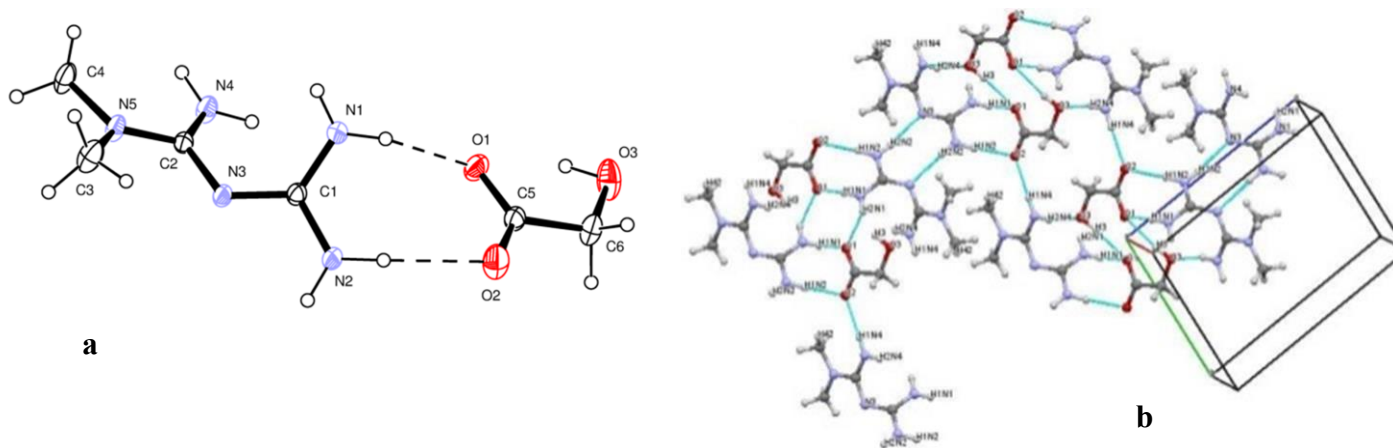
Fig.3.25a Packing motifs of the MET-Glycolic Acid 1:1

c

d
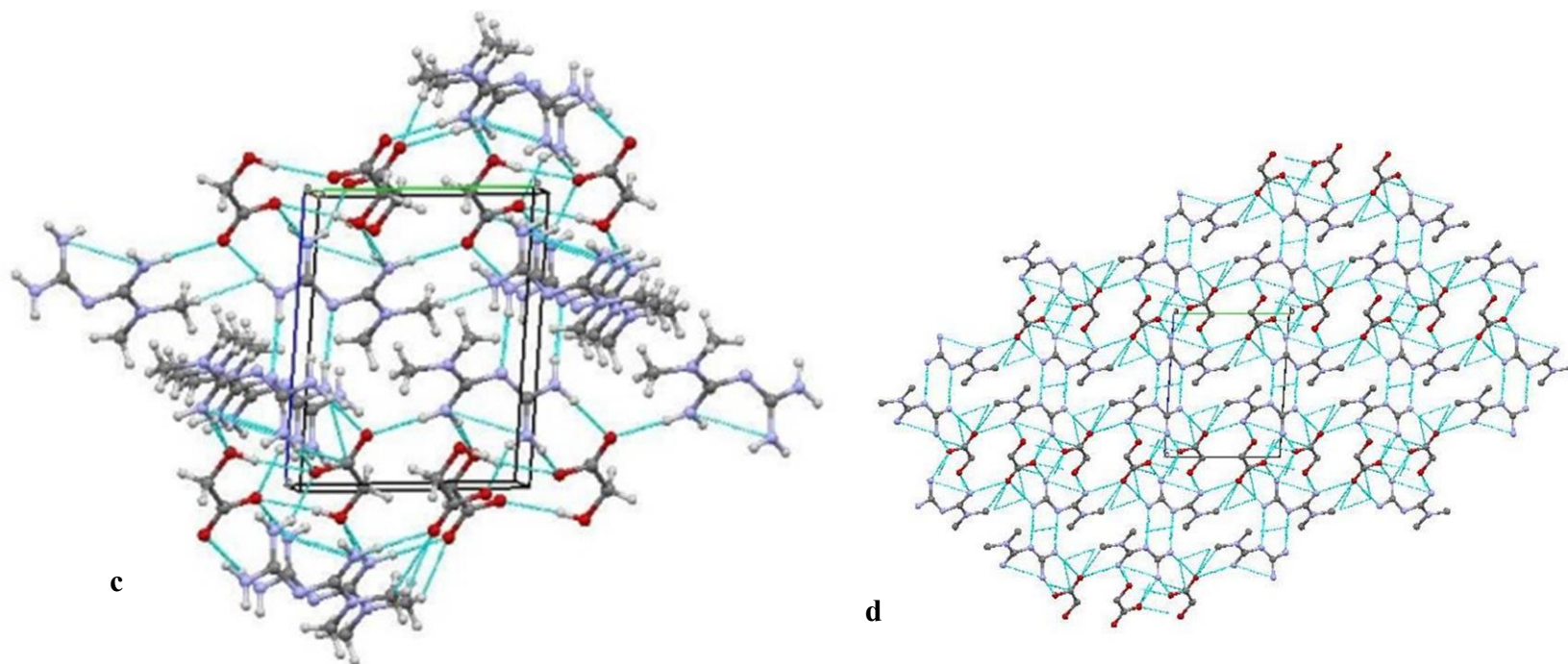
Fig.3.25b Packing motifs of the MET-Glycolic Acid 1:1

Table 3.8.22 Intremolecular contacts and Packing motifs of the MET-Diclofenac 1:1

22	MET-Diclofenac 1:1	D−H/Å	H···A/Å	D···A/Å	<D−H ···A/ °	Symmetry code
Lab code METDCF9	N−H···O dimer - $R_2^2(8)$					
	N1−H1···O1	0.84(3)	2.11(3)	2.931(3)	167(3)	x, y, z
	N2−H1···O2	0.89(2)	2.01(2)	2.900(3)	175(2)	x, y, z
	N−H···N dimer - $R_2^2(8)$					
	N2−H2−···N3	0.83(3)	2.25(3)	3.081(3)	174(3)	-x+1,-y+1,-z
	N−H···O tetramer - $R_4^2(8)$					
	N1−H1···O1	0.84(3)	2.11(3)	2.931(3)	167(3)	x, y, z
	N1−H2···O1	0.84(3)	2.03(3)	2.83(3)	158(3)	−x+1,−y,−z
	Other H-bonds					
	N4−H1···O2	0.74(3)	2.21(3)	2.938(2)	169(3)	x+1,+y,+z
	N6−H1···O2	0.79(3)	2.39(2)	2.985(3)	133(2)	x, y, z
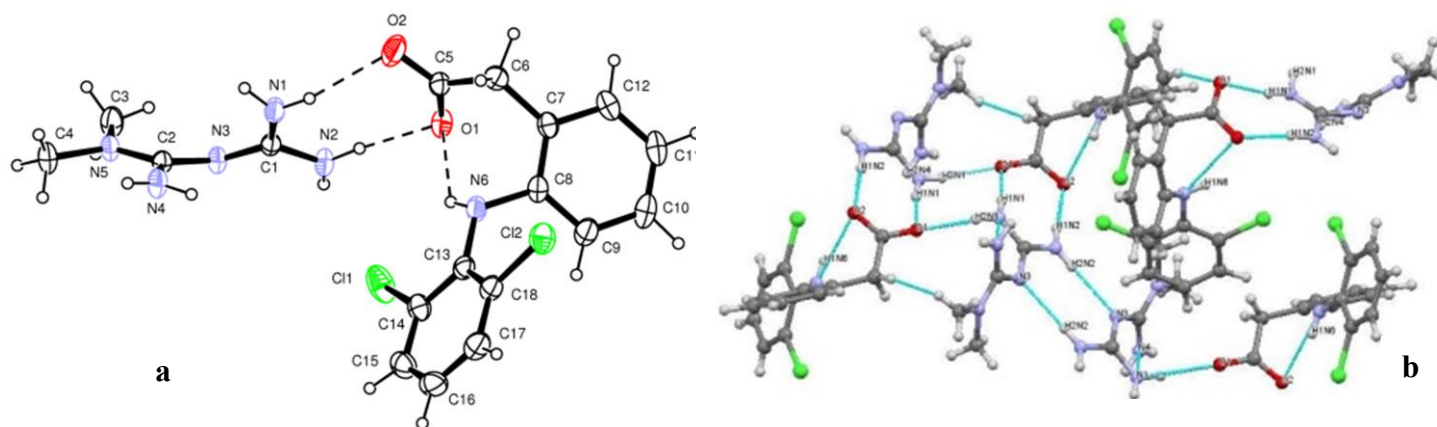
Fig.3.26a Packing motifs of the MET-Diclofenac 1:1
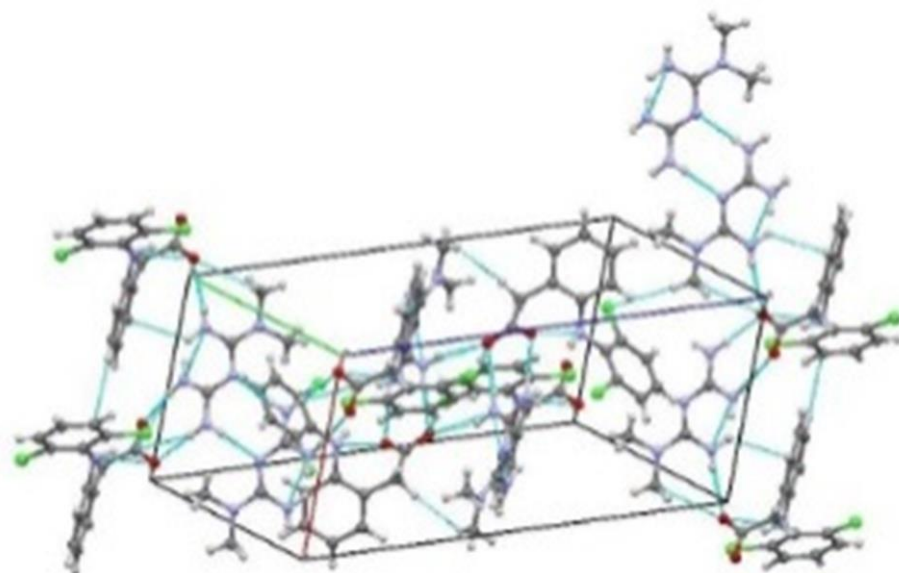
c
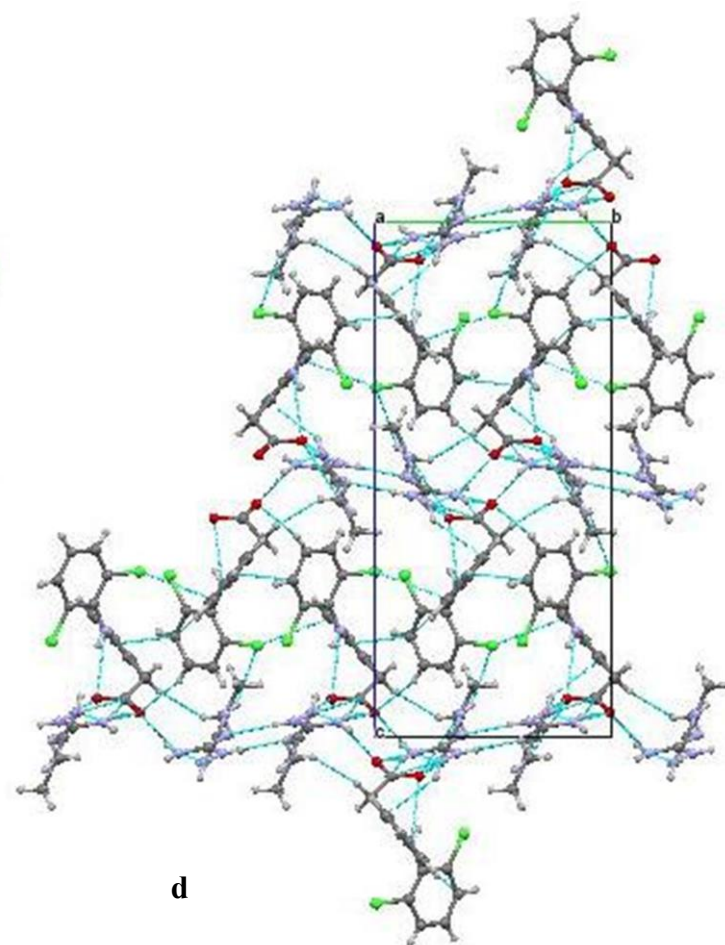
d

Fig.3.26b Packing motifs of the MET-Diclofenac 1:1

Table 3.8.23 Intremolecular contacts and Packing motifs of the MET-Salicylic acid 1:1

23	MET-Salicylic acid 1:1	D−H/Å	H···A/Å	D···A/Å	<D−H ···A/ °	Symmetry code
Lab code MET30	N−H···O tetramer - $R_4^2(8)$					
	N4−H1···O2	0.87(3)	2.25(3)	3.103(3)	1665(3)	-x,-y,-z+1
	N1−H2···O2	0.84(3)	2.55(4)	3.23(3)	140(3)	-x,-y+1,-z+1
	N4−H2···O1	0.95(4)	2.08(4)	3.005(4)	164(3)	x,+y-1,+z
	N1−H1···O1	0.89(4)	2.24(3)	3.030(3)	150(3)	x, y, z
	Other H-bonds					
	N4−H2···O1	0.95(4)	2.08(4)	3.005(4)	164(3)	x,+y-1,+z
	N2−H2···O1	0.93(3)	2.10(3)	3.011(3)	169(3)	-x+1/2,+y-1/2,-z+1/2+1
	N1−H2···O1	0.84(3)	2.49(3)	3.221(2)	147(3)	-x,-y+1,-z+1
	N1−H1···O2	0.88(4)	2.64(4)	3.46(4)	157(3)	x, y, z
	N2−H1···N3	0.87(3)	2.80(3)	3.35(3)	123(2)	-x+1/2,+y+1/2,-z+1/2+1
	Intramolecular H-bond in Salicylic acid					
	O3−H30···O2	0.94(4)	1.72(5)	2.561(4)	145(4)	x, y, z

a

b
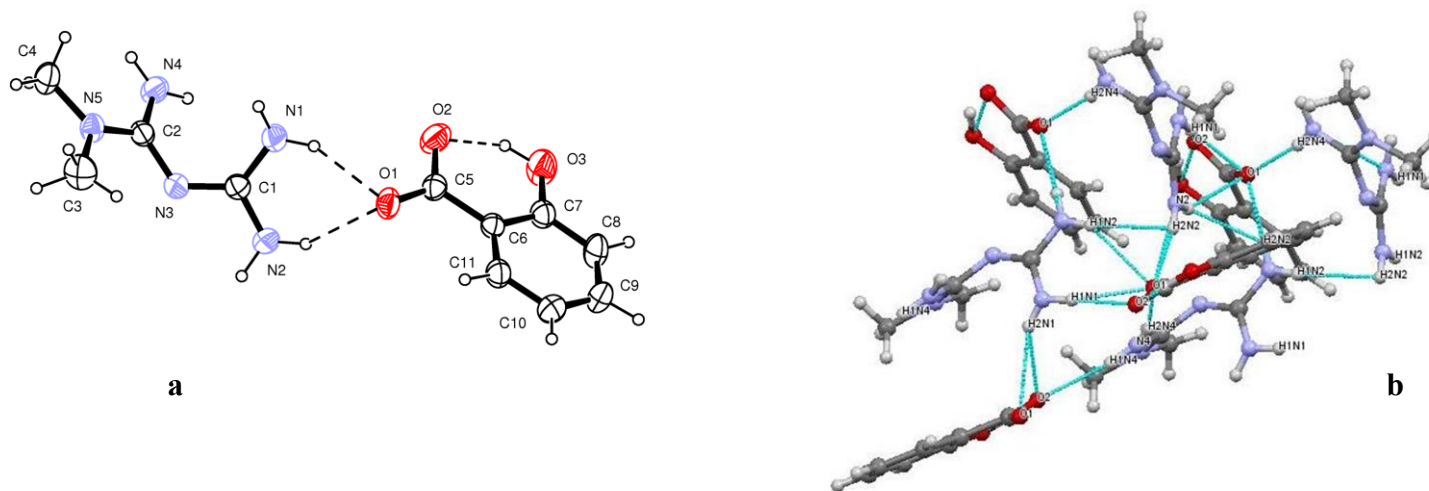
Fig.3.27a Packing motifs of the MET-Salicylic acid 1:1
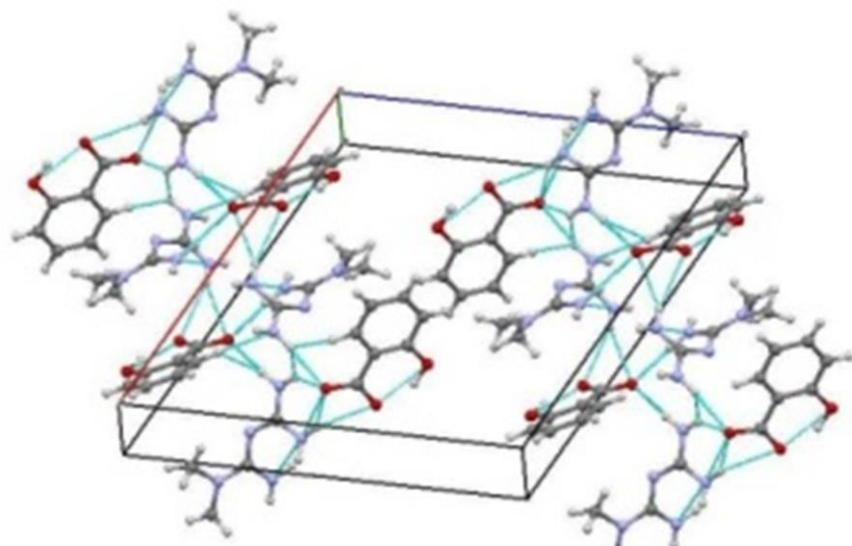
c
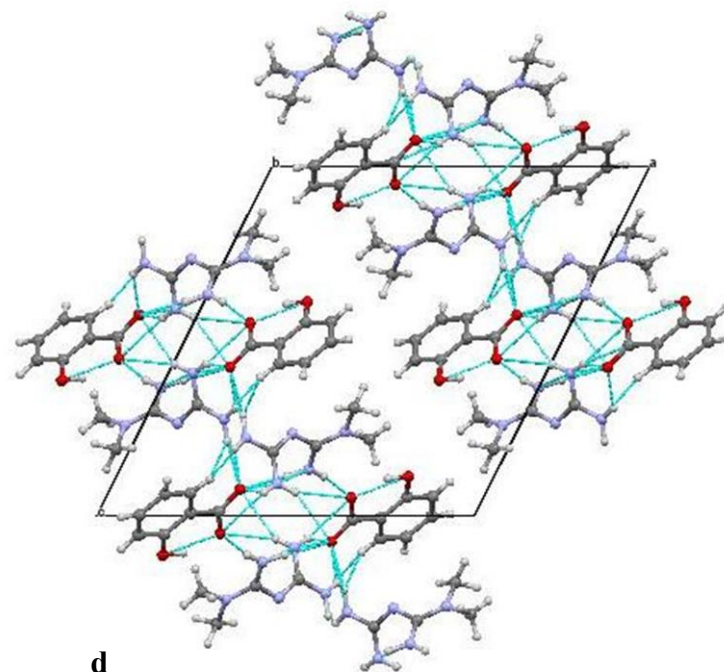
d

Fig.3.27b Packing motifs of the MET-Salicylic acid 1:1

Table 3.8.24 Intremolecular contacts and Packing motifs of the MET-Saccharine 1:1 polymorph I

24	MET-Saccharine 1:1 polymorph I	D−H/Å	H···A/Å	D···A/Å	<D−H ···A/ °	Symmetry code
	Trifurcated H-bond					
	N1−H1···O1	0.75(3)	2.26(3)	2.985(3)	164(3)	x, y, z
	N2−H2··O1	0.99(3)	1.96(3)	2.940(3)	175(3)	x-1/2,-y+1/2,-z
Lab code	N2−H1···O1	0.79(3)	2.47(3)	3.174(3)	149(3)	x, y, z
MET43	Other H-bonds					x+1/2,-y+1/2,-z
	N2−H1···N3	0.79(3)	2.79(3)	3.286(3)	123(2)	x+1/2,-y+1/2,-z
	N4−H2··O1	0.84(3)	2.98(3)	2.148(3)	167(3)	x-1,+y,+z
	N4−H1···O2	0.88(2)	2.12(2)	2.959(3)	162(2)	-x+1,+y-1/2,-z+1/2
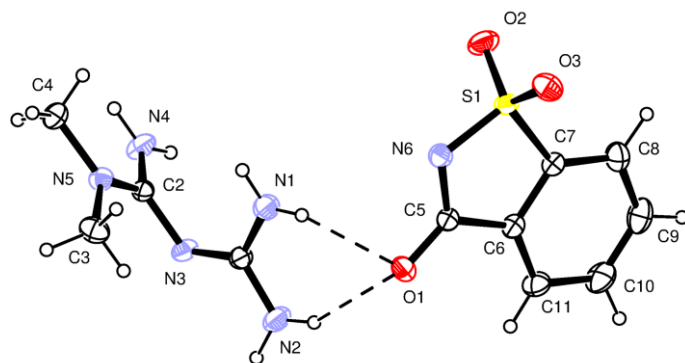
a
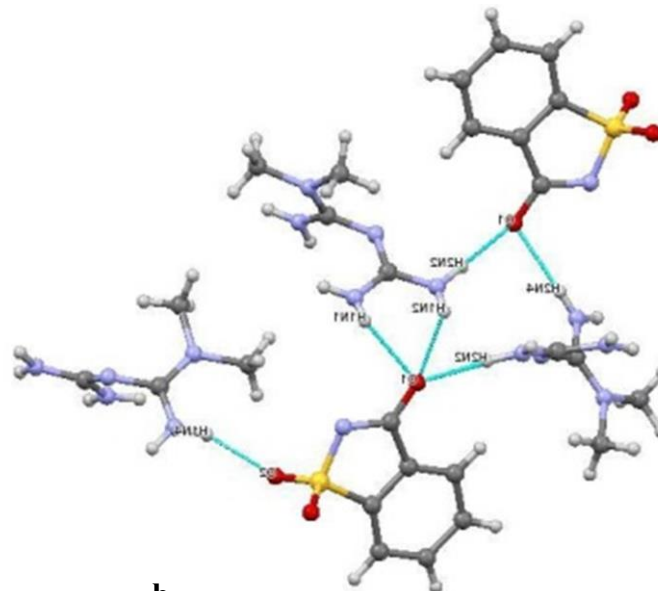
b

Fig.3.28a Packing motifs of the MET-Saccharine 1:1 polymorph I

c

d
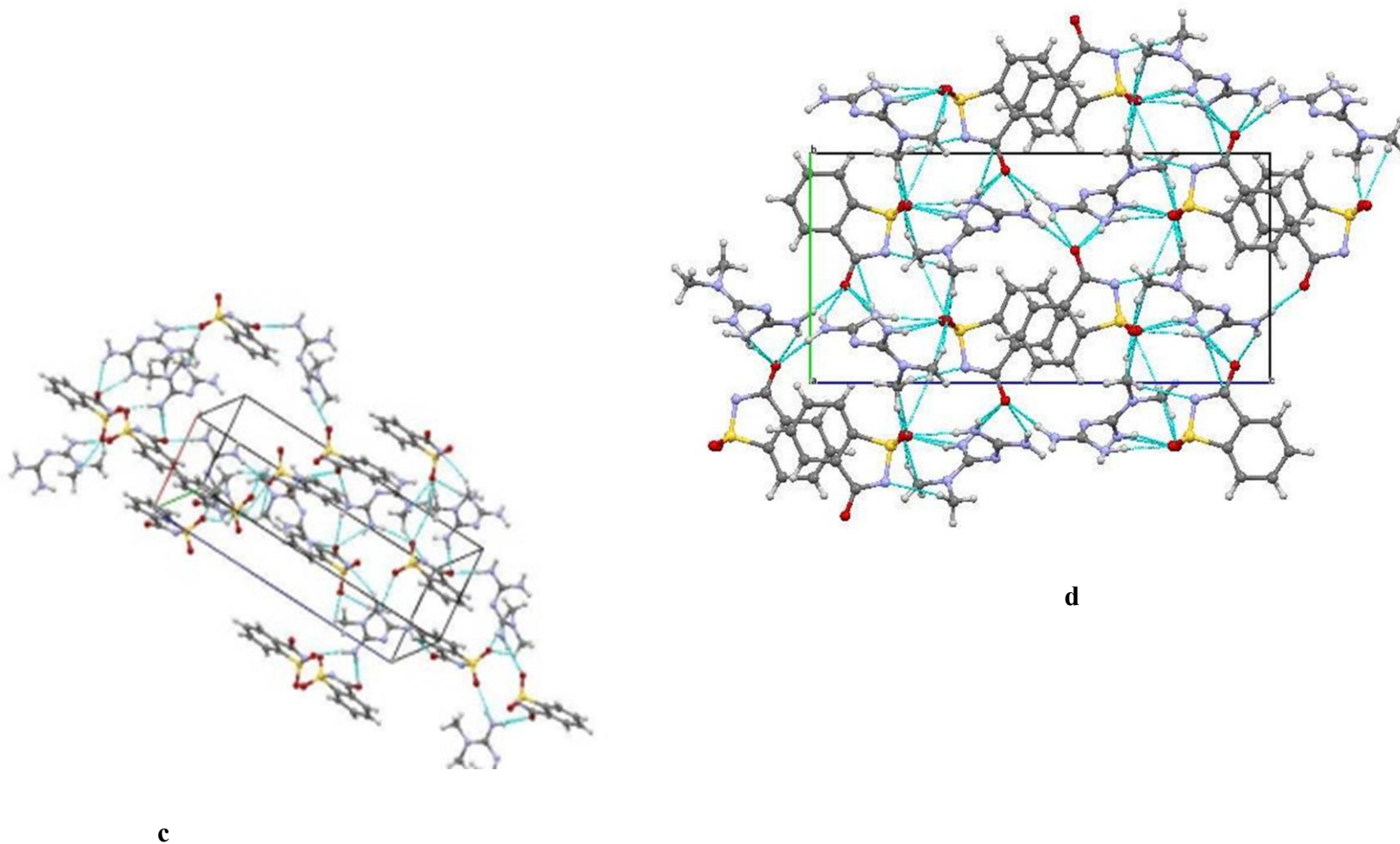
Fig.3.28b Packing motifs of the MET-Saccharine 1:1 polymorph I

Table 3.8.25 Intremolecular contacts and Packing motifs of the MET-Saccharine 1:1 Polymorph II

25	MET-Saccharine 1:1 Polymorph II	D−H/Å	H···A/Å	D···A/Å	<D−H ···A/ °	Symmetry code
Lab code METHCl6	Bifurcated H-bond					
	N1A−H11A···O1A	0.82(3)	2.27(3)	3.023(2)	153(2)	x, y, z
	N2A−H21A···O1A	0.84(2)	2.23(2)	2.988(2)	151(2)	x, y, z
	Dimer heteromeric					
	N1B−H11B···O1B	0.84(3)	2.00(3)	2.836(2)	171(2)	x, y, z
	N2B−H21B···N6B	0.85(3)	2.27(3)	3.114(2)	176(2)	x, y, z
	N−H···N dimer - $R_2^2(8)$					
	N2B−H22B···N3A	0.91(2)	2.24(2)	3.118(2)	163(2)	x, y, z
	N2A−H22A···N3B	0.91(3)	2.37(3)	3.265(2)	171(3)	x, y, z
	Other H-bonds					
	N2A−H21A···O1A	0.84(2)	2.23(2)	2.988(2)	151(2)	x, y, z
	N4B−H41B···O3A	0.88(2)	2.22(2)	3.047(2)	157(2)	-x+1/2+1,-y+1/2+2,-z+1
	N4A−H41A···O3B	0.86(2)	2.18(2)	3.010(2)	162(2)	-x+1,-y+1,-z+1
	N4A−H42A···O2A	0.82(3)	2.46(2)	3.197(3)	150(2)	-x+1/2+1,-y+1/2+1,-z+1
	N1B−H11B ···N6B	0.84(3)	2.99(2)	3.666(2)	139(21)	x, y, z
	N1B−H12B ···O1B	0.84(3)	2.28(2)	2.935(2)	136(2)	-x+1,+y,-z+1/2
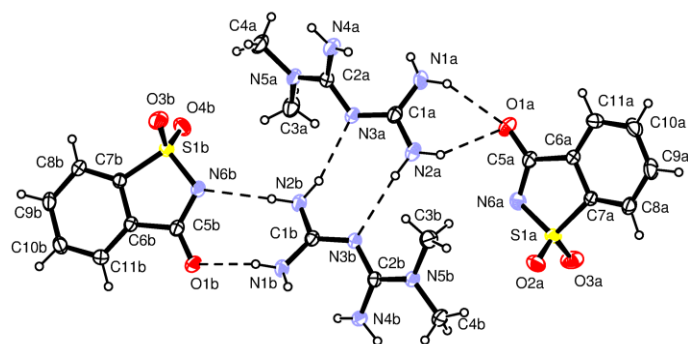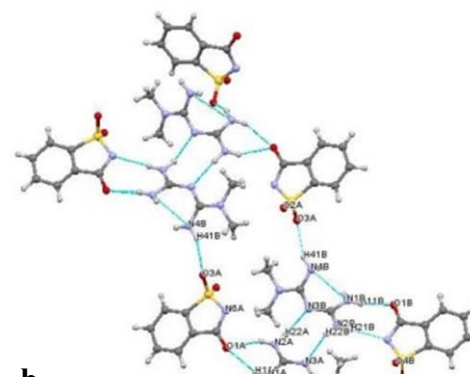
a   b

Fig.3.29a Packing motifs of the MET-Saccharine 1:1 Polymorph II

c

d
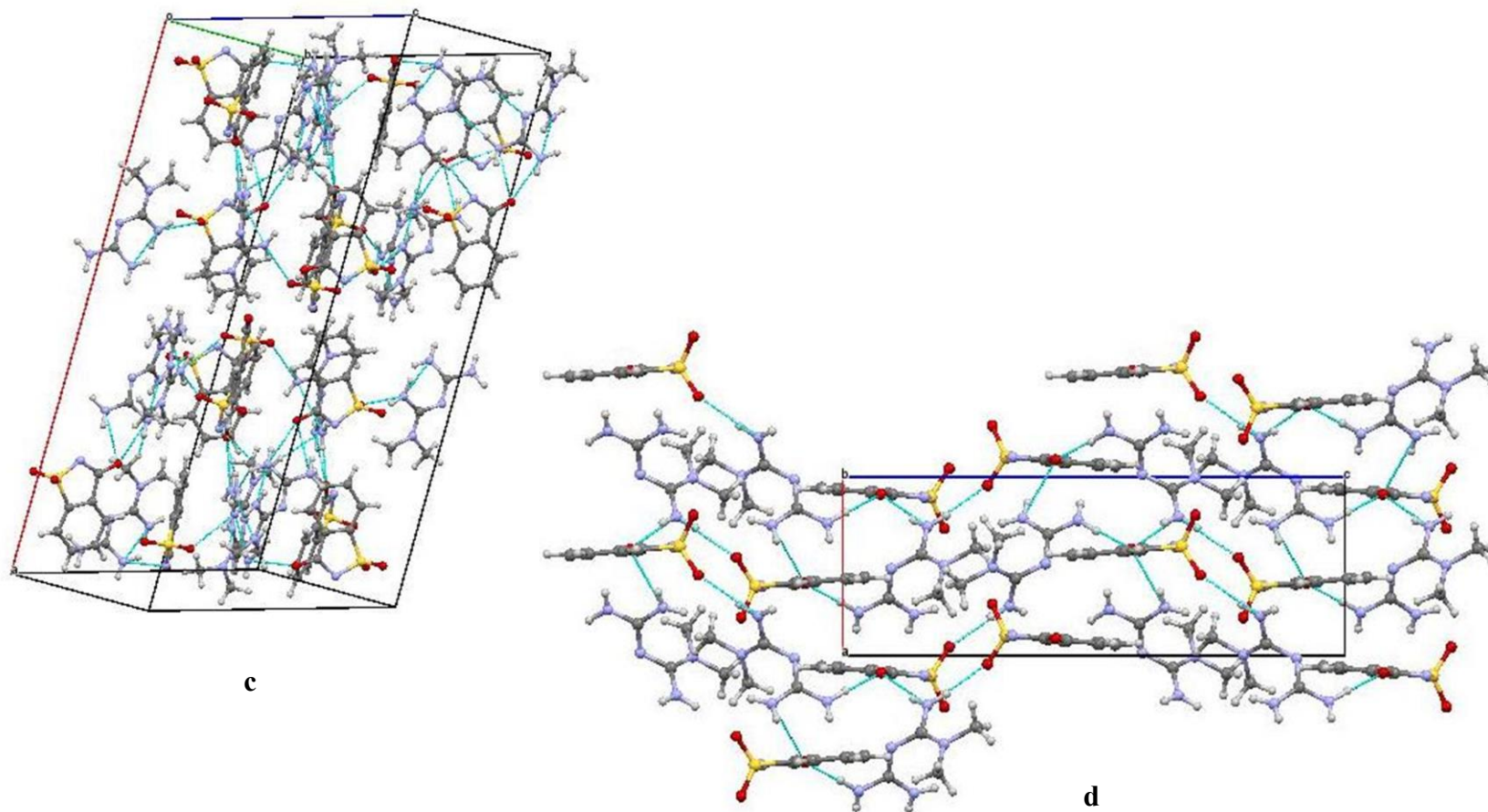
Fig.3.29b Packing motifs of the MET-Saccharine 1:1 Polymorph II

Table 3.1.26 Intremolecular contacts and Packing motifs of the MET-Acesulfame 1:1

26	MET-Acesulfame 1:1	D−H/Å	H···A/Å	D···A/Å	<D−H ···A/ °	Symmetry code
	N−H···N dimer - $R_2^2(8)$					
	N2−H2···N3	0.89(3)	2.24(3)	3.117(3)	171(3)	-x,-y+1,-z
	C−H···O dimer					
	C6−H6···O2	0.86(4)	2.71(3)	3.315(4)	129(3)	-x+1,-y+1,-z+1
	Bifurcated H-bonds					
	N4−H1···O1	0.85(3)	2.07(3)	2.88(3)	158(3)	x-1,+y,+z
	N2−H1···O1	0.85(3)	1.99(3)	2.836(3)	172(3)	x, y, z
Lab code METACSU7	Tetramer N−H···O; N−H···N					
	N1−H2···O2	0.80(3)	2.25(3)	3.040(4)	171(3)	-x,-y+1,-z+1
	N1−H1···N6	0.82(3)	2.26(3)	3.072(3)	170(3)	x, y, z
	Other H-bonds					
	N4−H2···O3	0.800(3)	2.15(3)	2.891(3)	155(3)	x-1/2,-y+1/2+1,+z-1/2
	N4−H2···O3	0.80(3)	2.15(3)	2.891(3)	155(3)	x-1/2,-y+1/2+1,+z-1/2
	N1−H1···O1	0.82(3)	2.83(3)	3.481(3)	138(2)	x, y, z
	C4−H42···O4'	0.89(4)	2.50(3)	3.24(6)	141(3)	-x,-y+1,-z+1
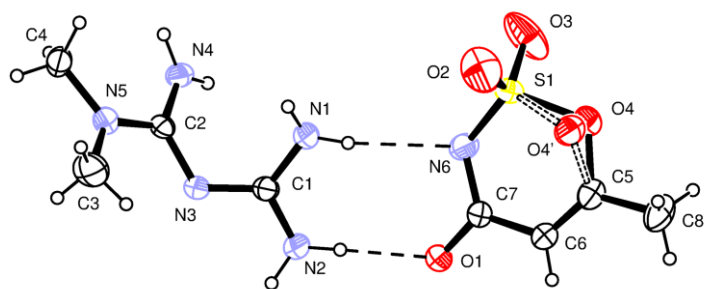
a
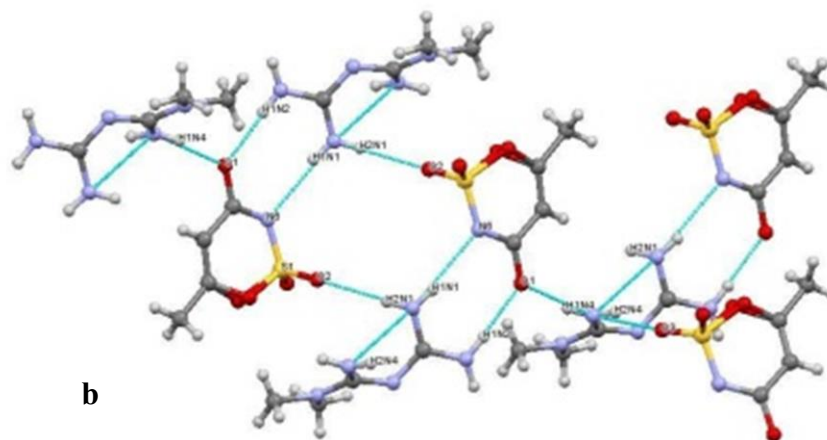
b

Fig.3.30a Packing motifs of the MET-Acesulfame 1:1

Fig.3.30b Packing motifs of the MET-Acesulfame 1:1

Table 3.9.1 Bond distances & conformation, MET PCC with strong acidic compounds

Nom	1	2	3	4	5
Lab code	**MET7b**	**MET3b**	**MET39**	**MET41**	**METFSQ**
PCC Data for geometry	MET-Nitric acid 1:1	MET-Phosphoric acid trihydrate 2:1:3	MET-Picric acid 1:1	MET-Picric acid 1:2	MET-Squaric acid-hydrate 1:1:1
d1 $C1 - N1$	1.333(2)	1.332(2)* 1.333(2)**	1.334(3)	1.317(3)	1.315(2)
d2 $C1 - N2$	1.330(2)	1.324(2)* 1.328(2)**	1.318(3)	1.303(5)	1.315(2)
d3 $C1 - N3$	1.334(2)	1.345(2)* 1.328(2)**	1.336(2)	1.368(4)	1.363(2)
d4 $C2 - N3$	1.345(2)	1.341(2)* 1.343(2)**	1.340(3)	1.374(5)	1.388(2)
d5 $C2 - N4$	1.331(2)	1.342(2)* 1.329(2)**	1.335(2)	1.306(4)	1.311(2)
d6 $C2 - N5$	1.333(2)	1.331(2)* 1.339(2)**	1.330(2)	1.310(4)	1.320(2)
d7 $N5 - C3$	1.459(2)	1.456(3)* 1.456(2)**	1.455(3)	1.464(6)	1.462(2)
d8 $N5 - C4$	1.454(3)	1.454(2)* 1.463(2)**	1.454(4)	1.465(8)	1.462(2)
$N1 \cdots N4$	2.932(2)	2.921(2)* 2.984(2)**	2.929(3)	2.968(5)	2.950(2)
Torsion $C_1N_3C_2N_5$	+146.4(1)	+156.3(1)* +146.5(1)**	142.6(2)	129.1(3)	142.8(1)
P1^P2	52.42	54.24 40.49	51.79	51.58	54.39
S.G.	*P-1*	*P-1*	*P2₁/c*	*P-1*	*P2₁/c*

* - A molecule of MET; ** - B molecule of MET

Table 3.9.2 Bond distances & Conformation, MET PCC with monocarboxylic acids

Nom	6	7	8	9	10	11
Lab code	METFORMA	MET10b	METClA6	METTRIFA	METTRIClA24	METTRIClA2
PCC data geometry	MET-Formic acid1:1	MET-Acetic acid 1:1	MET-Chloracetic acid 1:1	MET-Trifluoroacetic acid 1:1	MET-Trichloroacetic acid 1:1	MET-Trichloroacetic acid 1 :2
d1 C1—-N1	1.328(2)	1.334(1)	1.339(2)	1.336(3)	1.327(2)	1.299(7)* 1.310(8)**
d2 C1 — N2	1.329(2)	1.336(1)	1.336(2)	1.330(3)	1.327(2)	1.316(9)* 1.308(9)**
d3 C1 — N3	1.338(2)	1.338(1)	1.335(2)	1.334(3)	1.339(2)	1.368(7)* 1.369(8)**
d4 C2 — N3	1.347(2)	1.350(1)	1.352(2)	1.342(3)	1.337(2)	1.383(8)* 1.373(9)**
d5 C2 — N4	1.328(2)	1.334(2)	1.337(2)	1.333(3)	1.335(3)	1.306(8)* 1.307(9)**
d6 C2 — N5	1.335(2)	1.339(1)	1.331(2)	1.333(3)	1.338(3)	1.316 (7)* 1.322(8)**
d7 N5 — C3	1.451(2)	1.456(2)	1.456(2)	1.450(5)	1.456(4)	1.464(11)* 1.470(10)**
d8 N5 — C4	1.458(2)	1.453(2)	1.459(2)	1.457(3)	1.455(3)	1.455(10)* 1.472(12)**
N1··· N4	2.953(2)	2.981(2)	3.031(2)	3.000(3)	2.979(2)	2.987(7)* 2.961 (10)**
Torsion $C_1N_3C_2N_5$	−146.1(1)	143.0(1)	−137.1(1)	−142.0(2)	155.3(2)	+135.1(6)* −148.0(6)**
P1^P2	51.83	54.25	59.01	57.24	50.02	60.82 49.98
S.G.	$P2_1/n$	P2$_1$/n	$P2_1/n$	$P2_1/n$	$P2_1/n$	$P2_1/a$

* - A molecule of MET; ** - B molecule of MET

Table 3.9.3   Bond distances & conformation, MET PCC with dicarboxylic acids

Nom	12	13	14	15	16	17	18
Lab code	MET34	MET33	MET68	MET17	MET18	MET15	METADA22
PCC data for geometry	MET-Malonic acid 1:1	MET-Oxalic acid-hydrate 1:1:1	MET-Oxalic acid-hydrate 1:2.5:1	MET-Maleic acid 1:1	MET-Fumaric acid 1:0.5	MET-Succinic acid 1:0.5	MET-Adipic acid 1:1
d1 C1 ─-N1	1.333(2)	1.311(2)	1.289(7)	1.332(2)	1.336(3)	1.334(2)	1.327(2)
d2 C1 ─ N2	1.328(2)	1.320(2)	1.317(7)	1.340(2)	1.334(3)	1.333(2)	1.328(2)
d3 C1 ─ N3	1.338(2)	1.362(2)	1.365(8)	1.329(2)	1.333(2)	1.341(2)	1.343(2)
d4 C2 ─ N3	1.339(1)	1.381(1)	1.375(7)	1.359(2)	1.346(2)	1.348(2)	1.342(1)
d5 C2 ─ N4	1.334(2)	1.313(2)	1.305(6)	1.332(2)	1.331(3)	1.330(2)	1.332(2)
d6 C2 ─ N5	1.338(2)	1.323(2)	1.328(7)	1.325(2)	1.336(3)	1.338(2)	1.341(2)
d7 N5 ─ C3	1.451(2)	1.465(2)	1.462(8)	1.453(2)	1.454(3)	1.452(2)	1.446(2)
d8 N5 ─ C4	1.454(2)	1.460(20	1.451(10)	1.458(2)	1.455(3)	1.454(2)	1.456(2)
N1···N4	3.026(1)	2.970(2)	3.011(8)	2.989(2)	3.031(2)	2.989(2)	2.992(2)
Torsion $C_1N_3C_2N_5$	−149.8(1)	−143.6(1)	+140.9(5)	+136.1(1)	+141.7(2)	−144.3(1)	+152.4(1)
P1^P2	57.37	52.42	57.66	59.45	57.86	53.97	53.20
S.G.	*P2₁/c*	*P2₁/c*	*P -1*	*P2₁/n*	*P2₁/n*	*P2₁/n*	*P-1*

* - A molecule of MET; ** - B molecule of MET

Table 3.9.4 Bond distances & conformation, functional MET PCC

Nom	19	20	21	22	23	24	25	26
Lab code	METDIClA1	METDIClA3	METGLY23	METDCF9	MET30	MET43	METHCl6	METACSU7
PCC / Geometry	MET-Dichloroacetic acid 1:1	MET-Dichloroacetic acid 1:2	MET-Glycolic Acid 1:1	MET-Diclofenac 1:1	MET-Salicylic acid 1:1	MET-Saccharine 1:1, polymorph I	MET-Saccharine 1:1 Polymorph II	MET-Acesulfame 1:1
d1 C1 —- N1	1.312(3)	1.305(4)	1.328(1)	1.323(3)	1.335(3)	1.348(3)	1.330(2)* 1.334(2)**	1.338(3)
d2 C1 — N2	1.330(3)	1.311(4)	1.335(1)	1.334(3)	1.335(3)	1.339(3)	1.334(3)* 1.324(3)**	1.326(3)
d3 C1 — N3	1.336(3)	1.367(3)	1.340(1)	1.345(3)	1.314(3)	1.307(3)	1.325(2)* 1.344(2)**	1.336(3)
d4 C2 — N3	1.339(3)	1.380(4)	1.346(1)	1.350(2)	1.348(3)	1.369(2)	1.345(2)* 1.344(2)**	1.351(3)
d5 C2 — N4	1.335(4)	1.312(4)	1.342(2)	1.323(3)	1.332(3)	1.321(3)	1.339(2)* 1.347(20**	1.327(3)
d6 C2 — N5	1.335(3)	1.316(3)	1.339(1)	1.340(3)	1.323(4)	1.317(3)	1.325(3)* 1.333(2)**	1.331(3)
d7 N5 — C3	1.461(5)	1.465(5)	1.453(2)	1.451(3)	1.458(4)	1.466(3)	1.458(3)* 1.453(3)**	1.444(4)
d8 N5 — C4	1.453(3)	1.462(4)	1.449(1)	1.459(3)	1.460(4)	1.466(3)	1.453(3)* 1.454(3)**	1.457(3)
N1 · · · N4	2.963(3)	2.964(4)	2.979(1)	2.941(3)	3.058(3)	3.630(3)	3.000(2)* 2.821(2)**	2.937(3)
Torsion $C_1N_3C_2N_5$	153.2(2)	−142.9(3)	-151.8(1)	+148.2(2)	−136.1(2)	−71.2(3)	+146.3(2)* −162.7(1)**	−143.0(2)
P1^P2	46.00	51.53	52.65	50.88	56.94	72.03	54.05 38.50	55.09
S.G.	$P2_1/n$	$P\text{-}1$	$P\text{-}1$	$P2_1/c$	$P2_1/n$	$P2_12_12_1$	$C2/c$	$P2_1/n$

* - A molecule of MET; ** - B molecule of MET

Table no3.9.4 Bond distances & conformation, functional MET PCC

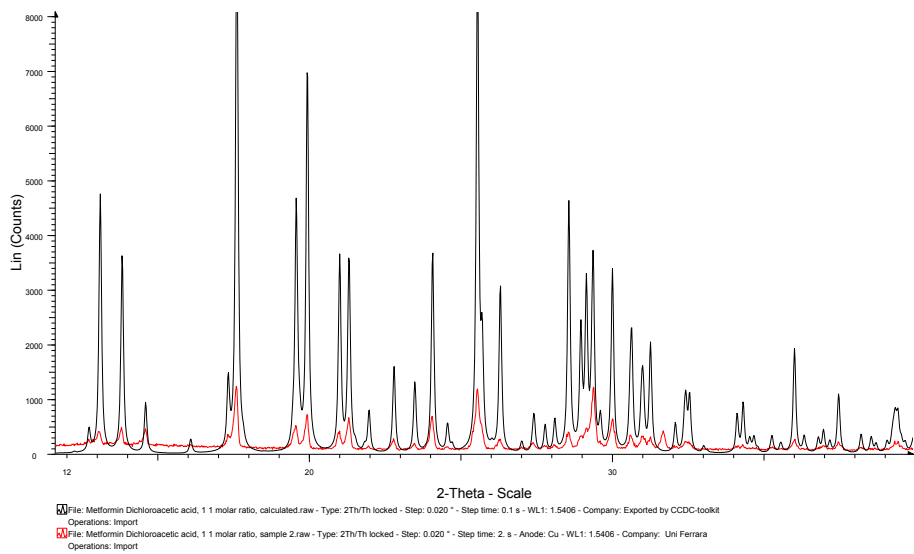| Nom	19	20	21	22	23	24	25	26
Lab code	METDIClA1	METDIClA3	METGLY23	METDCF9	MET30	MET43	METHCl6	METACSU7
PCC / Geometry	MET-Dichloroacetic acid 1:1	MET-Dichloroacetic acid 1:2	MET-Glycolic Acid 1:1	MET-Diclofenac 1:1	MET-Salicylic acid 1:1	MET-Saccharine 1:1, polymorph I	MET-Saccharine 1:1 Polymorph II	MET-Acesulfame 1:1
d1 C1 —- N1	1.312(3)	1.305(4)	1.328(1)	1.323(3)	1.335(3)	1.348(3)	1.330(2)* 1.334(2)**	1.338(3)
d2 C1 — N2	1.330(3)	1.311(4)	1.335(1)	1.334(3)	1.335(3)	1.339(3)	1.334(3)* 1.324(3)**	1.326(3)
d3 C1 — N3	1.336(3)	1.367(3)	1.340(1)	1.345(3)	1.314(3)	1.307(3)	1.325(2)* 1.344(2)**	1.336(3)
d4 C2 — N3	1.339(3)	1.380(4)	1.346(1)	1.350(2)	1.348(3)	1.369(2)	1.345(2)* 1.344(2)**	1.351(3)
d5 C2 — N4	1.335(4)	1.312(4)	1.342(2)	1.323(3)	1.332(3)	1.321(3)	1.339(2)* 1.347(20**	1.327(3)
d6 C2 — N5	1.335(3)	1.316(3)	1.339(1)	1.340(3)	1.323(4)	1.317(3)	1.325(3)* 1.333(2)**	1.331(3)
d7 N5 — C3	1.461(5)	1.465(5)	1.453(2)	1.451(3)	1.458(4)	1.466(3)	1.458(3)* 1.453(3)**	1.444(4)
d8 N5 — C4	1.453(3)	1.462(4)	1.449(1)	1.459(3)	1.460(4)	1.466(3)	1.453(3)* 1.454(3)**	1.457(3)
N1 · · · N4	2.963(3)	2.964(4)	2.979(1)	2.941(3)	3.058(3)	3.630(3)	3.000(2)* 2.821(2)**	2.937(3)
Torsion $C_1N_3C_2N_5$	153.2(2)	−142.9(3)	-151.8(1)	+148.2(2)	−136.1(2)	−71.2(3)	+146.3(2)* −162.7(1)**	−143.0(2)
P1^P2	46.00	51.53	52.65	50.88	56.94	72.03	54.05 38.50	55.09
S.G.	$P2_1/n$	$P-1$	$P-1$	$P2_1/c$	$P2_1/n$	$P2_12_12_1$	$C2/c$	$P2_1/n$

* - A molecule of MET; ** - B molecule of MET

Fig.e.3.31. XRPD patterns of MET-DCA acid 1:1 (a) and
MET-DCA acid 1:2 (b)
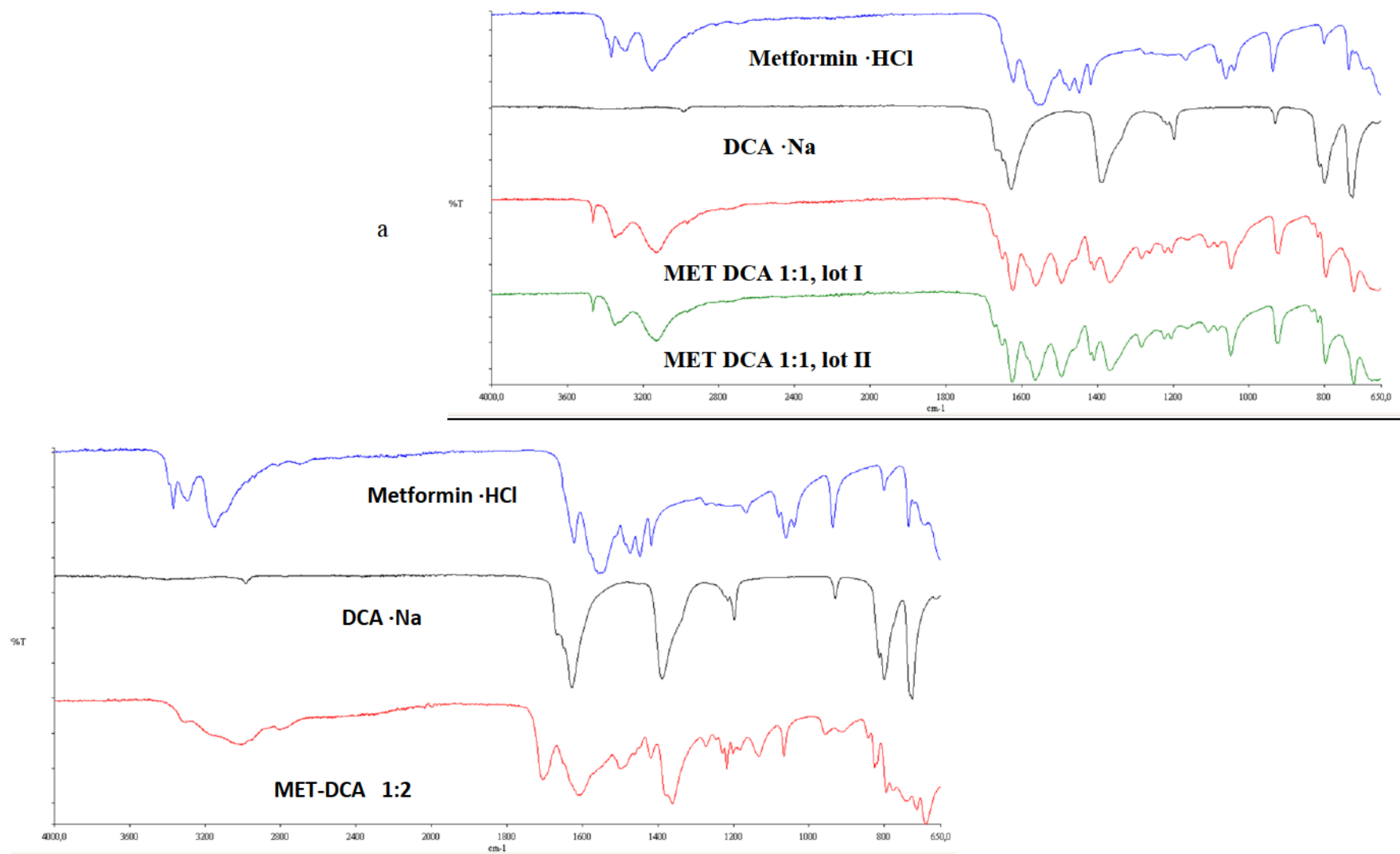
Fig..32. FT-IR Spectra: a - MET-DCA acid 1:1 PCC b MET-DCA acid 1:2 PCC
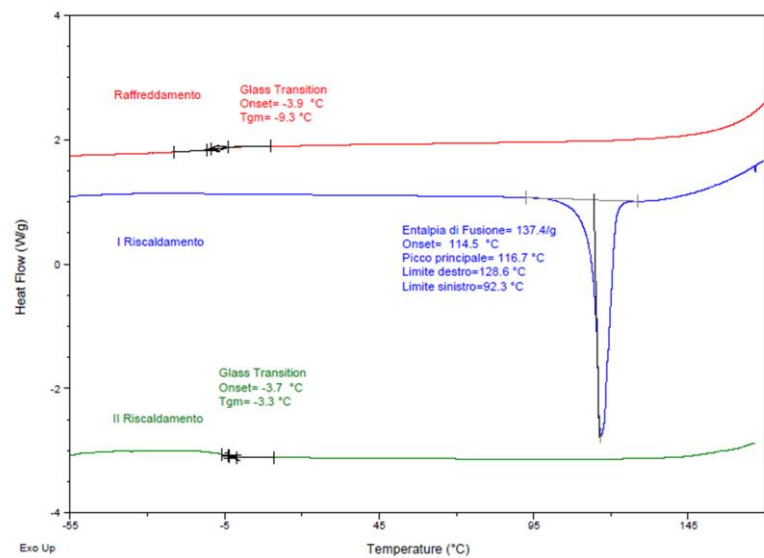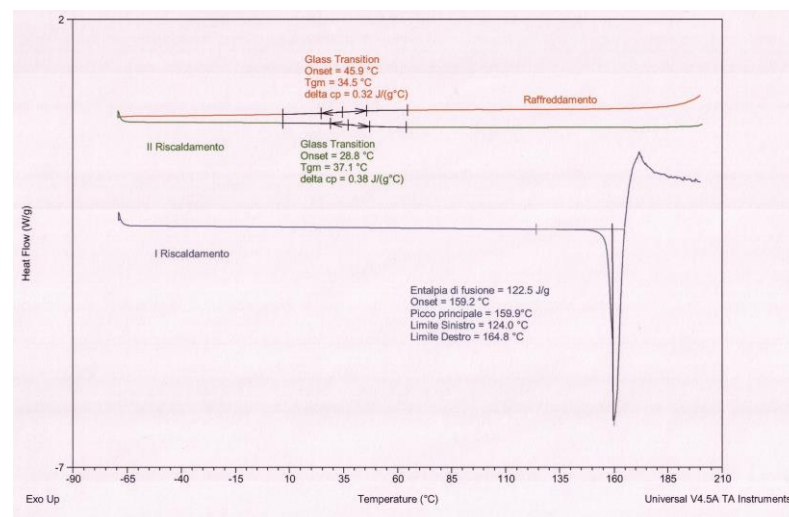
Fif. 3.33 DSC Thermograms: a - MET-DCA acid 1:1 b- MET-DCA acid 1:2

Table 3.11 In vitro cytotoxicity activity of Metformin-DCA 1:1 and Metformin-DCA 1:2 measurements on EHEB cell line

Esp. 30-3-15 EHEB	EHEB	
	Vitality	
Treatments	24h	48h
UNT	100	100
Metformin 15000uM	81	52
Metformin 1500uM	88	78
Metformin 150uM	95	86
DCA 15000uM	53	54
DCA 1500uM	86	89
DCA 150uM	100	97
Met-DCA 1:1 30000uM sale	31	5
Met-DCA 1:1 3000uM sale	69	51
Met-DCA 1:1 300uM sale	82	80
Met 15000uM + DCA 15000uM mix	40	16
Met 1500uM + DCA 1500uM mix	83	59
Met 150uM + DCA 150uM mix	94	87
UNT	100	100
Metformin 10000uM	97	58
Metformin 1000uM	99	86
Metformin 100uM	100	91
DCA 20000uM	51	41
DCA 2000uM	77	87
DCA 200uM	94	91
Met-DCA 1:2 30000uM sale	18	4
Met-DCA 1:2 3000uM sale	61	43
Met-DCA 1:2 300uM sale	67	76
Met 10000uM + DCA 20000uM mix	30	15
Met 1000uM + DCA 2000uM mix	72	66
Met 100uM + DCA 200uM mix	74	91

(Private communication – Prof. Paola Secchiero and Dr. Elisabetta Melloni Dip. Morfologia, Chirurgia e Medicina Sperimentale, Università di Ferrara)

Literature:

Aakeröy, C. B. , Desper J., Helfrich B. A. Heteromeric intermolecular interactions as synthetic tools for the formation of binary co-crystals, CrystEngComm, 2004, 6(5), 19–24

Aakeröy, C. B. , Hussain, I., Forbes, S., Desper J., Exploring the hydrogen-bond preference of N–H moieties in co-crystals assembled via O–H(acid)…N(py) intermolecular interactions, *CrystEngComm*, 2007, 9, 46–54

Aakeröy, C. B.; Hussain, I.; Desper, J. 2-Acetaminopyridine: A highly effective cocrystallizing agent. *Cryst. Growth Des.* 2006, *6*, 474-480.

Aakeröy, C.B, Fasulo, M.E., and Desper, J., , Cocrystal or Salt: Does It Really Matter? *Mol. Pharma.*, 4(3), 317 (2007)

Abu T.M. Serajuddin, Salt formation to improve drug solubility, Advanced Drug Delivery Reviews 59 (2007) 603–616; Paulekuhn GS, Dressman JB, Saal C., Trends in active pharmaceutical ingredient salt selection based on analysis of the Orange Book database, J Med Chem. 2007 Dec 27;50(26):6665-72]

Adams, H.; Hunter, C. A.; Lawson, K. R.; Perkins, J.; Spey, S. E.; Urch, C. J.; Sanderson, J. M. A Supramolecular System for Quantifying Aromatic Stacking Interactions. *Chem.Eur. J*. 2001, 7, 4863-4877.

Aher, S., Dhumal, R., Mahadik, K., Paradkar, A., York, P., 2010. Ultrasound assisted cocrystallization from solution (USSC) containing a non-congruently soluble cocrystal component pair: caffeine/maleic acid. Eur. J. Pharm. Sci. 41, 597–602

Aitipamula S., Vangala V.R., Chow P.S., R.B.H. Tan," CC Hydrate of an Antifungal Drug, Griseofulvin, with Promising Physicochemical Properties", *Cryst. Growth Des.* 2012, *12*, pp. 5858–5863.

Aitipamula S., Wong A.B.H.. Chow P.S., Tan R.B.H., "Pharmaceutical CCs of ethenzamide: structural, solubility and dissolution studies", *CrystEngComm*, 2012,

Algire C, Amrein L, Zakikhani M, Panasci L, Pollak M. Metformin blocks the stimulative effect of a high energy diet on colon carcinoma growth in vivo and is associated with reduced expression of fatty acid acid synthase. *Endocr Relat Cancer*. 2010;17(2):351–360.

Algire C, Moiseeva O, Deschênes-Simard X, Amrein L, Petruccelli L, Birman E, Viollet B, Ferbeyre G, Pollak MN., Metformin reduces endogenous reactive oxygen species and associated DNA damage, Cancer Prev Res (Phila). 2012 Apr;5(4):536-43. doi: 10.1158/1940-6207]

Ali S, Fonseca V. Overview of metformin: special focus on metformin extended release. Expert Opin Pharmacother 2012;13:1797–805.

Alizadeh, A. , Khodaei, M. M., Abdi, G. , Kordestani, D.,The First Report on Chemoselective Biguanide-Catalyzed Henry Reaction under Neat Conditions, Bull. Korean Chem. Soc. 2012, Vol. 33, No. 11, pp.3640-3644

Allen FH and Motherwell WDS. Application of the Cambridge Structural Database in organic chemistry and crystal chemistry. *Acta Cryst* B58: 407-422 (2002)

Almarsson, Ö. Zaworotko M. J., Crystal engineering of the composition of pharmaceutical phases. Do pharmaceutical co-crystals represent a new path to improved medicines? *Chem..Commun . ,*2004 , 1889 – 1896

Altomare, A.; Burla, M. C.; Camalli, M.; Cascarano, G. L.; Giacovazzo, C.; Guagliardi, A.; Moliterni, A. G.; Polidori, G.; Spagna, R. *SIR97, J. Appl. Crystallogr.* 1999, *32*, 115–119.

Amidines, Phosphazenes and Related Organocatalysts, 2009 John Wiley & Sons, Ltd, ISBN 978-0-470-51800-7

Amorha, K. C., Akinleye, M. O. , Oyetunde, O. O., In Vitro Drug Interactions Study of Lisinopril with Metformin, *IOSR Journal of Pharmacy and Biological Sciences (IOSR-JPBS) Volume 5, Issue 4 (Mar. – Apr. 2013), PP 12-18 iosrjournals.org/iosr-jpbs/papers/Vol5-issue4/D0541218.pdf*

Anderson, J.S., Structure of *organic molecular compounds Nature*, 1937, vol. 140, pp. 583–584

Andreetti, G.D. Crystallographic Studies of inclusion compounds In Atwood J.L., Davies, J.E.D., and MacNicol D.D., editors. *Inclusion Compounds* Vol. 3. pp. 129-146, London: Academic Press (1984)

Arora, K. K.; PrakashaReddy, J.; Pedireddi, V. R. Pyridine mediated supramolecular assemblies of 3,5-dinitro substituted benzoic acid, benzamide and benzonitrile. *Tetrahedron* 2005, *61*, 10793-10800.

Aschner *et al.*, Effect of the dipeptidyl peptidase-4 inhibitor sitagliptin as monotherapy on glycemic control in patients with type 2 diabetes, Diabetes Care. 2006 Dec;29(12):2632-7

Atipamula, S.; Banerjee, R.; Bansal, A. K.; Biradha, K.; Cheney, M. L.; Choudhury, A. R.; Desiraju, G. R.; Dikundwar, A. G.; Dubey, R.; Duggirala, N.; Ghogale, P. P.; Ghosh, S.; Goswami, P. K.; Goud, N. R.; Jetti, R. R. K. R.; Karpinski, P.; Kaushik, P.; Kumar, D.; Kumar, V.; Moulton, B.; Mukherjee, A.; Mukherjee, G.; Myerson, A. S.; Puri, V.; Ramanan, A.; Rajamannar, T.; Reddy, C. M.; Rodriguez-Hornedo, N.; Rogers, R. D.; Row, T. N. G.; Sanphui, P.; Shan, N.; Shete, G.; Singh, A.; Sun, C. C.; Swift, J. A.; Thaimattam, R.; Thakur, T. S.; Thaper, R. K.; Thomas, S. P.; Tothadi, S.; Vangala, V. R.; Variankaval, N.; Vishweshwar, P.; Weyna, D. R.; Zaworotko, M. J.. *Crys. Growth. Des*. 2012, 12, 2147−2152.

Atkinson M. B. J., Santhana Mariappan S.V., Bucar, D-K J. Baltrusaitis, J., Friščić T., Sinada, N.G., MacGillvray, R., Crystal engineering rescues a solution organic synthesis in a cocrystallization that confirms the configuration of a molecular ladder, *PNAS 2011*, *108*,. 10974-10979

Auffinger P. Hays F. A., Westhof E. Ho P. S., Halogen bonds in biological molecules, 2004 *Proc. Natl. Acad. Sci. U.S.A* 101 (48): 16789–16794

Babu NJ, Reddy LS, Nangia A. , Amide-N-oxide heterosynthon and amide dimer homosynthon in cocrystals of carboxamide drugs and pyridine N-oxides, *Mol Pharm.* 2007 May-Jun;4(3):417-34

Baile CJ., Metformin: its botanical background, *Pract Diab Int April 2004 Vol. 21 No. 3*

Bailey *Walsh,* R. D. , Bradner M. W., Fleischman, S., Morales, L. A., Moulton B., Rodríguez-Hornedo, N. Zaworotko, M. J., Crystal engineering of the composition of pharmaceutical phases, *Chem. Commun.*, 2003, 186-187

Barot, B.S., Parejiya, P.B., Patel, T.M., Parikh, R.K., & Gohel, M. C, Compactibility improvement of metformin hydrochloride by crystallization technique, Advanced Powder Technology 23 (2012) 814–823

Basavoju S., Bostroem D., Velaga S.P., "Pharmaceutical CC and salts of norfloxacin", *Cryst. Growth Des.*2006, *6*, pp. 2699–2708.

Basavoju, S., Bostrom, D., Velaga, S., 2008. Indomethacin–saccharin cocrystal: design, synthesis and preliminary pharmaceutical characterization. *Pharm. Res*. 25, 530–541

Bell PM, *Hadden* DR: *Metformin*. Endocrinol Metab Clin North Am 1997;26:523–537

Benghiat, V., Leiserowitz, L., Molecular packing modes. Part VI. Crystal and molecular structures of two modifications of tetrolic acid , *J. Chem. Soc., Perkin Trans. 2*, 1972, 1763-

Bernstein, J. (1993) Crystal growth, polymorphism and stucture-property relationships in organic crystals, *J. Phys. D: Appl. Phys.* 26, B66–B76.

Bernstein, J., Hagler, A. T. Conformational polymorphism. The influence of crystal structure on molecular conformation, *J. Am. Chem. Soc.*, 1978, 100 (3), pp 673–681

Berry, D.J., Seaton, C.C., Clegg, W., Harrington, R.W., Coles, S.J., Horton, P.N., Hursthouse, M.B., Storey, R., Jones, W., Friscic, T., Blagden, N., 2008. Applying hot-stage microscopy to co-crystal screening: a study of nicotinamide with seven active pharmaceutical ingredients. *Cryst. Growth Des.* 8, 1697–1712

Bertolasi, V., Gilli, P. Gilli, G. Hydrogen Bonding and Electron Donor-Acceptor (EDA) Interactions Controlling the Crystal Packing of Picric Acid and its Adducts with Nitrogen Bases. Their Rationalization in Terms of the pK_a Equalization and Electron-Pair Saturation Concepts. 2011, *Cryst. Growth Des.* 11: 2724-2735.

Bertolasi, V., Gilli, P. Gilli, G., Adducts of TCNQ with Neutral Nitrogen Bases. Their Rationalization in Terms of Intermolecular Charge-Transfer (CT) or Electron Donor–Acceptor (EDA) Interactions.2012, *Cryst. Growth Des.* 12: 4758-4770.

Bethune S.J., Schultheiss N., Henck J.O., "Improving the Poor Aqueous Solubility of Nutraceutical Compound Pterostilbene through CC Formation", *Cryst.Growth Des.* 2011, *11*, pp. 2817–2823.

Bharatam V. P., Patel S.D., Iqbal P., Pharmacophoric Features of Biguanide Derivatives: An Electronic and Structural Analysis, *J. Med. Chem.* 2005, *48,* 7615-7622

Bhatt P.M., Azim Y., Thakur T.S., Desiraju G.R.,"Co-crystals of the anti-HIV drugs lamivudine and zidovudine", *Cryst. Growth Des.* 2009, *9,* pp. 951–957.

Biradha K., Santra R., Crystal engineering of topochemical solid state reactions, *Chem.Soc.Rev.*,2013,42,950-967

Bis, J.A., Vishweshwar, P., Weyna, D., Zaworotko, M.J., 2007. Hierarchy of supramolecular synthons: persistent hydroxyl···pyridine hydrogen bonds in cocrystals that contain a cyano acceptor. *Mol. Pharm.* 4, 401–416

Blagden, N., Berry, D. J., Parkin, A., Javed, H., Ibrahim, A., Gavan, P. T., De Matos, L. L., and Seaton, C. C. (2008) Current directions in co-crystal growth. *New Journal of Chemistry*, 32(10). pp. 1659-1672

Blandino G, Valerio M, Cioce M, Mori F, Casadei L, Pulito C, Sacconi A, Biagioni F, Cortese F, Galanti S, Manetti C, Citro G, Muti P, Strano S., Metformin elicits anticancer effects through the sequential modulation of DICER and c-MYC., Nat Commun. 2012 May 29;3:865. doi: 10.1038/ncomms1859]

Blonde L, Dailey GE, Jabbour SA, et al. Gastrointestinal tolerability of extended-release metformin tablets compared to immediate-release metformin tablets: results of a retrospective cohort study. Curr Med Res Opin 2004;20:565–72.

Blume HH, Schug BH. 1996. The Biopharmaceutics Classification System (BCS): Class III drugs—Better candidates for BA/BE waiver? Eur J Pharm Sci 9:117–121

Bogacka *et al.*, The effect of pioglitazone on peroxisome proliferator-activated receptor-gamma target genes related to lipid storage in vivo, Diabetes Care. 2004 Jul;27(7):1660-7.

Bond A.D., What is a co-crystal? *CrystEngComm*, 2007,9, 833-834

Braga D, Grepioni F, Lampronti I. G., Maini L., and Turrina A., Ionic Co-crystals of Organic Molecules with Metal Halides: A New Prospect in the Solid Formulation of Active Pharmaceutical Ingredients, *Cryst. Growth Des.*, 2011, 11 (12), pp 5621–5627

Braga, D. and *Grepioni, F. (1994)* From molecule to molecular aggregation: clusters and crystals of clusters, *Acc. Chem. Res. 27, 51–56*

Braga, D., Grepioni, F., 2005. Making crystals from crystals: a green route to crystal engineering and polymorphism. *Chem. Commun*., 3635–3645

Braga, D.; *Desiraju, G. R.; Miller,* J. S.; Orpen, A. G.; Price, S. L. Innovation in crystal engineering, 4, 500-509, *CrystEngComm* 2002

Braga, D.; Grepioni, F.; Lampronti, G. I.; Maini, L.; Turrina, A. *Cryst. Growth. Des*. 2011, 11, 5621−5627

Braga, D.; Grepioni, F.; a ini, . Capucci, D. Nanna, S. Wouters, J. Aerts, . u r , L. *Chem. Commun*. 2012, 48, 8219−8221

Braga, D.; Grepioni, F.; Maini, L.; Prosperi, S.; Gobetto, R.; Chierotti, M. R. *Chem. Commun*. 2010, 46, 7715−7717

Bretnall AE, Clarke GS. 1998. Metformin hydrochloride. In Analytical profiles of drug substances and Excipients; Brittain HG, Ed. Vol. 25. San Diego, California: Academic Press, pp 243–293

British Herbal Pharmacopoeia. Keighley, UK: British Herbal Medicine Association, 1976.

Brittain, HG., & Byrn SR., Structural aspects of polymorphism. In: Brittain HG, editor. *Polymorphism of Pharmaceutical Solids*. New York: Marcel Dekker. Pp. 73-124. (1999)

Buerger MJ. *Elementary Crystallography*. New York: Eiley Interscience. pp 253-273 (1963)

Cahill C. L., de Lill D. T., Frisch . , "Homo- and Heterometallic Coordination Polymers from the f- Elements." *CrystEngComm,* 9, 15-26, 2007.

Carr R.L., Evaluating flow properties of solids, Chem. Eng. 72 (1965) 163–168.

Carter PW; Ward MD, Directing Polymorph Selectivity During Nucleation of Anthranilic Acid on Molecular Substrates, *J. Am. Chem. Soc.* 1994, *116(2) 769-770*

Chacra AR. Evolving Metformin Treatment Strategies in Type-2 Diabetes: From Immediate-Release Metformin Monotherapy to Extended-Release Combination Therapy. Am J Ther 2012. [PubMed]

Chatkon A., Barres A., Samart N., Boyl E. S., Halle J. K., Crans C. D., Guanylurea metformium double salt of decavanadate, $(HGU^+)_4(HMet^+)_2(V_{10}O_{28}{}^{6-})\cdot 2H_2O$, Inorganica Chimica Acta 420 (2014) 85–91

Chatkon A., Chatterjee B. P., Sedgwick A. M, Haller J.K., Crans C. D Counterion Affects Interaction with Interfaces: The Antidiabetic Drugs Metformin and Decavanadate, *Eur. J. Inorg. Chem.* 2013, 1859–1868

Chen, L.R., Young, V.G., Lechuga-Ballesteros, D & Grant, D.J.W., Solid state behavior of cromolyn sodium hydrates. *J. Pharm. Sci.* 88, 1191-1200 (1999)

Cheney M.L., Weyna D.R., Shan N., Hanna M., Wojtas L., Zaworotko M.J., "CF Selection in Pharmaceutical CC Development: a Case Study of a Meloxicam Aspirin CC That Exhibits Enhanced Solubility and Pharmacokinetics", *J. Pharm. Sci.* 2011, *100*, pp. 2172–2181.

Cheng CL, Yu LX, Lee HL, Yang CY, Lue CS, Chou CH. 2004., Biowaiver extension potential to BCS Class III high solubility–low permeability drugs: Bridging evidence for metformin immediate-release tablet. Eur J Pharm Sci 22:297–304

Chiarella, R. A., Davey, R. J., Peterson, M. L. Making Co-Crystals - the Utility of Ternary Phase Diagrams. Cryst. Growth Des. 2007, 7, 1223-1226

Childs L.S, Chyall J. L. Dunlap T.J., Coates A.D., Stahly C.B., Stahly G.P, A Metastable Polymorph of e tformin Hydrochloride: Isolation and Characterization Using Capillary Crystallization and Thermal Microscopy Techniques, *Crystal Growth & Design*, 2004, 4 (3), pp 441–449

Childs S. ., Chyall .J., Dunlap J.T., V.N., Smolenskaya Stahly B.C., Stahly G.P., "Crystal Engineering Approach to Forming CCs of Amine Hydrochlorides with Organic Acids. Molecular Complexes of Fluoxetine Hydrochloride with Benzoic, Succinic, and Fumaric Acids", *J. Am. Chem. Soc*. 2004, *126*, pp. 13335–13342

Childs, S. L.; Hardcastle, K. I. Cocrystals of piroxicam with carboxylic acids. *Cryst. Growth Des.* 2007, 7,1291−1304.

Childs, S.L., Rodriguez-Hornedo, N., Reddy, L.S., Jayasankar, A., Maheshwari, C., McCausland, L., Shipplett, R., Stahly, B.C., 2008. Screening strategies based on solubility and solution composition generate pharmaceutically acceptable cocrystals of carbamazepine. *CrystEngComm* 10, 856–864

Chin, D.N., Palmore, G.T.R., and Whitesides, G.M., Predicting Crystalline Packing Arrangements of Molecules That Form Hydrogen-Bonded Tapes", , *J. Am. Chem. Soc.*, 1999, *121*, 2115-2122.

Chow S.F., Chen . , Shi   ., Chow A.H.   ., Sun C.C., "Simultaneously improving stability, mechanical properties, and dissolution properties of ibuprofen and flurbiprofen by CClization with nicotinamide", *Pharm. Res*. 2012, *29*, pp. 1854–1865.

Clement B. Girreser U., Characterization of biguanides by ^{15}N NMR spectroscopy, Magnetic Resonance in Chemistry, Volume 37, Issue 9, pages 662–666, September 1999

Conover D., Andersen K., Makings of a Wide Moat in Diabetes Care, CFA, 03-28-14,

Crison JR, Timmins P, Keung A, Upreti VV, Boulton DW, Scheer BJ., biowaiver approach for biopharmaceutics classification system class 3 compound metformin hydrochloride using in silico modeling., J Pharm Sci. 2012 May;101(5):1773-82]Desai D, Wong B, Huang Y, Ye Q, Tang D, Guo H, Huang M, Timmins P., Surfactant-mediated dissolution of metformin hydrochloride tablets: wetting effects versus ion pairs diffusivity., J Pharm Sci. 2014 Mar;103(3):920-6

Cullity BD. *Elements of X-ray Diffraction* 3rd edn. New Jerse: Prentice Hall (2011);

D'Alessio D. The role of dysregulated glucagon secretion in type 2 diabetes. Diabetes Obes   etab.2010 13(Suppl 1):126–32. [PubMed: 21824266]

Dale S. H. , Elsegood M. R. J. , Hemmings M., Wilkinson L A., The co-crystallisation of pyridine with benzenepolycarboxylic acids: The interplay of strong and weak hydrogen bonding motifs, *CrystEngComm*, 2004,6, 207-214

Damiani A, De Santis P, Giglio E. The crystal structure of the 1:1 molecular complex between 1,3,7,9-tetramethyluric acids and pyrene. *Acta Crystallogr*. 1965;19:340.

Datta S, Grant DJ., Crystal structures of drugs: advances in determination, prediction and engineering, *Nat Rev Drug Discov.* 2004 Jan;3(1):42-57.

Derissen, J. L. & Smith, P. H, Refinement of the crystal structures of anhydrous α- and β-oxalic acids*, Acta Cryst*. (1974). B30, 2240–2242

Desiraju GR, *Crystal engineering: from molecule to crystal; J. Am. Chem. Soc.*, 2013, 135 (27), pp 9952–9967

Desiraju, G. R., *Crystal Engineering: the Design of Organic Solids*, Elsevier, 1989.

Desiraju, G. R., Supramolecular synthons in crystal engineering – a new organic synthesis, *Angew. Chem. Int. Ed.* 1995, *34*, 2311–2327

Dinsmoor R., Generic Drugs, 2008 http://www.diabetesselfmanagement.com/articles/oral-medicines/generic_drugs/print/]

Dokoumetzidis, A., Macheras, P., A century of dissolution research: From Noyes and Whitney to the Biopharmaceutics Classification System, *Int. J.Pharm*. 321 (2006) 1–11

Donnelly LA, Morris AD, Pearson ER. Adherence in patients transferred from immediate release metformin to a sustained release formulation: a population-based study. Diabetes Obes Metab 2009;11:338–42

Dowling R.J.O, Goodwin J.P, Stambolic V., Understanding the benefit of metformin use in cancer treatment, *BMC Medicine* 2011, 9:33

Dubey, M. S. Pavan, T. N. Guru Row and G. R. Desiraju, Crystal landscape in the orcinol:4,4′-bipyridine system: synthon modularity, polymorphism and transferability of multipole charge density parameters, *IUCrJ.* 2014 Jan 1; 1(Pt 1): 8–18

Duke JA. *Handbook of medicinal herbs*, 2nd edn. Boca Raton, Florida: CRC Press, 2002; 337 Dumitrescu, D. Legrand, Y.-M. Dumitrascu, F. Barboiu, M. Van Der Lee, A., Aminoguanidinium and diaminoguanidinium as adaptive cationic building blocks in guanidinium-organosulfonatecrystalline superstructures, *Cryst. Growth Des.*, 2012, 12 (8), pp 4258–4263

Dunitz D.J., Crystal and co-crystal: a second opinion, C*rystEngComm*, 2003,5, 506-506

E. Prugnard, M. Noel, Physicochemical Properties and Analytical Methods of Determination of Biguanides, Chapter 11, pp 287-304 in Handbook of Experimental Pharmacology Volume 119, 1996,

EMEA Committee for Medicinal Products for Human Use 2010. *Guideline on the Investigation of Bioequivalence,*European Medicines Agency, London

Engel K, Wang J., Interaction of organic cations with a newly identified plasma membrane monoamine transporter., Mol Pharmacol. 2005 Nov;68(5):1397-407

Etter M. C. and Reutzel S. M. Hydrogen bond directed cocrystallization and molecular recognition properties of acyclic imides, *J.Am. Chem. Soc*. 1991, *113*, 2586-2598

Etter, M.C. Encoding and decoding hydrogen-bond patterns of organic compounds *Ass. Chem. Res*. 1990, *23*, 120-126

Etter, M.C., MacDonald, J.C., Bernstein, J., 1990. Graph-set analysis of hydrogen-bond patterns in organic crystals. Acta Crystallogr., Sect. B 46, 256–262

European Medicines Agency (EMA); http://www.ema.europa.eu/ema/index.

Évora A.O.L., Castro R.A.E., Maria T.M.R., . Rosado M.T.S, Silva M.R., Beja A.M., Canotilho J., Eusébio . E.S., "Pyrazinamide-Diflunisal: A New Dual-Drug Co-Crystal", *Cryst. Growth Des.*, 2011, 11 (11), pp 4780–4788.

Fabbrizzi L., Micheloni M., Paoletti P., Thermochemical Consequences of *A* Delocalization in Metal-Biguanide Complexes, *Inorganic Chemistry, Vol, 17, No. 2, 1978,* 494-495

Farrugia, L. J. *WINGX, J. Appl. Crystallogr*. 1999, *32*, 837.

Feyman, R., *There's Plenty of Room at the Bottom. Eng. Sci.* 23 (5). 1960 pp. 22-36.

Florey, K. in *Analytical profiles of drug Substances* Vol. 2 ed. Florey, K. 1-62 (Academic, New York, 1973)

Foretz M, Hebrard S, Leclerc J, Zarrinpashneh E, Soty M, Mithieux G, Sakamoto K, Andreelli F,Viollet B. Inhibition of hepatic gluconeogenesis by metformin in the absence of LKB1-AMPK pathway: Role of hepatic energy state. Journal of Clinical Investigation. 2010; 120.

Forst *et al,*, Linagliptin (BI 1356), a potent and selective DPP-4 inhibitor, is safe and efficacious in combination with metformin in patients with inadequately controlled Type 2 diabetes, Diabet Med. 2010 Dec;27(12):1409-19

Frank E, Nothmann M, Wagner A.Uber synthetisch dargestellte Korpermit insulinartiger Wirkung auf den normalen und den diabetischen Organismus. *Klin Wschr* 1926; 5:2100–2107.

Friśčić, T., Jones, W., 2009. Recent advances in understanding the mechanism of cocrystal formation via grinding. *Cryst. Growth Des.* 9, 1621–1637

Fujioka K, Pans M, Joyal S. Glycemic control in patients with type 2 diabetes mellitus switched from twice-daily immediate-release metformin to a once-daily extended-release formulation. Clin Ther 2003;25:515–29.

Gao Y., Zu H., Zhang J., "Enhanced dissolution and stability of adefovir dipivoxil by CC formation", *J. Pharm. Pharmacol*. 2011, 63, pp. 483–490.

Gavezzotti, A. & Flack, H., Crystal Packing, Electronic Ed., pp. 5; http://www.iucr.org/iucr-top/comm/cteach/pamphlets/21/21.html

Gavezzotti, A.; Filippini, G. *J. Am. Chem. Soc.* 1995, *117*, 12299-12305.

Getsoian, A., Lodaya, R.M., Blackburn, A.C., One-solvent polymorph screen of carbamazepine, 2008, Int.J.Pharm. 348, 3-9

Gilli , G., Bertolasi, V. , Gilli, P. Solid-State N–H···O/O–H···N Tautomerism in Resonance-Assisted 1-(Arylazo)-2-Naphthols and its Trough-Space π*←π Perturbation in TCN Cocrystals. A Variable-Temperature X-Ray Crystal Study, 2013 *Cryst. Growth Des.* 13: 3308-3320.
Gilli, P. and Gilli, G., Hydrogen bond models and theories: The dual hydrogen bond model and its consequences 2010, *J. Mol. Struct.* 927: 2-10.
Gilli, P., Bertolasi, V., Ferretti, V., Gilli, G., Evidence for resonance-assisted hydrogen bonding. 4. Covalent nature of the strong homonuclear hydrogen bond. Study of the O–H···O system by crystal structure correlation methods, 1994, *J. Am. Chem. Soc.* 116: 909-915.
Gilli, P., Ferretti, V. , Bertolasi, V. , Gilli, G., A novel approach to hydrogen bonding theory.in *Advances in molecular structure research*, Vol. 2, M. Hargittai & I. Hargittai Eds., JAI Press Inc., Greenwich, CT, USA 1996, pp. 67-102.

Gilli, G; Gilli, P. *The Nature of the Hydrogen Bond. Outline of a Comprehensive Hydrogen Bond Theory*; Oxford University Press: Oxford, U.K., 2009.

Gilli, P. , Bertolasi, V., Ferretti, V. , Gilli, G. Evidence for intramolecular N–H···O resonance-assisted hydrogen bonding in *β*-enaminones and related heterodienes. A combined crystal-structural, IR and NMR spectroscopic, and quantum-mechanical investigation , 2000, *J. Am. Chem. Soc.* 122: 10405-10417.

Gilli, P., Pretto, L., Bertolasi, V., Gilli, G., Predicting Hydrogen-Bond Strengths from Acid-Base Molecular Properties. The pKa SlideRule: Toward the Solution of a Long-Lasting Problem, 2009, *Acc.Chem.Res.* 42:33-44.

Gilli, P., Pretto, L., Gilli, G., PA/pK_a equalization and the prediction of the hydrogen-bond strength: A synergism of classical thermodynamics and structural crystallography. 2007, *J. Mol. Struct.* 844-845: 328-339.

Giordano, F., Rossi, A., Mayano, J.R., Gazzaniga, A., Massarotti, V., Bini, M., Capasoni, D., Peveri, T., Redenti, E., Carima, L., Lorenza, A., Alberi, M.D., Zanol, M., Polymorphysm of rac-5,6-diisobutyryloxy-2-methylamino-1,2,3,4-tetrahydronaptha-lene Hydrochloride (CHF 1035). I., Thermal, spectroscopic, and X-ray diffraction properties. J.Pharm.Sci. 90, 1154-1163

Giovannucci E, Harlan DM, Archer MC, Bergenstal RM, Gapstur SM, Habel LA, Pollak M, Regensteiner JG, Yee D., Diabetes and cancer: a consensus report., Diabetes Care. 2010 Jul;33(7):1674-85. doi: 10.2337/dc10-0666

Giron, D. et al. Solid state characterizations of pharmaceutical hydrates. *J. Thermal Anl. Cal.* 68, 453-465 (2002)

Glossmann H, Reider N., A marriage of two "Methusalem" drugs for the treatment of psoriasis?: Arguments for a pilot trial with metformin as add-on for methotrexate, Dermatoendocrinol. 2013 Apr 1;5(2):252-63

Good, D.J., Rodríguez-Hornedo, N., 2009. Solubility advantage of pharmaceutical cocrystals. *Cryst. Growth Des.* 9, 2252–2264

Goshe A.J. Steele I. M. , Ceccarelli C., Rheingold A. L. , Bosnich B. Supramolecular recognition: On the kinetic lability of thermodynamically stable host–guest association complexes, *PNAS* 2002 99:*4823-4829*

Goud N.R., Gangavaram S., Suresh K., Pal S., a njunatha S.G., Nambiar S., Nangia A., "Novel Furosemide CCs and Selection of High Solubility Drug Forms", *J. Pharm. Sci.* 2012, *101*, pp. 664–680.

Grepioni F., Wouters J., Braga D., Nanna S., Fours B., Coquerel G., Longfils G., Rome S., Aerts L. and Quéré L., Ionic co-crystals of racetams: solid-state properties enhancement of neutral active pharmaceutical ingredients *via* addition of Mg^{2+} and Ca^{2+} chlorides, *CrystEngComm*, 2014,16, 5887-5896

Gridunova, G.V.,.Furmanova, N.G, Struchkov Y.. Ezhkova T, Z.I., Grigor'eva L.P., Chayanov B.A.; Crystal structures of two polymorphic modifications of m-Hydroxybenzoic acid. *Kristallografiya(Russ.)(Crystallogr.Rep.)* (1982), 27, 267

Grobelny, P., Mukherjee, A., Desiraju, G.R.: Drug-drug co-crystals: Temperature-dependent proton mobility in the molecular complex of isoniazid with 4-aminosalicylic acid. *CrystEngComm* 13, 4358-4364, (2011).

Grossmann H. Thiourea. Cryoscopy of organic mixtures and addition compounds. Chemiker-Zeitung. 1908;31:1195

Gryl M., Cenedese S., Stadnicka K.Crystal Engineering and Charge Density Study of Pharmaceutical Nonlinear Optical Material: Melamine-Barbital Co-Crystal, J. *Phys. Chem. C*, 2015, 119 (1), pp 590–598

Gu, C., Young, V., Grant, D.J.W., Polymorph screening: influence of solvents on the rate of solvent-mediated polymorphic transformation. 2001, J.Pharm.Sci. 90, 1878-1890

Guidance for industry. 2000. Waiver of *in vivo* bioavailability and bioequivalence studies for immediate release solid oral dosage forms based on a Biopharmaceutics Classification System. US Department of Health and Human Services Food and Drug Administration Center for Drug Evaluation and Research (CDER), Silver Spring, MD

Guzmán, H.R., Tawa, M., Zhang, Z., Ratabanangkoon, P., Shaw, P., Gardner, C.R., Moreau, J P., Almarrson, Ö., Remenar, J.F., 2007. Combined use of crystalline forms and precipitation inhibitors to improve oral absorption of celecoxib from solid oral formulations. *J. Pharm. Sci.* 96, 2686–2700

Han T, editor. *International Tables for Crystallography*, International Union of crystallography, Boston, MA (1987)

Hariharan M. , Structure of metformin hydrochloride, Acta Cryst. (1989). C45, 911-913

Haymarket Publications. Monthly Index of Medical Specialities (MIMS), August 2009 edition. London: Haymarket Publications, 2009.

Haynes, D. A.; Jones, W.; Motherwell, W. D. Cocrystallisation of succinic and fumaric acids with lutidines: a systematic study. *CrystEngComm* 2006, *8*, 830-840

He, G., Chow, P.S., Tan, R.B.H., 2010. Investigating the intermolecular interactions in concentration-dependent solution cocrystallization of caffeine and p-hydroxybenzoic acid *Cryst.Growth Des*. 10, 3763–3769

He, G., Chow, P.S., Tan, R.B.H., Investigating the intermolecular interactions in concentration-dependent solution cocrystallization of caffeine and p-hydroxybenzoic acid. 2010 *Cryst. Growth Des*. 10, 3763–3769.

He. G., Jacob. C., Guo. L., Chow, P.S., Tan, R.B. Screening for cocrystallization tendency: the role of intermolecular interactions, J Phys Chem B. 2008 Aug 14;112(32):9890-5.

Heckel W R.., Density–pressure relationship in powder compaction, Trans. Metall. Soc. AIME 221 (1961) 671–675.

Heldebrant D.J.,*et al*.,Performance of single-component CO2-binding organic liquids (CO2BOLs) for post combustion CO_2 capture, Chem.Eng.J. (2011), doi:10.1016/j.cej.2011.02.012

Hesse G, Taubmann G. Die Wirkung des Biguanids und seiner Derivate auf den Zuckerstoffwechsel. Naunyn-Schmiedebergs. *Arch Exp PathPharmacol* 1929; 142: 290–308

Hickey . B., Peterson . ., Scoppettuolo .A., "Performance comparison of a CC of carbamazepine with marketed product", *Eur. J. Pharma. Biopharma.* 2007, *67*, pp. 112–119.

Homsek I, Parojcic J, Dacevic M, Petrovic L, Javanovic D. 2010. Justification of metformin hydrochloride biowaiver criteria based on bioequivalence study. Arzneimittelforschung 60(9):553–559

http://www.hscic.gov.uk/searchcatalogue?productid=5461&q=title%3a%22prescription+cost+analysis%22&sort=Relevance&size=10&page=1#top;

Huang Z-F., Pan L., Zou J-J.,Zhang X., Wang L., Nanostructured bismuth vanadate-based materials for solar-energy-driven water oxidation: a review on recent progress, *Nanoscale*, 2014,6, 14044-14063

Hulliger, J. Chemistry and Crystal Growth, *Angew. Chem. Int. Ed. Engl. (1994) 33, 143-162.*

Inzucchi SE, et al. Efficacy and metabolic effects of metformin and troglitazone in type II diabetes mellitus. N Engl J Med. 1998; 338:867–72. [PubMed: 9516221]; Goodarzi MO, Bryer-Ash M.

Ishikawa T. General Aspects of Organosuperbases, pp.2, in *Superbases for Organic Synthesis: Guanidines,*

Issa N., Barnett S., Mohamed S. Braun, D.E., Copley R.C. B., Tocher D.A.   Price, S. L. Screening for cocrystals of succinic acid and 4-aminobenzoic acid *CrystEngComm,* 2012,14, 2454-2464

Janiak, C.. Engineering coordination polymers towards applications, *Dalton Trans*., 2003, 2781–2804

Jantratid E, Prakongpan S, Amidon GL, Dressman JB. 2006. Feasibility of biowaiver extension to biopharmaceutics classification system class III drug products. Cimetidine. Clin Pharmacokinet 45:385–399

Jantratid E, Prakongpan S, Dressman JB, Amidon GL, Junginger HE, Midha KK, Barends DM. 2006. Biowaiver monographs for mmediate release solid oral dosage forms: Cimetidine. J Pharm Sci 95:974–984

Jayasankar, A.; Reddy, L. S.; Bethune, S. J. ; Rodríguez-Hornedo, N. Role of Cocrystal and Solution Chemistry on the Formation and Stability of Cocrystals with Different Stoichiometry *Cryst. Growth Des.* 2009, *9* (2), 889-897

Jiang G, Zhang BB. Glucagon and regulation of glucose metabolism. Am J Physiol Endocrinol Metab. 2003; 284:E671–8. [PubMed: 12626323];

Kaljurand, I., Kűutt, A., Soovaäli, . et al. (2005) Extension of the self-consistent pectrophotometric basicity scale in acetonitrile to a full span of 28 pKa units: unification of different basicity scales. The Journal of Organic Chemistry, 70, 1019–1028.

Kalra S, Emerging role of dipeptidyl peptidase-IV (DPP-4) inhibitor vildagliptin in the management of type 2 diabetes, J Assoc Physicians India. 2011 Apr;59:237-45.

Kanters, J. A. , Roelofsen, G. Hydrogen-bond motifs of carboxylic acids: the α-form of monochloroacetic acid, *Acta Cryst.* (1976). B32, 3328-3331

Kanters, J. A. , Roelofsen, G., Feenstra, T., Hydrogen-bond motifs of carboxylic acids: the β-form of monochloroacetic acid, *Acta Cryst.* (1976). B32, 3331-3333

Kastelic J., Kikelj D., Leban I., Lah, N., Fluconazole–malonic acid (1/1) *Acta Crystallogr Sect* E 2013 1; 69(Pt 3): o378–o379

Kavuru P., Aboarayes D., Arora K.K. , Clarke H. D., Kennedy A., Marshall L., Ong T. T., Perman J., Pujari T., Wojtas Ł., Zaworotko M.J. Hierarchy of Supramolecular Synthons: Persistent Hydrogen Bonds Between Carboxylates and Weakly Acidic Hydroxyl Moieties in Cocrystals of Zwitterions *Cryst. Growth Des.*, 2010, 10 (8), pp 3568–3584

Kawakita K., Ludde K.H., Some consideration of powder compression equations, PowderTechnol. 4 (1971)61–68.

Kerns, E.H.; Li, D. *Drug-Like Properties: Concept, Structure Design and Methods*; Elsevier: San Diego, CA, USA, 2008

Khandoudi N *et al*., Rosiglitazone, a peroxisome proliferator-activated receptor-gamma, inhibits the Jun NH(2)-terminal kinase/activating protein 1 pathway and protects the heart from ischemia/reperfusion injury, Diabetes. 2002 May

Khater MH, Gharib K, Abdelbary EH, Abd El-haleem MR (2014) A Comparative Study of Glycolic Acid Versus Mixture of Trichloroacetic Acid and Glycolic Acid Peeling for Treatment of Three Benign Epidermal Lesions. J Clin Exp Dermatol Res 5:251

Kitaigorodsky A. I., *Organicheskaya kristallokhimiya*, Ed.Akademii Nauk SSSR-a, Moskva 1955, pp. 139–236. Klepser TB, Kelly MW., Metformin hydrochloride: an ntihyperglycemic agent, Am J Health Syst Pharm. 1997 Apr 15;54(8):893-903

Klussmann, M.; White, A. J. P.; Armstrong, A.; Blackmond, D. G. Rationalization and Prediction of Solution Enantiomeric Excess in Ternary Phase Systems *Angew. Chem., Int. Ed.* 2006, *45* (47), 7985–7989

Koepsell H., Organic cation transporters in intestine, kidney, liver and brain, Annual Review of Physiology, 1998, Vol. 60: 243-266

Kootiratrakarn T., Kampirapap K., Chunhasewee C, Epidermal Permeability Barrier in the Treatment of Keratosis Pilaris, Dermatology Research and Practice, Volume 2015 (2015)

Koradia, V., Chawla, G., Bansal, A.K., (2004) Qualitative and quantitative analysis of clopidogrel bisulphate polymorphs. Acta Pharm 54: 193–204.

Kortejarvi H, Urtti A, Yliperttula M. 2007. Pharmacokinetic simulation of biowaiver criteria: The effects of gastric emptying, dissolution, absorption, and elimination rates. Eur J Pharm Sci 30(2):155–166

Koseki N., Kawashita H., Niina M., Nagae Y., Masuda N., Development and validation for high selective quantitative determination of metformin in human plasma by cation exchanging with normal-phase LC/MS/MS. *J. Pharm. Biomed. Anal.* 36: 1063–72 (2005)

Kotar-Jordan, B., Simonič, I., Zupet, R., Ružič, . , Grčman, . , Pečaver, A. (2005) Crystallization of solid forms of clopidogrel addition salts.WO2005/016931. Chem Abstr 142: 266759.

Lalau JD, Lactic acidosis induced by metformin: incidence, management and prevention, Drug Saf. 2010 Sep 1;33(9):727-40

Larsson O, et al. Distinct perturbation of the translatome by the antidiabetic drug metformin. *Proc Natl Acad Sci U S A*. 2012;109(23):8977–8982].

Lebovitz *et al.* , Mechanism of action of the second-generation sulfonylurea glipizide, Am J Med. 1983 Nov 30;75(5B):46-54

Lehn, J. M. Supramolecular Chemistry - Scope and Perspectives Molecules, Supermolecules, and Molecular Devices (Nobel Lecture), *Angew. Chem. Int. Ed. Engl.* 1988, *27*, 89-112

Lemmerer, A. Bernstein, J., Kahlenberg, V., Covalent assistance in supramolecular synthesis: *in situ* modification and masking of the hydrogen bonding functionality of the supramolecular reagent isoniazid in co-crystals, *CrystEngComm*, 2011,13, 5692-5708

Li M, Ding W, Smee J.J, Baruah B, Willsky GR, Crans DC., Anti-diabetic effects of vanadium(III, IV, V)-chlorodipicolinate complexes in streptozotocin-induced diabetic rats., Biometals. 2009 ec;22(6):895-905

Li, Z. J.; Abramov, Y.; Bordner, J.; Leonard, J.; Medek, A.; Trask, A. V. Solid-state acid-base interactions in complexes of heterocyclic bases with dicarboxylic acids: Crystallography, hydrogen bond analysis, and 15N NMR spectroscopy. *J. Am. Chem. Soc.* 2006, *128*, 8199-210

Lipinski, C.A. Drug-like properties and the causes of poor solubility and poor permeability. *J. Pharmacol. Toxicol. Methods* 2000, *44*, 239–245.;

Lipinski, C.A.; Lombardo, F. Experimental and computational approaches to estimated solubility and permeability in drug discovery and development settings. *Adv. Drug Deliv. Rev.* 2001, *46*, 3–26].

Liu, X.; Chhipa, R. R.; Pooya, S.; Wortman, M.; Yachyshin, S.; Chow, L. M. L.; Kumar, A.; Zhou, X.; Sun, Y.; Quinn, B.; McPherson, C.; Warnick, R. E.; Kendler, A.; Giri, S.; Poels, J.; Norga, K.; Viollet, B.; Grabowski, G. A.; Dasgupta, B., Discrete mechanisms of mTOR and cell cycle regulation by AMPK agonists independent of AMPK, PNAS, 2014 vol. 111 no. 4, E435–E444

Logie L, Harthill J, Patel K, Bacon S, Hamilton DL, Macrae K, McDougall G, Wang HH, Xue L, Jiang H, Sakamoto K, Prescott AR, Rena G., Cellular responses to the metal-binding properties of metformin.

Logie L, Harthill J, Patel K, Bacon S, Hamilton DL, Macrae K, McDougall G, Wang HH, Xue L, Jiang H, Sakamoto K, Prescott AR, Rena G.., Cellular responses to the metal-binding properties of metformin., Diabetes. 2012 Jun;61(6):1423-33.]

uo Y., Sun B., "Pharmaceutical Co-crystals of Pyrazinecarboxamide (PZA) with Various Carboxylic acids: Crystallography, Hirshfeld Surfaces and Dissolution Study", *Cryst. Growth Des.* 2013, *13*(5), pp. 2098–2106.

Lynch, D. E.; Smith, G.; Freney, D.; Byriel, K. A.; Kennard, C. H. L. Molecular Cocrystals of Carboxylic-Acids. XV. Preparation and Characterization of Heterocyclic Base Adducts with a Series of Carboxylic-Acids, and the Crystal-Structures of the Adducts of 2-Aminopyrimidine with 2,6-Dihydroxybenzoic Acid, 4-Aminobenzoic Acid, Phenoxyacetic Acid, (2,4-Dichlorophenoxy)-Acetic Acid, (3,4-Dichlorophenoxy)-Acetic Acid and Salicylic-Acid, and 2-Aminopyridine with 2,6-Dihydroxybenzoic Acid.*Aust. J. Chem.* 1994, *47*, 1097-1115

M.Kim, J.W.Park, Reversible, solid state capture of CO2 by hydroxylated amidines, Chem.Commun.46(2010)2507–2509

MacDonald J.C., Whitesides G. M., Solid-State Structures of Hydrogen-Bonded Tapes Based on Cyclic Secondary Diamides, *Chem.Rev*, 1994. 94,2383-24

Macrae, C. F.; Bruno, I. J.; Chisholm, J. A.; Edgington, P. R.; McCabe, P.; Pidcock, E.; Rodriguez-Monge, L.; Taylor, R.; van de Streek, J.; Wood, P. A. *J. Appl. Crystallogr*. 2008, *41,* 466–470.

Maddox, J., Crystals from first principles *Nature* 1988, 335, 201

Majerz, I.; Malarski, Z.; Sobczyk, L. Proton transfer and correlations between the C-O, O-H, N-H and O···N bond lengths in amine phenolates. *Chem. Phys. Lett.* 1997, *274*, 361-364.

Marchi A. , Marvelli L. , Cattabriga M. , Rossi R. , Neves M. , Bertolasi V. Ferretti, V., Technetium(V) and rhenium(V) complexes of biguanide derivatives. Crystal structures, ***J. Chem. Soc., Dalton Trans.***, 1999, 1937-1944, DOI: 10.1039/A900798I

Margetic D., Physico-Chemical Properties of Organosuperbases, pp. 25 in in *Superbases for Organic Synthesis: Guanidines, Amidines, Phosphazenes and Related Organocatalysts*, 2009 John Wiley & Sons, Ltd, ISBN 978-0-470-51800-7

Marianne Ashford, Biopharmaceutical principles of Drug Delivery, pp 318 in Aulton's Pharmaceutics: The Design and Manufacture of Medicines, edited by Michael E. Aulton, Kevin M. G. Taylor, fourth edition, 2013 Churchill Livingstone*/Elsevier]*.

Martell, A. E.; Smith, R. M.; Motekaitis, R. J. *NIST Critically Selected StabilityConstants of Metal Complexes*, NIST Standard Reference Database Number 46, Version 8.0; NIST: Gaithersburg, MD, May 2004.

McIntyre, G. J. J. Crystal Engineering and Correspondence between Molecular and Crystal Structures. Are 2- and 3-Aminophenols Anomalous? *Am. Chem. Soc*. 1997, 119, 3477−3480

McMahon J. A., Bis J. A., Vishweshwar P., Shattock T. R., McLaughlin O. L. Zaworotko M. J., Crystal Engineering of the Composition of Pharmaceutical Phases 3. Primary Amide Supramolecular Heterosynthons and Their Role in the Design of Pharmaceutical Co-Crystals, *Z. Kristallogr., 2005*, 220, 340

c Namara, D.P., Childs, S. ., Giordano, J., Iarriccio, A., Cassidy, J., Shet, . S., a nnion, R., O'Donnell, E., Park, A., 2006. Use of a glutaric acid cocrystal to improve oral bioavailability of a low solubility API. Pharm. Res. 23, 1888–1897

Metformin revisited: re-evaluation of its properties and role in the pharmacopoeia of modern antidiabetic agents. Diabetes Obes Metab. 2005; 7:654–65. [PubMed:16219009]]

Metrangolo, P.; Resnati, G. (2001), "Halogen Bonding: A Paradigm in Supramolecular Chemistry", Chem. Eur. J 7 (12): 2511–2519.

Miller RA, Chu Q, Xie J, Foretz M, Viollet B, Birnbaum MJ. Biguanides suppress hepatic glucagon signalling by decreasing production of cyclic AMP., Nature. 2013 Feb 14;494(7436):256-60. doi: 10.1038/nature11808.

Moamen S. Refat, Mohamed I. Kobeasy, Synthesis, spectroscopic, thermal, free radical scavenging ability, and antitumor activity studies of cobalt(II) metformin complex, Russian Journal of General Chemistry , April 2014, Volume 84, Issue 4, pp 767-774

Morissette SL, Almarsson O, Peterson ML, *et al*. *High-throughput* crystallization: polymorphs, salts, co-crystals and solvates of pharmaceutical solids. *Adv Drug Delivery Rew* v56 n3 2004 pp 275-300.

Morris, K.& Rodrígues-Hornedo, N. in *Encyclopedia of Pharmaceutical Technology* Vol.7 (eds Swarbrick, J. & Boylan, J.C.) 393-440 (marcel Dekker, New York, 1993)

Morris, K.R., Griesser, U.J., Eckhardt, C.J. & Stowell, J.G. Theoretiocal approaches to physical transformations of active pharmaceutical ingredients during manufacturing processes. *Adv. Drug Deliv. Rev*., 48, 91-114 (2001)

Mueller-Dethlefs, K.; Hobza, P. Noncovalent Interactions: A Challenge for Experiment and Theory. Chem. Rev. 2000, 100, 143-167

Muller H, Rheinwein H. Pharmacology of galegin. *Arch Exp Path Pharmacol* 1927; 125: 212–228.

N,N-dimethylbiguanide is used as oral antidiabetic drug, well known as Metformin (MET). It directly improves insulin action and is the only approved hypoglycemic drug of the biguanide class. It is the drug of first choice for oral therapy of the type 2 diabetes, marketed as hydrochloride, embonat (pamoate) and *p-chlorophenoxy acetate salt*.

Nair A.K., Anand O., Chun N., Conner D.P., Mehta M.U., Nhu D.T., Polli J.E., Yu L.X., Davit B. . , "Statistics on BCS Classification of Generic Drug Products Approved Between 2000 and 2011 in the USA", *AAPS Journal*, 2012, *14*,(4), pp. 664–666.

Nangia, A. Conformational polymorphism in organic crystals *Acc Chem Res*. 2008 May;41(5):595-604

Nangia, A., Supramolecular chemistry and crystal engineering, *J. Chem. Sci*.,. 2010, 122, 295–310

Nanubolu J. B., Sridhar B., Ravikumar K., Sawant D.K., Naik AT., Patkar N.L., Cherukuvada S., Sreedhar B., Polymorphism in metformin embonate salt – recurrence of dimeric and tetrameric guanidinium–carboxylate synthons ,*CrystEngComm*, 2013,**15**, 4448-4464

Nanubolu J. B., Sridhar B., Ravikumar K., Sawant D.K., Naik AT., Patkar N.L., Cherukuvada S., Sreedhar B., Polymorphism in metformin embonate salt – recurrence of dimeric and tetrameric guanidinium–carboxylate synthons ,*CrystEngComm*, 2013,15, 4448-4464

Nardelli, M. *J. Appl. Crystallogr*. 1995, *28*, 659.

Ndefo, *et al.,* Alogliptin: A new dipeptidyl peptidase-4 inhibitor for the management of type 2 diabetes mellitus, *American Journal of Health-System Pharmacy January 15, 2014 vol. 71 no. 2 103-109*

Nehm, S. J.; Rodríguez-Spong, B.; Rodríguez-Hornedo, N. Phase Solubility Diagrams of Cocrystals Are Explained by Solubility Product and Solution Complexation *Cryst.Growth Des.* 2006, 6, 592−600

Nelson C.G., Diclofenac gel in the treatment of actinic keratosis, Ther Clin Risk Manag. 2011; 7: 207–211.

Nicklin P, Keates AC, Page T, Bailey CJ. 1996. Transfer of metformin across monolayes of human intestinal Caco-2 cells and across rat intestine. Int J Pharm 128:155–162. 4. Proctor WR, Bourdet DL,

Nicoli, S.; Bilzi, S.; Santi, P.; Caira, M. R.; Li, J.; Bettini, R. Ethyl-paraben and nicotinamide mixtures: Apparent solubility, thermal behavior and X-ray structure of the 1:1 co-crystal *J. Pharm.Sci.* 2008, *97* (11), 4830-4839

Nisly SA *et al.*, Canagliflozin, a new sodium-glucose cotransporter 2 inhibitor, in the treatment of diabetes, Am J Health Syst Pharm. 2013 Feb 15;70(4):311-9

Otwinowski, Z.; Minor, W. *Methods Enzymol.* 1997, *276*, 307–326.

Padrela, L., Rodrigues, M.A., Velaga, S.P., Fernandes, A.C., Matos, H.A., de Azevedo, E.G., 2010. Screening for pharmaceutical cocrystals using the supercritical fluid enhanced atomization process. *J. Supercrit. Fluids* 53, 156–164

Papandreou I, Goliasova T, Denko NC. Anticancer drugs that target metabolism: Is dichloroacetate the new paradigm?, Int J Cancer. 2011 Mar 1;128(5):1001-8

Pekker, S., Kovats, E., Oszlanyi, G., et al., Rotor–stator molecular crystals of fullerenes with cubane   *Nature Mat.,*2005, vol. 4, pp. 764–767.

Pérez-Fernández R., Fresno N., Goya P., Elguero J., Menéndez-Taboada L., García-Granda S., Marco C., Structure and Thermodynamical Properties of Metformin Salicylate, *Cryst. Growth Des.*, 2013, 13 (4), pp 1780–1785.

Perlstein, J., *Molecular self-assemblies. 2. A computational method for the prediction of the* structure of one-dimensional screw, glide, and inversion molecular aggregates and implications for the packing of molecules in monolayers and crystals, *J. Am. Chem. Soc.*, 1994, 116 (2), pp 455–470

Perlstein, J., Molecular Self-Assemblies. 3. Quantitative Predictions for the Packing Geometry of Perylenedicarboximide Translation Aggregates and the Effects of Flexible End Groups. Implications for Monolayers and Three-Dimensional Crystal Structure Predictions, Chem. Mater., 1994, 6 (3), pp 319–326

Pernicova I, Korbonits M., Metformin—mode of action and clinical implications for diabetes and cancer, Nat Rev Endocrinol. 2014 Mar;10(3):143-56.doi:10.1038/nrendo.2013.256]

Peterson, L.M; Hickey B.M., Zaworotko J.M., Almersson Ö., Expanding the Scope of Crystal Form Evaluation in Pharmaceutical Science, *J. Pharma Pharmaceut Sci.* 9(3): 317-326, 2006

Pharmaceutical Industry Practices on Genotoxic Impurities, Edited by Heewon Lee. CRC Press, 2014 pp 396]

PharmaTrac data(India),; England NHS Prescription Cost Analysis report 2011,

Plosker GL , Dapagliflozin: a review of its use in type 2 diabetes mellitus, Drugs. 2012 Dec 3;72(17):2289-312

Poisonous Plant Database. U.S. Department of Health and Human Services. U.S. Food & Drug Administration, Center for Food

Pollak Michael, Potential applications for biguanides in oncology, *J Clin Invest.* 2013;123(9):3693–3700.]

Prins, L. J.; Reinhoudt, D. N.; Timmerman, P. Noncovalent Synthesis using Hydrogen Bonding. *Angew. Chem.*, Int. Ed. 2001, 40, 2382-2426.

Qu, H., Louhi-Kultanen, V., Kallas, J., Solubility and stability of anhydrate/hydrate in solvent mixtures.2006*, Int.J.Pharm*. 321, 101-107

Rainbolt, J., Yonker C.R., Ang T., Liang C., Jessop P.G., Reversible zwitterionic liquids, the reaction of alkanolguanidines alkanolamidines and diamines with CO2, GreenChem.12(2010)713– 721.;

Remenar J.F., o rissette S. ., Peterson . ., o ulton B., a cPhee J., Guzmán H.R., Almarsson Ö., "Crystal engineering of novel CCs of a Triazole drug with 1,4-dicarboxylic acids", *J. Am. Chem. Soc.*2003, *125*, pp. 8456– 8457.

Remyga, S.A., Myasnikova, R. M., and Kitaigorodski, A.I., An example of a mixed binary molecular crystal with doubly-random disorder in the arrangements of the molecules, *Zh. Strukt. Khim*., 1969, vol. 10, pp. 1131–1133

Rodríguez-Hornedo, N.; Nehm, S. J.; Seefeldt, K. F.; Pagan-Torres, Y.; Falkiewicz, C. J. Reaction Crystallization of Pharmaceutical Molecular Complexes.*Mol. Pharm.* 2006, *3* (3), 362–7

Safety & Applied Nutrition. Office of Plant and Dairy Foods and Beverages.

Samanta R., Kanaujia S. and Reddy C M., New co-crystal and salt form of sulfathiazole with carboxylic acid and amide, J. Chem. Sci. Vol. 126, No. 5, September 2014, pp. 1363–1367

Sanphui P., Goud N.R., Khandavilli U.B.R., Nangia A., "Fast Dissolving Curcumin CCs", *Cryst. Growth Des*.2011, *11*, pp. 4135–4145.

Schartman, R.R., On the thermodynamics of cocrystal formation*, Int.J.Pharm* 365 (2009), 77-80

Scheen AJ, Clinical pharmacokinetics of metformin, Clin Pharmacokinet. 1996 May;30(5):359-71.1996 May;30(5):359-71.

Schmidt, G.M.J., Photodimerization in the solid state, Pure Appl. Chem. 1971, 27, 647-67

Schultheiss, N., Newman, A., Pharmaceutical Cocrystals and Their Physicochemical Proprieties, 2009, *Cryst. Growth Des.* Vol .9, No.6, 2950-2967

Schwartz S, Fonseca V, Berner B, et al. Efficacy, tolerability, and safety of a novel once-daily extended-release metformin in patients with type 2 diabetes. Diabetes Care 2006;29:759–64. [PubMed]

Seaton, C.C., 2008. Current directions in co-crystal growth. New J. Chem. 32, 1659–1672

Seaton, C.C., Blagden, N., Muns, T., Scowen, I.J. Creation of ternary multicomponent crystals by exploitation of charge-transfer interactions, *Chemistry - A European Journal.* 2013 Aug 5;19(32):10663-7

Serajuddin, A.T.M., 2007. Salt formation to improve drug solubility. *Adv. Drug Del.Rev*. 59, 603–616

Shapiro L. S, Parrino A. V, Freedman L., Hypoglycemic Agents. III.[1—3] N[1]-Alkyl- and Aralkyl biguanides, *J. Am. Chem. Soc.*, 1959, 81 (14), pp 3728–3736

Sharma V.K., Nautiyal V., Goel K.K., Sharma A., Assessment of Thermal Stability of Metformin Hydrochloride, *Asian Journal of Chemistry,* Vol. 22, No. 5 (2010), 3561-3566

Shattock T. R., Arora K. K., Vishweshwar P., Zaworotko M. J Hierarchy of Supramolecular Synthons: Persistent Carboxylic Acid···Pyridine Hydrogen Bonds in Cocrystals That also Contain a Hydroxyl Moiety . *Cryst. Growth Des.*, 2008, 8 (12), pp 4533–4545

Shaw RJ, et al. The kinase LKB1 mediates glucose homeostasis in liver and therapeutic effects of metformin. Science. 2005; 310:1642–6. [PubMed: 16308421];

Sheldrick, G. M. *SHELX-97, Program for Crystal Structure Refinement*, University of Gőttingen, Germany, 1997.

Sherman, B. C. , U.S. Patent 6,077,542, 2000.

Shu Y, Brown C, Castro RA. 2008. Effect of genetic variation in the organic cation transporter 1, OCT1, on metformin pharmacokinetics. Clin Pharm Ther 83:273–280

Simonnet H, Tanret G. Sur les propietes hypoglycemiantes du sulfate de galegine. *Bull Soc Chim Biol Paris*1927; 8.

Sinko PJ, Leesman GD, Amidon GL. 1991. Predicting fraction dose absorbed in humans using a macroscopic mass balance approach. Pharm Res 8(8):979–988

Smith A.J., Kavuru P., Wojtas L., Zaworotko . J., Shytle R.D., "C0crystals of quercetin with improved solubility and oral bioavailability", *Mol. Pharmaceutics* 2011, *8*,

Smith, A. J., Kim, S-H., Duggirala, N.K., Jin J., Wojtas, L., Ehrhart, J., Giunta, B., Tan, J., Zaworotko, M.J. and Shytle, R. D., Improving Lithium Therapeutics by Crystal Engineering of Novel Ionic Cocrystals, *Mol. Pharmaceutics* 2013, 10, 4728−4738

Spek, A. L. *PLATON, A Multipurpose Crystallographic Tool*, Utrecht University, The Netherlands, 2002.

Stahly, G. P., A Survey of Cocrystals Reported Prior to 2000, *Crystal Growth & Design* 2009, 9 , 4212 - 4229.

Stahly, G. P..Diversity in Single - and Multiple – Component Crystals. The Search for and Prevalence of Polymorphs and Cocrystals, *Crystal Growth & Design* 2007,7, 1007-1026

Stanton . K., Bak A., "Physicochemical Properties of Pharmaceutical Co-Crystals: A Case Study of Ten AMG 517 Co-Crystals", *Cryst. Growth Des.* 2008, *8*, pp. 3856–3862.

Steiner T, The hydrogen bond in the solid state, *Angew Chem* Int Ed Engl. 2002 Jan 4;41(1):49-76.

Steiner, T.; Majerz, I.; Wilson, C. C. First O-H-N Hydrogen Bond with a Centered Proton Obtained by Thermally Induced Proton Migration. *Angew. Chem., Int. Ed.* 2001, *40*, 2651-2654

Steiner, T.; Majerz, I.; Wilson, C. C. First O-H-N Hydrogen Bond with a Centered Proton Obtained by Thermally Induced Proton Migration. *Angew. Chem., Int. Ed.* 2001, *40*, 2651-2654

Sterne J. Du nouveau dans les antidiabetiques.La NN dimethylamine guanyl guanide (N.N.D.G.). *MarocMed* 1957; 36: 1295–1296.

Sugawara, Y., Kamiya, N., Iwasiki, H., Ito, T. & Satow, Y. Humidity controlled reversible structure transition of disodium adenosine 5'-triphosphate dehydrate and trihydrate in the single crystal state. *J.Am. Chem. Soc*. 113, 5440-5445 (1991)

Sun C.C., Corystallization for successful drug delivery, Expert Opin. Drug Deliv. (2013) 10(2); 201-213

Sun, W.-Y.; Yoshizawa, M.; Kusukawa, T.; Fujita, M. MultiComponent Metal-Ligand Self-Assembly. *Curr. Opin. Chem. Biol.* 2002, 6, 757-764.

Tahrani *et al.*, Saxagliptin: a new DPP-4 inhibitor for the treatment of type 2 diabetes mellitus, Adv Ther. 2009 Mar;26(3):249-62

Thakker DR. 2008. Mechanisms underlying saturable intestinal absorption of metformin. Drug Metab Dispos 36:1650–1658

Thakur, T. S. Kirchner, . T. Bläser, D.; Boese, R.; Desiraju, G. R. *CrystEngComm* 2010, 12, 2079−2085

Thalladi, V. R. Weiss, H.-C. Bläser, D. Boese, R. Nangia, A. Desiraju, G. R. C−H···F Interactions in the Crystal Structures of Some Fluorobenzene, *J. Am. Chem. Soc.* 1998, 120, 8702−8710

Thayer , A. . , "Finding solutions", *Chem. Eng. News* 2010, *88*, pp. 13–18.

The 2013 Drug Trend Report, The Express Scripts, April 2014

Top 20 generic molecules worldwide, November 20, 2012, http://www.fiercepharma.com/special-reports/top-20-generic-molecules-worldwide

Top 200 Drugs of 2012, Michael Bartholow, PharmD, CACP, Published Online: Wednesday, July 17, 2013- See more at: http://www.pharmacytimes.com/publications/issue/2013/July2013/Top-200-Drugs-of-2012#sthash.GxN7Ir2Z.dpuf

Trask A.V, and Jones W., Crystal engineering of organic cocrystals by solid-state grinding approach, *Top Curr.Chem*. (2005) 254:41-70

Trask A.V., o therwell W.D.S., Jones W., "Pharmaceutical Cocrystallization: Engineering a Remedy for Caffeine Hydration", *Cryst. Growth Des*. 2005, *5*, pp. 1013–1021.

Trask, A.V., Motherwell, W.D.S., Jones, W., *Solvent-drop grinding: green polymorph* control of cocrystallization. *Chem Commun 2004*; 10: 890–1.

Trouillas P., Marchetti C., Bonnefont-Rousselot D., Lazzaroni R., Jore D., Garde`s-Albert M., Collin F., Mechanism of one-electron oxidation of metformin in aqueous solution, *Phys. Chem. Chem. Phys.*, 2013,15, 9871-9878

Tsume Y, Amidon GL. 2010. The Biowaiver extension for BCS class III drugs: The effect of dissolution rate on the bioequivalence of BCS class III immediate-release drugspredicted by computer simulation. Mol Pharm 7(4):1295–1243

Tucker GT, Casey C, Phillips PJ, Conor H, Ward JD, Woods HF. 1981. Metformin kinetics in healthy subjects and in patients with diabetesmellitus. Br J Clin Pharmacol 12:235–246

UK Prospective Diabetes Study (UKPDS) Group. Effect of intensive blood glucose control with metformin on complications in overweight patients with type 2 diabetes (UKPDS 34). *Lancet* 1998; 352: 854–865.

UK's British National Formulary (a rch, 2013) http://www.bnf.org/bnf/index.htm

Unger RH, Cherrington AD. Glucagonocentric restructuring of diabetes: a pathophysiologic and therapeutic makeover. J Clin Invest. 2012, 122:4–12. PubMed: 22214853

Van Niekerk, J.N. and Saunder, D.H., The crystal structure of the molecular complex of 4,4'-dinitrobiphenyl with biphenyl. Acta Crystallogr. 1948;1:44.

Vasudevan M, Ravi J., Ravisankar S., Suresh B., Ion-pair liquid chromatography technique for the estimation of metformin in its multicomponent dosage forms. *J. Pharm. Biomed. Anal.*25: 77–84 (2001).

Vippagunta RR, LoBrutto R, Pan C, Lakshman JP., Investigation of Metformin HCl lot-to-lot variation on flowability differences exhibited during drug product processing., J Pharm Sci. 2010 Dec;99(12):5030-9.

Wang DS, Jonker JW, Kato Y, Kusuhara H, Schinkel AH, Sugiyama Y., Involvement of Organic Cation Transporter 1 in Hepatic and Intestinal Distribution of Metformin, J Pharmacol Exp Ther. 2002 Aug;302(2):510-5

Watanabe CK. Studies in the metabolic changes induced by administration of guanidine bases. *J.Biol Chem* 1918; 33: 253–265

Wenger, M., & Bernstein, J. Designing a Cocrystal of γ-Amino Butyric Acid, *Angew. Chem* Vol. 118 - Issue 47 - 2006 - pp. 8134-8137

Weyna, D.R., Shattock, T., Vishweshwar, P., Zaworotko, M.J., 2009. Synthesis and structural characterization of cocrystals and pharmaceutical cocrystals: mechanochemistry vs slow evaporation from solution. *Cryst. Growth Des*. 9, 1106–1123

Wiechert, D.; Mootz, D. Molecular beside ionic: Crystal structures of a 1/1 and a 1/4 adduct of pyridine and formic acid. *Angew. Chem., Int. Ed.* 1999, *38*, 1974-1976.

Wilson, C. C. Migration of the proton in the strong O-H.O hydrogen bond in urea-phosphoric acid (1/1). *Acta Crystallogr.,Sect. B: Struct. Sci.* 2001, *57*, 435-439

Wilson, C. C., Migration of the proton in the strong O-H▪ ▪O hydrogen bond in urea-phosphoric acid (1/1), *Acta Cryst.* (2001). B57, 435-439

Wriedt, M.; Yakovenko, A.; Halder, G.; Prosvirin, A.; Dunbar, K.R.; Zhou, H.C, Reversible Switching from Antiferro- to Ferromagnetic Behavior by Solvent-Mediated, Thermally-Induced Phase Transitions in a Trimorphic MOF-Based Magnetic Sponge System, *J.Am.Chem.Soc*. 2013, 135, 4040 −4050

Zakikhani M, Dowling R, Fantus IG, Sonenberg N, Pollak M. Metformin is an AMP kinase-dependent growth inhibitor for breast cancer cells. *Cancer Res*.2006;66(21):10269–10273.

Zerkowski, J.A.; MacDonald, J.C.; Whitesides, G.M. Polymorphic Packing Arrangements in a Class of Engineered Organic Crystals *Chem. Mater*. 1997, 9, 1933-1941

Zhang M., Moore G.A., Lever M., Gardiner S.J., Kirkpatrick C.M., Begg E.J., Rapid and simple high-performance liquid chromatographic assay for the determination of metformin in humanplasma and breast milk. *J. Chromatogr. B* 766: 175–79 (2001).

Zhanga S., Rasmuson A.C., "The theophylline–oxalic acid co-crystal system: solid phases, thermodynamics and crystallization", *CrystEngComm*, 2012, *14*, pp. 4644–4655.

Zhou G, et al. Role of AMP-activated protein kinase in mechanism of metformin action. J Clin Invest. 2001; 108:1167–74. PubMed: 11602624

Zhou M, Xia L,Wang J. 2007. Metformin transport by a newly cloned proton-stimulated organic cation transporter (plasma membrane monoamine transporter) expressed in human intestine. Drug Metab Dispos 35:1956–1962

Zhu, H., Grant, D.J.W., Influence of water activity in organic solvent + water mixtures on the nature of the crystallizing drug phase 2. Ampicillin., *Int.J. Pharm* 1996, 139, 33-43

Zhu, H., Yuen, C., Grant, D.J.W., Influence of water activity in organic solvent+water mixtures on the nature if the crystallization drug phase 1. Theophylline, 2007, *Int.J..Pharm* 135, 151-160

Zhu, J., Padden, B.E., Munson, E.J. & Grant, D.J.W. Physicochemical characterization of nedocromil bivalent metal salt hydrates 2. Nedocromil zinc. *J. Pharm. Sci*. 86, 418-428 (1997)

Zhu*, M., Lu, L., Yang, P., & Jin, X.* (2002 May) *Bis*(*1,1-dimethylbiguanido*)*copper*(*II*) *octahydrate*. 58 (5),